THESIS

This is to certify that the

dissertation entitled

VOLTAGE COLLAPSE BIFURCATION OF A POWER
SYSTEM TRANSIENT STABILITY MODEL

presented by

I-PUNG HU

has been accepted towards fulfillment
of the requirements for

_____Ph.D._____ degree in _Electrical_ Engineering

*Robert A. Schluter*

Major professor

Date _8/8/90_____

PLACE IN RETURN BOX to remove this checkout from your record.
TO AVOID FINES return on or before date due.

| DATE DUE | DATE DUE | DATE DUE |
|----------|----------|----------|
|          |          |          |
|          |          |          |
|          |          |          |
|          |          |          |
|          |          |          |
|          |          |          |
|          |          |          |

MSU Is An Affirmative Action/Equal Opportunity Institution

c:\circ\datedue.pm3-p.1

VOLTAGE COLLAPSE BIFURCATION OF A POWER

SYSTEM TRANSIENT STABILITY MODEL

By

I-Pung Hu

A DISSERTATION

**ABSTRACT**

## VOLTAGE COLLAPSE BIFURCATION OF A POWER SYSTEM TRANSIENT STABILITY MODEL

By

I-Pung Hu

A complete power system model, which is composed of an algebraic load flow model and dynamic generator/exciter model, is developed. This complete power system model is formulated to point out the similarities and differences between the load flow models and the complete power system model that includes electrical generator/exciter and generator mechanical dynamics. Comparison of the load flow and the complete power system model simulation results indicate a converged load flow simulation may not imply voltage stability and will not accurately assess the proximity to voltage instability in the complete power system model. The effects of line drop compensation, excitation system control, machine saturation, and field current limits must be modelled precisely if accurate assessments of proximity to voltage collapse are to be obtained. These effects can be accurately modelled in a transient stability simulation but are not accurately modelled in current load flow models. A modified load flow model and simulation method is proposed that includes the effects of line drop compensation, excitation system control, machine saturation, and field current limits.

Voltage instabilities are classified into two categories. Load flow voltage instability is caused by supply and demand problem. Dynamic voltage instability is caused by the instability of the flux decay and exciter dynamics. Four voltage bifurcation tests, algebraic, algebraic/dynamic, dynamic/algebraic, and flux decay bifurcation tests are developed in this thesis. The algebraic bifurcation test can identify the supply and demand problem in the distribution system. algebraic/dynamic and dynamic/algebraic bifurcation tests can detect

ii

the instability of the generator dynamics. These tests are applied to analyze a two bus system and a twelve bus system. The results indicate the dynamic generator/exciter portion of the complete model becomes voltage unstable before the algebraic load flow portion of the complete model violates the widely used load flow based tests for voltage instability. Thus, new limits for stable operation must be established based on the instability of the dynamic portion of the complete power system model. Simulations show that generators in a coherent group of buses will lose their flux decay voltage stability when the reactive generation reserves in that coherent group of buses are exhausted.

## ACKNOWLEDGEMENTS

# TABLE OF CONTENTS

**LIST OF TABLE**

# LIST OF FIGURE

## LIST OF SYMBOLS

$l$:     number of generators with no field current upper limit violation. Internal, terminal, or high side transformer buses connected to these generators are called controllable.

$m$:    number of generators with field current limits violations. Internal, terminal, or high side transformer buses that are connected to these generators are called uncontrollable.

$n$:     number of load buses.

$i$:      $i=1,...,l$

$j$:      $j=1,...,m$

$k$:     $k=1,...,n$

$E'_{qi}$:    controllable internal bus voltage

$E'_{qj}$:    uncontrollable internal bus voltage

$V_{Ti}$:    controllable terminal bus voltage

$V_{Tj}$:    uncontrollable terminal bus voltage

$V_{Hi}$:    controllable high side transformer bus voltage

$V_{Hj}$:    uncontrollable high side transformer bus voltage

$V_k$:  load bus voltage

$\delta_i$:  controllable internal bus angle

$\delta_j$:  uncontrollable internal bus angle

$\theta_{Ti}$:  controllable terminal bus angle

$\theta_{Tj}$:  uncontrollable terminal bus angle

$\theta_{Hi}$:  controllable high side transformer bus angle

$\theta_{Hj}$:  uncontrollable high side transformer bus angle

$\theta_k$:  load bus angle

$\omega_i$:  controllable internal bus frequency

$\omega_j$:  uncontrollable internal bus frequency

$E_{fdi}$:  controllable internal bus field voltage

$E_{fdj}$:  uncontrollable internal bus field voltage, a constant

$P_{Mi}$:  mechanical power supplied by the steam turbine at controllable generator

$P_{Mj}$:  mechanical power supplied by the steam turbine at uncontrollable generator

$P_i^e$:  real power generated at controllable generator

$P_j^e$:  real power generated at uncontrollable generator

$P_{Ti}^e$:  real power received at controllable terminal bus

$P_{Tj}^e$:  real power received at uncontrollable terminal bus

$P_{Hi}^d$:     real power load at controllable high side transformer bus

$P_{Hj}^d$:     real power load at uncontrollable high side transformer bus

$P_k^d$:     real power load at load bus

$Q_i^e$:     reactive power generated at controllable generator

$Q_j^e$:     reactive power generated at uncontrollable generator

$Q_{Ti}^e$:     reactive power received at controllable terminal bus

$Q_{Tj}^e$:     reactive power received at uncontrollable terminal bus

$Q_{Hi}^d$:     reactive power load at controllable high side transformer bus

$Q_{Hj}^d$:     reactive power load at uncontrollable high side transformer bus

$Q_k^d$:     reactive power load at load bus

$V_{1i}$:     measured voltage

$V_{3i}$:     stabilizer output voltage

$V_{Ri}$:     amplifier output voltage

$V_{REFi}$: reference voltage

$\tau'_{d0i}$     generator direct axis transient open circuit time constant at controllable internal bus

$\tau'_{d0j}$:     generator direct axis transient open circuit time constant at uncontrollable internal bus

$M_i$:     generator per unit inertia constant at controllable internal bus

$M_j$:    generator per unit inertia constant at uncontrollable internal bus

$D_i$:    generator load damping coefficient at controllable internal bus

$D_j$:    generator load damping coefficient at uncontrollable internal bus

$\tau_{Ri}$:    regulator input filter time constant

$\tau_{Fi}$:    regulator stabilizing circuit time constant

$\tau_{Ei}$:    exciter time constant

$\tau_{Ai}$:    amplifier input filter time constant

$x_{ci}$:    line drop compensation reactance

$K_{Fi}$:    regulator stabilizing circuit gain

$K_{Ei}$:    exciter self excitation at full load field voltage

$K_{Ai}$:    amplifier circuit gain

$S_{Ei}$:    rotating exciter saturation at ceiling voltage

$S_{Di}$:    generator saturation function applied to direct axis reactance at controllable internal bus

$S_{Dj}$:    generator saturation function applied to direct axis reactance at uncontrollable internal bus

$x'_{di}$:    transient direct axis reactance at controllable internal bus

$x'_{dj}$:    transient direct axis reactance at controllable internal bus

$x_{di}$:    steady state direct axis reactance at controllable internal bus

$x_{dj}$:    steady state direct axis reactance at uncontrollable internal bus

$x_{qi}$:  steady state quadrature axis reactance at controllable internal bus

$x_{dj}$:  steady state quadrature axis reactance at uncontrollable internal bus

CHAPTER 1

INTRODUCTION

1.1   Voltage Collapse

Voltage collapse of the interconnected power system has been a subject that is becoming of concern to utilities around the world. Voltage collapse is a concern because of the transfer of power over long distances and the inability to add generation close to load centers due to environmental and political constraints.

Voltage collapse is a slow continuous decline of voltage over a 10 to 20 minute interval and followed by a rapid decline of voltage (Fig. 1.1). In some cases, this voltage decline can occur over an interval as short as one minute and yet in other rare cases the voltage decline can occur over a several hour period.

Although much research has been undertaken to establish the precise model and causes of voltage collapse, there still isn't a complete understanding or agreement on the exact model to be used to simulate voltage collapse. This thesis develops a precise model and investigates the contribution of each element in this precise model to voltage collapse. After the precise model is developed and understood, the causes of voltage collapse, the measures or conditions for assessing the proximity to voltage collapse are investigated. The operating and planning criteria that will ensure adequate safety margins against voltage collapse, and the network enhancement strategy that would most effectively and economically in-

# CHAPTER 1

# INTRODUCTION

## 1.1 Voltage Collapse

Voltage collapse of the interconnected power system has been observed frequently and is of concern to utilities around the world. Voltage collapse has been associated with the transfer of power over long distances and the trend of siting generators far from load centers due to environmental and political concerns.

Voltage collapse is a slow continuous decline of voltage over a 10 to 20 minute interval and followed by a rapid decline of voltage (Fig. 1.1). In some cases, this voltage decline can occur over an interval as short as one minute and yet in other rare cases the voltage decline can occur over a several hour period.

Although much research has been undertaken to establish the precise model and causes of voltage collapse, there still isn't a complete understanding or agreement on the exact model to be used to simulate voltage collapse. This thesis develops a precise model and investigates the contribution of each element in this precise model to voltage collapse. After the precise model is developed and understood, the causes of voltage collapse, the measures or conditions for assessing the proximity to voltage collapse are investigated. The operating and planning criteria that will ensure adequate safety margins against voltage collapse, and the network enhancement strategy that would most effectively and economically in-

1

crease margins for voltage collapse problems are then topics for future investigation.
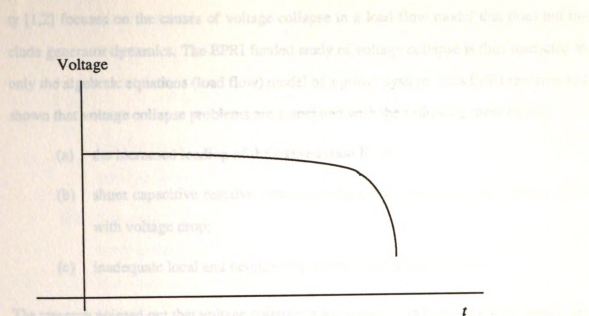
Voltage



Figure 1.1 Voltage collapse phenomenon

## 1.2    The Purpose of This Thesis

The purpose of this thesis is to

    (a)   greatly extend the understanding of the modeling of generator dynamics needed to accurately assess proximity to voltage collapse;

    (b)   show that the causes of voltage collapse not only occur in the algebraic equations of the model but also in the differential equations of the model;

    (c)   determine tests that indicate the proximity to voltage collapse;

    (d)   extend the understanding of the various types of voltage collapse and how each is caused to occur.

## 1.3    Load Flow Collapse

The Electric Power Research Institute (EPRI) funded research at Michigan State Universi-
ty [1,2] focuses on the causes of voltage collapse in a load flow model that does not in-
clude generator dynamics. The EPRI funded study of voltage collapse is thus restricted to
only the algebraic equations (load flow) model of a power system. This EPRI research has
shown that voltage collapse problems are associated with the following three factors

    (a)   the increased loading of the transmission lines;

    (b)   shunt capacitive reactive power withdrawal and increased line losses ($I^2X$)
           with voltage drop;

    (c)   inadequate local and neighboring reactive generation support.

The research pointed out that voltage collapse is associated with reactive power supply de-
mand problems in voltage control areas. These voltage control areas are groups of buses
that are coherent in both transient and steady state response in both voltage magnitude and
phase to all disturbances that occur outside the voltage control area. This type of coheren-
cy is due to the weakness of the transmission network cutset that isolates the coherent
group of buses called a voltage control area. An algorithm was developed that could deter-
mine these voltage control areas for very large data bases.

Voltage collapse can occur if

    (a)   there are no reactive generation reserves on synchronous generation or on
           static var compensators, or if under load tap changers are at the limits on tap
           changing action, or if there is no capacitive reactive reserve on mechanically
           switched capacitors. If a voltage control area has no supply of reactive power
           from any of the above sources, maybe vulnerable to severe voltage decline.
           The voltage decline can be large because the reactive power voltage jacobian
           elements associated with branches in the voltage control area boundary are
           small compared with branches connecting buses within the voltage control

areas. (The algorithm for determining voltage control areas identifies and eliminates the branches with the smallest reactive power jacobian elements connected to each bus. The groups of buses that are isolated by the elimination of these branches with the smallest reactive power voltage jacobian elements are the voltage control areas) The voltage decline needed to import reactive power across the branches in the voltage control area boundary with small jacobian element values must necessarily be large;

(b)  The weak voltage control area boundary branches clog up and can't effectively transfer reactive power between voltage control areas. These boundary branches not only clog up but become "drains", where both ends of the branch send reactive power into the branch to meet the large $I^2X$ losses on the branch. Branches become drains with large SIL loading levels as bus voltage drops on both ends of the branch or as real power transfer over the branch increases. A boundary branch that acts as a drain does not effectively ship reactive power from one voltage control area with reactive reserves to a voltage control area that has no reactive reserves and needs reactive power. A branch that acts as a drain sucks the reactive power needed to meet it's $I^2X$ reactive losses from both buses it connects in the two voltage control areas. The voltage control area with the higher voltage level will provide more of the reactive power needed to meet $I^2X$ losses on the branch;

(c)  Voltage control areas that do not have reactive power reserves and have boundary branches with drain problems have difficulty in meeting increased reactive demand. If the voltage control area is at EHV (Extra High Voltage) voltage level and is connected by long transmission lines or underground lines, the shunt capacitive support may be large. If voltages drop in a voltage control area with

(1)   no reactive reserves

(2)   a weak boundary with a significant number of branches with drain problems

(3)   significant shunt capacitive reactive power support,

the large shunt capacitive reactive power withdrawal at buses in the voltage control area with voltage drop may not be met by the limited amount of reactive power that can be drawn in across the voltage control area boundary. This results in a lack of a stable load flow solution and thus voltage collapse.

As a summary, the increased loading of transmission lines clog up the ability of these lines to supply reactive power to the load area, line losses increase the reactive power load in the load area, and capacitor reactive power withdrawal decreases the local reactive power supply in load areas. If there is no other way to bring in reactive power support, the voltage will keep decreasing until a point where the load flow solution associated with the buses in the load area can not be solved. This kind of voltage instability is caused by reactive power supply and demand problems and has nothing to do with the flux decay and exciter dynamics of the generator. This kind of voltage instability is called load flow voltage instability. It will be shown in this thesis that load flow voltage instability could be one of the causes of system voltage instability.

## 1.4    Review of Load Flow Voltage Collapse Methods

Load flow voltage collapse methods, developed by using load flow model and solution algorithms, have been widely used in the utilities for voltage collapse analysis. It is assumed that a lack of convergence to a load flow solution is related to voltage collapse. The singularity of a jacobian matrix or part of a jacobian matrix indicates that the load flow solution algorithm may not converge to a solution and that the solution (if computed) may be a

point of bifurcation (a point where two or more solutions merge).

Tamura[12,13] showed that existence of closely related multiple load flow solutions were likely to appear under heavy load condition. A pair of closely located load flow solutions seems to be related to the voltage collapse. The closely located load flow solutions are caused by the singularity of the Jacobian matrix. The voltage instability proximity indicator developed in [12,13] is basically another method to detect the singularity of the jacobian matrix.

Sensitivity analysis based voltage collapse tests place conditions on the relationship between changes in states or outputs and changes in inputs. Borremans [28] provided conditions of sensitivity matrices $S_{Q_G Q_L}$ and $S_{Q_L V}^{-1}$ for voltage stability. Carpentier [8] provided a condition for $S_{Q_G Q_L}$. Schlueter [3] defined PQ and PV controllability and developed sensitivity matrix tests on $S_{Q_G E}$, $S_{VE}$, $S_{Q_G Q_L}$, and $S_{Q_L V}^{-1}$ that assure PQ and PV controllability. It is shown that all known tests for voltage collapse can be derived based on assuming PQ and PV controllability hold.

It will be shown in this thesis that the load flow model based voltage collapse tests are incorrect, especially when the system is stressed. The load flow voltage collapse methods only investigate the supply and demand problems of the transmission and distribution system. The instability of the generator dynamics can not be analyzed by load flow voltage collapse methods. It is shown in this thesis that the instability of generator dynamics will cause one type of voltage instability of the power system and that load flow methods investigate the other type of voltage instability.

## 1.5    Review of Dynamic Voltage Collapse Methods

Dynamic voltage collapse methods take the dynamics of the generator into account. Only mechanical dynamics of the generator have been included in the dynamic model used in

[7, 27]. The importance of flux decay and excitation system dynamics to voltage collapse have been pointed out by Schlueter [1,2,3,4].

Venikov [7] recognized that a sign change of the determinant of the jacobian of equilibrium equations of a transient power system stability model may indicate voltage instability of the power system. Kwatny [27] showed that the static bifurcations of the equilibrium (load flow) equations were associated with either voltage collapse or steady state angle stability. Kwatny [27] separated divergence instability (singularity of the jacobian of the equilibrium equations of both the differential and algebraic equations) from loss of causality (singularity of the jacobian of just the algebraic equations). The implications of divergence instability and loss of causality with regard to voltage instability will be studied more completely in this thesis. The differential equations used in this model represented only the mechanical dynamics of the generator. The algebraic equations represent the real and reactive power balance equations at load buses. Schlueter [1,2,3,4] extended Kwatny's [27] work by developing conditions for static voltage collapse that included the flux decay dynamics and excitation system dynamics of the generators. Loss of causality in this extended model will be associated with load flow voltage collapse and divergence stability will be associated with dynamic voltage instability. Schlueter [1,2,3,4] defined parameters $\lambda$ that change slowly over time and can cause the equilibrium point to move to a point of bifurcation. Schlueter [1,2,3,4] also showed that PV and PQ controllability could assure that the transient stability model of [27, 7] could not experience divergence instability or loss of causality. Sauer and Pai [19] presented the relationship between a power system dynamic model and standard load flow model. Only generator mechanical dynamics were included in his model.

This thesis shows that instability of the flux decay and excitation system dynamics may result in voltage collapse. The causes of flux decay and excitation system instability are identified.

## 1.6    Thesis Contribution

This thesis will investigate system voltage instability which occurs in a power system model that includes both generator and exciter dynamics and the algebraic equations associated with the real and reactive power balance equations at buses in the transmission network. A necessary condition for system voltage instability is that the jacobian of the equations that describe the equilibrium point of this set of differential and algebraic equations (general power system model) be singular. A necessary condition for load flow voltage instability is that the jacobian of the real and reactive power balance equations of a load flow model be singular at some equilibrium point. Since the real and reactive power balance equations in a load flow and in the mid term transient stability model are different, the necessary conditions for load flow voltage collapse may not indicate a system voltage instability and vice versa.

The primary contribution of this thesis is the development of a power system model that includes the following three factors:

    (1)   air gap saturation in the synchronous machine model,

    (2)   line drop compensation in the excitation system model,

    (3)   field current limitation and the field current limit controller in the excitation system,

and shows their influence on proximity to voltage collapse. All of these factors are associated with how voltage control is accomplished in the set of differential and algebraic equations of the system voltage instability model. These factors are greatly simplified in a load flow model and can cause large error in predicting proximity to voltage collapse.

It will be shown that the load flow equilibrium point and the equilibrium point of the set of differential and algebraic equations (general power system model) that describe system

voltage instability model diverge as the equilibrium points of the two models approach voltage instability. These three factors

    (a)    are the factors that cause the differences in the equilibrium point of the load flow and the equilibrium point of the set of differential and algebraic equations;

    (b)    cause the tests for system voltage instability to give different results from the test for load flow voltage instability even when the same equilibrium point is used in both models.

The line drop compensation decides the bus or fictitious point in the network where voltage is going to be controlled by the generator exciter. In most cases, the generator terminal voltage and current are measured because these variables are easier to measure. Line drop compensators utilize the measured terminal voltage and current and a model of the network connected to the generator to calculate the voltage and current at some other point (fictitious or real) where the exciter attempts to hold voltage to some reference value. The actual point in the network where the exciter's line drop compensator selects to control voltage, significantly changes the amount of the local reactive power demand supplied by this generator and can significantly affect the voltages observed in the network after a contingency or a change in operating conditions.

The air gap saturation of the generator is the magnetic saturation of iron in the rotor and in the stator. Before saturation, the field current will generate enough flux to induce sufficient stator voltage to control the generator terminal bus voltage. When air gap saturation happens, the ability of the exciter to increase the induced stator voltage will be reduced even though field current is increased.

Field current limits are thermal limits of generator rotor and prevent overheating of the generator rotor. The field current limit is given as a curve that plots the level of field cur-

rent versus the time duration of that level of field current. If the field current limit is exceeded, there will be a control to disable the exciter in the generator and reduce the field current down to continuous rating levels that can be sustained indefinitely. Air gap saturation effects certainly contribute to a machine reaching its field current limit.

The second contribution of this thesis is the classification of the various types of system voltage instability and the development of proximity test for each type of system voltage instability. The necessary condition for system voltage instability is based on singularity of the jacobian of the set of differential and algebraic equations that describe the equilibrium point for this general power system model. The necessary conditions for load flow voltage instability are based on the singularity of the jacobian of the algebraic equations of the load flow model. The jacobian for testing for system voltage instability is evaluated at the equilibrium point for the set of differential and algebraic equations. The jacobian for testing for load flow voltage instability is evaluated at the equilibrium point of the load flow algebraic equations.

It should be noted that the focus of this thesis is to study only those bifurcations and singularities that can occur when the state of the dynamic and algebraic model is at the equilibrium point. Furthermore, the focus is toward describing the necessary conditions for different types of bifurcations and singularities that cause voltage collapse at the equilibrium points rather than describing the bifurcation itself or the dynamical behavior near or after the bifurcation occurs.

The test conditions for system voltage instability and load flow instability do not necessarily indicate that a bifurcation will occur at that equilibrium point because the test conditions are necessary and not sufficient conditions. Furthermore, the test conditions do not indicate that a voltage collapse bifurcation occurs even if a bifurcation (change in the number of solutions) occurred at a specific equilibrium point $x_0(\lambda_0)$ as operating condition $\lambda$ is varied over $[\lambda_a, \lambda_b]$ and passes through $\lambda_0$. Several different types of bifurcation

could occur (saddle node bifurcation, steady state angle stability bifurcation) and thus the necessary conditions for bifurcation do not indicate that a voltage collapse bifurcation has occurred. A system algebraic voltage instability bifurcation can occur due to a bifurcation of the algebraic equations when coupling of the algebraic and differential equations is ignored or there are linearly dependent rows in the linearized real and reactive power balance equations of load buses. This system algebraic voltage instability is related to load flow voltage instability but is based on the equilibrium point of the set of algebraic and differential equations whereas load flow voltage instability is based on the load flow set of algebraic equations and their equilibrium point. A system dynamic bifurcation occurs when rows of the jacobian of the system voltage instability model associated with generator flux decay and exciter dynamics are linearly dependent with the rows associated with the real and reactive power balance equations at generator terminal, high side transformer, or load buses.

The third contribution is to develop and test proximity measures for dynamic system voltage instability and algebraic system voltage instability. There are four test conditions developed in this thesis. The algebraic bifurcation test can be used to test for algebraic (load flow) system voltage instability. Testing singularity of the submatrix of the system voltage stability model jacobian associated with the real and reactive power balance of generator terminal, high side transformer, and load buses (the algebraic bifurcation test jacobian) establishes whether loss of causality occurs and whether reactive demand supply problems exist. If the reactive demand supply problems occur at load and high buses, the test is similar to a load flow bifurcation test and would satisfy the system voltage collapse bifurcation test. If the row dependence of the algebraic bifurcation test includes rows associated with generator terminal buses, the algebraic bifurcation test indicates possible singularity of the power system model but does not assure that the system bifurcation test is satisfied. The algebraic/dynamic test is equivalent to the system jacobian matrix test since the algebraic/dynamic test matrix is singular if and only if the system voltage stability model jaco-

bian is singular. The dynamic/algebraic test shows the stability of the dynamic states of the power system with the assumption that no algebraic bifurcation has occurred. The flux decay bifurcation test can be used to explain the cause of system dynamic voltage instability since it indicates whether system voltage instability is related to instability of the flux decay dynamics.

This thesis has shown that the tests for voltage instability based exclusively on the load flow are invalid because the load flow does not accurately model the exciter and generator. The model which is developed in this thesis is necessary not only to compute the true equilibrium point of the system but also to develop tests for system voltage instability.

The primary contribution of this thesis is the development of a power system model that permits simulation of voltage instability. The development of a complete dynamic system analysis of the bifurcations and singularities of this model that are related to voltage collapse is impossible. A test condition for system bifurcation (change in the number of solutions at equilibria) is developed and an effort is made toward a classification of the types of bifurcations and singularities (loss of causality) of the model. It should be noted that the development of a complete dynamical system analysis of the power system model developed in this thesis is not easy since the theory for describing bifurcations and singularities of constrained differential equations is not complete.

In Chapter 2, a precise power system model is developed. The inability of getting correct steady state solution of the load flow model is also shown in Chapter 2. The tests for voltage collapse and the classification of voltage collapse are provided in Chapter 3. In Chapter 4, a two bus system and a twelve bus system are tested using the theory developed in Chapter 3. In Chapter 5, conclusions and topics for future research are given.

**CHAPTER 2**

**POWER SYSTEM MODELING**

## 2.1    Introduction

A general power system model, which includes mechanical dynamics, flux decay dynam-

ics, and excitation system dynamics of a generator and real and reactive power balance

equations for each network bus, is developed in this chapter. This model can be used to

test for algebraic voltage instability and system voltage instability. There are two different

kinds of nonlinear equations in this general power system model. One is a set of nonlinear

differential equations which represents the dynamics of the generator. Another is a set of

nonlinear algebraic equations which represents the real and reactive power balance equa-

tion for each bus in the network.

Differential Equation Model

$$\dot{x}(t) = f(x(t), y(t), \lambda(t)) \qquad \lambda(t) \in [\lambda_a, \lambda_b]$$

Algebraic Equation Model

$$0 = g(x(t), y(t), \lambda(t))$$

where

$x(t)$ :  state vector of the generator dynamics,

$y(t)$ : state vector of bus voltage and angle of terminal buses, high side transformer buses, and load buses, and

$\lambda(t)$ : state vector of the slow varying operating parameter.

$\lambda(t)$ is the set of operating parameters that change over time. $\lambda(t)$ can be used to represent real and reactive power load, generation dispatch, under load tap changers, and switchable shunt capacitors. As $\lambda(t)$ varies over $[\lambda_a, \lambda_b]$, there is assumed to be at least one equilibrium point for each $\lambda$, $(x_0(\lambda), y_0(\lambda))$. A necessary condition for the system to experience system voltage instability is that the jacobian

$$ J = \begin{vmatrix} \dfrac{\partial f}{\partial x} & \dfrac{\partial f}{\partial y} \\ \dfrac{\partial g}{\partial x} & \dfrac{\partial g}{\partial y} \end{vmatrix} $$

be singular at some $\lambda_0$ and $(x_0(\lambda_0), y_0(\lambda_0))$.

Section 2.2 discusses the derivation of each element in the general power system model. The air gap saturation, line drop compensation, field current limit, and excitation system control are discussed in detailed. Section 2.3 presents a general power system model which has $l$ controllable generator buses, m uncontrollable generator buses, and n load buses.

We also show that the conventional voltage instability test, which is implemented using a load flow power system model simulation, has problems getting correct solutions when the system is stressed. Simulation results which show the inability of load flow simulation to get the correct solution are provided in Section 2.4.

## 2.2 Single Bus System Model

The differential equation model includes the mechanical dynamics, flux decay dynamics,

and excitation system dynamics of the generator. The air gap saturation, field current limit, and line drop compensation should be included in this model.

### 2.2.1 Mechanical Dynamics

$$M\ddot{\delta} + D\dot{\delta} = P_M - P^e(E, \delta, V, \theta) \qquad (2.1)$$

where

M: generator per unit inertia constant

D: generator load damping coefficient

$\delta$: internal bus angle with respect to a synchronous rotating reference line

$P_M$: input mechanical power

$P^e$: output electrical power

The nonlinear differential equation (2.1) is called the swing equation because it is the same equation which describes the "swinging" of a pendulum in a uniform gravitational field. It describes the "swings" in the power angle $\delta$ during a transient. If it is assumed that there is no angle stability problem,

$$P_M = P^e(E, \delta, V, \theta),$$

the nonlinear differential equation (2.1) becomes a nonlinear algebraic equation. It is assumed there is no angle stability problem in the analysis of flux decay bifurcation test in Chapter 3 and the two bus system simulation in Chapter 4, .

### 2.2.2 Flux Decay Dynamics

The flux decay equation for each generator is

$$\tau'_{d0}\dot{E}_q = E_{fd} - E_q = E_{fd} - (E'_q + I_d(x_d - x'_d))$$

$$= E_{fd} - \left( E'_q + \frac{Q_{GE}}{E'_q} (x_d - x'_d) \right)$$

$$= E_{fd} - \frac{x_d E'_q}{x'_d} + \frac{(x_d - x'_d) V \cos(\delta - \theta)}{x'_d}$$

where

$E_q$:  internal generator voltage proportional to field flux linkage behind steady state direct axis reactance

$E'_q$:  internal generator voltage proportional to field flux linkage behind transient direct axis reactance

$E_{fd}$:  generator field voltage

$I_d$:  projection of terminal current on direct axis

$V$:  generator terminal voltage

$x'_d$:  transient direct axis reactance

$x_d$:  steady state direct axis reactance

$Q_{GE}$:  generator reactive power generation

$\tau'_{d0}$:  generator direct axis transient open circuit time constant

Notice that $Q_{GE}$ is the reactive power out of the generator. If $x'_d = x_q$, $Q_{GE}$ is the reactive power out of the internal bus.

It is necessary to include the air gap saturation for studying voltage instability. In Fig 2.1, $E_p$ is the voltage behind Potier leakage reactance. Before the air gap saturates, $E_p < A$, the increase of $I_{fd}$ can effectively increase $E_p$. If $E_p \geq A$, $I_{fd}$ can no longer control $E_p$ effectively due to the air gap saturation. The ability of the exciter to control the induced voltage has subsequently been reduced.
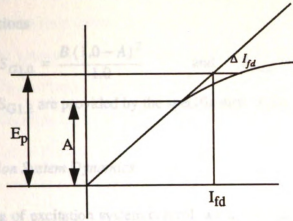
Figure 2.1 Air gap saturation

The model that includes air gap saturation is

$$\tau'_{d0}\dot{E}'_q = E_{fd} - (1 + S_D(E_p)) E_q$$

$$= E_{fd} - (1 + S_D(E_p)) \left( E'_q + \frac{I_d(x_d - x'_d)}{1 + S_D(E_p)} \right)$$

$$= E_{fd} - (1 + S_D(E_p)) E'_q - \frac{Q_{GE}(x_d - x'_d)}{E'_q}$$

where

$$S_D(E_p) = \frac{B(E_p - A)}{E_p}$$

$$V'_d = V_d - I_q x_p = V_d - \frac{V_d x_p}{x_{qs}}$$

$$V'_q = V_q + I_d x_p = V_q - \frac{(E'_q - V_q) x_p}{x'_{ds}}$$

$$E_p = \sqrt{V'^2_d + V'^2_q}$$

$V_d, V_q$ :   Projections of terminal voltage on generator d and q axes

$E_p$ :        Voltage behind the potier leakage reactance

The parameters A and B of the generator saturation function $S_D$ are evaluated from the following equations

$$S_{G1.0} = \frac{B(1.0-A)^2}{1.0} \quad \text{and} \quad S_{G1.2} = \frac{B(1.2-A)^2}{1.2}$$

The $S_{G1.0}$ and $S_{G1.2}$ are provided by the specification of the generator.

## 2.2.3 *Excitation System Dynamics*

In the modeling of excitation system control, we include the transfer function of the line drop compensator, amplifier, exciter, stabilizer, and measurement device (Figure 2.2). The line drop compensator is selected in the design of the excitation system. The excitation system feedback voltage is determined from measuring the generator terminal voltage V and current I and computing $V_c = V + jx_c I$ using a fictitious reactance $x_c$. By varying $x_c$, $V_c$ can be the voltage close to the internal bus, terminal bus, or a fictitious bus out somewhere in the network. The generator's excitation system will react to a disturbance very differently for different line drop compensation values $x_c$.
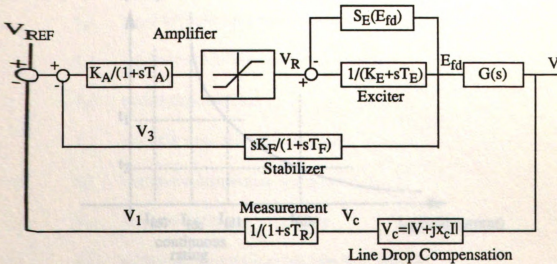


Figure 2.2 Excitation system model

Field current limit is a curve that relates the field current value to the duration of the interval during which the field current exceeds that value. If the field current exceeds the field current limit, the generator rotor will over heat and a field current limit control automatically disables the excitation system control and brings the field current down to a level (continuous rating) that can be sustained indefinitely without overheating the generator rotor. For example, in Figure 2.3, if the field current is at $I_{fd2}$, the time period that allows field current to remain at that value is $t_2$. After that period of time ($t_2$), the field current will be brought down to its continuous rating to prevent any damage of the exciter. If the field current is lower than its continuous rating ($I_{fd0}$), it can remain at that value for infinite time. The action of the field current control will be approximated by setting $K_a$ to zero and setting $E_{fd}$ to the value appropriate to produce the continuous rating of field current. This model of the field current limiter is not available in all transient stability programs and this approximate model is quite adequate for assessing retention or loss of voltage stability.
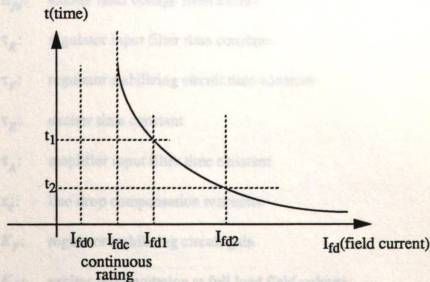


Figure 2.3 Field current limit controller

If we write a set of state equations to represent excitation system dynamics we get the following state equations.

$$\dot{V}_1 = \frac{-V_1 + |V + jx_c I|}{\tau_R}$$

$$\dot{V}_3 = \frac{1}{\tau_F}\left(-V_3 + \frac{K_F V_R}{\tau_E} - \frac{K_F E_{fd}\left(S_E\left(E_{fd}\right) + K_E\right)}{\tau_E}\right)$$

$$\dot{V}_R = \frac{1}{\tau_A}\left(K_A\left(V_{REF} - V_1 - V_3\right) - V_R\right)$$

$$\dot{E}_{fd} = \frac{1}{\tau_E}\left(V_R - \left(S_E\left(E_{fd}\right) + K_E\right)E_{fd}\right)$$

where

$V_1$:      measured voltage

$V_3$:      stabilizer output voltage

$V_R$:      amplifier output voltage

$E_{fd}$:     exciter field voltage from exciter

$\tau_R$:      regulator input filter time constant

$\tau_F$:      regulator stabilizing circuit time constant

$\tau_E$:      exciter time constant

$\tau_A$:      amplifier input filter time constant

$x_c$:      line drop compensation reactance

$K_F$:      regulator stabilizing circuit gain

$K_E$:      exciter self-excitation at full load field voltage

$K_A$:      amplifier circuit gain

$S_E$:      rotating exciter saturation at ceiling voltage

$V_{REF}$: reference voltage

## 2.2.4 Algebraic Equation Model

The algebraic equation model is the real and reactive power balance equation which represent the power flow at each bus in the network. If the air gap saturation is considered at the generator internal bus and terminal bus, the algebraic equation model is

$$S_D = \frac{B\,(E_p - A)^2}{E_p}$$

$$S_Q = \frac{x_q S_D}{x_d}$$

$$x'_{ds} = \frac{x'_d - x_p}{1 + S_D} + x_p$$

$$x_{qs} = \frac{x_q - x_p}{1 + S_Q} + x_p$$

$$P^e = \frac{E'_q V \sin(\delta - \theta)}{x'_{ds}} + \frac{V^2}{2}\left(\frac{1}{x_{qs}} - \frac{1}{x'_{ds}}\right)\sin(2(\delta - \theta))$$

$$= \frac{E'_q V \sin(\delta - \theta)(1 + S_D)}{x'_d + S_D x_p} +$$

$$\frac{V^2}{2}\left(\frac{x_d + x_q S_D}{x_d x_q + x_q S_D x_p} - \frac{(1 + S_D)}{x'_d + S_D x_p}\right)\sin(2(\delta - \theta))$$

$$Q^e = \frac{2E'_q V \sin(\delta - \theta) - E'_q V \cos(\delta - \theta) - V^2 \sin^2(\delta - \theta)}{x'_{ds}} +$$

$$\frac{x_{qs}(E'_q - V \sin(\delta - \theta))^2}{x'^2_{ds}}$$

$$= \frac{(1 + S_D)}{x'_d + S_D x_p}(2E'_q V \sin(\delta - \theta) - E'_q V \cos(\delta - \theta) - V^2 \sin^2(\delta - \theta)) +$$

$$\frac{(x_d x_q + x_q x_p S_D)\,(1 + S_D)^2\,(E'_q - V\sin(\delta - \theta)\,)^2}{(x'_d + S_D x_p)^2\,(x_d + x_q S_D)}$$

$$P_G = \frac{E'_q V \sin(\delta - \theta)}{x'_{ds}} + \frac{V^2}{2}\left(\frac{1}{x_{qs}} - \frac{1}{x'_{ds}}\right)\sin(2(\delta - \theta))$$

$$= \frac{E'_q V \sin(\delta - \theta)\,(1 + S_D)}{x'_d + S_D x_p} +$$

$$\frac{V^2}{2}\left(\frac{x_d + x_q S_D}{x_d x_q + x_q S_D x_p} - \frac{(1 + S_D)}{x'_d + S_D x_p}\right)\sin(2(\delta - \theta))$$

$$Q_G = \frac{E'_q V \cos(\delta - \theta)}{x'_{ds}} - V^2\left(\frac{\cos(\delta - \theta)^2}{x'_{ds}} + \frac{\sin(\delta - \theta)^2}{x_{qs}}\right)$$

$$= \frac{E'_q V \cos(\delta - \theta)\,(1 + S_D)}{x'_d + S_D x_p} -$$

$$V^2\left(\frac{\cos(\delta - \theta)^2(1 + S_D)}{x'_d + S_D x_p} + \frac{\sin(\delta - \theta)^2(x_d + x_q S_D)}{x_d x_q + x_q S_D x_p}\right)$$

$$P_G - P_H^d = \sum_{j=1}^{n} V_H V_{Lj} Y_{Lj} \cos(\theta - \theta_{Lj} - \gamma_{Lj})$$

$$Q_G - Q_H^d = \sum_{j=1}^{n} V_H V_{Lj} Y_{Lj} \sin(\theta - \theta_{Lj} - \gamma_{Lj})$$

where

$P^e$:  generator real power generation at internal bus

$Q^e$:  generator reactive power generation at internal bus

$P_G$:  real power injection at generator terminal bus

$Q_G$:  reactive power injection at generator terminal bus

$P_H^d$:  real power load at high side transformer bus

$Q_H^d$:  reactive power load at high side transformer bus

$S_D$:     generator saturation function applied to direct axis reactance

$S_Q$:     generator saturation function applied to quadrature axis reactance

$x_p$:     potier reactance

$E'_q$:     internal bus voltage

$\delta$:     internal bus angle

$V$:     terminal bus voltage

$\theta$:     terminal bus angle

$V_H$:     high side transformer bus voltage

$\theta_H$:     high side transformer bus angle

$V_L$:     load bus voltage

$\theta_L$:     load bus angle

## 2.3 General Power System Model

The variable and parameters that are used in this section are defined in LIST OF SYM-

BOLS.

$$\dot{\omega}_i = \left(\frac{1}{M_i}\right)(P_{Mi} - D_i\omega_i - P_i^e) \tag{2.1}$$

$$\dot{\omega}_j = \left(\frac{1}{M_j}\right)(P_{Mj} - D_j\omega_j - P_j^e) \tag{2.2}$$

$$\dot{\delta}_i = \omega_i \tag{2.3}$$

$$\dot{\delta}_j = \omega_j \tag{2.4}$$

$$\dot{E}'_{qi} = \left(\frac{1}{\tau_{d0i}}\right)\left(\left(\frac{-x_{dsi}E'_{qi}}{x'_{dsi}} + \frac{(x_{dsi} - x'_{dsi})V_{Ti}\cos(\delta_i - \theta_{Ti})}{x'_{dsi}}\right)(1 + S_{Di}) + E_{fdi}\right)$$

$$= \frac{1 + S_{Di}}{\tau_{d0i}}\left(\frac{-(x_{di} + S_{Di}x_{pi})E'_{qi}}{x'_{di} + S_{Di}x_{pi}} + \frac{(x_{di} - x'_{di})V_{Ti}\cos(\delta_i - \theta_{Ti})}{x'_{di} + S_{Di}x_{pi}}\right) + \frac{E_{fdi}}{\tau_{d0i}}$$

$$= \left(\frac{1}{\tau_{d0i}}\right)\left(E_{fdi} - (1 + S_{Di})E'_{qi} - \frac{Q_i^e(x_{di} - x'_{di})}{E'_{qi}}\right) \tag{2.5}$$

$$\dot{E}'_{qj} = \left(\frac{1}{\tau_{d0j}}\right)\left(\left(\frac{-x_{dsj}E'_{qj}}{x'_{dsj}} + \frac{(x_{dsj} - x'_{dsj})V_{Tj}\cos(\delta_j - \theta_{Tj})}{x'_{dsj}}\right)(1 + S_{Dj}) + E_{fdj}\right)$$

$$= \frac{1 + S_{Dj}}{\tau_{d0j}}\left(\frac{-(x_{dj} + S_{Dj}x_{pj})E'_{qi}}{x'_{dj} + S_{Dj}x_{pj}} + \frac{(x_{dj} - x'_{dj})V_{Tj}\cos(\delta_j - \theta_{Tj})}{x'_{dj} + S_{Dj}x_{pj}}\right) + \frac{E_{fdj}}{\tau_{d0j}}$$

$$= \left(\frac{1}{\tau_{d0j}}\right)\left(E_{fdj} - (1 + S_{Dj})E'_{qj} - \frac{Q_j^e(x_{dj} - x'_{dj})}{E'_{qj}}\right) \tag{2.6}$$

$$\dot{V}_{1i} = \left(\frac{1}{\tau_{Ri}}\right)\left(-V_{1i} + |V_{Ti} + j(I_{Ti}x_{ci})|\right) \tag{2.7}$$

$$\dot{V}_{3i} = \left(\frac{1}{\tau_{Fi}}\right)\left(-V_{3i} + \frac{K_{Fi}V_{Ri}}{\tau_{Ei}} - \frac{K_{Fi}E_{fdi}(S_{Ei}(E_{fdi}) + K_{Ei})}{\tau_{Ei}}\right) \tag{2.8}$$

$$\dot{V}_{Ri} = \left(\frac{1}{\tau_{Ai}}\right)(K_{Ai}(V_{REFi} - V_{1i} - V_{3i}) - V_{Ri}) \tag{2.9}$$

$$\dot{E}_{fdi} = \left(\frac{1}{\tau_{Ei}}\right)(V_{Ri} - (S_{Ei}(E_{fdi}) + K_{Ei})E_{fdi}) \tag{2.10}$$

$$P_i^e = P_{Ti}^e = \frac{E'_{qi}V_{Ti}\sin(\delta_i - \theta_{Ti})(1 + S_{Di})}{x'_{di} + S_{Di}x_{pi}} +$$

$$\frac{V_{Ti}^2}{2}\left(\frac{x_{di} + x_{qi}S_{Di}}{x_{di}x_{qi} + x_{qi}S_{Di}x_{pi}} - \frac{(1 + S_{Di})}{x'_{di} + S_{Di}x_{pi}}\right)\sin(2(\delta_i - \theta_{Ti})) \tag{2.11}$$

$$P_j^e = P_{Tj}^e = \frac{E'_{qj}V_{Tj}\sin(\delta_j - \theta_{Tj})(1 + S_{Dj})}{x'_{dj} + S_{Dj}x_{pj}} +$$

$$\frac{V_{Tj}^2}{2}\left(\frac{x_{dj} + x_{qj}S_{Dj}}{x_{dj}x_{qj} + x_{qj}S_{Dj}x_{pj}} - \frac{(1 + S_{Dj})}{x'_{dj} + S_{Dj}x_{pj}}\right)\sin(2(\delta_j - \theta_{Tj})) \tag{2.12}$$

$$P_{Ti}^e - P_{Ti}^d = V_{Ti}V_{Hi}Y_{TiHi}\cos(\theta_{Ti} - \theta_{Hi} - \gamma_{TiHi}) + V_{Ti}^2 Y_{TiHi}\cos(\gamma_{TiHi}) \tag{2.13}$$

$$P_{Tj}^e - P_{Tj}^d = V_{Tj}V_{Hj}Y_{TjHj}\cos(\theta_{Tj} - \theta_{Hj} - \gamma_{TjHj}) + V_{Tj}^2 Y_{TjHj}\cos(\gamma_{TjHj}) \tag{2.14}$$

$$-P_{Hi}^d = \sum_{s=1}^{l} V_{Hi}V_{Hs}Y_{HiHs}\cos(\theta_{Hi} - \theta_{Hs} - \gamma_{HiHs}) +$$

$$\sum_{j=1}^{m} V_{Hi}V_{Hj}Y_{HiHj}\cos(\theta_{Hi} - \theta_{Hj} - \gamma_{HiHj}) +$$

$$\sum_{k=1}^{n} V_{Hi}V_k Y_{cij}\cos(\theta_{Hi} - \theta_k - \gamma_{Hik}) +$$

$$V_{Hi}V_{Ti}Y_{HiTi}\cos\left(\theta_{Hi}-\theta_{Ti}-\gamma_{HiTi}\right) \tag{2.15}$$

$$-P_{Hj}^{d} = \sum_{i=1}^{l} V_{Hj}V_{Hi}Y_{HjHi}\cos\left(\theta_{Hj}-\theta_{Hi}-\gamma_{HjHi}\right) +$$

$$\sum_{s=1}^{m} V_{Hj}V_{Hs}Y_{HiHs}\cos\left(\theta_{Hj}-\theta_{Hs}-\gamma_{HiHs}\right) +$$

$$\sum_{k=1}^{n} V_{Hj}V_{k}Y_{Hjk}\cos\left(\theta_{Hj}-\theta_{k}-\gamma_{Hjk}\right) +$$

$$V_{Hj}V_{Tj}Y_{HjTj}\cos\left(\theta_{Hj}-\theta_{Tj}-\gamma_{HjTj}\right) \tag{2.16}$$

$$-P_{k}^{d} = \sum_{i=1}^{l} V_{k}V_{Hi}Y_{kHi}\cos\left(\theta_{k}-\theta_{Hi}-\gamma_{kHi}\right) +$$

$$\sum_{j=1}^{m} V_{k}V_{Hj}Y_{kHj}\cos\left(\theta_{k}-\theta_{Hj}-\gamma_{kHj}\right) +$$

$$\sum_{s=1}^{n} V_{k}V_{s}Y_{ks}\cos\left(\theta_{k}-\theta_{s}-\gamma_{ks}\right) \tag{2.17}$$

$$Q_{i}^{e} = \frac{(1+S_{Di})V_{Ti}\left(2E'_{qi}\sin\left(\delta_{i}-\theta_{Ti}\right) - E'_{qi}\cos\left(\delta_{i}-\theta_{Ti}\right) - V_{Ti}\sin^{2}\left(\delta_{i}-\theta_{Ti}\right)\right)}{x'_{di}+S_{Di}x_{pi}} +$$

$$\frac{(x_{qi}x_{di}+x_{qi}x_{pi}S_{Di})\,(1+S_{Di})^{2}\,(E'_{qi}-V_{Ti}\sin(\delta_{i}-\theta_{Ti})\,)^{2}}{(x'_{di}+S_{Di}x_{pi})^{2}\,(x_{di}+x_{qi}S_{Di})} \tag{2.18}$$

$$Q_{j}^{e} = \frac{(1+S_{Dj})V_{Tj}\left(2E'_{qj}\sin\left(\delta_{j}-\theta_{Tj}\right) - E'_{qj}\cos\left(\delta_{j}-\theta_{Tj}\right) - V_{Tj}\sin^{2}\left(\delta_{j}-\theta_{Tj}\right)\right)}{x'_{dj}+S_{Dj}x_{pj}} +$$

$$\frac{(x_{qj}x_{dj}+x_{qj}x_{pj}S_{Dj})\,(1+S_{Dj})^{2}\,(E'_{qj}-V_{Tj}\sin(\delta_{j}-\theta_{Tj})\,)^{2}}{(x'_{dj}+S_{Dj}x_{pj})^{2}\,(x_{dj}+x_{qj}S_{Dj})} \tag{2.19}$$

$$Q_{Ti}^e = \frac{E'_{qi} V_{Ti} \cos(\delta_i - \theta_{Ti})(1 + S_{Di})}{x'_{di} + S_{Di} x_{pi}} -$$

$$V_{Ti}^2 \left( \frac{\cos(\delta_i - \theta_{Ti})^2 (1 + S_{Di})}{x'_{di} + S_{Di} x_{pi}} + \frac{\sin(\delta_i - \theta_{Ti})^2 (x_{di} + x_{qi} S_{Di})}{x_{di} x_{qi} + x_{qi} S_{Di} x_{pi}} \right) \quad (2.20)$$

$$Q_{Tj}^e = \frac{E'_{qj} V_{Tj} \cos(\delta_j - \theta_{Tj})(1 + S_{Dj})}{x'_{dj} + S_{Dj} x_{pj}} -$$

$$V_{Tj}^2 \left( \frac{\cos(\delta_j - \theta_{Tj})^2 (1 + S_{Dj})}{x'_{dj} + S_{Dj} x_{pj}} + \frac{\sin(\delta_j - \theta_{Tj})^2 (x_{dj} + x_{qj} S_{Dj})}{x_{dj} x_{qj} + x_{qj} S_{Dj} x_{pj}} \right) \quad (2.21)$$

$$Q_{Ti}^e - Q_{Ti}^d = V_{Ti} V_{Hi} Y_{TiHi} \sin(\theta_{Ti} - \theta_{Hi} - \gamma_{TiHi}) - V_{Ti}^2 Y_{TiHi} \sin(\gamma_{TiHi}) \quad (2.22)$$

$$Q_{Tj}^e - Q_{Tj}^d = V_{Tj} V_{Hj} Y_{TjHj} \sin(\theta_{Tj} - \theta_{Hj} - \gamma_{TjHj}) - V_{Tj}^2 Y_{TjHj} \sin(\gamma_{TjHj}) \quad (2.23)$$

$$-Q_{Hi}^d = \sum_{s=1}^{l} V_{Hi} V_{Hs} Y_{HiHs} \sin(\theta_{Hi} - \theta_{Hs} - \gamma_{HiHs}) +$$

$$\sum_{j=1}^{m} V_{Hi} V_{Hj} Y_{HiHJ} \sin(\theta_{Hi} - \theta_{Hj} - \gamma_{HiHj}) +$$

$$\sum_{k=1}^{n} V_{Hi} V_k Y_{Hik} \sin(\theta_{Hi} - \theta_k - \gamma_{Hik}) +$$

$$V_{Hi} V_{Ti} Y_{HiTi} \sin(\theta_{Hi} - \theta_{Ti} - \gamma_{HiTi}) \quad (2.24)$$

$$-Q_{Hj}^d = \sum_{i=1}^{l} V_{Hj} V_{Hi} Y_{HjHi} \sin(\theta_{Hj} - \theta_{Hi} - \gamma_{HjHi}) +$$

$$\sum_{s=1}^{m} V_{Hj} V_{Hs} Y_{HjHs} \sin(\theta_{Hj} - \theta_{Hs} - \gamma_{HjHs}) +$$

$$\sum_{k=1}^{n} V_{Hj} V_k Y_{Hjk} \sin(\theta_{Hj} - \theta_k - \gamma_{Hjk}) +$$

$$V_{Hj} V_{Tj} Y_{HjTj} \sin(\theta_{Hj} - \theta_{Tj} - \gamma_{HjTj}) \tag{2.25}$$

$$-Q_k^d = \sum_{i=1}^{l} V_k V_{Hi} Y_{kHi} \sin(\theta_k - \theta_{Hi} - \gamma_{kHi}) +$$

$$\sum_{j=1}^{m} V_k V_{Hj} Y_{kHj} \sin(\theta_k - \theta_{Hj} - \gamma_{kHj}) +$$

$$\sum_{s=1}^{n} V_k V_s Y_{ks} \sin(\theta_k - \theta_s - \gamma_{ks}) \tag{2.26}$$

$$S_{Di} = \frac{B_i (E_{pi} - A_i)^2}{E_{pi}} \tag{2.27}$$

$$S_{Dj} = \frac{B_j (E_{pj} - A_j)^2}{E_{pj}} \tag{2.28}$$

## 2.4    Comparison of Load Flow and General Power System Steady State Simulations

Load flow simulation has been used as a standard tool to analyze voltage instability. The solution of load flow equations is assumed to be the steady state solution (equilibrium point) of the power system. In this section, we show that the solution of the load flow equations is similar to the equilibrium point of the general power system model only under light load conditions. These two solutions tend to diverge as the power system is stressed. Since the voltage instability usually occurs in heavy load conditions, we will not be able to get the correct data to analyze voltage instability problems by using load flow simulation.

Figure 2.4 shows the network diagram of a 12 bus system model [23] which is used for the simulations of this thesis. There are three internal buses, three terminal buses (low side transformer buses), three high side transformer buses, and three load buses. In the simulation, we increase the reactive power load at bus LOAD2 and solve for the solutions of a load flow model and general power system model. The reason we choose to increase the reactive power load at bus LOAD2 is that generator bus GEN3 has relatively small reactive generation capacity compared with GEN1 and GEN2. It is easier to exhaust reactive generation capability of GEN3 in the load flow simulation and the field current capability of GEN3 in a general power system model simulation. In the simulation results of Figure 2.5 and Figure 2.6, we assume the voltage of terminal buses are controlled by the generators in both the load flow model and the general power system model. The only difference between Figure 2.5 and Figure 2.6 is that in Figure 2.5 we use a smaller exciter amplifier gain ($K_A=50$) and in Figure 2.6 we use a larger exciter amplifier gain ($K_A=200$) for all the exciters in the general power system model. In each figure, we show the voltage magnitude differences of load flow model and general power system model solutions for high side transformer buses (HST1, HST2, and HST3) and load buses (LOAD1, LOAD2, and LOAD3). The x axis is the reactive power load at bus LOAD2 and y axis is the voltage magnitude difference of those two different models.

In both Figure 2.5 and Figure 2.6, the solutions of both models are quite similar when the reactive power load at bus LOAD2 is less than 100 MVar. The solutions start to diverge at the point where the reactive power load at bus LOAD2 exceeds 100 MVar. This is because the load flow model fixed the terminal bus or high side transformer bus voltage and approximates the field current limit by a reactive power limit. The general power system model does not specify the generator terminal or high side transformer bus voltage but attempts to regulate it through the effects of generator flux decay dynamics, generator air gap saturation as well as the exciter loop voltage regulation dynamics. Furthermore, the exciter's line drop compensator generally does not regulate voltage at either the terminal
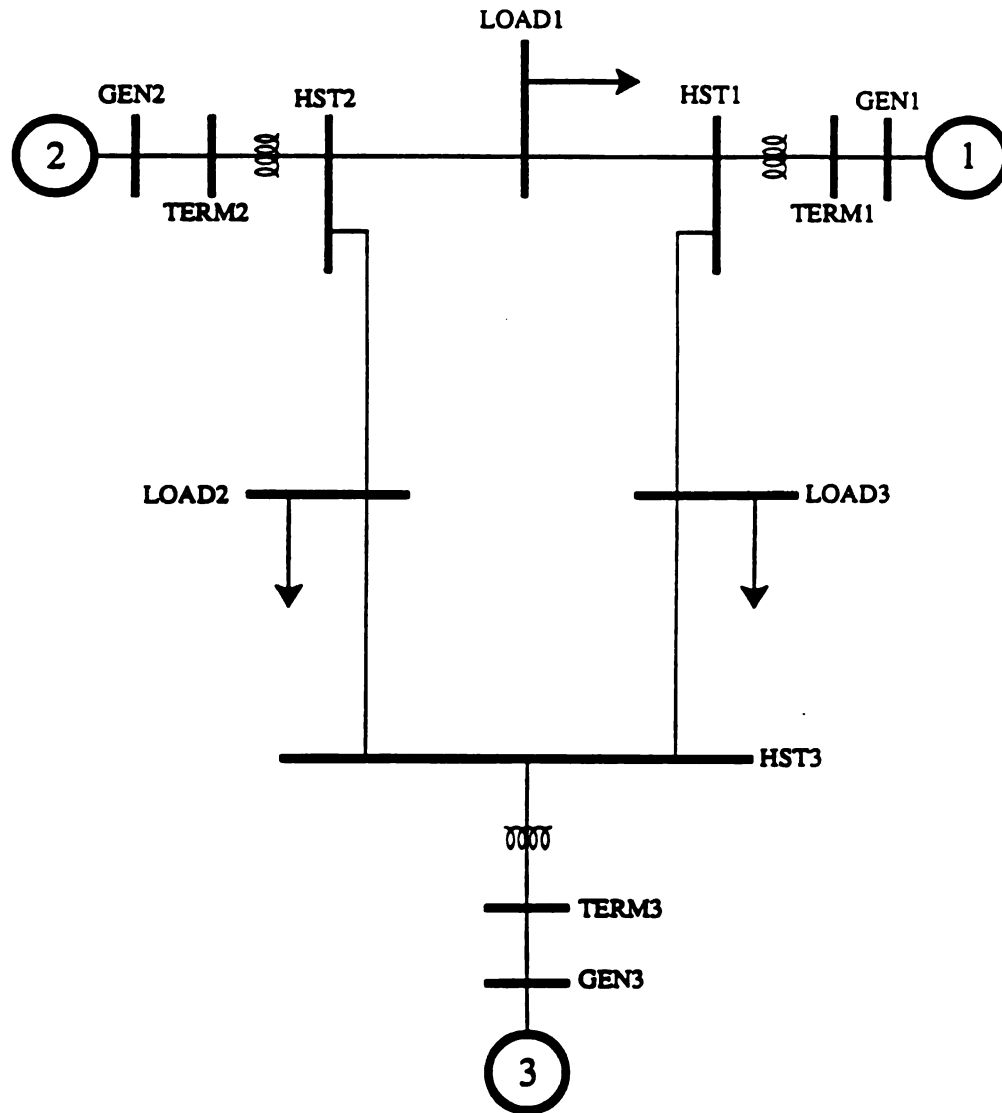
Figure 2.4 Twelve bus test system model
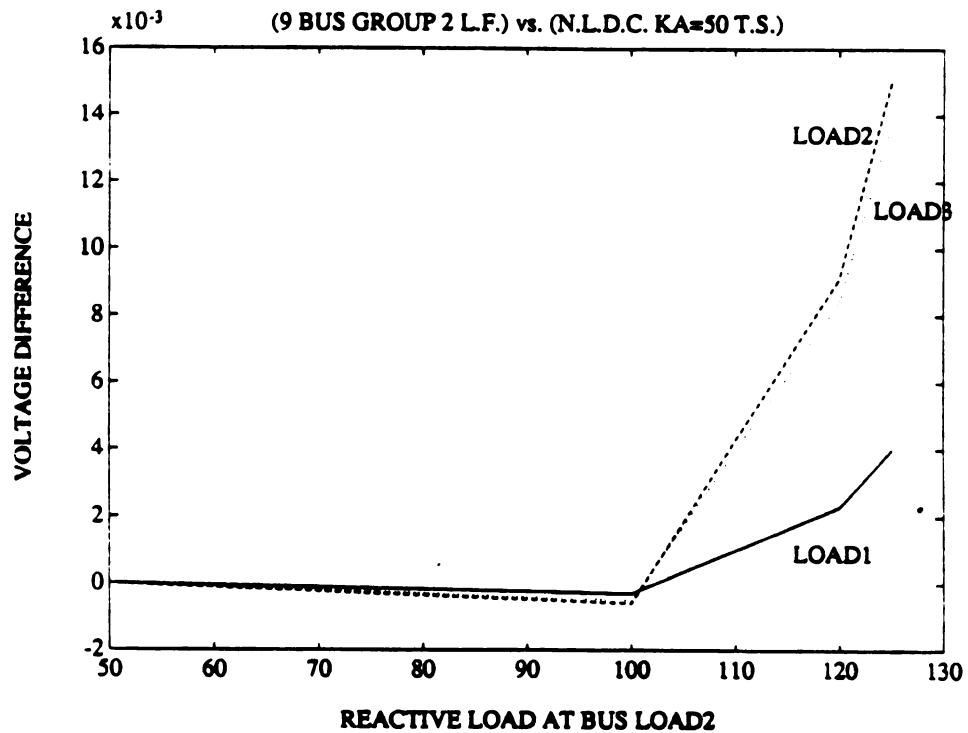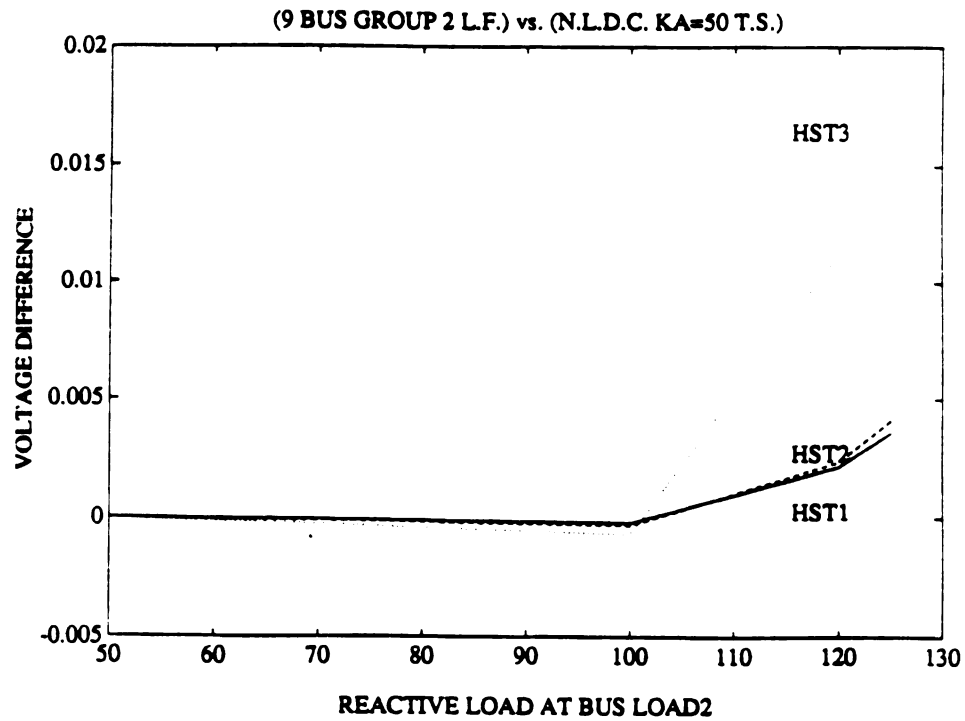
Figure 2.5 Comparaison of the solutions of load flow model and general power system model ($K_A$=50 )
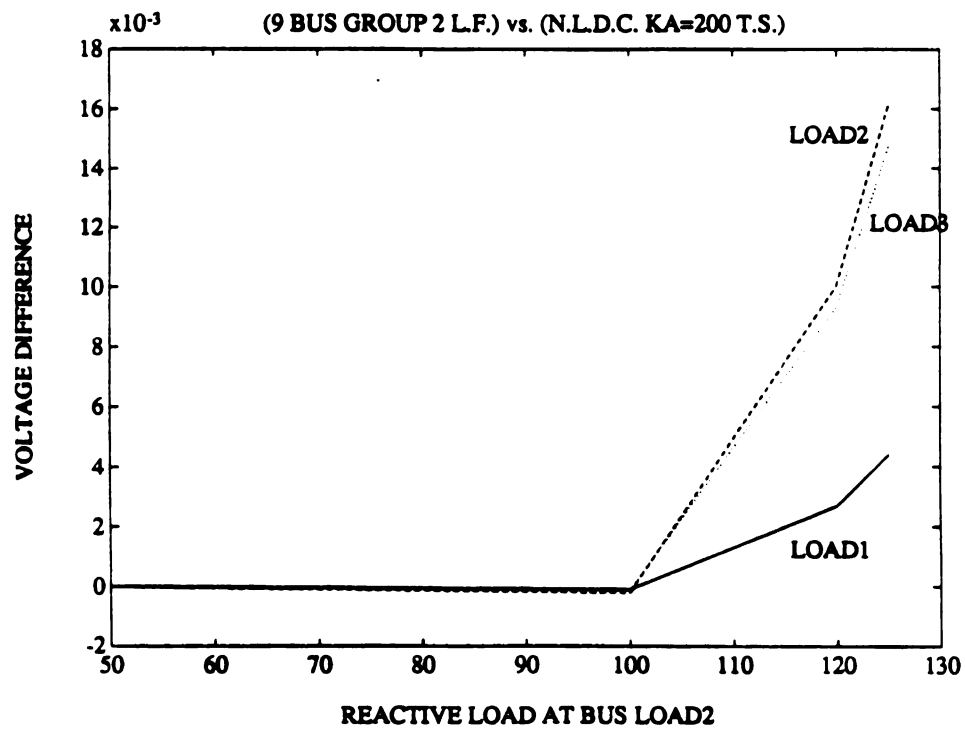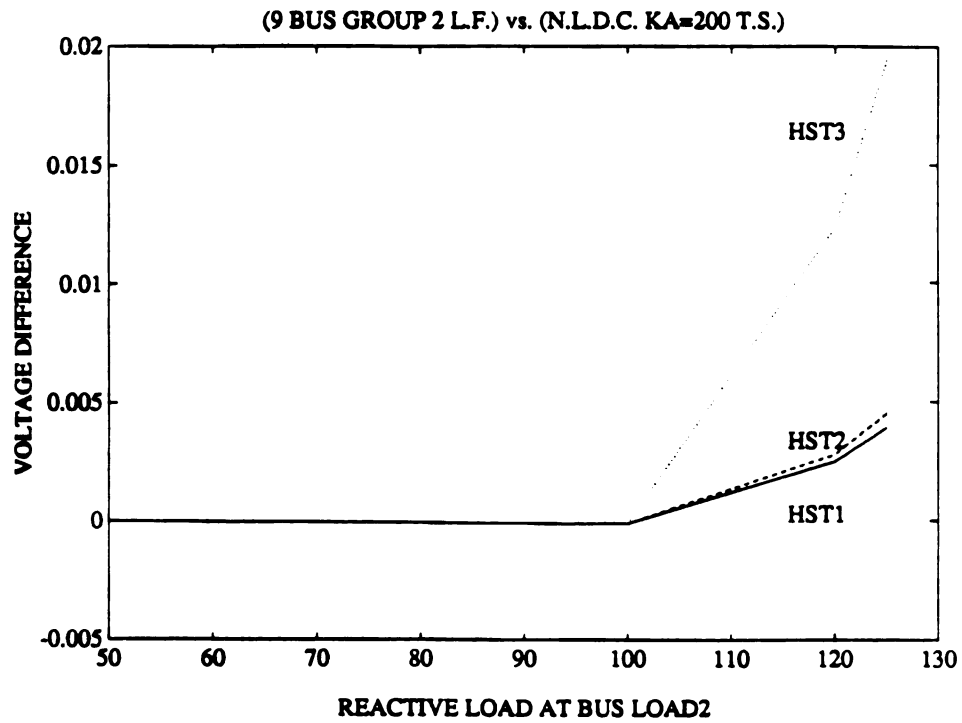
Figure 2.6 Comparaison of the solutions of load flow model and general power system model ($K_A$=200 )

bus or high side transformer bus voltage as with load flow but regulates some fictitious point that can be anywhere between the internal generator bus and some point out in the network. Finally, the reactive power limit in a load flow model is an approximation to the reactive power produced by the generator after the field current limit of the generator is hit and the field current limit controller has brought the field current down to its continuous rating level. Thus, the general power system model would allow a much higher field current level than indicated by the continuous field current level for durations indicated by a field current capability curve. The computational results presented compare the equilibrium point of the general power system model before field current limits are hit (the exciter is not disabled by the field current limit controller and field current is not reduced to continuous rating level) with that obtained from a load flow that contains a reactive generation limit that is related to continuous rating limit. This result will show a divergence between the general power system model equilibrium point and the load flow power system model equilibrium point even before field current limit is hit in the general power system model; that is when the system has not yet progressed to the point where generators have lost control of voltage. A second comparison of the equilibrium points of the load flow with continuous rating reactive limits with the equilibrium of the general power system model could be conducted when the field current limit is hit and the field current limiter has disconnected the exciter and reduced field current down to continuous rating levels with the equilibrium. The comparison of the load flow and general power system model equilibria should be quite close if the continuous rating of field current is at a level where saturation effects are negligible or have been accurately modeled and the generator is operating close to the point at which the correspondence between the field current and reactive power limit is computed.

It shows in our simulations that the solution of the general power system model diverged at 125 MVar which is much less than the reactive load level of 182 MVar at which the load flow diverges. The assumption that the load flow simulation is conservative, which has

been widely applied, is not true. The general power system model is more vulnerable to voltage collapse and lack of a converged solution than the load flow model.

Figure 2.5 and Figure 2.6 show that the divergence of solutions of HST3, LOAD2, and LOAD3 are much larger than the other buses. This is because the reactive reserve at bus GEN3 has been exhausted in the heavy load condition and LOAD2 and LOAD3 are close to GEN3.

The solutions in Figure 2.6 for an exciter amplifier gain of $K_A$=200 are far closer than the solutions in Figure 2.5 for $K_A$=50 in light load conditions. The reason that there is better agreement between the equilibria of the load flow and general power system model at large exciter gain is that the load flow model assumes the exciter gain is infinite so that the control of terminal voltage has no error. The general power system model has a finite excitation system closed loop gain $K_{EX}$ and an error in regulating voltage proportional to the inverse of $K_{EX}$ ($K^{-1}_{EX}$). Since $K_{EX}$ is proportional to the exciter amplifier gain $K_A$ and inversely related to air gap saturation, the agreement between the models increases with $K_A$ and decreases as the air gap saturation and reactive generation increase.

The reasons for the divergence of the load flow model from the general power system model are summarized in the following:

(a) the load flow simulation uses reactive power generation to regulate bus voltage and the general power system model uses field current to regulate bus voltage,

(b) the general power system model takes into account the air gap saturation, which affects the closed loop gain of the exciter control loop, but the load flow model does not,

(c) the load flow model assumes $K_A$ is infinite but $K_A$ is a finite value in the general power system model; The exciter loop gain $K_{EX}$ is proportional to the

exciter amplifier gain and inversely proportional to air gap saturation. The error in regulating voltage is proportional to $K^{-1}_{EX}$.

(d)  generators in the load flow model regulate either their high side transformer bus voltage or terminal bus voltage but the general power system model which takes line drop compensation into account allows any point between the generator internal bus and some fictitious point out in the network to be regulated.

# CHAPTER 3

# TESTS FOR VOLTAGE COLLAPSE

## 3.1 Introduction

Voltage instability problems are classified into two different categories in this thesis. These two kinds of voltage instability are results of very different types and locations of stress. Load flow voltage instability is caused by the inability of the transmission system to supply the reactive load when there is no reactive power supply at that load voltage control area. System voltage instability is caused by either the instability of generator dynamics or the links between dynamic states and algebraic states in a stressed network. Four voltage instability tests are discussed in this chapter.

## 3.2 Classification of Types of Voltage Instability

In a power system, there are strong connections and weak connections in the transmission system. We define the strength of the branch in terms of reactive power transferring capability of the branch. A strong connection has no problem in transferring both real and reactive power. A weak connection has difficulty in transferring reactive power in the sense that if the operating condition of the system is changed the weak transmission line gets clogged up and can not transfer reactive power without significant losses and voltage difference across the branch. It can be shown that the strength of a connection is dependent

on the reactance of the transmission line and the operating condition. A heavily loaded transmission line with large line reactance usually has difficulty in transferring reactive power. If we put any kind of disturbance in the system, the buses connected with strong connections will respond to the disturbance coherently in both voltage magnitude and phase. If we collect those buses with strong connections, we can form a coherent group of buses and we call this coherent group of buses a Voltage Control Area(VCA). (Schlueter/ Costi[9])

### 3.2.1   Load Flow Voltage Instability

Load flow voltage instability problems are reactive supply and demand problems. They are caused by the weak boundary connections among voltage control areas and capacitive reactive withdrawal with voltage drop inside the voltage control areas. A voltage decrease in a voltage control area will increase line reactive losses and weaken the strength of boundary connections to the neighboring areas. Because of the decrease of voltage, the re-active power supplied by line charging and shunt capacitors in that area will be decreased. Thus the voltage decrease at an area will not only decrease the shunt capacitive reactive power supply in that area but also reduce the capability of boundary transmission lines to transfer reactive power from other areas. It will come to a point where the load flow equations associated with the buses in that area can not be solved and the jacobian matrix becomes singular at that point. We call this kind of voltage instability load flow instability.

In this thesis, we show that

(1)   weak boundary transmission lines may get clogged up and become a reactive drain that sucks reactive power from both buses they are connected to;

(2)   the voltage instability caused by supply and demand problems can be analyzed by load flow simulation and the singularity of the load flow jacobian matrix indicates this kind of problem;

(3) load flow voltage instability, a particular type of system voltage instability, can not occur when there is plenty of reactive supply close to the point of stress. In contrast, system dynamic voltage instability may occur in an area even when there is plenty of reactive power supply close to it.

It will be shown in the Voltage Instability Tests chapter that load flow voltage instability (supply and demand problems) satisfy the necessary condition for bifurcation of the constrained differential equation if the jacobian matrix associated with the real and reactive power equations at high side transformer buses or load buses have linearly dependent rows. This would confirm the validity of the methods that apply load flow jacobian analysis to investigate voltage instability problems. It should be noted that load flow instability, that includes the real and reactive power balance equations at generator terminal buses, may not imply system voltage instability. More importantly, system voltage instability will be shown to occur without load flow voltage instability. This indicates that the load flow jacobian analysis is not conservative enough to predict all the possible types of voltage instability. The load flow instability test can be used to test for system voltage instability that result from reactive supply/demand problems at high side transformer and load buses.

### 3.2.2 System Voltage Instability

System voltage instability occurs due to two possible reasons. One reason is the reactive demand supply imbalance and the other is the instability of generator dynamics. There are four factors, air gap saturation, field current limit controller, line drop compensator, and excitation system control which may cause the instability of generator dynamics. These four factors have been modelled in Chapter 2.

Air gap saturation reduces the ability of a generator to create reactive power and control voltage. As air gap saturation increases, the increase in field current needed to control a specific terminal voltage change increases. If the field current limit is hit, the excitation

system is disconnected and field current is reduced to it's continuous rating level. The bus voltage controlled by the exciter is no longer controlled. It will be shown that increased air gap saturation and increased reactive generation in a stressed network will move the eigenvalues of dynamic states toward the right half plane and system voltage instability may occur. If the fictitious bus voltage controlled by the line drop compensator is located far out in the network, field current will be closer to saturation and the generator will be required to produce more reactive generation. It will be shown that the flux decay and exciter eigenvalues are generally complex if the field current limit is not hit and the excitation system is still in control of terminal bus voltage. It will be shown that, in some cases, these complex eigenvalues of the flux decay and exciter or the generator mechanical dynamics move to the right half plane and a Hopf bifurcation may occur. The loss of stability associated with Hopf bifurcation may cause the field current limit to be hit before the reactive loads on the machine would have caused the field current limit to be hit. Thus, the generator excitation system may be disabled and the field current reduces to continuous rating if either the field current limit is hit or if the flux decay and exciter or generator mechanical dynamics experience a Hopf bifurcation. Both air gap saturation and increased reactive generation will be shown to move the flux decay eigenvalues close to the right half plane. If the field current limit is hit, the exciter is disconnected, and field current is reduced to it's continuous rating. It will be shown that the flux decay eigenvalues will generally be real rather than complex as they were before the field current is hit and will be far closer to the $j\omega$ axis. After the field current limit is hit, the flux decay eigenvalue may be positive or become positive with increased reactive load. The generator's response after the flux decay eigenvalue becomes positive will be shown to result in monotone decreasing field current, induced voltage, and reactive power output. All of these would explain why voltage collapse is observed to be a continuous decline of voltage. This kind of voltage instability can be detected by using a dynamic/algebraic test to be defined. It will be also shown that this dynamic voltage collapse may occur even if the field current limits aren't reached and

the exciter is not disabled.

The other type of system voltage instability is caused by the stress on the transmission and distribution system and is tested using the algebraic/dynamic test to be defined. This type of voltage instability will be shown to not only capture load flow instability at high side transformer and load buses that do not interact with generator flux decay dynamics as well as the voltage instability caused by interaction between the generator and the network at generator terminal, high side transformer, and load buses. The system voltage instability caused by interaction of flux decay dynamics with the network at terminal, high side transformer, and load buses can be tested by the algebraic/dynamic test since the algebraic/dynamic test can test for every type of voltage instability.

## 3.3 Voltage Instability Tests

It should be noted that the focus of this thesis is to study only those bifurcations and singularities that occur when the state of the algebraic and dynamic models are at the equilibrium point. Furthermore, the focus is toward describing the necessary conditions for different types of bifurcations and singularities rather than describing the bifurcation or describing the dynamical behavior before or after the bifurcation occurs. This thesis provides different types of tests for voltage instability. The algebraic bifurcation test will be used for testing for load flow voltage instability. The algebraic/dynamic and dynamic/algebraic bifurcation tests are tests for dynamic voltage instability. The algebraic, algebraic/dynamic, and dynamic/algebraic tests for voltage instability are not tests for the same type of voltage instability. The types of voltage instability tested for in each of these three tests will be described. A flux decay bifurcation test is a test for instability of the flux decay dynamics under the assumption that there are no angle stability problem. This flux decay bifurcation test shows theoretically that the sensitivity matrix $S_{Q_G E}$, $S_{VE}$ and the air gap saturation, excitation system control, and reactive power generation decide the stability of

generator flux decay dynamics.

### 3.3.1 Model Linearization

$$\dot{x}(t) = f(x(t), y(t), \lambda(t))  \tag{3.1}$$

$$0 = g(x(t), y(t), \lambda(t))  \tag{3.2}$$

where

x(t): state vector of the generator dynamics

y(t): state vector of bus voltage and angle of terminal buses, high side transformer buses, and load buses

$\lambda(t)$ : state vector of the slow varying operating parameter, $\lambda(t) \in [\lambda_a, \lambda_b]$

$$J = \begin{bmatrix} \dfrac{df}{dx} & \dfrac{df}{dy} \\ \dfrac{dg}{dx} & \dfrac{dg}{dy} \end{bmatrix} = \begin{bmatrix} A(x_0, y_0, \lambda_0) & B(x_0, y_0, \lambda_0) \\ C(x_0, y_0, \lambda_0) & D(x_0, y_0, \lambda_0) \end{bmatrix}  \tag{3.3}$$

where matrix A, B, C, and D are a function of initial values of $x_0$, $y_0$, and $\lambda_0$.

We can write a set of linearized equations

$$\Delta \dot{x}(t) = A \Delta x(t) + B \Delta y(t)  \tag{3.4}$$

$$0 = C \Delta x(t) + D \Delta y(t)  \tag{3.5}$$

$\Delta y$ contains the changes of bus voltage and angle of terminal buses, high side transformer buses, and load buses. We can further divide $\Delta y$ into $\Delta y_1$ and $\Delta y_2$ where $\Delta y_1$ is the changes of bus voltage and angle of terminal buses, and $\Delta y_2$ is the changes of bus voltage and angle of high side transformer buses and load buses. Equation (3.4) and (3.5) become

$$\Delta \dot{x}(t) = A \Delta x(t) + \begin{bmatrix} B_1 & B_2 \end{bmatrix} \begin{bmatrix} \Delta y_1(t) \\ \Delta y_2(t) \end{bmatrix}  \tag{3.4.1}$$

$$0 = \begin{bmatrix} C_1 \\ 0 \end{bmatrix} \Delta x (t) + \begin{bmatrix} D_1 & D_2 \\ D_3 & D_4 \end{bmatrix} \begin{bmatrix} \Delta y_1 (t) \\ \Delta y_2 (t) \end{bmatrix}$$ (3.5.1)

where

$$\begin{bmatrix} B_1 & B_2 \end{bmatrix} = B$$

$$\begin{bmatrix} C_1 \\ C_2 \end{bmatrix} = C \qquad\qquad C_2 = 0$$

$$\begin{bmatrix} D_1 & D_2 \\ D_3 & D_4 \end{bmatrix} = D$$

The $C_2$ matrix is zero because there is no direct connection from internal buses to high side transformer buses or load buses.

### 3.3.2   System Bifurcation Test

It should be pointed out that for each $\lambda (t)$ value there are several solutions (equilibrium points) $(x_0^{\lambda(t)}, y_0^{\lambda(t)})$ of equations 3.1 and 3.2. Some of these equilibria are stable and others are not stable. It is assumed that the system is operating at a stable equilibrium at t=0 and that the bus voltages are near 1.0 p.u. and angle differences are less than $45^{\circ}$ in this solution. As $\lambda (t)$ slowly varies for t>0, the equilibrium point $(x_0^{\lambda(t)}, y_0^{\lambda(t)})$ changes until at some point

$$(\tilde{\lambda} = \lambda (t)) \in [\lambda_a, \lambda_b],$$

the jacobian matrix J becomes singular. The condition

$$det \left\{ J \left( x_0^{\tilde{\lambda}}, y_0^{\tilde{\lambda}}, \tilde{\lambda} \right) \right\} = 0$$

is a necessary condition for static bifurcation of the general power system model. Singularity of J does not imply a bifurcation (change in the number of solutions at $\left( x_0^{\tilde{\lambda}}, y_0^{\tilde{\lambda}}, \tilde{\lambda} \right)$ as $\lambda (t)$ passes through $\tilde{\lambda}$). If a system bifurcation occurs, it may not be a bifurcation that

causes voltage instability but could result in angle instability or some other type of bifurcation.

If the bifurcation occurs that results in voltage instability and it may result in one of at least three types of system voltage instability.

It should be noted that the development of a complete dynamical system analysis of the power system model developed in this thesis is not easy. The theory for describing bifurcation and singularities of constrained differential equation system models is not complete and the degree of complexity is too high to be handled by today's state of the art computer system. For example, it takes six nonlinear differential equations and four nonlinear algebraic equations to describe a generator and its terminal and high side transformer buses. A simplified two bus system with one generator bus and one terminal bus will be investigated in this thesis. It will be shown that we have to make crude assumptions to make this two bus system model valid and this model can only be used to investigate a limited number of causes of voltage instability.

### 3.3.3  Algebraic Bifurcation Test

Algebraic bifurcation is a change in the number of solutions in the algebraic equation

$$0 = g(x(t), y(t), \lambda(t)) \tag{3.7}$$

as a function of $y(x(t), \lambda(t))$ in a neighborhood around a point $(\tilde{x}, \tilde{\lambda})$. A necessary condition for algebraic bifurcation is that

$$\frac{\partial}{\partial y} g(\tilde{x}, \tilde{y}, \tilde{\lambda}) = D$$

is singular at $(\tilde{x}, \tilde{y}, \tilde{\lambda})$. The test condition for algebraic bifurcation is a test condition for loss of causality [27] of the transient stability model. Loss of causality indicates that the transient stability simulation packages that iteratively updated x using the differential

equations and update y using the algebraic equations may not obtain unique solutions and will generally terminate due to numerical failure as singularity of D is approached. Algebraic bifurcation does not guarantee that a system bifurcation will occur as will be discussed in more detail shortly. However, algebraic bifurcation indicates a point where the transient stability simulation will fail and where strange (chaotic) behavior may occur[21] under stressed operating conditions.

The algebraic bifurcation test is similar to the widely used load flow jacobian test. If

$$det\,(D|_{x_0,\,y_0,\,\lambda_0}) \;=\; 0$$

then algebraic bifurcation occurs. At the bifurcation point $(x_0, y_0, \lambda_0)$, two closely located load flow solutions merge into one and matrix D becomes singular at this bifurcation point. The singularity of matrix D indicates that there is lack of a solution to satisfy the supply and demand problem. It is usually caused by the weak boundaries of voltage control areas that reduce the ability to import reactive power, the shunt capacitive reactive supply withdrawal with voltage decline, and the lack of sufficient reactive supply in critical voltage control areas.

The difference between algebraic bifurcation test and load flow jacobian test is that the steady state solutions we use to determine the singularity of matrix D are different. In an algebraic bifurcation test, we use the solutions of

$$0 = f(x\,(t),y\,(t),\lambda\,(t)) \qquad\qquad (3.6)$$

$$0 = g\,(x\,(t),y\,(t),\lambda\,(t)) \qquad\qquad (3.7)$$

to test the singularity of matrix D. In widely used load flow jacobian test, the solution of

$$0 = \bar{g}\,(x_0,\,(y_0,y_1\,(t)),\lambda\,(t)) \qquad\qquad (3.8)$$

is used, where $\bar{g}$ includes the real power balance equations at terminal high side trans-

former, and load buses; retains reactive power balance equations at high side transformer and load buses, but eliminates reactive power balance equation at generator terminal buses that are included in $g$. The $y(t)$ vector is thus divided into a vector $y_1(t)$ of the angle at all buses and the voltage at all high side transformer and load buses. $y_0$ represents the generator voltage setpoint at terminal buses. The test for load flow bifurcation is then based on the singularity or nonsingularity of

$$\frac{\partial \bar{g}}{\partial y_1}$$

We have shown that the solutions of (3.6) and (3.7) and the solutions of (3.8) tend to diverge at heavy load condition but before the field current limits are hit. The results of the algebraic bifurcation test and the load flow jacobian test will also diverge as we move the system close to load flow voltage instability. Note that if algebraic bifurcation test shows that the matrix D is singular, the system jacobian matrix J will not be singular unless $D - CA^{-1}B$ is singular as will be discussed in the next subsection.

If the singularity of matrix D is caused by the linear dependency of two or more rows in matrix $\begin{bmatrix} D_3 & D_4 \end{bmatrix}$ in equation (3.5.1), this implies that there are linearly dependent rows in the system jacobian matrix J because the submatrix $C_2$ is a zero matrix. Linearly dependent rows of $\begin{bmatrix} D_3 & D_4 \end{bmatrix}$ thus implies the system jacobian matrix J becomes a singular matrix and that a system bifurcation may occur. This indicates that the linear dependency of the rows of the real and reactive power jacobian associated with high side transformer and load buses is one of the ways to cause system bifurcation. It shows that the methods which use the algebraic bifurcation test to investigate voltage instability problems are valid if the voltage instability is caused by linearly dependent rows of $\begin{bmatrix} D_3 & D_4 \end{bmatrix}$ associated with high side transformer buses or load buses.

The matrix $\begin{bmatrix} D_1 & D_2 \end{bmatrix}$ has the form

$$D_1 = \begin{bmatrix} \dfrac{\partial P_T}{\partial \theta_T} & \dfrac{\partial P_T}{\partial V_T} \\[2mm] \dfrac{\partial Q_T}{\partial \theta_T} & \dfrac{\partial Q_T}{\partial V_T} \end{bmatrix} = \begin{bmatrix} D_{n,n}^{13} & D_{n,n}^{14} \\[1mm] D_{n,n}^{23} & D_{n,n}^{24} \end{bmatrix}$$

$$D_2 = \begin{bmatrix} \dfrac{\partial P_T}{\partial \theta_H} & 0 & \dfrac{\partial P_T}{\partial V_H} & 0 \\[2mm] \dfrac{\partial Q_T}{\partial \theta_H} & 0 & \dfrac{\partial Q_T}{\partial V_H} & 0 \end{bmatrix} = \begin{bmatrix} D_{n,n}^{15} & 0_{n,m} & D_{n,n}^{16} & 0_{n,m} \\[1mm] D_{n,n}^{25} & 0_{n,m} & D_{n,n}^{26} & 0_{n,m} \end{bmatrix}$$

where $\dfrac{\partial P_T}{\partial \theta_T}, \dfrac{\partial P_T}{\partial V_T}, \dfrac{\partial Q_T}{\partial \theta_T}, \dfrac{\partial Q_T}{\partial V_T}, \dfrac{\partial P_T}{\partial \theta_H}, \dfrac{\partial P_T}{\partial V_H}, \dfrac{\partial Q_T}{\partial \theta_H}$, and $\dfrac{\partial Q_T}{\partial V_H}$ are diagonal matrices represented

by the notation $D_{n,n}^{ij}$.

Rows of $\begin{bmatrix} D_1 & D_2 \end{bmatrix}$ can not be dependent unless the ith row of $\begin{bmatrix} D_1 & D_2 \end{bmatrix}$ is linearly dependent with the i+nth row. If $\begin{bmatrix} D_1 & D_2 \end{bmatrix}$ has linearly dependent rows or if one or more rows of $\begin{bmatrix} D_1 & D_2 \end{bmatrix}$ are linearly dependent with one or more rows of $\begin{bmatrix} D_3 & D_4 \end{bmatrix}$, then an algebraic bifurcation (loss of causality) may exist that will not necessarily cause system bifurcation which requires J to be singular. An algebraic bifurcation (loss of causality) that does not cause a static system bifurcation can result in chaos [21] and possibly other unacceptable behavior which may or may not be associated with voltage collapse. A loss of causality that does not cause system bifurcation is studied for a two bus example system in the next chapter. A general investigation of loss of causality (algebraic bifurcation) and it's impacts on the behavior of the system behavior is beyond the scope of this thesis.

### 3.3.4 Algebraic/Dynamic System Bifurcation Test

If matrix A is nonsingular, the system jacobian J is nonsingular(singular) if and only if

$$M_1 = D - CA^{-1}B$$

is nonsingular(singular)[24].

Since it is shown that matrix A is always nonsingular in Appendix B.3, the algebraic/dynamic system bifurcation test is always valid for testing the singularity of the system jacobian matrix J. We have indicated that the (loss of causality) algebraic bifurcation test on D can be used to test the singularity of the system jacobian matrix if $\begin{bmatrix} D_3 & D_4 \end{bmatrix}$ have linearly dependent rows of D. If these linearly dependent rows of D belong to $\begin{bmatrix} D_1 & D_2 \end{bmatrix}$ or both $\begin{bmatrix} D_1 & D_2 \end{bmatrix}$ and $\begin{bmatrix} D_3 & D_4 \end{bmatrix}$, there is a loss of causality (possibly chaotic behavior) but no steady state system bifurcation. Likewise, there are system bifurcations of the algebraic equations (and obviously also the set of differential and algebraic equations) that can't be detected by the algebraic bifurcation test. Two such cases are

(a)   linearly dependent rows in matrix $\begin{bmatrix} C_1 & D_1 & D_2 \end{bmatrix}$, or

(b)   linearly dependent rows in matrix $\begin{bmatrix} D_3 & D_4 \end{bmatrix}$ and $\begin{bmatrix} C_1 & D_1 & D_2 \end{bmatrix}$.

A method that will identify the linearly dependent rows in the matrix $\begin{bmatrix} C_1 & D_1 & D_2 \end{bmatrix}$ is presented here. The matrix $\begin{bmatrix} C_1 & D_1 & D_2 \end{bmatrix}$ can be represented by

$$\begin{bmatrix} C_1 & D_1 & D_2 \end{bmatrix} = \begin{bmatrix} 0_{n,n} & D^{11}_{n,n} & D^{12}_{n,n} & 0_{n,4n} & D^{13}_{n,n} & D^{14}_{n,n} & D^{15}_{n,n} & 0_{n,m} & D^{16}_{n,n} & 0_{n,m} \\ 0_{n,n} & D^{21}_{n,n} & D^{22}_{n,n} & 0_{n,4n} & D^{23}_{n,n} & D^{24}_{n,n} & D^{25}_{n,n} & 0_{n,m} & D^{26}_{n,n} & 0_{n,m} \end{bmatrix} = \begin{bmatrix} K_1 \\ K_2 \end{bmatrix}$$

where $D^{11}_{n,n} = \dfrac{\partial P_T}{\partial \delta}$, $D^{12}_{n,n} = \dfrac{\partial P_T}{\partial E'_q}$, $D^{21}_{n,n} = \dfrac{\partial Q_T}{\partial \delta}$, and $D^{22}_{n,n} = \dfrac{\partial Q_T}{\partial E'_q}$ and the other diagonal matrices that belong to $D_1$ and $D_2$ have been previously defined in section 3.3.4. There are n generator buses and m high side transformer buses and load buses in this example. If

there are linearly dependent rows in the matrix $\begin{bmatrix} C_1 & D_1 & D_2 \end{bmatrix}$, it has to be one row in the matrix $K_1$ and another row in the matrix $K_2$. It is only possible that the ith row of $K_1$ is linearly dependent on the ith row of $K_2$. The ith row in the matrix $K_1$ can never be linearly dependent on the jth row of the matrix $K_2$ if i is not equal to j. The algorithm for identifying the linearly dependent row in the matrix $\begin{bmatrix} C_1 & D_1 & D_2 \end{bmatrix}$ is given in Figure 3.1. The computation effort is less than or equal to

6n (scalar division) + 7n (scalar comparison) + n (scalar addition)

where n is the number of generator buses.

### 3.3.5   Dynamic/Algebraic System Bifurcation Test

If matrix D is nonsingular, the system jacobian matrix J is nonsingular(singular) if and only if

$$M_2 = A - BD^{-1}C$$

is nonsingular(singular).

If D is nonsingular, both $M_1$ and $M_2$ can be used to test for system bifurcation (singularity of J). Both $M_1$ and $M_2$ can be used to test for singularity of J when D and A are nonsingular because the singularity of J depends on the row dependence of rows of $\begin{bmatrix} C & D \end{bmatrix}$ and $\begin{bmatrix} A & B \end{bmatrix}$ rather that row dependence in $\begin{bmatrix} A & B \end{bmatrix}$ or $\begin{bmatrix} C & D \end{bmatrix}$ alone. $M_2$ represents the system matrix of the nonlinear constrained differential equation modeled linearized at an equilibrium point $x_0$, $y_0$, $\lambda_0$ and thus defines the eigenvalues of the equivalent unconstrained dynamical system. If the real parts of the eigenvalues of $M_2$ are all negative, the equivalent unconstrained dynamical system is locally stable in the neighborhood of the equilibrium point. A dynamic/algebraic system bifurcation test can be used to test the stability of the dynamic states if the matrix D is nonsingular. If there are complex eigenvalues with zero
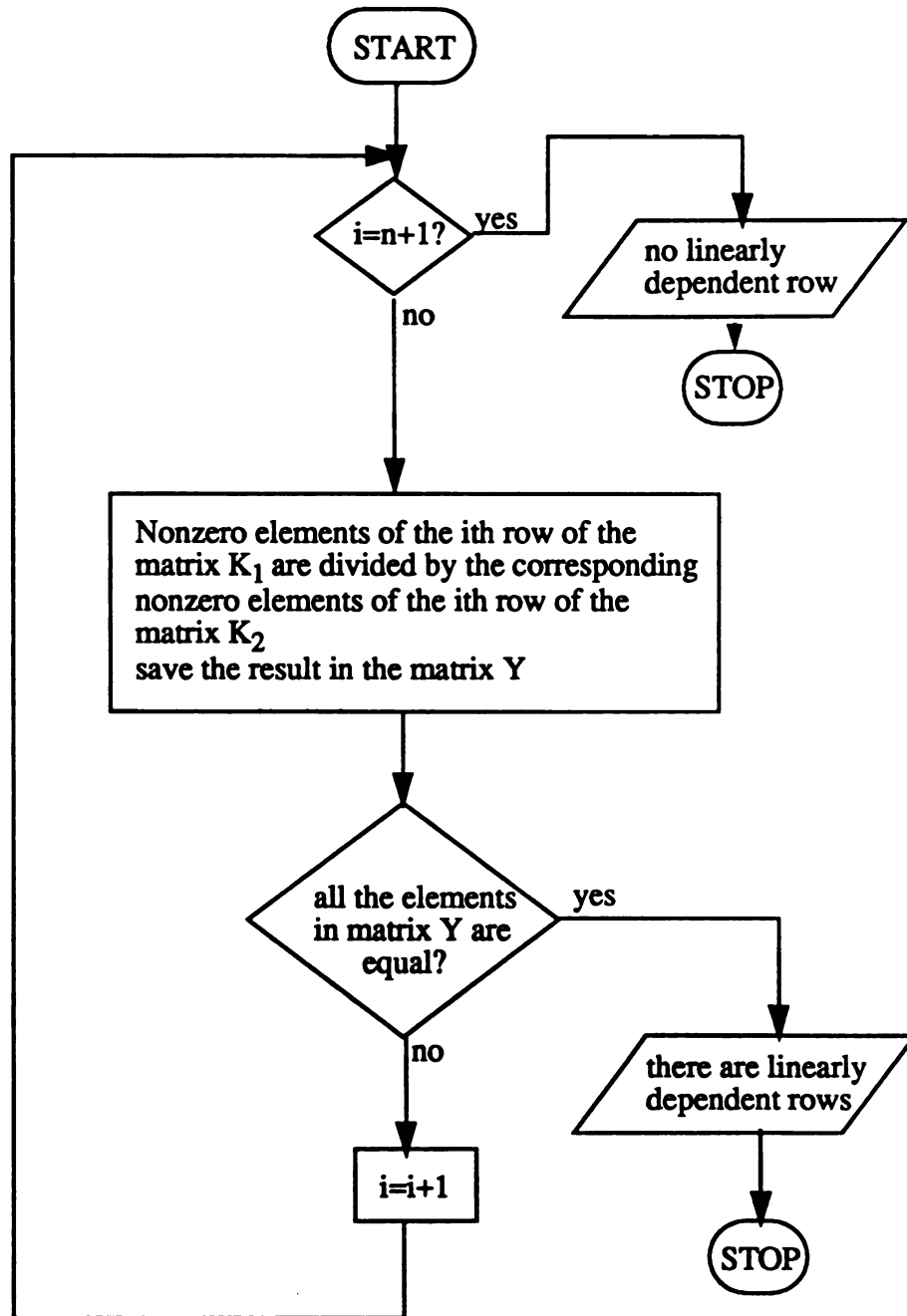
Figure 3.1 Algorithm for identifying the linearly dependent rows

in the matrix $\begin{bmatrix} C_1 & D_1 & D_2 \end{bmatrix}$

real parts, the system may experience Hopf bifurcation and yet J and $M_2$ will be nonsingular. Thus, singularity of J and $M_2$ will not indicate all possible bifurcations but only static bifurcations. A fundamental assumption, which is confirmed by our computational results, is that voltage collapse bifurcations are static bifurcation that can be tested for by singularity of J, $M_2$, or $M_1$. Examples of singularities, that are not detected by singularity of J, $M_1$, and $M_2$ and are not necessarily associated with voltage collapse, are

(a)  Hopf bifurcations which occur when eigenvalues of $M_2$ are complex with zero real parts and

(b)  algebraic bifurcation (loss of causality)

$$det(D) = det\left(\begin{bmatrix} D_1 & D_2 \\ D_3 & D_4 \end{bmatrix}\right) = 0$$

where rows of $\begin{bmatrix} D_1 & D_2 \end{bmatrix}$ are dependent on rows of $\begin{bmatrix} D_3 & D_4 \end{bmatrix}$. (Note that row dependence in $\begin{bmatrix} D_3 & D_4 \end{bmatrix}$ are detected in J and $M_1$ and is associated with load flow bifurcation which are reactive demand/supply related voltage collapse bifurcations) It should be noted that despite the above theoretical results and the computational results in the next chapter that confirms this theory, there is no doubt that our understanding of bifurcations of this system is not complete.

This $M_2$ test for system static bifurcation is a test for bifurcation of a type that are not related to algebraic bifurcation or the bifurcations that occur in equation (3.8) are related to load flow bifurcation. The singularity of $M_2$ as $\lambda(t)$ varies indicates that J is singular and that a bifurcation may have occurred in the dynamical system where the algebraic constraints have been eliminated. Whether a bifurcation occurs or not and whether the bifurcation is related to voltage instability or not, the system will become unstable if the real part of the eigenvalue that became zero becomes positive as $\lambda(t)$ continues to vary. This instability could be related to voltage collapse even if no bifurcation occurs when $M_2$ and

J were singular. Zaborsky[21] discusses this type of dynamic/algebraic bifurcation on a two bus system and provides some preliminary results on it's dynamical system behaviors.

### 3.3.6 Flux Decay Bifurcation Test

In flux decay system bifurcation test, we assume that there is no angle instability.

$$\dot{x}_1(t) = f_1(x_1(t), x_2(t), y(t), \lambda(t))$$

$$\dot{x}_2(t) = f_2(x_1(t), x_2(t), y(t), \lambda(t))$$

$$0 = g(x_1(t), x_2(t), y(t), \lambda(t))$$

x(t) in equation (3.1) is divided into $x_1$(t) and $x_2$(t). $x_1$(t) represents the flux decay states of the generator. $x_2$(t) represents the states of mechanical and exciter dynamics.

The jacobian of the above equations is

$$J = \begin{bmatrix} \dfrac{\partial f_1}{\partial x_1} & \dfrac{\partial f_1}{\partial x_2} & \dfrac{\partial f_1}{\partial y} \\ \dfrac{\partial f_2}{\partial x_1} & \dfrac{\partial f_2}{\partial x_2} & \dfrac{\partial f_2}{\partial y} \\ \dfrac{\partial g}{\partial x_1} & \dfrac{\partial g}{\partial x_2} & \dfrac{\partial g}{\partial y} \end{bmatrix} = \begin{bmatrix} T_1 & T_2 \\ T_3 & T_4 \end{bmatrix}$$

where

$$T_1 = \begin{bmatrix} \dfrac{\partial f_1}{\partial x_1} \end{bmatrix}$$

$$T_2 = \begin{bmatrix} \dfrac{\partial f_1}{\partial x_2} & \dfrac{\partial f_1}{\partial y} \end{bmatrix}$$

$$T_3 = \begin{bmatrix} \dfrac{\partial f_2}{\partial x_1} \\[2ex] \dfrac{\partial g}{\partial x_1} \end{bmatrix}$$

$$T_4 = \begin{bmatrix} \dfrac{\partial f_2}{\partial x_2} & \dfrac{\partial f_2}{\partial y} \\[2ex] \dfrac{\partial g}{\partial x_2} & \dfrac{\partial g}{\partial y} \end{bmatrix}$$

If there are linearly dependent rows where one or more occur in $\begin{bmatrix} T_1 & T_2 \end{bmatrix}$ and the remaining rows occur in $\begin{bmatrix} T_3 & T_4 \end{bmatrix}$, the dynamic/algebraic test of this new jacobian will be singular if J is singular and $\begin{bmatrix} T_1 & T_2 \end{bmatrix}$ is linearly independent and $\begin{bmatrix} T_3 & T_4 \end{bmatrix}$ is linearly independent. Singularity or existence of positive eigenvalues of

$$M_3 = T_1 - T_2 T_3^{-1} T_4 = T$$

indicates that the voltage instability may be related to dynamic voltage instability associated with flux decay dynamics. Matrix T represents the matrix associated with flux decay dynamics when the excitation system dynamics, generator mechanical dynamics, and algebraic equations have been eliminated at the equilibrium point. Matrix T is used as a test for the flux decay dynamics in a manner similar to the AESOPS algorithms tests for the stability of mechanical system eigenvalue. The results indicate $M_3$ does not change significantly as the excitation system of every generator remains in control of terminal bus voltage. However, if the field current limit is hit on one generator, then $M_3$ varies significantly.

Note that singularity of $M_2$ may not be an appropriate test for dynamic instability of the flux decay dynamics when D is singular. However $M_3$ may be a valid test for flux decay bifurcation when D is singular since D is a submatrix of $T_3$ which mat be nonsingular when D is singular. The flux decay bifurcation test can point out how the air gap saturation, line drop compensation, field current limit, sensitivity matrices, and reactive generation will influence the stability of flux decay dynamics.

Computational results in the next chapter indicate that when a generator has not hit field current limit the eigenvalues associated with both the mechanical dynamics or the generator flux decay dynamics and the exciter dynamics are generally complex. Although real parts of these eigenvalues will be shown to approach zero and possibly result in Hopf bifurcation that can cause field current limit violation as reactive load network and network stress, it does not appear that it will cause voltage instability. The disablement of the excitation system and the reduction of the field current to continuous rating levels caused by the oscillation generally seems to extinguish the Hopf bifurcation. The resultant system after the excitation system is disabled has real eigenvalues rather than complex eigenvalues in the examples discussed in the next chapter. If the real eigenvalues associated with the generator flux decay dynamics are negative the system is stable and J remains nonsingular. If the eigenvalues associated with the flux decay dynamics are positive, the system experiences a dynamic voltage collapse where the induced flux, field current, and reactive power out of the generator approach zero forcing the voltage collapse in the system. When the eigenvalues associated with this flux decay dynamics become positive, the determinant of J changes sign. A specific flux decay bifurcation test is desired which would indicate when the eigenvalues associated with the flux decay dynamics become real rather than being complex and indicate whether the eigenvalue is positive or negative.

It should be noted that it is possible to effectively disable the excitation system if the field current is above continuous rating and the air gap saturation has reduced the excitation loop gain to small values. In this case, the flux decay eigenvalue will be shown to approach the right half plane if $S_{Q_L V}^{-1}$ and $S_{VE}$ have negative elements. In this case, the algebraic voltage collapse test was violated indicating a reactive demand supply problem has occurred that could have brought on dynamic collapse where generator field current flux are unstable and approach zero.

An analysis of flux decay bifurcation in undertaken. To perform this analysis, it will be

necessary to assume that steady state angle instability has not occurred so that the required sensitivity matrices are well defined. Since voltage collapse is assumed to be a static bifurcation, the derivatives $\dot{\delta}$ and $\dot{\omega}$ can be set to zero and the swing equations are deleted and replaced by an algebraic real power balance equation of the generator. The reactive power balance equation of the generator internal bus is also added because it will be used for sensitivity matrix analysis in this section.

$$P^e = f_1 (\delta, \theta, E, V)$$

$$Q^e = f_2 (\delta, \theta, E, V)$$

The sensitivity matrix model has the form (Appendix II)

$$\Delta Q^e = S_{Q_G E} \Delta E + S_{Q_G Q_L} \Delta Q_L \tag{3.9}$$

$$\Delta V = S^{-1}_{Q_L V} \Delta Q_L + S_{VE} \Delta E \tag{3.10}$$

We also set the derivative of exciter states belonging to $x_2$ in the general power system model to be zero and we obtain another set of algebraic equations. We can solve for the field voltage in terms of the terminal bus voltage.

$$E_{fd} = diag \left( \frac{-K_{Ai} K_{Ri}}{S_{Ei} (E_{fdi}) + K_{Ei}} \right) V_T$$

$$\Delta E_{fd} = diag \left( \frac{-K_{Ai} K_{Ri}}{S_{Ei} (E_{fd0i}) + K_{Ei} + \dot{S}_{Ei} (E_{fd0i}) E_{fd0i}} \right) \Delta V_T \tag{3.11}$$

where $E_{fd}$ is the vector of generator field voltage and $V_T$ is the vector of terminal bus voltage.

The only linearized dynamic equations left are for flux decay equations

$$\Delta \dot{E'}_q = \frac{1}{\tau_{do}} \left( \Delta E_{fd} - \Delta E'_q + \frac{Q_0^e (x_d - x'_d)}{E'^2_{qi0}} \Delta E'_q - \frac{(x_d - x'_d) \Delta Q^e}{E'^2_{qi0}} \right) \tag{3.12}$$

Substituting (3.9), (3.10), and (3.11) into (3.12) we obtain

$$\Delta \dot{E}'_q = \left( diag\left(\frac{1}{\tau'_{d0i}}\right)\right)\left(diag\left(-1 + \frac{Q^e_{i0}(x_{di} - x'_{di})}{E'^2_{qi0}}\right)\right.$$

$$+ diag\left(\frac{-K_{Ai}K_{Ri}V_{i0}}{S_{Ei} + K_{Ei} + \dot{S}_{Ei}E_{fdi0}}\right)WS_{VE}$$

$$\left.- diag\left(\frac{x_{di} - x'_{di}}{E'^2_{qi0}}\right)S_{Q_GE}\right)\Delta E'_q + \eta\Delta Q_L\right) = T\Delta E + \eta'\Delta Q_L \qquad (3.13)$$

where $\underline{W}$ selects the terminal bus voltage vector out of the vector $\underline{V}$ that includes voltage at terminal, high side transformer, and load buses.

Matrix $T$ is a diagonally dominant matrix and all the eigenvalues of matrix $T$ has negative real parts in the normal operating condition. As the system becomes stressed, the reactive power generation $Q^e_{i0}$ of generators start to increase in a speed faster than $E'^2_{qi0}$. This will reduce the negative diagonal dominance of matrix $T$ and move $T$ toward singularity. When the generator experiences excitation system saturation, the term

$$S_{Ei}(E_{fdi0}) + K_{Ei} + \dot{S}_{Ei}(E_{fdi0})E_{fdi0}$$

may increase and force the diagonal elements of matrix $T$ to become less negative. If there is a terminal bus voltage deviation such that $S_{VE}$ elements and row sums increase, the diagonal dominance of matrix $T$ is even further reduced. The loss of diagonal dominance of T indicates the matrix is approaching singularity since T is a diagonally dominant M matrix. The sensitivity matrix $S_{Q_GE}$ has the property that the negative off diagonal elements become more negative and the positive diagonal elements become less positive as the system is stressed. This would also contribute to the loss of diagonal dominance and singularity of matrix $T$. The air gap saturation will help to move the field current to its up-

per limit. Air gap saturation can significantly reduce $x'_{ds}$ and $x_{ds}$. Thus, both the diagonal and off diagonal elements of the third term of equation 3.13 associated with $\alpha$ diagonally dominant matrix $S_{Q_GE}$ will move toward zero which has the effect of moving the eigenvalues associated with equation 3.13 toward the right half plane.

If the field current limit is hit, the excitation system is disabled and the second term

$$\frac{-K_{Ai}K_{Ri}V_{i0}}{S_{Ei}(E_{fdi0}) + K_{Ei} + \dot{S}_{Ei}((E_{fdi0})E_{fdi0})}$$

becomes zero. This means that a large negative diagonal element of matrix $T$ will be removed. The eigenvalues of matrix $T$ will be moved to a point where either it is very close to the origin or even becomes positive. When the excitation system is disabled, the field current is reduced to continuous rating which reduces air gap saturation. The reduction of field current and air gap saturation has the effect of causing the eigenvalues associated with the third term in equation 3.13 to be more negative.

PQ controllability requires $S_{VE}$ to be nonnegative. Strong PQ controllability requires row sums of $S_{VE}$ to be near 1. PV controllability requires that $S_{Q_GE}$ have positive diagonal elements, be an M matrix, and be $\alpha$ diagonally dominant. Loss of PQ controllability occurs when elements of row sums of $S_{VE}$ approach infinite and then instantly go negative. Note that if elements of $S_{VE}$ are negative, it is virtually certain that the eigenvalue of matrix $T$ will be positive since the diagonal matrix

$$diag\left(\frac{-K_{Ai}K_{Ri}V_{i0}}{S_{Ei}(E_{fdi0}) + K_{Ei} + \dot{S}_{Ei}((E_{fdi0})E_{fdi0})}\right) \tag{3.14}$$

is so large. Loss of PV controllability results in loss of the M matrix and $\alpha$ diagonal dominance property of $S_{Q_GE}$. When the exciter is disabled due to field current limitation and the second term in equation 3.13 is missing, the loss of PV controllability can cause the eigenvalues of T to become positive, since the term

$$diag\left(\frac{1}{\tau_{d0i}}\right)diag\left(\frac{x_{di}-x'_{di}}{E_{qi}^2}\right)S_{Q_GE}$$

is not small compared to the first term. If $S_{Q_GE}$ is $\alpha$ diagonally dominant, the above term has positive eigenvalues, but if $S_{Q_GE}$ is no longer $\alpha$ diagonally dominant or loses its M matrix property, then the eigenvalues of the term will be negative and the eigenvalues of T can become positive.

Loss of PV controllability can also contribute to eigenvalues of $T$ becoming positive when the excitation system is not disabled due to field current limitation, but its effect should be small compared to loss of PQ controllability.

This simplified power system model shows clearly how a dynamic voltage instability would happen and indicates the contribution of each element to voltage instability.

## 3.4   Relationship to Literature

There is a large amount of literature on the voltage stability problem. Most of this literature deals with the existence of load flow solutions in the steady state or static condition of the power system. Research efforts have resulted in several different methodologies for the coordination and utilization of the reactive power and voltage control resources of the system.

It has been known that there will be two static load flow solutions which eventually merge into one in a two bus system when a bus with an increasing real or reactive power load is fed through a transmission line from a fixed magnitude voltage source. With increasing load beyond the critical load value, there exists no load flow solution. In mathematical terms, this is a static or saddle node bifurcation. A similar event occurs on a large power system if real or reactive load ($\lambda_i(t)$) is increased at a critical bus. Before $\lambda_i(t)$ is increased, there are many solutions under normal operating conditions. One or more of the

numerous load flow solutions will converge together and merge into one and the jacobian matrix becomes singular, which indicates a bifurcation and voltage collapse if the bifurcation is associated with voltage collapse. Many research efforts of voltage stability are devoted to this static bifurcation event.

Tamura [12,13] has confirmed that closely related multiple load flow solutions that merge are likely to appear under heavy load conditions. He showed that a pair of load flow solutions located close to each other is related to voltage instability. A voltage instability proximity index which measures the closeness of a pair of load flow solutions and proximity of the jacobian matrix to singularity are developed in his research. A method for computing these multiple load flow solutions are provided in his recent research.

Much of the voltage collapse literature [28,29,8,12,13] uses a conventional load flow model to analyze voltage instability. Generator dynamics are not included in their research. This kind of voltage stability problem has been classified as a demand/supply problem. In this thesis, we use algebraic bifurcation test to investigate the supply demand problems of the power system. The difference between an algebraic bifurcation test and the widely used load flow jacobian test is that in an algebraic bifurcation test we use the equilibrium point from a general power system model which includes the mechanical dynamics, flux decay dynamics, and excitation system dynamics and the test for voltage collapse is a test for row dependence of

$$D = \begin{bmatrix} D_1 & D_2 \\ D_3 & D_4 \end{bmatrix}.$$

Load flow bifurcation utilizes the equilibrium point of just the real power balance equation at terminal, high side transformer, and load buses and the reactive power balance equations at high side transformer and load buses. The load flow bifurcation test of the singularity of $\begin{bmatrix} D_3 & D_4 \end{bmatrix}$ are based on the load flow equilibrium points. It has been shown in this thesis that the conventional load flow model is not suitable for voltage instability

analysis under heavy load conditions and that generator dynamics are strongly related to the voltage stability.

Venikov [7] recognized the significance of a degeneracy in the real power angle jacobian matrix with respect to the steady state stability of a transient power system stability model. He observed that in load flow calculations performed by Newton's method one can estimate the steady state stability of the operating condition in question. Under certain conditions, a change in the sign of the determinant of the jacobian matrix during a continuous variation of parameters coincides with the movement of the operating condition from a voltage stable to a voltage unstable condition.

Kwatny[27] attempted to relate static voltage instability and voltage collapse to bifurcation phenomena. Only generator mechanical dynamics and real and reactive power balance load flow equations were included in this model. It was shown that static bifurcations of the load flow equations were associated with either divergence type instability or loss of causality. The bifurcation tests were shown to be tests for steady state angle stability or voltage collapse in a load flow model.

Schlueter[1,2,3,4] pointed out that the dynamics of flux decay and excitation system has tremendous impact on the voltage instability of a power system. These generator dynamics are included in his model for theoretical analysis. He also identified the component of $\lambda$ which is the operating parameters which may drive the power system to bifurcation. $\lambda$ may be used to represent changes in real or reactive power load, real or reactive power transfer, changes in real power generation on generators due to inertial, governor, automatic generation control, or economic dispatch response to loss of generation contingencies, or actions of under load tap changers or switchable shunt capacitors in the distribution system. A definition of PQ controllability is hypothesized on the proper response of voltage at load buses and voltage set point changes at generator buses. The PQ controllability definition results in an array of tests for voltage collapse that

encompass all the tests that developed for voltage collapse. The PQ controllability tests on sensitivity matrix $S_{Q_LV}$ and $S_{VE}$ assure that the load flow and transient mid term stability model will not experience bifurcation.

Sauer and Pai[19] presented the relationship between a detailed power system dynamic model and a standard load flow model. The field current limit controller and line drop compensator were not included in their model and the flux decay and excitation system dynamics were ignored in the analysis.The linearized dynamic model is examined to show how the load flow jacobian appears in the system dynamic state jacobian for evaluating steady state stability in two special cases where the load flow jacobian is the jacobian of the constrained differential equation model. The singularity of the load flow jacobian was shown to imply singularity of the system dynamic state jacobian for a special case where reactance and resistances of the generator model are ignored, exciter dynamics and flux decay dynamics are ignored and field current limits and line drop compensation are ignored. If all of these factors are taken into account, this thesis shows that the tests for system bifurcation are very different from those for load flow bifurcation. The differences between load flow and system bifurcation not only occur due to these model differences and their resulting differences in equilibrium points but also because eliminating the modeling differences eliminates the property of dynamic/algebraic bifurcation that can't occur in a load flow or in Pai and Sauer's simplified dynamic model [19].

There are papers which discuss the stability of the voltage controllers, such as under load tap changer and switchable shunt capacitors in the distribution system. Abe[14], Liu and Wu[22], and Illic[16,17] have developed test conditions for stability of the control of under load tap changers that are similar to the test conditions developed in this thesis for flux decay bifurcation tests of the general power system model.

There are papers which apply sensitivity analysis to determine voltage instability. The sensitivity analysis develops the relations of the changes of states and inputs. Borremans

[28] suggested two conditions

$$S_{Q_G Q_L} > 0 \qquad \text{and} \qquad S_{Q_L V}^{-1} > 0$$

for voltage stability. $S_{Q_G Q_L} > 0$ is the requirement that the generator correctly responds to a reactive load increase and $S_{Q_L V}^{-1} > 0$ is the requirement that an increase in reactive demand will cause a decrease in voltages. Carpentier[8] also derived a voltage stability indicator and pointed out that

$$0 \le S_{Q_G Q_L \, ij} < K \qquad \text{and} \qquad \text{column sum } S_{Q_G Q_L} \approx 1$$

This is a stronger condition than Borremans', and can be used as an indicator to determine an overloaded system. Glavitsch[29] provided another sensitivity test, $S_{VE}$, to investigate the relationship of load bus voltage and generator bus voltage. Schlueter[3] has shown that all the sensitivity tests are a subset of the tests that can be derived based on assuming PQ and PV controllability hold.

The sensitivity matrices used in the flux decay bifurcation tests in this thesis have the same definition as Schlueter [3] using a load flow model but use the constrained dynamical model equilibrium rather than a load flow equilibrium to evaluate the sensitivity matrices.

# CHAPTER 4

# SIMULATION RESULTS ON VOLTAGE INSTABILITY OF

# POWER SYSTEM MODELS

A two bus and a twelve bus power system models are simulated in this chapter. The simplicity of the two bus system model allows us to investigate the voltage instability problems by using a two dimensional phase portrait. The simulation results of a two bus system model confirm the validity of our voltage instability tests. Since the air gap saturation, field current limit, line drop compensation, exciter system control, and the distribution system are eliminated in the two bus system model, the voltage instability caused by those factors can not be seen in a two bus system model.

The twelve bus system model includes the air gap saturation, field current limit, line drop compensation, exciter system control, and the network. Because of the complexity of the twelve bus system, it is impossible to investigate the system voltage instability by using a phase portrait. The voltage instability tests are applied to determine the system voltage stability and the causes of voltage instability. A Q-V curve for bus LOAD2 is also provided for each simulation case to monitor the effects of the change of the network operating condition to the system voltage instability. All the data shown in this chapter are in per unit base.

It will be shown in section 4.1 that the only system bifurcation which can occur in a two

bus system where exciters are disabled is when the high and low voltage solutions merge together. The eigenvalue of the flux decay dynamics are negative real values which approach zero as the solutions merge. It indicates that the merging point is a bifurcation point. A simple exciter control is included and the effects of this exciter control on the trajectory of the system is discussed. An algebraic bifurcation due to linearly dependence in $\begin{bmatrix} D_1 & D_2 \end{bmatrix}$ can occur which does not cause system bifurcation. This singularity is associated with possible chaotic behavior. The two bus system model is shown to have a stable low voltage solution at small reactive load levels and an unstable low voltage solution at higher reactive load levels. The boundary where the low voltage solution is no longer stable is where the chaotic behavior can occur.

In section 4.2, algebraic bifurcation and load flow bifurcation of a 12 bus model are studied. Two cases are studied. In the first case, line reactances of the two lines that connect a load bus to the rest of the system are increased. This bus is a voltage control area. The weakening of the boundary of the voltage control area is theoretically sufficient to cause a voltage collapse bifurcation. The collapse must occur because a theoretical upper bound on the small eigenvalue associated with a voltage control area is the maximum of the sum of the magnitude of boundary jacobian elements connected to a bus. Since there is only one bus and the boundary jacobian elements approach zero, the upper bound on the small eigenvalue associated with the voltage control area approaches zero. Since an eigenvalue approaches zero, the necessary conditions for a bifurcation must occur. The computational results confirm that collapse occurs but also indicates that the algebraic bifurcation is due to a reactive demand supply problem associated with shipping reactive power into this voltage control area. The shunt capacitive reactive supply at the bus is shown to be reduced due to the large bus voltage drop needed to ship the reactive and real power to the bus over the weakened voltage control area boundary. The branches in the voltage control area boundary are shown to experience geometrically increased reactive losses as the line reactances of the voltage control area boundary increases. The ability of the boundary

branches to ship reactive power declines as the branches become drains and suck reactive power from both buses they are connected to. Thus, the reactive demand supply problem develop at a bus despite the fact that there is ample reactive generation reserves on all of the generators in the system.

The second case confirms that an algebraic bifurcation at a load bus will cause a system bifurcation in the general power system model. The results also indicate that as algebraic bifurcation is approached, the transient stability program will not converge to a solution. This is similar to a Newton Raphson load flow where voltage collapse occurs when an eigenvalue of the load flow jacobian is zero but may not converge when an eigenvalue of the jacobian is less than one. Since the EPRI Transient Mid Term Stability Program utilizes a Newton Raphson algorithm to solve the algebraic equations, the program puts out a diagnostic that a solution can not be found before voltage collapse bifurcation occurs.

The second case shows theoretically and computationally that the bifurcation test results are confirmed by a Q-V curve. Q-V curves are widely used in the utility industry to assess proximity to voltage collapse. The Q-V curve is a stress test where reactive load is added at a bus until the system can no longer supply that load. It has been shown that Q-V curve is lower bound on the small eigenvalue of the reactive power voltage jacobian matrix for the reactive deficient voltage control area where bus at which the Q-V curve is calculated resides. The reactive power voltage jacobian $S_{Q_L V}$ is a submatrix of D and singularity of this submatrix does not necessarily indicate singularity of J. However, singularity of $S_{Q_L V}$ has been shown to be associated with violation of virtually every known test for voltage collapse. Since the Q-V curve is a lower bound on the small eigenvalue of $S_{Q_L V}$ associated with a voltage control area, it is theoretically related to load flow bifurcation, transient mid term stability model bifurcation tests, load flow sensitivity voltage collapse tests, and linearized dynamic voltage collapse test. The Q-V curve never reaches the knee at which voltage collapse bifurcation should occur on the Q-V curve. These results indicate the sys-

tem under study comes close but never achieves a voltage collapse bifurcation as reactive load is increased at the bus which is an isolated voltage control area from the first case. This confirms the results of the algebraic bifurcation and system bifurcation tests where the system bifurcation test matrix and algebraic bifurcation test matrix approach singularity but are never singular for increasing reactive load at this same bus.

The test results indicate that the 12 bus test system is not vulnerable to algebraic bifurcation and reactive demand and supply problem. The system was modified to make it far more susceptible to reactive demand supply problem by increasing series reactances and shunt susceptances of lines. However, the EPRI Transient Mid Term Stability Program would not converge to an equilibrium when the 12 bus system model was modified to make it more susceptible to reactive demand supply voltage collapse problems. The Newton Raphson algorithm in the Transient Mid Term Stability Program attempts to solve the real and reactive power balance equations together with the differential equations. Since the transient stability model has no generator terminal PV buses, as the load flow model has, the Newton Raphson algorithm in the transient stability program does not converge but the load flow Newton Raphson program converges. A program for solving for the equilibrium of the general stability model is needed if proximity to voltage collapse is to be accurately assessed.

Dynamic/algebraic bifurcation problems are analyzed in Section 4.3 and 4.4. In Section 4.3, a generator and its terminal bus are isolated from the rest of the system by increasing the transformer reactance that connects the generator to the rest of the twelve bus system. The purpose of this particular case is to establish whether the results obtained for the two bus system composed of the generator internal and terminal bus in Section 4.1 are valid in a general system. The conclusion is that the results on the two bus system can be used to describe the dynamic/algebraic bifurcation that can occur due to the bifurcation of the load flow, flux decay manifold, and control manifold of that generator. The generator dynamics

are stable with no oscillations for increase in reactive load at the generator terminal bus if the field current limit has not been reached and the exciter has not been disabled. However, if the continuous rating field current limit is exceeded and the excitation system is not disabled, the excitation system dynamics approach a dynamic bifurcation. Static relationship between reactive generation and reactive load and reactive load and voltage indicate the element $S_{Q_L V}^{-1}$ and $S_{Q_G Q_L}$ associated with the generator terminal bus are negative. A root locus analysis indicates that the system could experience a dynamic/algebraic bifurcation although none occurred as reactive load was increased before the transient stability program would no longer converge to an equilibrium. The system experienced a dynamic/ algebraic voltage collapse bifurcation when the excitation system was disabled at the reactive load level where the field current was at the continuous rating limit. A time simulation indicates that there is a rapid decline of terminal voltage, field current, and reactive power output. The flux decay bifurcation test, and the dynamic algebraic bifurcation test confirm the eigenvalue analysis and transient stability simulation results that there is a dynamic voltage collapse problem.

The two bus voltage control area case of a generator internal and terminal bus is extended to a three bus voltage control area composed of a generator, terminal, and load bus in Section 4.4. The test for voltage collapse is performed by increasing reactive load at the load bus rather than at the generator terminal bus as in the case studied in Section 4.3. The results indicate an oscillation develops before the field current limit is reached. A eigenvalue/eigenvector analysis as reactive load is increased indicates the oscillation occurs at the generator flux decay and exciter dynamics. A root locus is performed to explain why the oscillation develops. The system never approaches an algebraic system bifurcation based on a Q-V curve and on the algebraic bifurcation test. The system never approaches a dynamic/ algebraic bifurcation as reactive load and the field current limit is reached. After the continuous field current limit is hit and the excitation system is disabled, the system experiences a dynamic/algebraic bifurcation. The transient stability program fails to be

## 4.1

Th

b

si

E

a

is

la

able to simulate this unstable system response.


## 4.1 Simulation Results of A Two Bus Power System Model

The two bus power system model is composed of a generator internal bus and terminal bus. The analysis used is taken from [21] but the computational results and the relationships to the theory in Chapter 3 are new. This two bus model is shown in Figure 4.1. $E' \angle \delta'$ is the internal bus voltage magnitude and phase angle. The $P_L$ and $Q_L$ are real and reactive power loads at the terminal bus and are assumed to be constant. The generator is assumed to be a round rotor machine, so $x'_d = x_q$. This model is valid for simulating large power system if

(a)     large reactances of the transformers isolate every generator from the rest of the system, and

(b)     the rest of the system can be modeled as an equivalent bus with constant real and reactive power loads.

All the data shown in this section are in per unit base.
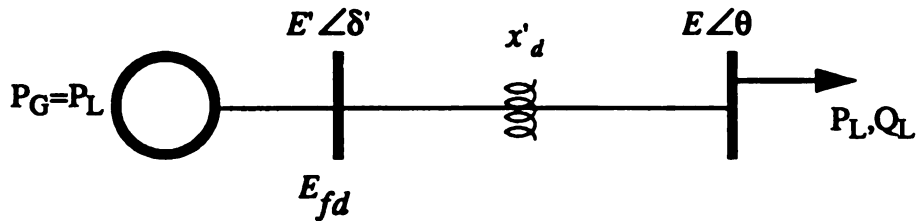


Figure 4.1 Two Bus Power System Model

## 4.1.1  Mathematical Models

The mathematical model without exciter dynamics of a two bus power system can be stated as follows

$$\tau'_{d0}\dot{E}' = \frac{-x_d}{x'_d}E' + \frac{x_d - x'_d}{x'_d}E\cos\delta + E_{fd} \tag{4.1}$$

$$P_L = \frac{E'E\sin\delta}{x'_d} \tag{4.2}$$

$$Q_L = \frac{E'E\cos\delta - E^2}{x'_d} \tag{4.3}$$

where

$$\delta = \delta' - \theta$$

Since we assume that there is no angle instability problem, $\delta$ can be eliminated and leave a second order nonlinear system.

From (4.2)

$$\sin\delta = \frac{P_L x'_d}{E'E}$$

From (4.3)

$$\cos\delta = \frac{Q_L x'_d + E^2}{E'E} \tag{4.4}$$

and

$$\cos^2\delta + \sin^2\delta = 1 = \frac{(P_L x'_d)^2 + (Q_L x'_d + E^2)^2}{(E'E)^2}$$

$$\Rightarrow g(E, E') = (E'E)^2 - (P_L x'_d)^2 - (Q_L x'_d + E^2)^2 = 0 \tag{4.5}$$

Plug equation (4.4) into equation (4.1) we get

$$\tau'_{d0}\dot{E}' = \frac{-x_d}{x'_d}E' + \frac{x_d - x'_d}{x'_d E'}E^2 + \frac{x_d - x'_d}{E'}Q_L + E_{fd} \tag{4.6}$$

Equation (4.6) is a constrained differential equation. It is constrained by equation(4.5). The states E and E' have to always stay in a manifold defined by equation (4.5). We call this manifold the load flow manifold.

If we set $\dot{E}' = 0$, equation (4.6) becomes

$$f(E, E') = \frac{-x_d}{x'_d}E'^2 + \frac{x_d - x'_d}{x'_d}E^2 + (x_d - x'_d)Q_L + E_{fd} = 0 \tag{4.7}$$

It turns out that the equilibrium point of the flux decay equation (4.6) has to always stay in a manifold defined by equation (4.7). We call this manifold the equilibrium manifold or the flux decay manifold. The intersections of the load flow manifold (4.5) and flux decay manifold (4.7) are the equilibrium points of the system. In Figure 4.2, the dotted line is the load flow manifold and the solid line is the flux decay manifold. There are two intersections that stand for two steady state solutions or equilibrium points. One is at $(E_h, E'_h) = (0.99, 1.01)$ and we call it high voltage solution. This solution is usually within the acceptable voltage range. Another one is at $(E_l, E'_l) = (0.22, 0.4129)$ and we call it low voltage solution. $(E_u, E'_u) = (0.26, 0.404)$ is the point that has the minimum $E'$ of a load flow manifold. Since the flux decay manifold is derived by setting $\dot{E}' = 0$, $\dot{E}' > 0$ for the area below flux decay manifold and $\dot{E}' < 0$ for the area above flux decay manifold. Since the trajectory is constrained within the load flow manifold by (4.5), it follows that

$$\frac{\partial g}{\partial E}dE + \frac{\partial g}{\partial E'}dE' = 0$$

$$\Rightarrow \frac{dE'}{dE} = -\frac{\frac{\partial g}{\partial E}}{\frac{\partial g}{\partial E'}} = -\frac{E'^2 - 2(x'_d Q_L + E^2)}{E'E} \tag{4.8}$$

At the minimum point of $E'$ of the load flow manifold $(E_u, E'_u)$

$$\frac{dE'}{dE} = 0$$

$$\Rightarrow E'^2_u = 2\,(x'_d Q_L + E^2_u) \tag{4.9}$$

If E>E$_u$, by equations (4.5) and (4.8)

$$\frac{dE'}{dE} > 0, \text{ and}$$

if E<E$_u$, by equations (4.5) and (4.8)

$$\frac{dE'}{dE} < 0.$$

The sign of $\frac{dE'}{dE}$ gives the direction in which the state is moving on its trajectory along the load flow manifold in Figure 4.2. Since $\frac{dE'}{dE} = 0$ at the point $(E_u, E'_u)$, the point $(E_u, E'_u)$ is a third equilibrium point of the system 4.1-4.3. The sign of $\frac{dE'}{dE}$ shows that the point $(E_u, E'_u)$ acts like a source and moves the trajectory moves away from it in both directions. The point $(E_u, E'_u)$ is thus an unstable equilibrium point of 4.1-4.3. Note that as reactive load Q$_L$ becomes more positive, from equation 4.9, the value of $E'_u$ increases since if Q$_L$=0 $E'_u = E_u = 0$.

In Figure 4.2, since $E_l < E_u$ for Q$_L$=0.07, an initial value $(E_0, E'_0)$ will converge to $(E_l, E'_l)$ if $E_0 < E_u$ and will converge to $(E_h, E'_h)$ if $E_0 > E_u$. It indicates that both $(E_h, E'_h)$ and $(E_l, E'_l)$ are stable equilibrium points in this case. It is known that the equilibrium point after sudden rise in load for the recent Tokyo voltage collapse was a stable low voltage solution. Thus, voltage collapse, that occurs after a disturbance or contingency, may be due to the system being dislodged from a stable high voltage solution and converges to a low voltage stable solution. A system that experiences load flow demand/supply problems could experience a voltage decline and ultimately converges to a low voltage solution.

It is also possible that the low voltage steady state solution intersects with the lowest point

P=0.33,Q=0.07,Efd=1.055,Xd=0.66,Xd(Prime)=0.2

Eh=0.9950, Eh(Prime)=1.0114
El=0.2200, El(Prime)=0.4129
Eu=0.2600, Eu(Prime)=0.4037
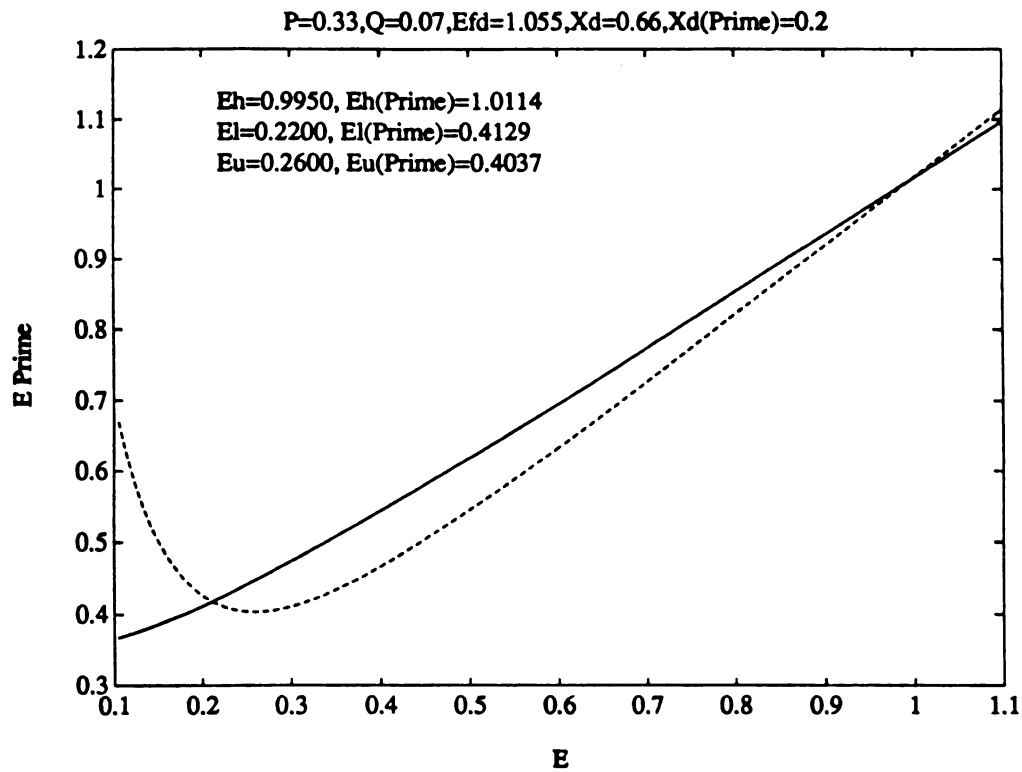
Figure 4.2 Load flow and equilibrium manifolds for two stable equilibrium points

P=0.33,Q=0.32,Efd=1.22,Xd=0.66,Xd(Prime)=0.2

Eh=0.9959, Eh(Prime)=1.0614
El=0.3000, El(Prime)=0.5585
Eu=0.3000, Eu(Prime)=0.5585
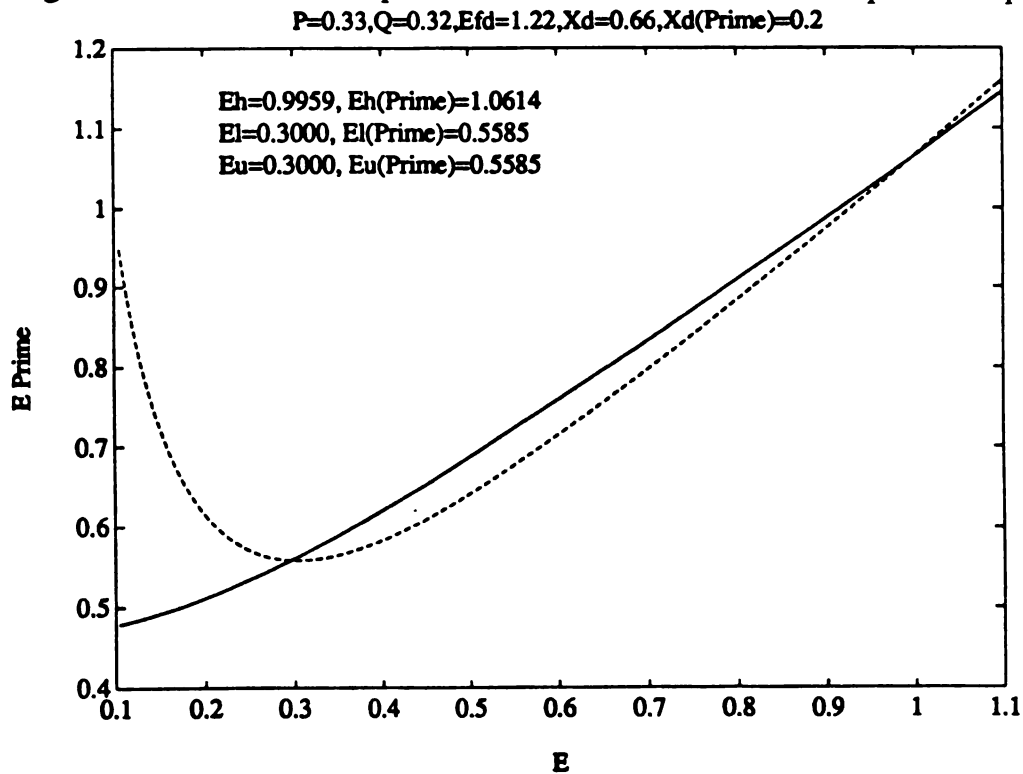
Figure 4.3 Load flow and equilibrium manifolds for loss of causality
at low voltage solution

of the load flow manifold if reactive power $Q_L$ increases to 0.32. In Figure 4.3,

$(E_l, E'_l) = (E_u, E'_u)$. The system loses its causality (det(D)=0) at the unstable equilibrium point $(E_u, E'_u)$. The system would remain at the unstable equilibrium point

$(E_u, E'_u)$ unless some disturbance occurs. The disturbance would cause the trajectory to either approach $(E_h, E'_h)$ or to experience dynamic collapse as E declines and E' increases. If there were external dynamics in the system 4.1-4.3 , the dynamical system theory may not be mature enough to define what will happen at this point. It has been shown that chaotic behavior occurs in the simulation [21] if there are external dynamics. It will be shown in the following section that as the system moves to algebraic bifurcation, the stability of the system at low voltage equilibrium point becomes unpredictable because the simulation does not converge and dynamical system theory can not currently predict what will happen. Notice that the high voltage solution $(E_h, E'_h)$ where the power system is usually operated at is still a stable equilibrium point. The chaotic behavior or loss of voltage stability would occur only if the system is operated at the low voltage solution. Note that the reactive load increase causes the stable low voltage solution to experience loss of causality and the possible loss of voltage stability or chaotic behavior.

Figure 4.4 is the case where $E_l > E_u$ for an additional increase in $Q_L$ to 0.47. There are two intersections of load flow and equilibrium manifolds. The high voltage solution $(E_h, E'_h)$ is stable. The low voltage solution $(E_l, E'_l)$ is unstable. The equilibrium points are closer if we compare with the case in Figure 4.2 and Figure 4.3. It will be shown in Figure 4.5 and Figure 4.6 that these two equilibrium points will merge together and disappear as $Q_L$ continuous to increase.

Figure 4.5 is the case where there is only one intersection of the load flow manifold and the equilibrium manifold at $Q_L$=0.8326. This is the point that violates the conditions of dynamic/algebraic and algebraic/ dynamic tests and the system jacobian matrix becomes singular. It will be shown in the following section that two equilibrium points merge to-

P=0.33,Q=0.47,Efd=1.315,Xd=0.66,Xd(Prime)=0.2

Eh=0.9950, Eh(Prime)=1.0912
El=0.3750, El(Prime)=0.6500
Eu=0.3425, Eu(Prime)=0.6463
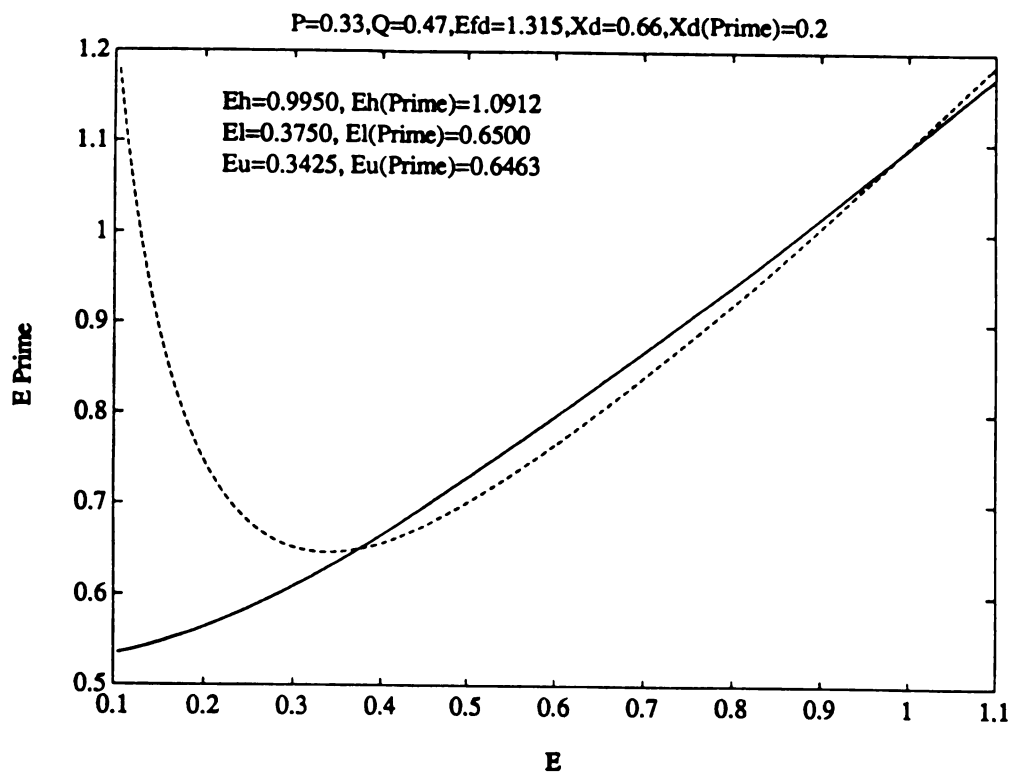
**Figure 4.4 Load flow and equilibrium manifolds with one stable and one unstable equilibrium points**

P=0.33,Q=0.8326,Efd=1.5,Xd=0.66,Xd(Prime)=0.2

Et=0.7650, Et(Prime)=0.9863
Eu=0.4250, Eu(Prime)=0.8314
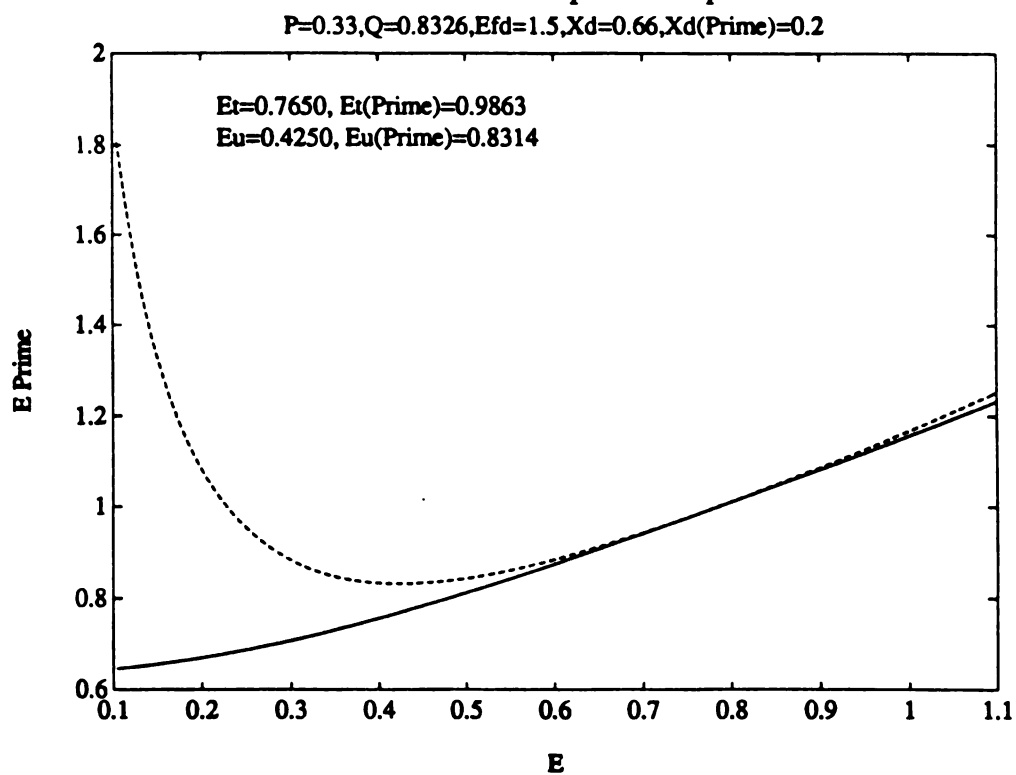
**Figure 4.5 Load flow and equilibrium manifolds with one intersection**

P=0.33,Q=0.85,Efd=1.5,Xd=0.66,Xd(Prime)=0.2

Eu=0.4250, Eu(Prime)=0.8395
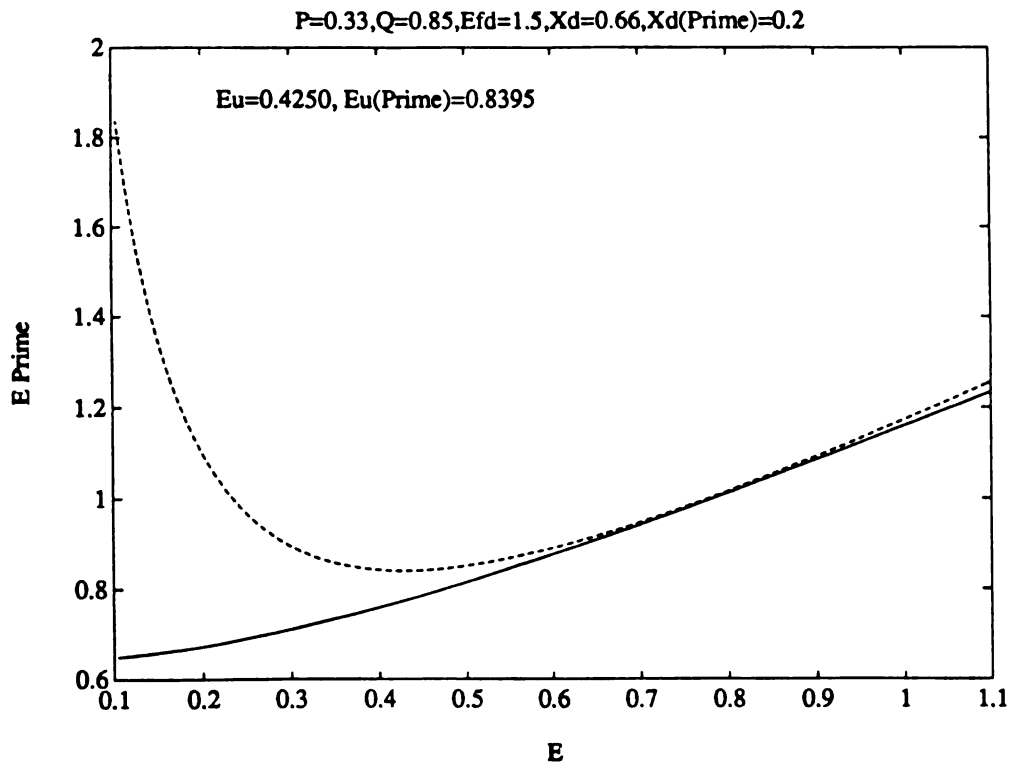
Figure 4.6 Load flow and equilibrium manifolds with no intersection

Equilibrium Manifolds for different Efds

Solid Line: Equilibrium Manifold(Efd=0.8)
Dashed Line: Equilibrium Manifold(Efd=1.05)
Dotted Line: Load Flow Manifold
P=0.33, Q=0.07, Xd=0.66, Xd(Prime)=0.2
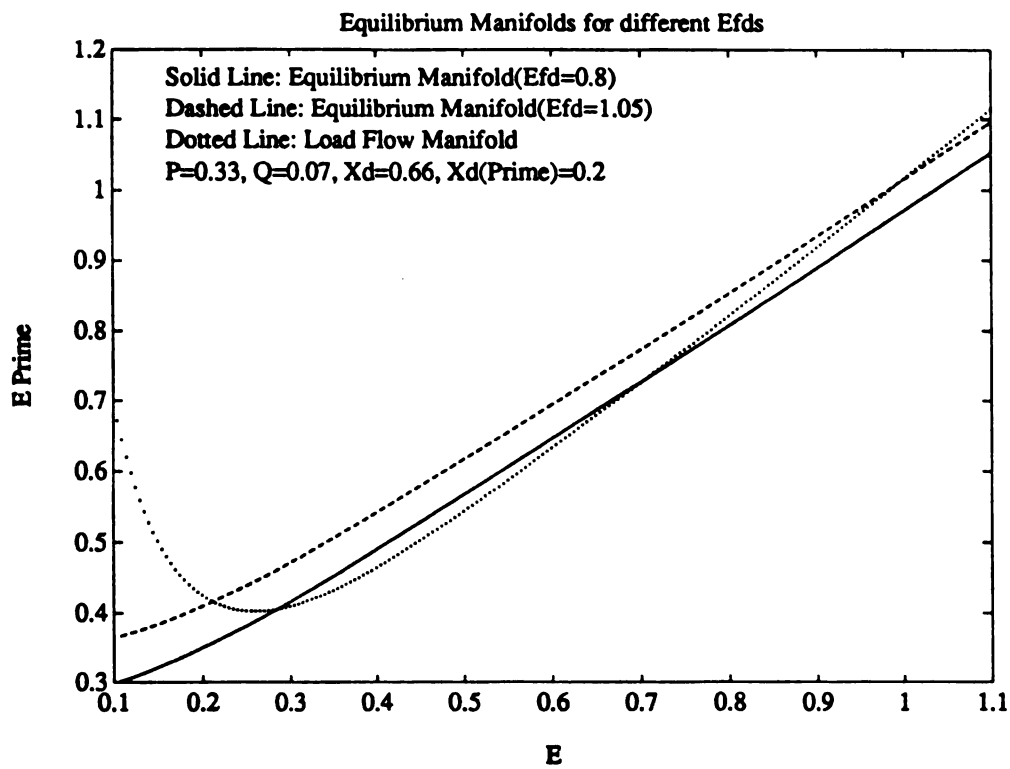
Figure 4.7 Load flow and equilibrium manifolds for different field voltages

gether and the system becomes unstable with the voltage $E$ and $E'$ decaying toward zero. This type of loss of voltage stability is observed in the slow continuous decline in voltage. It will be clear in the 12 bus system example that when a generator hits field current limit and the excitation system is disabled, a dynamic voltage instability results in continuous decline in induced voltage field current and terminal bus voltage that are caused by the loss of stability of generator dynamics.

Figure 4.6 is the case where $Q_L$=0.85 and there exists no solution when field current limits are hit and the excitation system is disabled. The case where the exciter is not disabled is discussed in the next section. It will be shown that if the exciter is not disabled, this case would never happen. An increase of field current when there is a real or reactive load increase will move the high and low voltage solutions far away from each other to preserve the stability of the system voltage. The effects of changes of field current, real power load, and reactive power load will be now discussed in Figure 4.7, 4.8, and 4.9.

Position and shape of these two manifolds change with parameter values like $E_{fd}$, $P_L$, and $Q_L$. Figure 4.7 shows the changes in the flux decay manifold for different $E_{fd}$ values. Since load flow manifold is not a function of $E_{fd}$, there is no change in both position and shape of the load flow manifold. In Figure 4.7, the solid line represents the equilibrium manifold with $E_{fd} = 0.8$, and the dotted line represents the load flow manifold. The intersections of these two manifolds are at (0.7, 0.71) and (0.29, 0.405). Notice that the high voltage solution is not within the acceptable range in a normal system. If we increase the $E_{fd}$ from 0.8 to 1.05, the equilibrium manifold can be move up and represented by a dashed line. The new intersections of the load flow manifold and equilibrium manifold become (0.98, 1.05) and (0.215, 0.42). The high voltage solution is now in the acceptable range. By increasing field voltage (field current), the system voltage $E$ can be increased. This indicates the important role that adjustment of $E_{fd}$ has in maintaining the system voltage at the desired value.
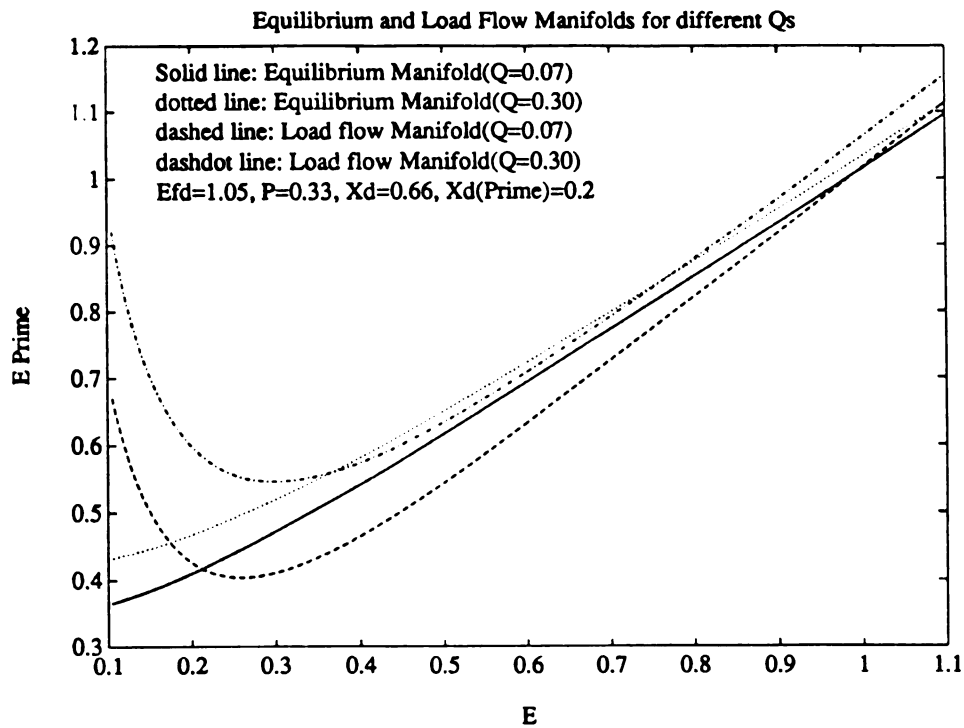
Figure 4.8 Load flow and equilibrium manifolds for different reactive loads
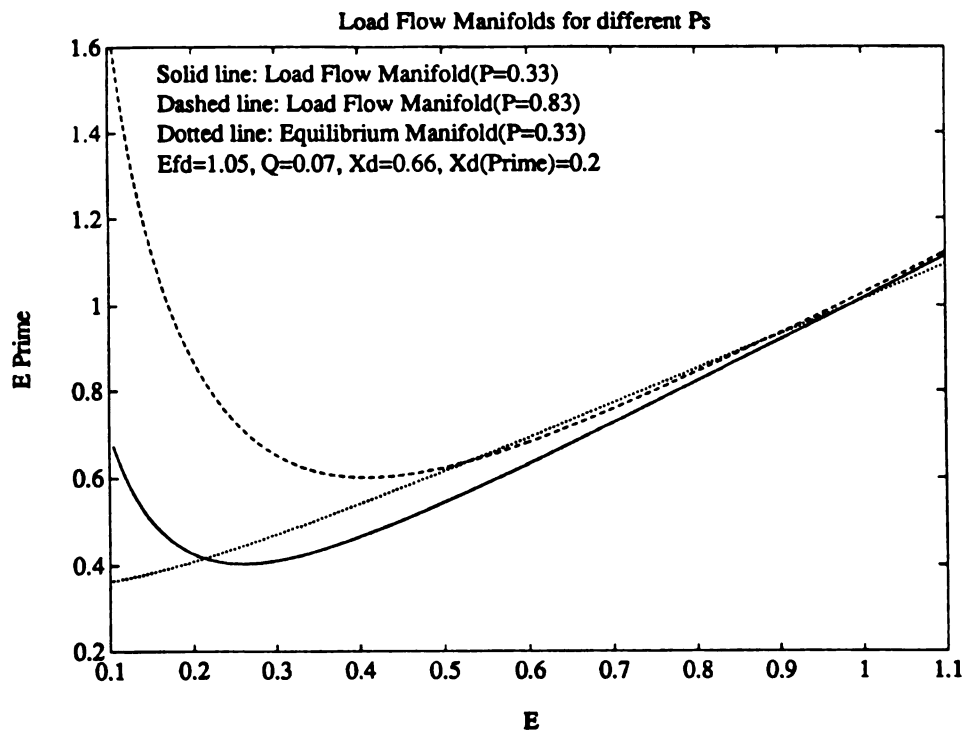


Figure 4.9 Load flow and equilibrium manifolds for different real power loads

In Figure 4.8, solid line and dotted line represent the equilibrium manifold and load flow manifold at reactive power load at 0.07 respectively. The high and low voltage steady state solutions are (0.95, 0.95) and (0.215, 0.42) respectively. Since both the load flow manifold and equilibrium manifold are functions of the reactive power load, the position and shape of both of the manifolds will change if there is a change in the reactive power load. If the reactive power load is increased from 0.07 to 0.3, the new equilibrium manifold and load flow manifolds are represented by dashed line and dashdotted line. The new high and low voltage steady state solutions become (0.76, 0.85) and (0.37, 0.58). This is the case where there is no excitation system control. It indicates that if the system loses its excitation system control, a reactive power load increase will cause a system voltage decrease. In this special case, we can also see that the increase of reactive power load will move the system from two stable equilibrium points to one stable equilibrium point $(E_h, E'_h)$ and one unstable equilibrium point $(E_l, E'_l)$. The equilibrium points become closer to each other as we increase the reactive power load. It will be shown that as we increase the reactive power load even further, the two equilibrium points will merge together and become an unstable equilibrium point. This is the point where the algebraic/dynamic test condition is violated and bifurcation may occur at this point.

Figure 4.9 shows the effects of changes of the real power load. Since the real power load is a function of the load flow manifold but not a function of the equilibrium manifold, only the position and shape of the load flow manifold will be changed for a real power load change. The dotted line represents the equilibrium manifold. The solid line represents the load flow manifold where the real power load is at 0.33. The high and low voltage solutions are (0.95, 1.0) and (0.215, 0.43).

Equation (4.5)

$$g(E, E') = (E'E)^2 - (P_L x'_d)^2 - (Q_L x'_d + E^2)^2 = 0 \qquad (4.5)$$

shows that real power load is neither a coefficient of E nor E'. It indicates that the change of real power load will influence the solutions of lower voltage and has less impact on high voltage solutions. The load flow manifolds for different real power loads will converge as E and E' increase. This phenomenon can be seen in the Figure 4.9.

The dashed line is the load flow manifold when the real power load is at 0.83. The new high and load voltage steady state solutions become (0.88, 0.9) and (0.53, 0.62). The system is moving from two stable equilibrium points, (0.95, 1.0) and (0.215, 0.43), to one stable equilibrium point (0.88, 0.9) and one unstable equilibrium point (0.53, 0.62). If there is no excitation system control and real power load is further increased, those two equilibrium points will merge together just like the case of increasing reactive power load and the algebraic/dynamic test conditions will be violated.

### 4.1.2   Two Bus System Simulation With Excitation System Control included

The mathematical model developed in section 4.1.1 does not include the excitation system control. The field voltage ($E_{fd}$) is an assigned value for each simulation in section 4.1.1. In a real power system, field voltage plays an important role in maintaining terminal bus voltage at a preset value. In this section, the exciter system control is included. The exciter is assumed to have infinite gain so that as long as the field current is below its upper limit the terminal bus voltage can be held at its preset value. It is also assumed that the exciter can respond to disturbances infinitely fast. If the field current hits its upper limit, a field current limiter will disable the excitation system control and field voltage is assume to remain at its upper limit.

A computer program is developed for the two bus system with the exciter control simulation. The algorithm for this computer program is in Figure 4.10. The program reads in the initial values of the field voltage ($E_{fd0}$), the desire terminal bus voltage ($E_{ref}$), and the reactive power load condition. In the first iteration, the program solves equations (4.5) and

```
                        ┌─────────────┐
                        │    START    │
                        └──────┬──────┘
                               │
                               ▼
                  ┌───────────────────────┐
                  │       Read in         │
                  │  E_fd0, E_ref, and Q_L │
                  └───────────────────────┘
```

$E_{fd0}$, $E_{ref}$, and $Q_L$

Solve equations (4.7) and (4.5) for $E$ and $E'$

$E_{fd}=E_{fd}+\lambda$

$E_{fd}=E_{fd}^-$

$E<E_{REF}$    Yes / No

$|E-E_{ref}| < \varepsilon$    No

$E_{fd}<E_{fdmax}$    Yes / No

Yes

Output
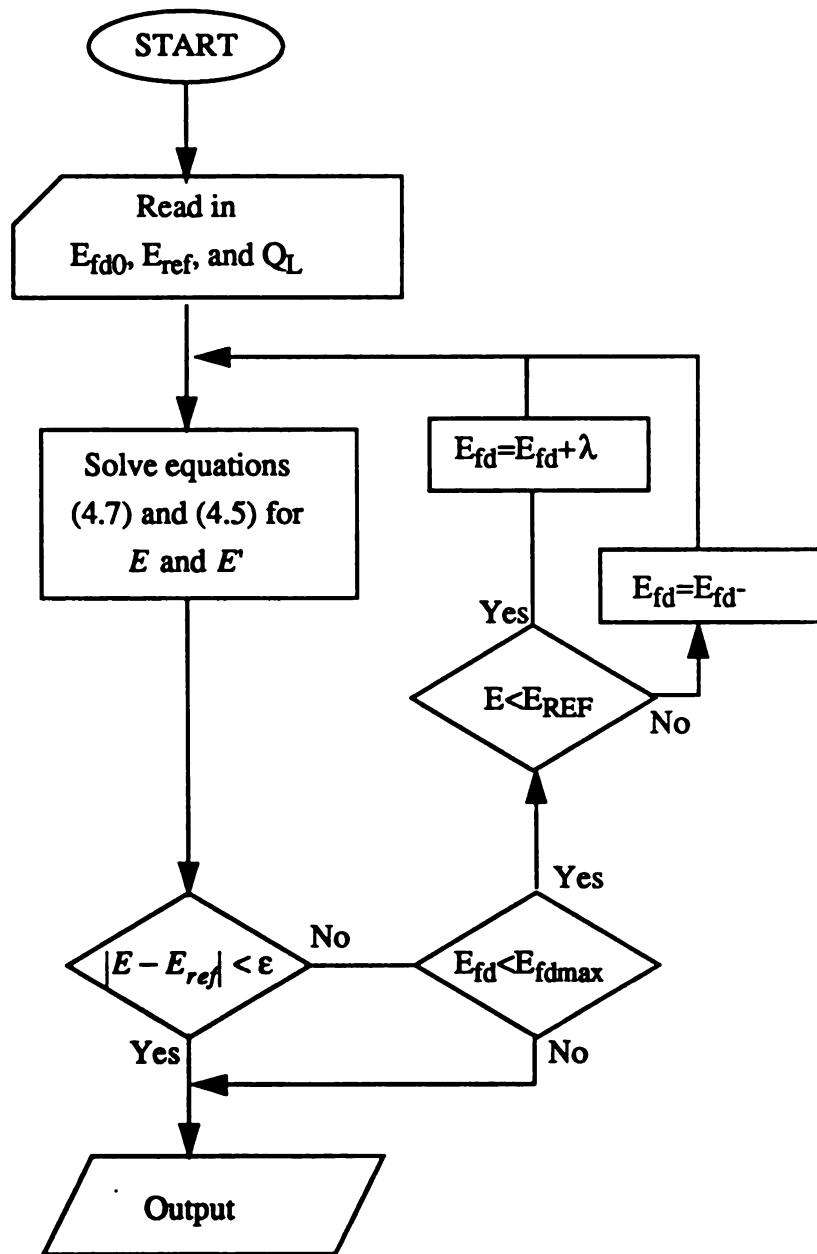
Figure 4.10 Algorithm of a computer program that includes
the exciter effects in a two bus system model

(4.7) for terminal bus voltage ($E$) and internal bus voltage ($E'$). E is then compared with the $E_{ref}$. If the absolute value of the difference of E and $E_{ref}$ is less than the tolerance $\varepsilon$, the program stops at this iteration and provide an output for the specified reactive power load condition. If the difference between E and $E_{ref}$ is larger than $\varepsilon$, the program checks if the field current is on its upper limit or not. If the field current is on its upper limit, it indicates that the generator loses its capability of controlling voltage. The program provides the output $E$ and $E'$ and stops. If the field current is still within its acceptable operating range, the field voltage will be increased (or decreased) by a small value $\lambda$. The increase or decrease of field voltage is dependent on whether the terminal bus voltage is lower or higher than the desired terminal bus voltage. After the field voltage is adjusted, the program starts its second iteration to solve the equations (4.7) and (4.5). The program will stop when either the difference of terminal bus voltage and desired terminal bus voltage is within the tolerance or the field current hits its upper limit.

The procedure of this simulation is shown in Figure 4.11.

The purpose of this simulation is to

(a)    confirm the validity of voltage instability tests by using phase portrait analysis method,

(b)    show the voltage instability occurs in the flux decay dynamics much earlier than the load flow jacobian matrix becomes singular in the case that the system is operated at the neighborhood of the high voltage solution, and

(c)    investigate the voltage instability in the neighborhood of low voltage solution.

The line drop compensation, air gap saturation, and precise exciter control are not included in this simulation and will be included in the twelve bus system simulation. Table 4.1
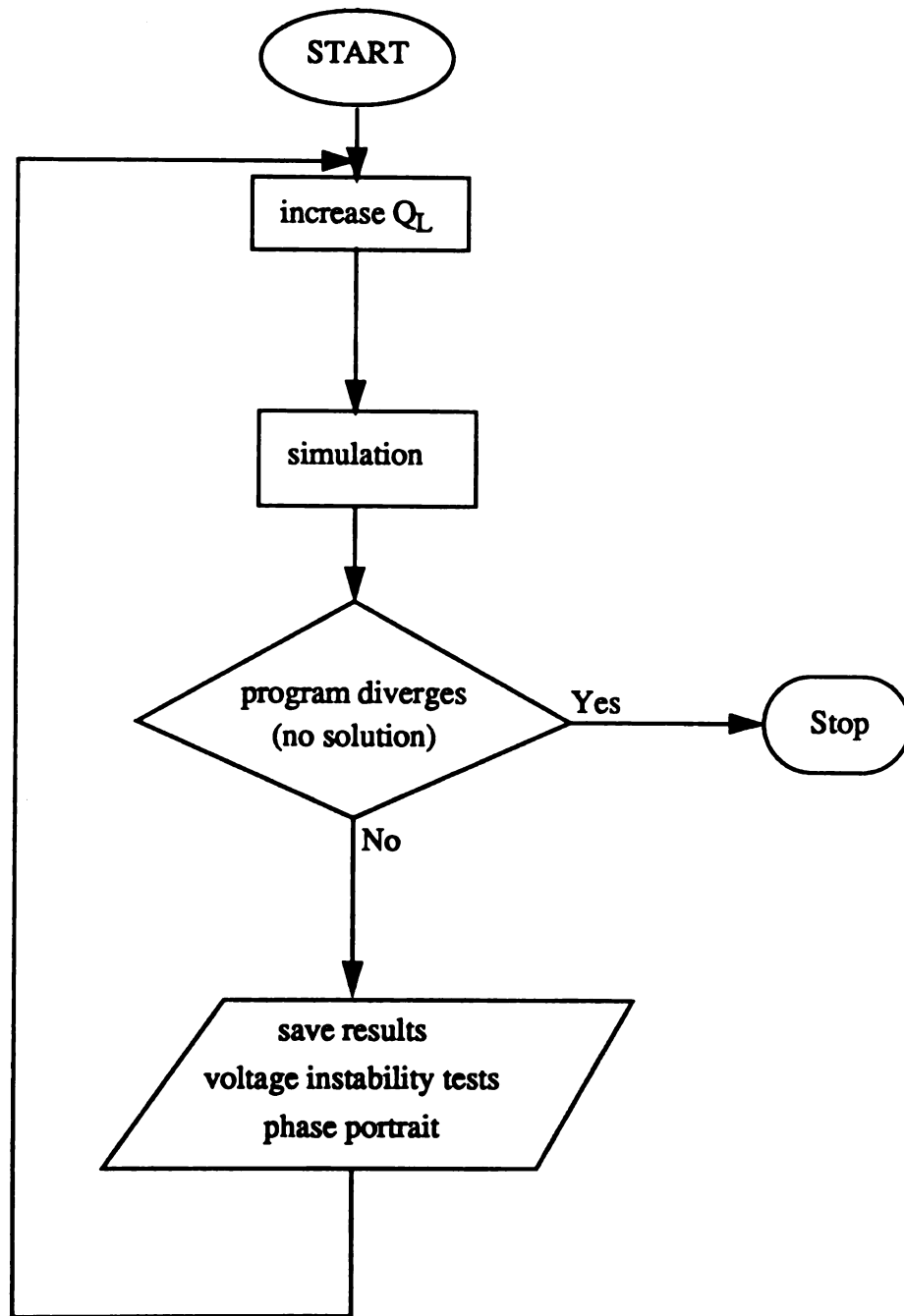
Figure 4.11 Procedure of two bus simulation

shows the base case data for this two bus system simulation. All of these data are in per unit base.

Table 4.1 Base case data for the two bus system simulation

| P | Q | $E_{fd}$ | $E_{fdmax}$ | $E_{ref}$ | $x_d$ | $x'_d$ |
|------|------|-------|-------|-----|------|------|
| 0.33 | 0.07 | 1.055 | 1.5 | 1.0 | 0.66 | 0.2 |

The equations are restated here to formulate the voltage instability matrices.

$$\tau'_{d0}\dot{E}' = \frac{-x_d}{x'_d}E' + \frac{x_d - x'_d}{x'_d}E\cos\delta + E_{fd} \tag{4.1}$$

$$P_L = \frac{E'E\sin\delta}{x'_d} \tag{4.2}$$

$$Q_L = \frac{E'E\cos\delta - E^2}{x'_d} \tag{4.3}$$

The jacobian matrix of these nonlinear equations is

$$J = \begin{bmatrix} \dfrac{-x_d}{x'_d} & \dfrac{(x_d - x'_d)\cos\delta_0}{x'_d} & \dfrac{(x'_d - x_d)E_0\sin\delta_0}{x'_d} \\[2mm] \dfrac{E_0\sin\delta_0}{x'_d} & \dfrac{E'_0\sin\delta_0}{x'_d} & \dfrac{E'_0E_0\cos\delta_0}{x'_d} \\[2mm] \dfrac{E_0\cos\delta_0}{x'_d} & \dfrac{E'_0\cos\delta_0 - 2E_0}{x'_d} & \dfrac{-E'_0E_0\sin\delta_0}{x'_d} \end{bmatrix} = \begin{bmatrix} A & B \\ C & D \end{bmatrix}$$

where

$$A = \frac{-x_d}{x'_d}$$

$$B = \left[ \dfrac{(x_d - x'_d)\cos\delta_0}{x'_d} \quad \dfrac{(x'_d - x_d)E_0\sin\delta_0}{x'_d} \right]$$

$$C = \left[ \begin{array}{c} \dfrac{E_0\sin\delta_0}{x'_d} \\ \dfrac{E_0\cos\delta_0}{x'_d} \end{array} \right]$$

$$D = \left[ \begin{array}{cc} \dfrac{E'_0\sin\delta_0}{x'_d} & \dfrac{E'_0 E_0\cos\delta_0}{x'_d} \\ \dfrac{E'_0\cos\delta_0 - 2E_0}{x'_d} & \dfrac{-E'_0 E_0\sin\delta_0}{x'_d} \end{array} \right]$$

The algebraic bifurcation test matrix is D.

The dynamic/algebraic bifurcation test matrix is

$$\hat{A} = A - BD^{-1}C$$

The algebraic/dynamic bifurcation test matrix is

$$\hat{D} = D - CA^{-1}B$$

Since in this two bus system model we assumed there is no angle stability problem and the excitation system control can respond to the disturbance infinitely fast, the dynamic/algebraic bifurcation test is the same as the flux decay bifurcation test.

Figure 4.12 is the phase portrait for the base case data. Since $E_l = 0.22$ is less than $E_u = 0.26$, both high and low voltage steady state solutions are stable. It is confirmed by the voltage instability tests in Table 4.2. The eigenvalues of dynamic/algebraic bifurcation test matrix $\hat{A}$ are negative for both high and low voltage solutions. The condition number of the algebraic bifurcation test matrix D for low voltage solution indicates that if the system is operated at a point near the low voltage solution, the system is very close to a loss of causality
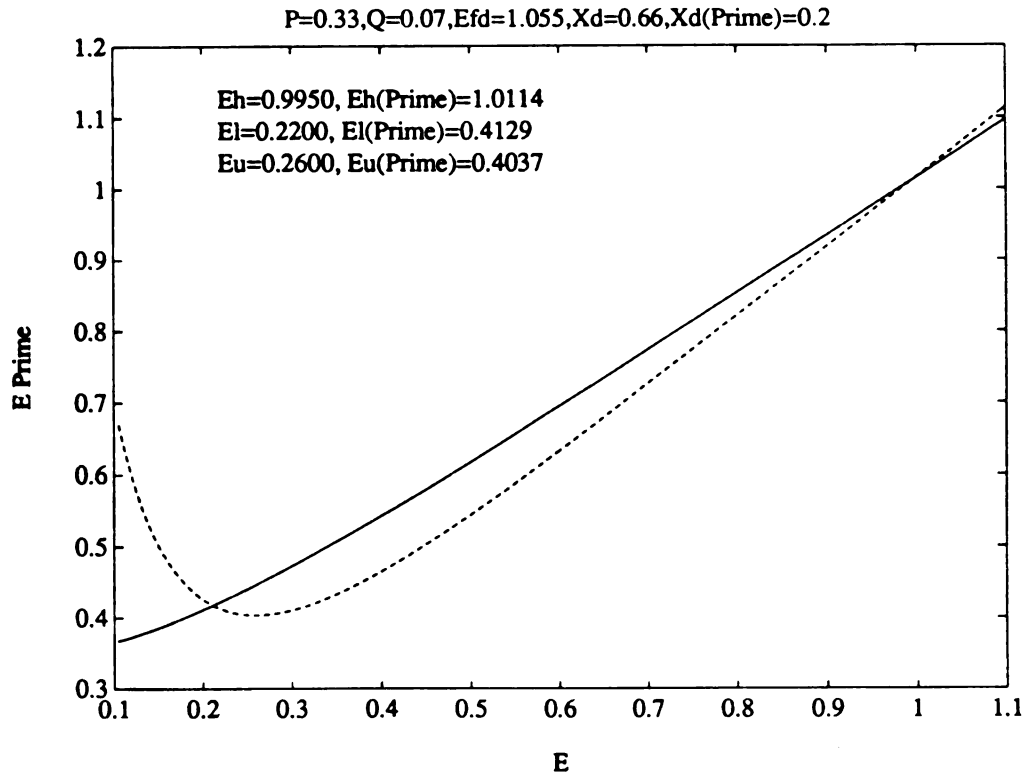
Figure 4.12 Phase portrait for Q=0.07

Table 4.2 Voltage instability tests for Q=0.07

|  | $E$ | $E'$ | 1/cond(D) | 1/cond($\hat{D}$) | eig($\hat{A}$) |
|---|---|---|---|---|---|
| High voltage | 0.995 | 1.0114 | 0.8732 | 0.2683 | -0.9364 |
| Low voltage | 0.22 | 0.4037 | 0.077 | 0.1736 | -9.1857 |

P=0.33,Q=0.27,Efd=1.185,Xd=0.66,Xd(Prime)=0.2

Eh=0.9950, Eh(Prime)=1.0514
El=0.2850, El(Prime)=0.5285
Eu=0.2925, Eu(Prime)=0.5278
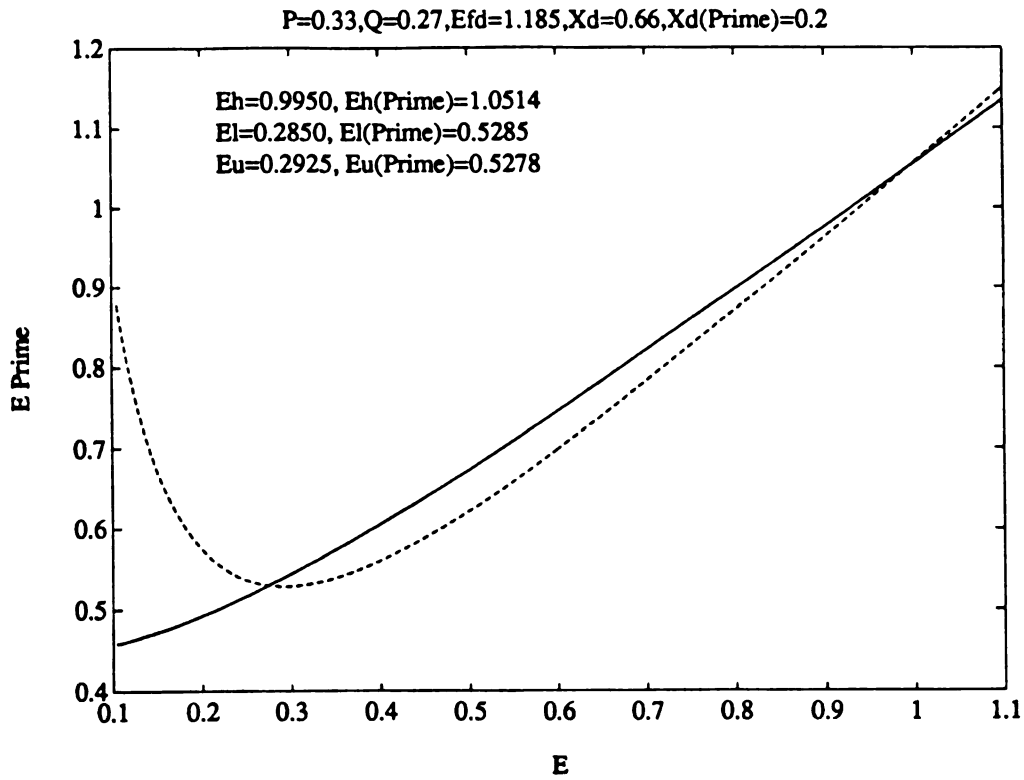
Figure 4.13 Phase portrait for Q=0.27

Table 4.3 Voltage instability tests for Q=0.27

|  | $E$ | $E'$ | 1/cond(D) | 1/cond($\hat{D}$) | eig($\hat{A}$) |
|---|---|---|---|---|---|
| High voltage | 0.995 | 1.0514 | 0.844 | 0.2225 | -0.8379 |
| Low voltage | 0.285 | 0.5285 | 0.0285 | 0.3161 | -48.2318 |

problem. The condition number of the algebraic/dynamic bifurcation test matrix $\hat{D}$ indicates the system is far away from the system bifurcation point for both the high and low voltage solutions.

In Figure 4.13, the reactive power load is increased to 0.27. Since the field voltage $E_{fd}$ is within its acceptable limit, the high voltage solution of the terminal bus is close to its pre-set value 1.0. The high and low voltage solutions are both stable. The condition number of the algebraic bifurcation test matrix D in Table 4.3 for the low voltage solution indicates that the increase of reactive power load may cause loss of causality problems in the algebraic equations if the system is operated at the low voltage solution. Comparing Figure 4.12 and 4.13, the high and low voltage solutions move closer to each other for an increase in reactive power load even when there is still plenty of field current reserve. The field current reserve can only guarantee two steady state solutions but can not guarantee both of these two steady state solutions to be stable.

Figure 4.14 and Table 4.4 are for the case where the reactive power load is further increased to 0.32. The low voltage solution is "almost" at the minimum of the load flow manifold. Because of the round off error of the computer, it is impossible to find the exact point. Table 4.4 shows that the system is very close to loss of causality in low voltage solution (1/cond(D)=0.014). The eigenvalue of $\hat{A}$ for low voltage solution starts to move to negative infinity if $E_l$ is less than but very close to $E_u$. If $E_l$ is larger than but very close to $E_u$, we will see a very large positive eigenvalue of $\hat{A}$. It indicates that at the neighborhood of the unstable equilibrium point of 4.1-4.3 $(E_u, E'_u) = (E_l, E'_l)$, the eigenvalue of $\hat{A}$ can be either close to positive infinity or negative infinity. The loss of causality of the algebraic equation causes this kind of chaotic phenomena. The eigenvalue of $\hat{A}$ for high voltage solution is negative in Table 4.4 but is moving toward the right half plane for increase in $Q_L$ if we compare the eigenvalue of $\hat{A}$ in Table 4.3.

If the reactive power load is increased to be at 0.37, the low voltage solution becomes an

P=0.33,Q=0.32,Efd=1.22,Xd=0.66,Xd(Prime)=0.2
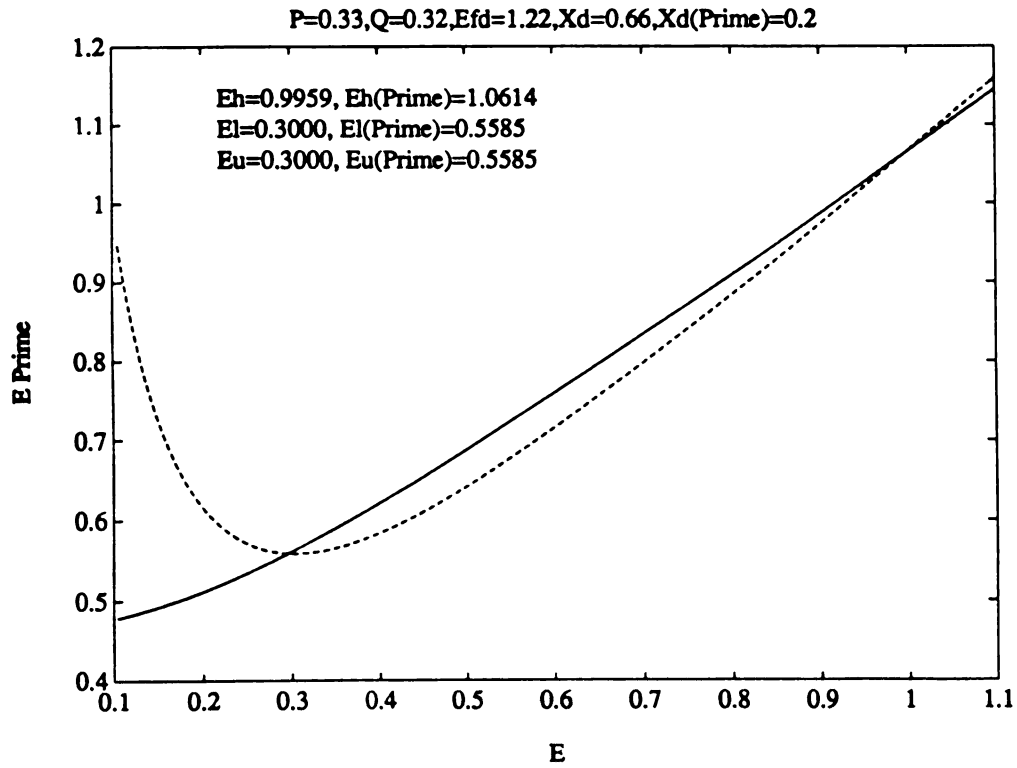


Figure 4.14 Phase portrait for Q=0.32

Table 4.4 Voltage instability tests for Q=0.32

|  | $E$ | $E'$ | 1/cond(D) | 1/cond($\hat{D}$) | eig($\hat{A}$) |
|---|---|---|---|---|---|
| High voltage | 0.995 | 1.0614 | 0.8329 | 0.2115 | -0.8119 |
| Low voltage | 0.3 | 0.5585 | 0.014 | 0.3556 | -110.1627 |
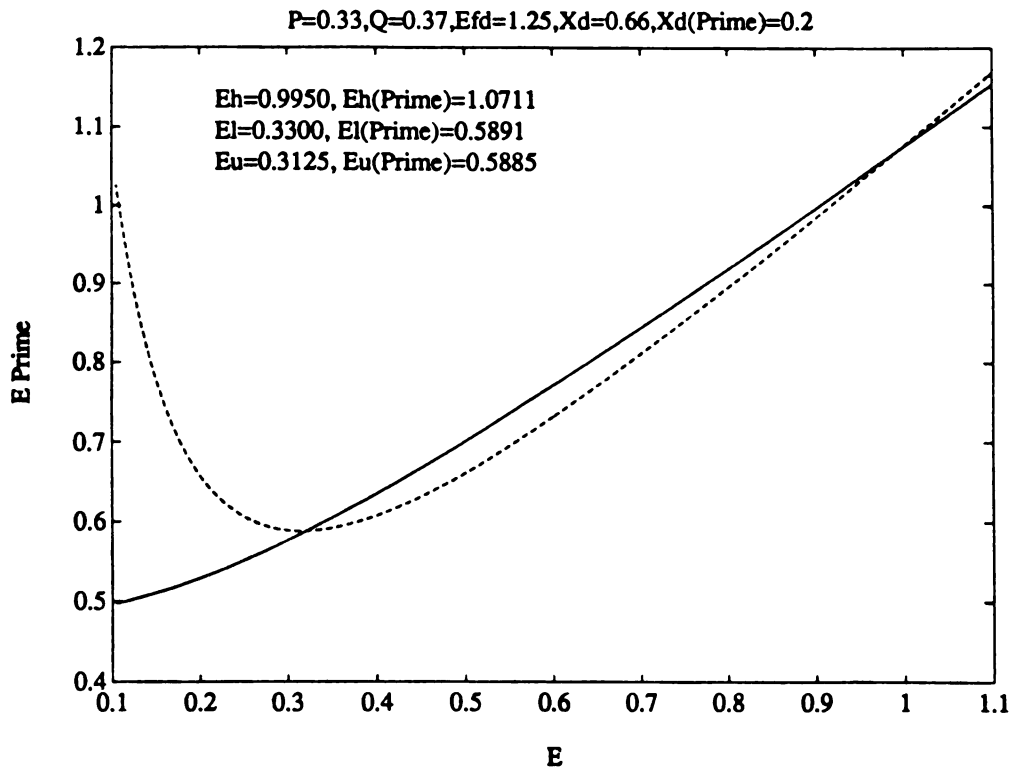
Figure 4.15 Phase portrait for Q=0.37

Table 4.5 Voltage instability tests for Q=0.37

|  | $E$ | $E'$ | 1/cond(D) | 1/cond($\hat{D}$) | eig($\hat{A}$) |
|---|---|---|---|---|---|
| High voltage | 0.995 | 1.0711 | 0.8214 | 0.2 | -0.7861 |
| Low voltage | 0.33 | 0.5891 | 0.0696 | 0.3915 | 22.3132 |
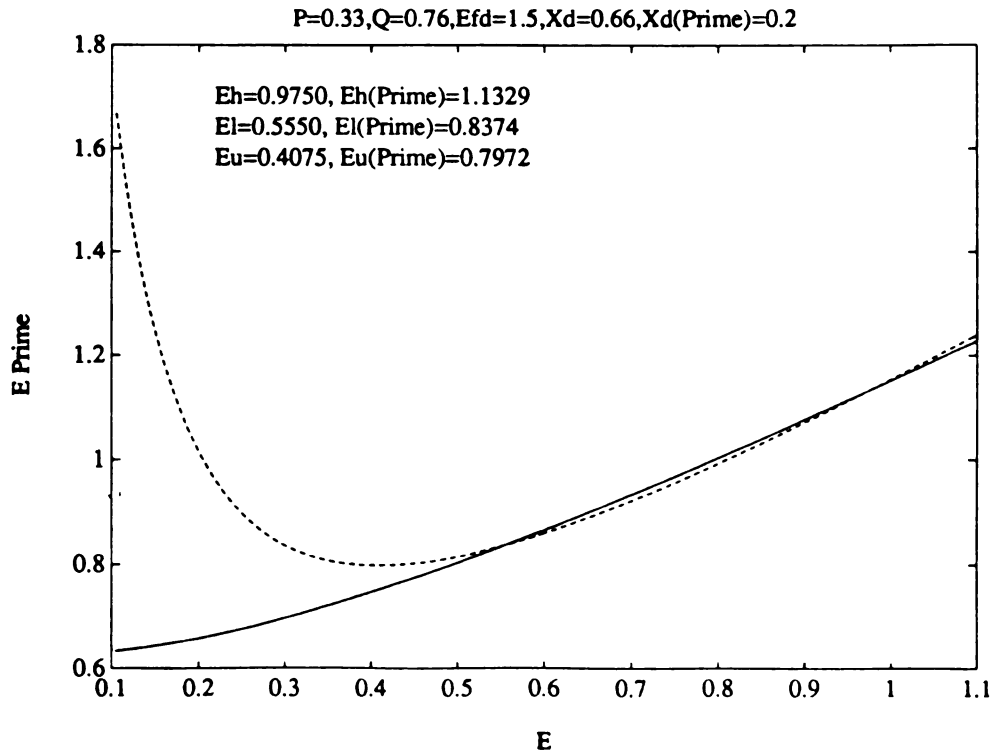
Figure 4.16 Phase portrait for Q=0.76

Table 4.6 Voltage instability tests for Q=0.76

|  | $E$ | $E'$ | 1/cond(D) | 1/cond($\hat{D}$) | eig($\hat{A}$) |
|---|---|---|---|---|---|
| High voltage | 0.975 | 1.1329 | 0.7196 | 0.1171 | -0.5318 |
| Low voltage | 0.555 | 0.8374 | 0.4855 | 0.2544 | 1.6653 |

unstable equilibrium point because of $E_l > E_u$. The instability of the low voltage equilibrium point $(E_l, E'_l) = (0.33, 0.589)$ is also shown in Table 4.5 because the eigenvalue of $\hat{A}$ becomes positive. The trajectory close to this unstable equilibrium point will move away from it. The magnitude of the eigenvalue of $\hat{A}$ for the high voltage solution is also decreased if it is compared with the eigenvalues in the Table 4.3 and 4.4. Although the exciter can still hold the terminal bus voltage at its preset value as we increase the reactive power load, the level of the stability of the dynamic states is decreased because the eigenvalue of $\hat{A}$ is moving toward the right half plane.

When Q is at 0.76, $E_{fd}=E_{fdmax}$ in Figure 4.16. The exciter control is disabled and the terminal bus voltage can not be held at its desired value. The indicators of system bifurcation $1/cond(\hat{D})$ for both high and low voltage solutions decrease. It indicates that the system jacobian becomes more singular and the system is moving to a system bifurcation point. Since the equilibrium points are far away from the minimum point of the load flow manifold, the indicator of algebraic bifurcation $1/cond(D)$ is large.

In Figure 4.17, there is only one intersection of the load flow and equilibrium manifolds at Q=0.8326. This point is the system bifurcation point. The high and low voltage solutions merge together. Our system bifurcation test indicator $1/cond(\hat{D})$ shows the algebraic/dynamic test matrix is extremely close to a singular matrix. Because of the limitation of the precision of computer, the eigenvalue of $\hat{A}$ is still negative but very close to zero. This is the point of dynamic voltage instability since the equilibrium point is unstable since all points on $g\ (E, E')$ above $(E_u, E'_u)$ would converge to $(E_u, E'_u)$. The trajectory would result in $E$ and $E'$ approaching zero that results in voltage collapse due to the dynamic stability problem. Note that the dynamic voltage collapse occurred after the field current limit is hit which disabled the excitation system. The dynamic instability that caused dynamic voltage instability occurred for very small reactive load increase above that where the field current limit is hit which disabled the excitation system. The dynamic instability that

P=0.33,Q=0.8326,Efd=1.5,Xd=0.66,Xd(Prime)=0.2

Et=0.7650, Et(Prime)=0.9863
Eu=0.4250, Eu(Prime)=0.8314
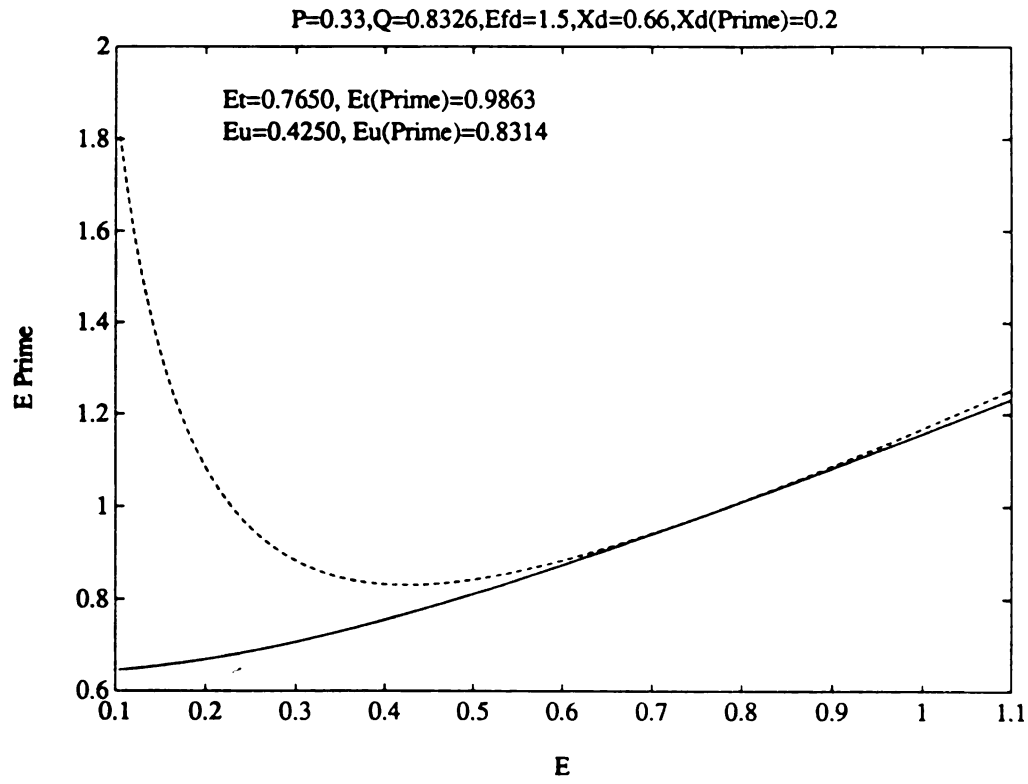
Figure 4.17 Phase portrait for Q=0.8326

Table 4.7 Voltage instability tests for Q=0.8326

|  | $E$ | $E'$ | 1/cond(D) | 1/cond($\hat{D}$) | eig($\hat{A}$) |
|---|---|---|---|---|---|
| High voltage | 0.765 | 0.9863 | 0.6722 | 0.000472 | -0.0023 |
| Low voltage | 0.765 | 0.9863 | 0.6722 | 0.000472 | -0.0023 |
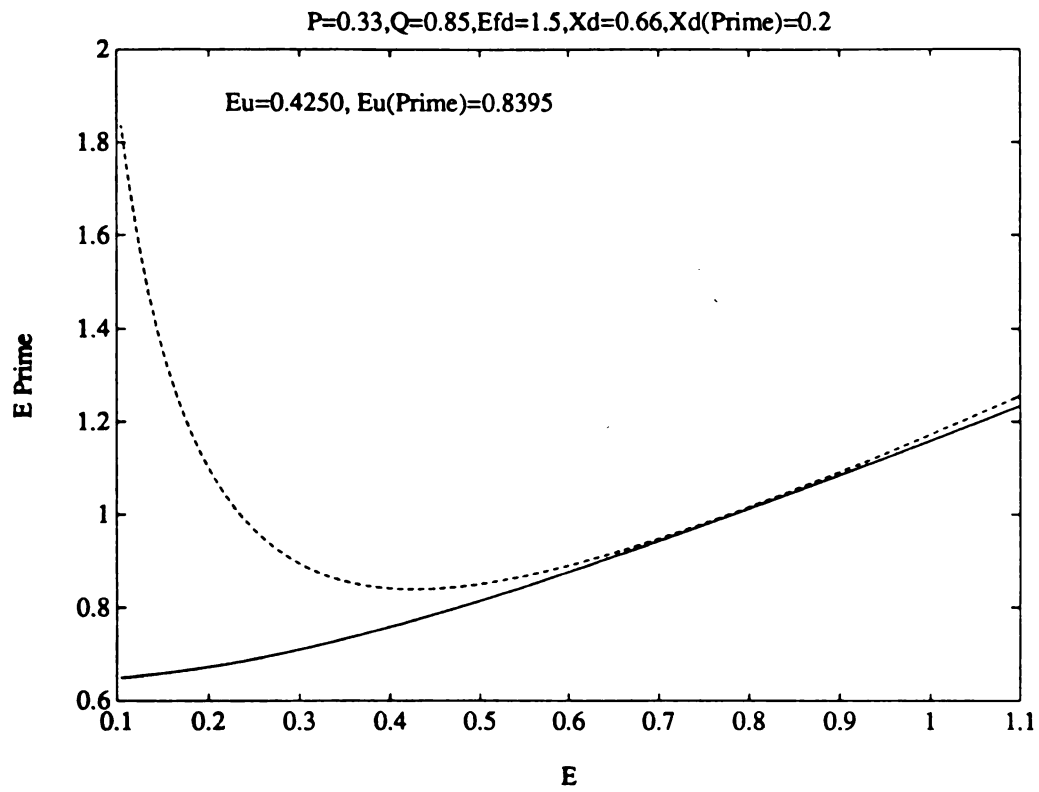
Figure 4.18 Phase portrait for Q=0.85

Table 4.8a Summary of voltage instability test for high voltage solution

| Q | E | E' | 1/cond($D$) | det($D$) | 1/cond($\dot{D}$) | det($\dot{D}$) | eig($\hat{A}$) | $E_{fd}$ |
|---|---|---|---|---|---|---|---|---|
| 0.07 | 0.995 | 1.0114 | 0.8732 | 24.51 | 0.2683 | 6.9552 | -0.9364 | 1.055 |
| 0.17 | 0.995 | 1.0313 | 0.8624 | 24.489 | 0.2452 | 6.5929 | -0.8884 | 1.12 |
| 0.27 | 0.995 | 1.0514 | 0.844 | 24.444 | 0.2235 | 6.206 | -0.8379 | 1.185 |
| 0.32 | 0.995 | 1.0614 | 0.8329 | 24.41 | 0.2115 | 6.01 | -0.8118 | 1.22 |
| 0.37 | 0.995 | 1.0711 | 0.8214 | 24.381 | 0.201 | 5.808 | -0.7861 | 1.25 |
| 0.76 | 0.975 | 1.1329 | 0.7196 | 22.467 | 0.1171 | 3.62 | -0.5318 | 1.5 |
| 0.81 | 0.875 | 1.0628 | 0.7079 | 15.874 | 0.0732 | 1.6138 | -0.3355 | 1.5 |
| 0.8326 | 0.765 | 0.9863 | 0.6722 | 10.145 | 0.00047 | 0.00698 | -0.0023 | 1.5 |

Table 4.8b Summary of voltage instability test for low voltage solution

| Q | E | E' | 1/cond($D$) | det($D$) | 1/cond($\dot{D}$) | det($\dot{D}$) | eig($\hat{A}$) | $E_{fd}$ |
|---|---|---|---|---|---|---|---|---|
| 0.07 | 0.22 | 0.4037 | 0.077 | -0.2426 | 0.1736 | -0.6754 | -9.1857 | 1.055 |
| 0.17 | 0.24 | 0.4704 | 0.0941 | -0.229 | 0.2358 | -0.7762 | -11.2086 | 1.12 |
| 0.27 | 0.285 | 0.5285 | 0.0285 | -0.0611 | 0.3161 | -0.888 | -48.2318 | 1.185 |
| 0.32 | 0.3 | 0.5585 | 0.014 | -0.029 | 0.3556 | -0.98 | -110.1627 | 1.22 |
| 0.37 | 0.33 | 0.5891 | 0.0696 | 0.154 | 0.3915 | -1.042 | 22.3132 | 1.25 |
| 0.76 | 0.555 | 0.8374 | 0.4855 | 3.036 | 0.2544 | -1.5325 | 1.6653 | 1.5 |
| 0.81 | 0.65 | 0.9049 | 0.5973 | 5.689 | 0.1144 | -1.051 | 0.6096 | 1.5 |
| 0.8326 | 0.765 | 0.9863 | 0.6722 | 10.145 | 0.00047 | 0.00698 | -0.0023 | 1.5 |

caused dynamic voltage instability occurred for very small reactive load increase above that where the field current limit is reached. If the reactive power load is increased to be at 0.85, there is no intersection of the load flow and equilibrium manifolds. This is shown in Figure 4.18.

Table 4.8a and 4.8b are summaries of voltage instability tests for high and low voltage solutions respectively. Note that the signs of the determinant of $\hat{D}$ are always negative for low voltage solutions and positive for high voltage solutions. The sign of $\hat{D}$ and the sign of the eigenvalue of $\hat{A}$ are always in agreement indicating the determinant of $\hat{D}$ is a good test for dynamic voltage stability. This would be an important indicator for determining where the operating point of the system is, especially when the system is close to system bifurcation.

## 4.2    Load Flow and Algebraic Bifurcations

### 4.2.1    Introduction

A twelve bus system (Figure 4.19) with generator dynamics included is the sample system of this section. The air gap saturation, excitation system control, field current limit, and line drop compensation are precisely modeled. It is shown in this section that voltage instability may occur due to load flow or algebraic bifurcation.

### 4.2.2    Load Flow Voltage Instability Simulations

This section demonstrates that

(a)    the load flow voltage instability may occur at a voltage control area of the transmission network which is weakly connected to the rest of the system,
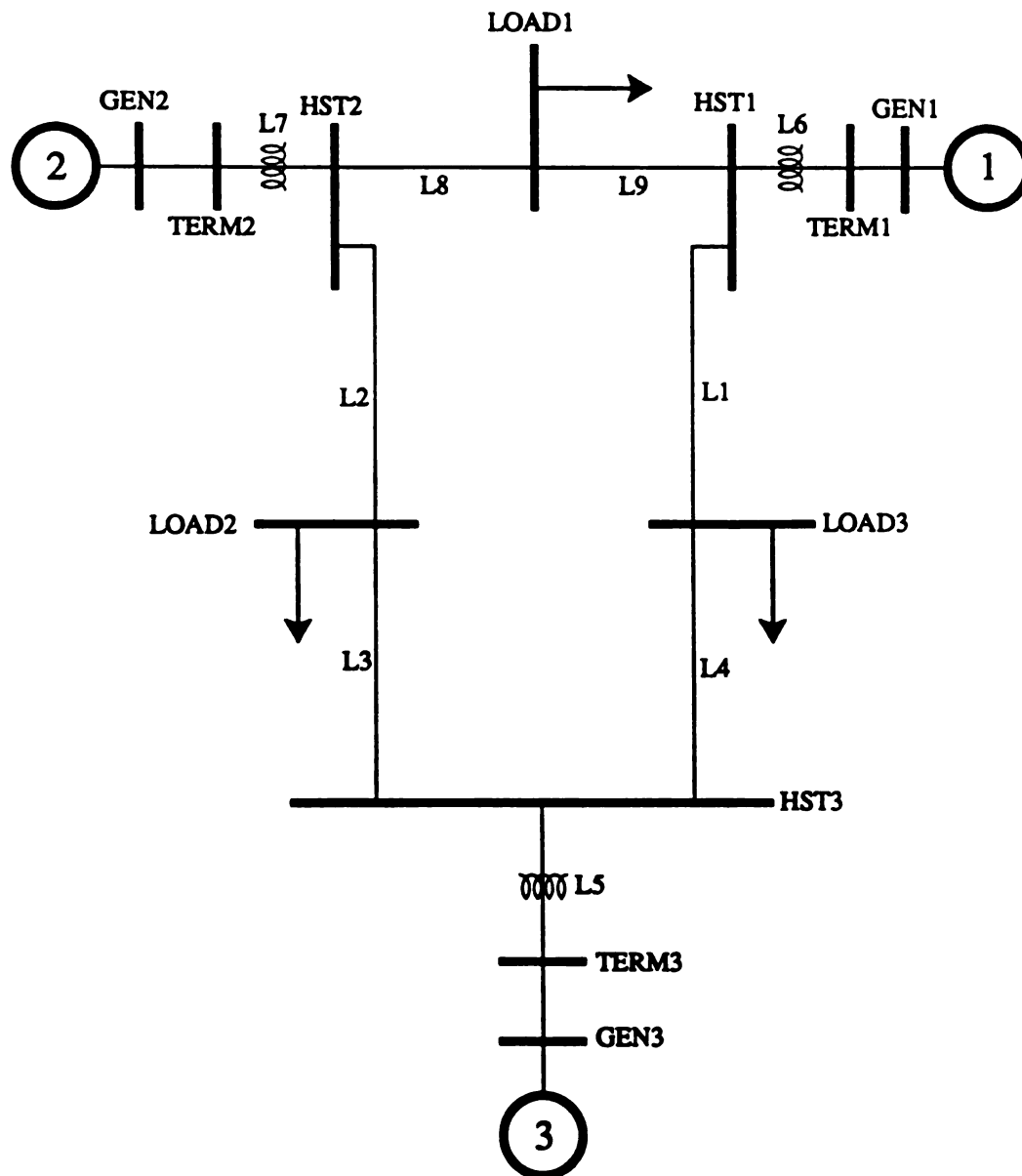
Figure 4.19 A twelve bus test system

(b)   reactive generation reserve can be available on generators at the outside of the voltage control areas but the reactive power can not be transferred through the weak connected transmission lines to the area that needs the reactive power support,

(c)   the load flow voltage instability is a supply and demand problem, and

(d)   the transient stability program is not robust enough to simulate a load flow voltage collapse problem.

In the simulation, the reactances of the transmission lines L2 and L3 are increased by factors of 2.0, 3.0, 4.0, and 4.1. The simulation was performed using the load flow program because

(a)   it is a reactive supply and demand problem and

(b)   the load flow program is much more robust than the transient stability program in solving a stressed network since the load flow assumes the generator terminal bus voltages are specified and need not be solved for but the generator terminal bus voltage must be solved for in the transient stability model. Solving for the algebraic equations for bus voltages at generator terminal buses as well as the high side transformer and load buses and the angles at terminal, high side transformer and load buses in the transient stability model is like solving a load flow without generator PV buses, which is very difficult to solve.

Complete load flow simulation results are given in Appendix C. It should be noted that increasing reactances on L2 and L3 has the effect of causing bus LOAD2 to become a voltage control area. It has been shown that the maximum of the small eigenvalue associated with a voltage control area is the maximum of the sum of the voltage control area bound-

Table 4.9 Load flow simulation for the increase of line reactances at L2 and L3

| Reactance (times) | 1 | 2 | 3 | 4 | 4.1 |
|---|---|---|---|---|---|
| Voltage* (LOAD2) | 0.9576 | 0.9239 | 0.8740 | 0.7946 | 0.7106 |
| Angle* (LOAD2) | -9.1 | -14.5 | -20.4 | -27.4 | -31.8 |
| Voltage (HST2) | 0.9962 | 0.9910 | 0.9864 | 0.9804 | 0.9719 |
| Angle (HST2) | -1.0 | 0.3 | 1.0 | 1.7 | 1.8 |
| Voltage (HST3) | 0.9870 | 0.9833 | 0.9773 | 0.9603 | 0.9206 |
| Angle (HST3) | -7.2 | -9.1 | -10.3 | -11.5 | -11.6 |
| Losses* (L2) | -16.8 | -8.09 | 0.6 | 11.38 | 22.83 |
| Losses (L3) | -14.38 | -9.15 | -0.69 | 12.96 | 23.67 |
| Angle Dif. (L2) | 8.1 | 14.8 | 21.4 | 29.1 | 33.6 |
| Angle Dif. (L3) | 1.9 | 5.5 | 10.1 | 15.9 | 20.2 |

*Angle in degree, voltage in p.u., and losses in MVar.

ary branches connected to any bus. Increasing the reactances of L2 and L3 have the effect of reducing the maximum eigenvalue of this LOAD2 bus voltage control area to zero, assuring that a voltage collapse bifurcation will ultimately occur. These results will establish that load flow bifurcation is a reactive demand supply problem.

Table 4.9 shows

      (a)   the changes of voltages,

      (b)   angle differences between buses HST2 and LOAD2 and buses HST3 and LOAD2, and

      (c)   the line losses of the transmission lines which are connected to bus LOAD2 as reactances L2 and L3 are increased.

In Figure 4.20, load bus voltages are plotted as a function of the magnitude of the line reactances. Figure 4.21 shows dramatic increase in line losses for the increase of the line reactance. Figure 4.22 shows the angle differences of HST2 and HST3 versus the increase in line reactances.

In Figure 4.20, the voltage of bus LOAD2 decreases as we increase the reactances. When the reactances are four times greater than the base case line reactances, the voltage of bus LOAD2 has reached an unacceptable value of 0.7946. The voltages of buses LOAD1 and LOAD3 remain high before the reactances are increased by a factor of 4.1. The PV buses TERM1 and TERM2 have plenty of generation reserve for each of these five cases. The reactive generation reserves at buses TERM1 and TERM2 can not be transferred to LOAD2 area because of the weak connections. It indicates that the load flow voltage instability is a reactive supply and demand problem at the LOAD2 bus.

As the reactances are increased to two times the base case value, the voltage at bus LOAD2 decreases to 0.9239. This voltage decline results in a reactive power supply with-

**Load Bus Voltages**



Dashed line: Bus voltage at LOAD1
Solid line: Bus voltage at LOAD2
Dotted line: Bus voltage at LOAD3
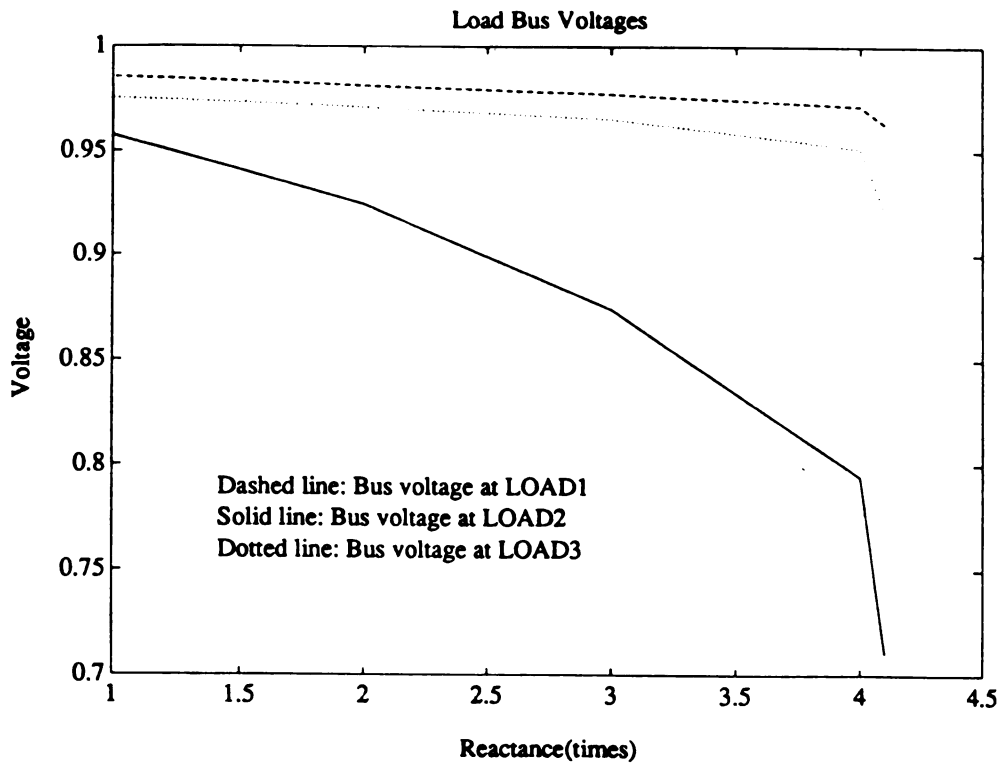
Figure 4.20 Load bus voltages at different line reactances

**Line Losses at L2 and L3**



Dashed line: Line losses(L3)
Solid line: Line losses(L2)
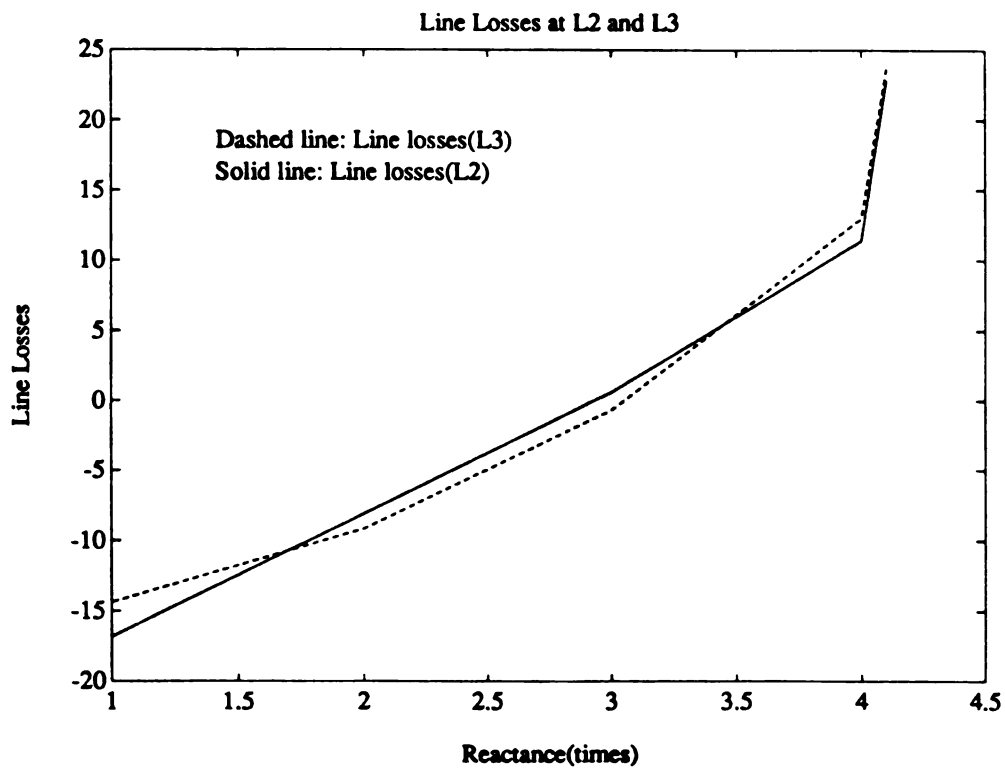
Figure 4.21 Line losses for different line reactances

drawal associated with line charging (Figure 4.21) since the losses are negative when the reactances of L2 and L3 are small and positive as L2 and L3 reactances increase. The negative line losses on L2 and L3 indicate the shunt reactive power provided by the line charging of long transmission lines are greater than the $I^2X$ reactive power losses on the lines when the line reactances are small. As the series reactances increase, the $I^2X$ losses increase dramatically and the reactive power supplied by line charging on these long transmission lines decrease due to voltage drop at LOAD2. Thus, the total reactive losses in Figure 4.21 increase with line reactances. Note that the line losses increase geometrically when line reactance is increased by a factor greater than 4. This geometric increase in reactive losses occurs when the line becomes a drain with SIL greater than 1 and sucks large amounts of reactive power from both buses it is connected to. The development of severe drain problems on voltage control area boundary branches can be shown to occur when branch angle differences exceed a threshold. Note that the angle differences in Figure 4.21 increase and suddenly grow geometrically as drains developed on the boundary branches.

Notice that the voltage at buses LOAD1 and LOAD3 do not respond to the decrease of voltage at bus LOAD2 because the bus LOAD2 is isolated by weak connection and there is plenty of reactive power reserve close to buses LOAD1 and LOAD3 to hold their voltages high.

As the reactances become three times larger than the base case values, the increase of angle differences (Figure 4.22), the decrease of voltage at bus LOAD2, and the increase of line losses at L2 and L3 further weaken the ability of bus LOAD2 to obtain reactive power supply. The voltage at bus LOAD2 decreases to 0.874. The voltage of bus LOAD2 is further decreased to 0.7946 when the reactances of L2 and L3 are increased to four times of their regular values. This voltage is well below the acceptable range. The line losses are about fifteen times larger than the line losses at smaller reactances (3 times the normal values).
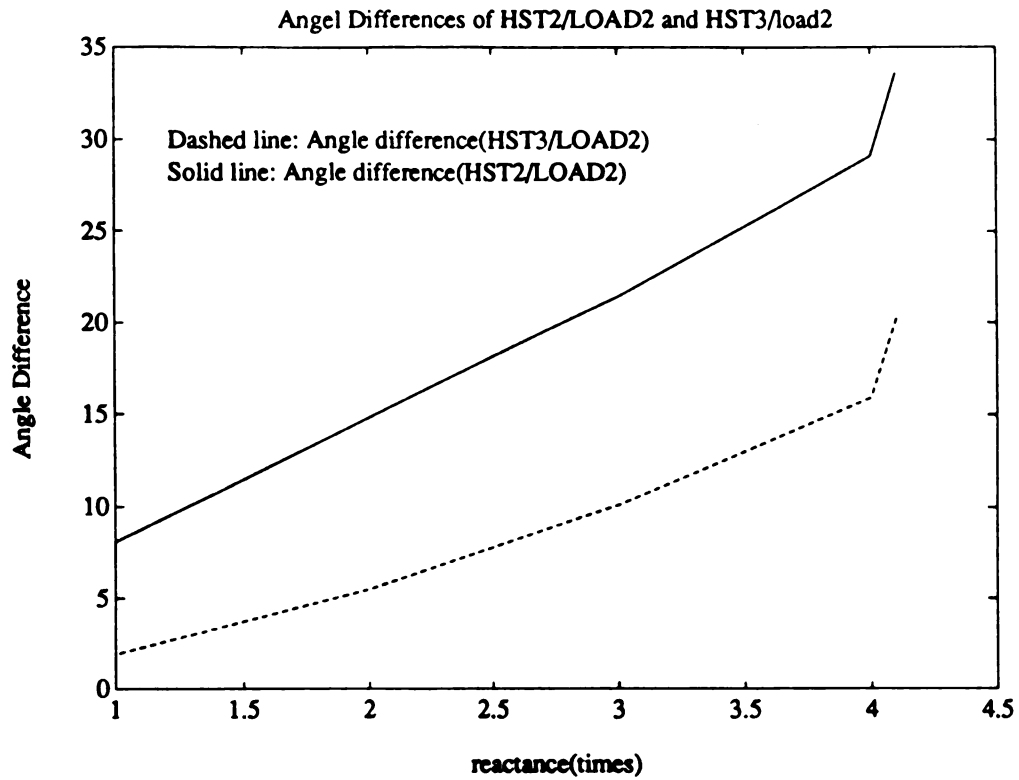
Figure 4.22 Angle differences of HST2/LOAD2 and HST3/LOAD2
at different line reactances

As the reactances of L2 and L3 are increased to be 4.1 times of their base case values, the voltage at bus LOAD2 decreases sharply. The line losses and angle differences are increased tremendously. This indicates this voltage problem is truly a reactive demand and supply problem at bus LOAD2. These results confirm that the algebraic bifurcations are reactive demand supply problems. Large shunt capacitive reactive supply withdrawal at buses in the voltage control area and geometrically increasing reactive losses on voltage control area boundary branches bring on the reactive demand supply problem. Note that the results also confirm that voltage collapse can be forced to occur when the voltage control area boundary is weakened causing the upper bound on the small eigenvalues associated with that voltage control area to approach zero.

### 4.2.3 Algebraic Voltage Instability Simulations

In Section 4.2.2, It was suggested and analytically justified that if the transmission system is stressed by increasing the reactances of L2 and L3, the transient stability program has difficulty in obtaining converged equilibrium solutions. These equilibrium solutions are obtained by simulating the transient stability model based on the converged load flow solution. The lack of convergence of the equilibrium program (steady state solution of the transient stability program) is caused by large real and reactive power load on the transmission system and the increase of the reactances at L2 and L3. In this section, the reactances of L2 and L3 are increased but the real power loads at buses LOAD1, LOAD2, and LOAD3 are decreased by a total of 150 MW. The decrease of the real power load can increase the strength of the network and help the equilibrium program to obtain converged results.

In the simulation, the reactive power load at bus LOAD2 is increased from 40 MVar to 61 MVar. If the reactive power load is equal or larger than 62 MVar, an error message says "error in solving the network discontinuity" would be produced by the equilibrium pro-

gram. The ill-conditioned network matrix prevents the equilibrium program from obtaining a converged solution. The eigenvalues, eigenvectors, condition number, and determinant of the system jacobian matrix, algebraic/dynamic test matrix, and flux decay test matrix are computed for each converged steady state solution. The complete simulation results are provided in Appendix C.

Table 4.10 Changes of the ratio of the determinant of the algebraic
test matrix and the jacobian matrix

| Load level(MVar) | 40 | 45 | 50 | 55 | 58 | 60 |
|---|---|---|---|---|---|---|
| $det(D_{load})/det(D_{40})$ | 1 | 0.7486 | 0.5129 | 0.2816 | 0.1490 | 0.0669 |
| $det(J_{load})/det(J_{40})$ | 1 | 0.8381 | 0.6892 | 0.5180 | 0.4201 | 0.3608 |

Table 4.10 shows the changes of the ratio of the determinant of the algebraic bifurcation test matrix and the jacobian matrix as the reactive power load at bus LOAD2 is increased from 40 MVar to 60 MVar. The ratio drops dramatically in the algebraic bifurcation test matrix. It indicates the transmission network is under stressed and has difficulty in transferring reactive power to bus LOAD2. The ratio for the system jacobian matrix is also decreased from 1.0 to 0.3608. It indicates that the system jacobian matrix is becoming singular and is caused by the singularity of the algebraic bifurcation test matrix because the algebraic bifurcation test is approaching singularity faster. This confirms that a reactive supply and demand program in serving reactive load at load bus is one of the reasons that will cause system voltage instability.

All of the eigenvalues of the jacobian matrix (eigjj) and algebraic bifurcation matrix (eigd) in Appendix C decrease as we increase the reactive power load. This is another method of showing both the system jacobian matrix and the algebraic bifurcation test matrix are approaching singularity.

We have shown that the simulation algorithm of the equilibrium program is less robust than the Newton-Raphson algorithm of the load flow program in the last section. The necessary condition for a Newton-Raphson method to obtain a converged solution is that

$$|\lambda_i|_{min} > 1$$

where $|\lambda_i|_{min}$ is the minimum absolute eigenvalue of the matrix. If any eigenvalue of the load flow jacobian matrix has an absolute value less than one may cause the divergence of the Newton-Raphson algorithm. In the simulation results (Appendix C), the smallest eigenvalue of the system jacobian matrix decreases to 0.0511 and the smallest eigenvalue of the algebraic bifurcation test matrix decreases to 0.1268. These eigenvalues are small enough to violate the necessary condition for Newton Raphson method to guarantee a converged solution. Thus, the equilibrium program that uses a Newton Raphson algorithm to solve the algebraic equations no longer converges when the reactive load at LOAD2 exceeds 62 MVar. A more robust algorithm might allow the load flow and equilibrium programs to converge to solutions at points right up to the point where bifurcation occurs $\lambda_{min} = 0$. Since the equilibrium and load flow program utilize a Newton Raphson algorithm, the solutions very close to bifurcation can not be computed.

Tables in Appendix C.2 shows the equilibrium point for each load level. All of the generators still have plenty of reactive generation reserve since there is no field current limit violation. This result implies that the algebraic bifurcation in the network does not cause significant reactive generation response from the generators due to the weakness of lines L2 and L3.

Algebraic bifurcation simulation(5 time, 55 MVar)

Solid line: GEN3
Dashed line: GEN2
Dotted line: GEN1

time(second)
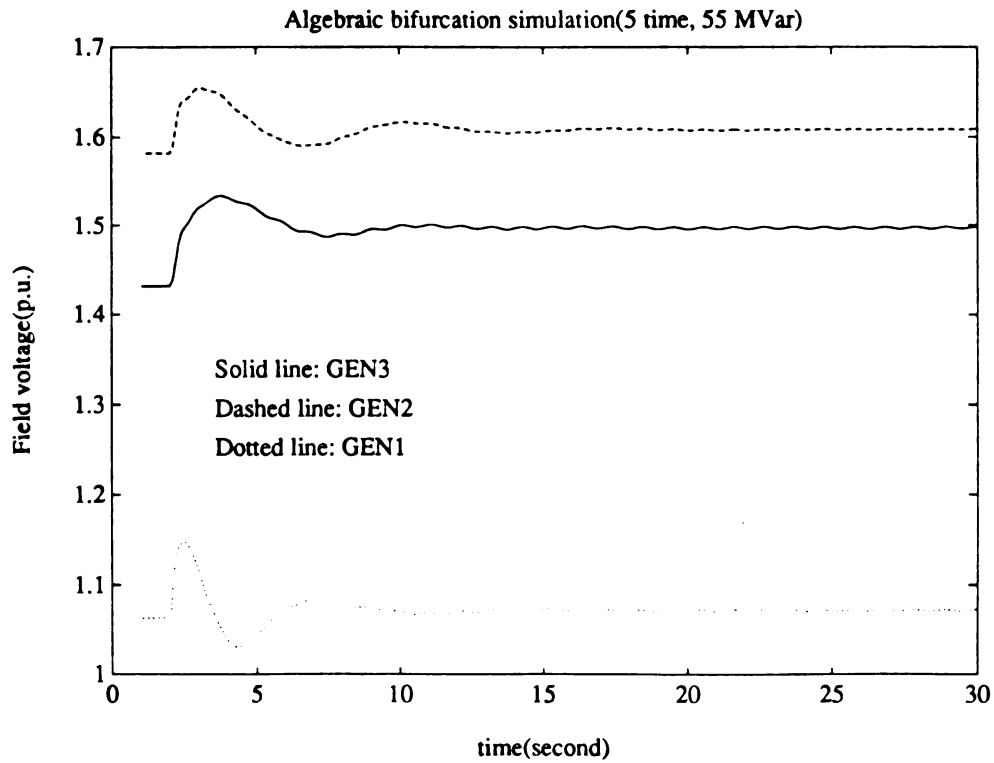
Figure 4.23 Algebraic bifurcation simulation (field voltage)

Algebraic bifurcation simulation(5 time, 55 MVar)

Solid line: GEN3
Dashed line: GEN2
Dotted line: GEN1

time(second)
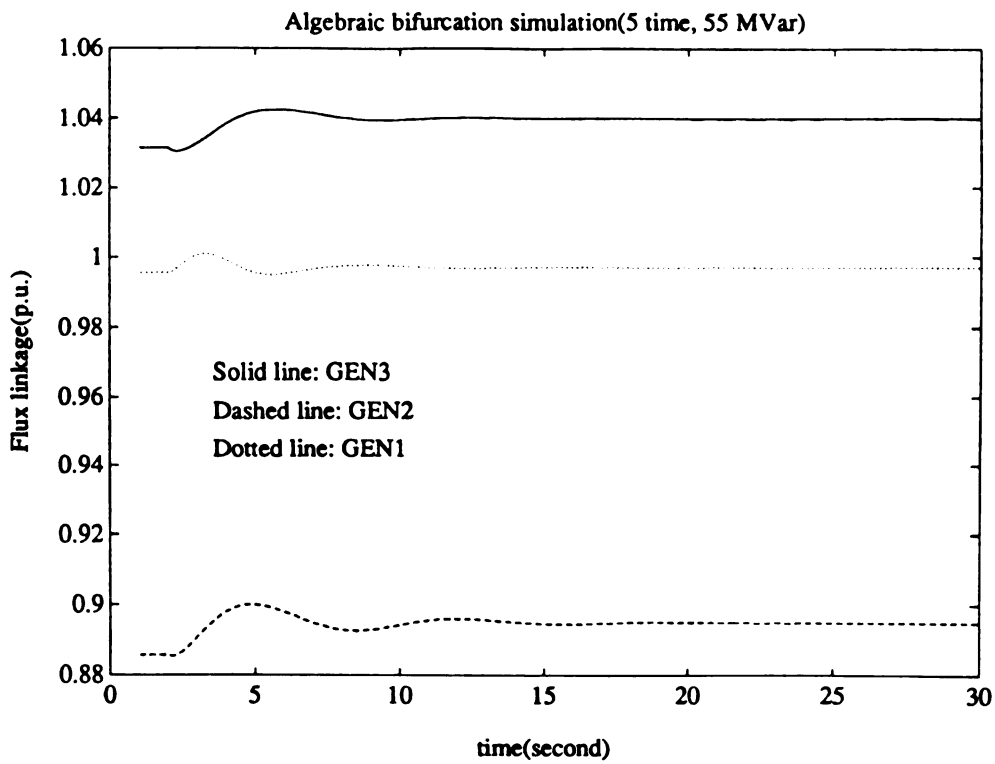
Figure 4.24 Algebraic bifurcation simulation (internal bus voltage)
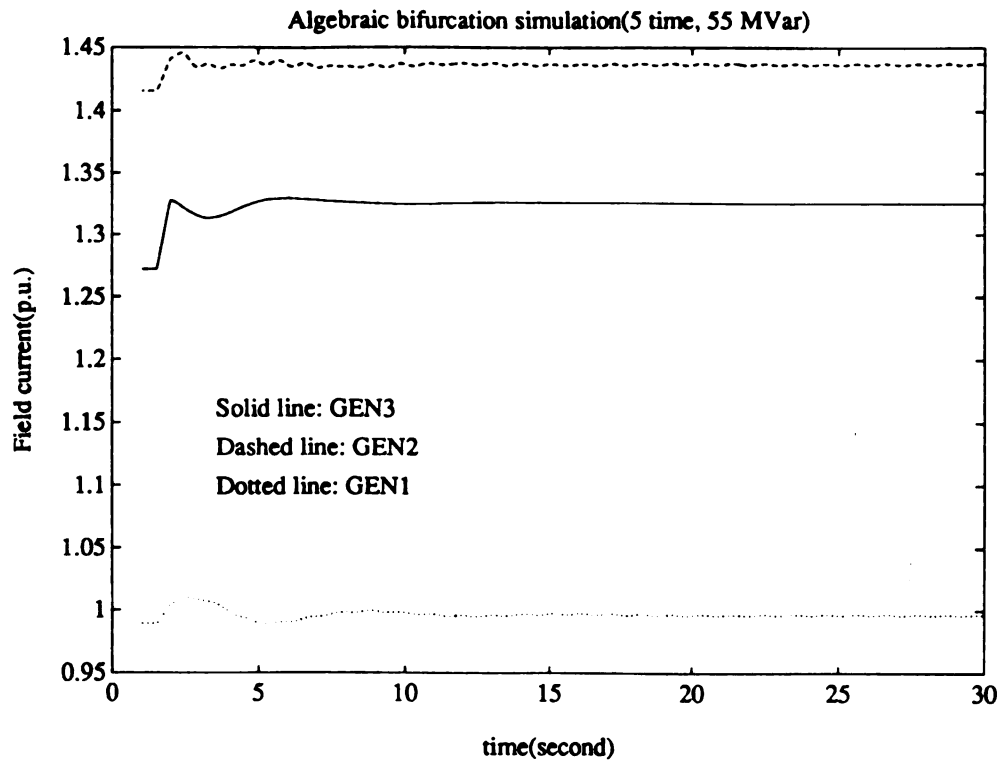
Figure 4.25 Algebraic bifurcation simulation (field current)
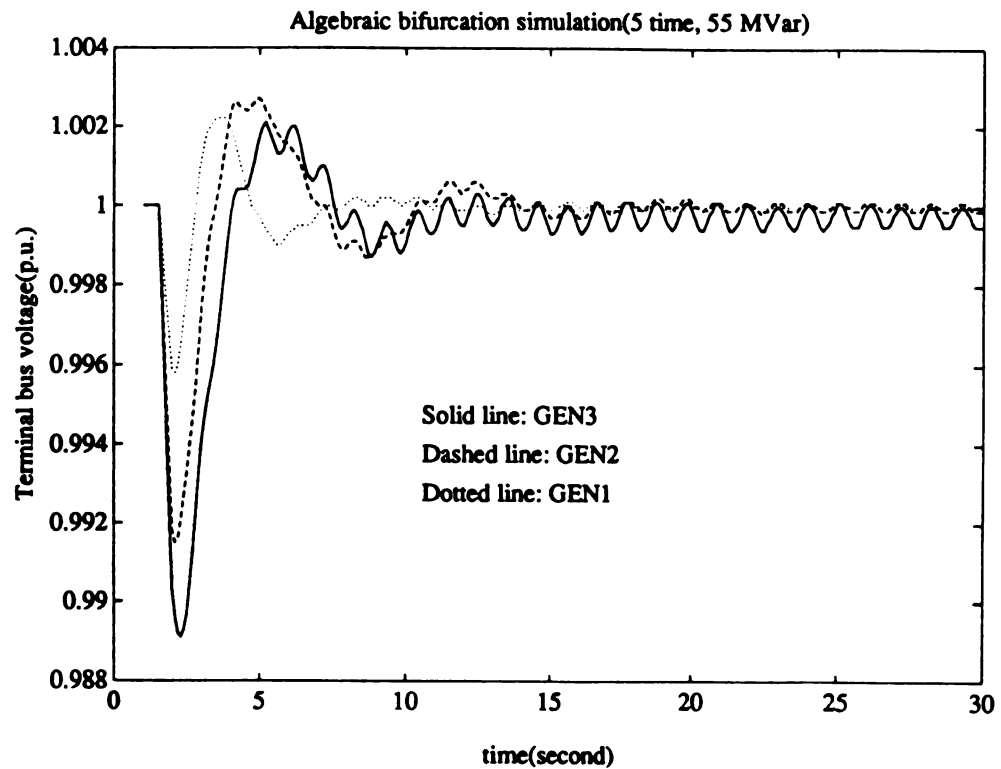


Figure 4.26 Algebraic bifurcation simulation (terminal bus voltage)

Time simulations for field voltage, internal bus voltage, field current, and terminal bus voltage are provided in Figure 4.23, 4.24, 4.25, and 4.26 for the reactive power load at 60 MVar. In Figure 4.23, the field voltages of all three generators are increased to pick up the reactive power load increase at the bus LOAD2. All the field voltage converged to a steady state solution and bus GEN3 and GEN2 pick up most of the reactive power load increase. No field voltage upper limit is hit in this case. Figure 4.24 shows that internal bus voltages of all the generators reach a stable steady state solution. No field current limit (2.2 p.u.) violation occurs as shown in Figure 4.25. In Figure 4.26, all the terminal bus voltages are decreased by the disturbance at the time when the disturbance is introduced. The terminal bus voltages are restored at about 13 seconds. Small oscillations occur in the voltage at the terminal buses. The magnitude of these small oscillations are decreasing and will be damp out if the time simulation is continued. The time simulation results confirm there is no dynamic voltage collapse when the reactive load at LOAD2 is increased from 40 to 60 MVars. These results agree with the results in Table 4.10. Thus, although the system is approaching algebraic bifurcation and a system bifurcation, no voltage collapse bifurcation has occurred.

A lower bound on the minimum eigenvalue associated with a voltage control area is

$$\lambda_{min} \le min \{ \sum_{j=1}^{n+m} \{S_{Q_L V}\}_{ij} \}$$

If the reactive power angle coupling is ignored

$$\hat{\lambda}_i \le min_i \{Q_i - V_i^2 B_{ii} + \sum_{\{(j=1), (j \ne i)\}}^{n+m} V_i V_j B_{ij} \sin(\theta_i - \theta_j - \gamma_{ij}) \}$$

$$\le min_i \{2Q_i\}$$

since there are no PV buses in the network algebraic equations. Thus, if the reactive load $Q_{Li}$ ($Q_i = Q_{Gi} - Q_{Li}$) at a bus in increased as a stress test for a voltage control area, the lower

bound on the minimum eigenvalue decreases. The Q-V curve; which is produced by making a bus in a reactive deficient region a PV bus, reducing the setpoint voltage, and plotting the reactive power generated at the bus, is a plot of the stress test of adding reactive load at the test bus. The parabolic shape of the Q-V curve is shown in Figure 4.28. The knee of the Q-V curve (at which $\frac{dQ}{dV} = 0$) occurs when no more reactive load can be added since the series $I^2X$ losses with voltage drop and the shunt capacitive reactive supply withdrawal with voltage drop overcome the ability to obtain reactive power from the sources of reactive power (synchronous generators). It has thus been shown that the Q-V curve in the general power system model, is a test to determine how small the minimum eigenvalue of a submatrix of $\begin{bmatrix} D_3\ D_4 \end{bmatrix}$ associated with a voltage control area can be. It is clear that the fact that the minimum of a lower bound on a minimum eigenvalue estimate of a submatrix $(S_{Q_LV})$ of $\begin{bmatrix} D_3\ D_4 \end{bmatrix}$ doesn't necessarily indicate a point of singularity of $\begin{bmatrix} D_3\ D_4 \end{bmatrix}$ and J. However, the singularity of $S_{Q_LV}$ has been theoretically shown to relate to every known test [1, 12, 13, 28, 29, 8, 27, 14, 22, 16, 17] for voltage collapse. Showing the Q-V curve is related to a lower bound on the small eigenvalue of $S_{Q_LV}$ associated with a voltage control area links the Q-V curve to all other tests for voltage collapse including the algebraic bifurcation test [27]. The Q-V curve is a standard tool used by industry for assessing proximity to voltage collapse in a load flow. It has been shown to relate the singularity and possible bifurcation of the reactive power balance equations in the general power system model as well as every known test for voltage collapse.

The bifurcation tests results in Table 4.10 indicate that the system is approaching an algebraic bifurcation but the load flow and equilibrium programs do not converge and the EPRI load flow will not solve. The Q-V curve is computed using the equilibrium program and load flow program when reactive load is increased at bus LOAD2.

Figure 4.27a shows the Q-V curve for both load flow and equilibrium program simulation. Since there is no PV bus in the equilibrium program computation, the Q-V curve for equi-
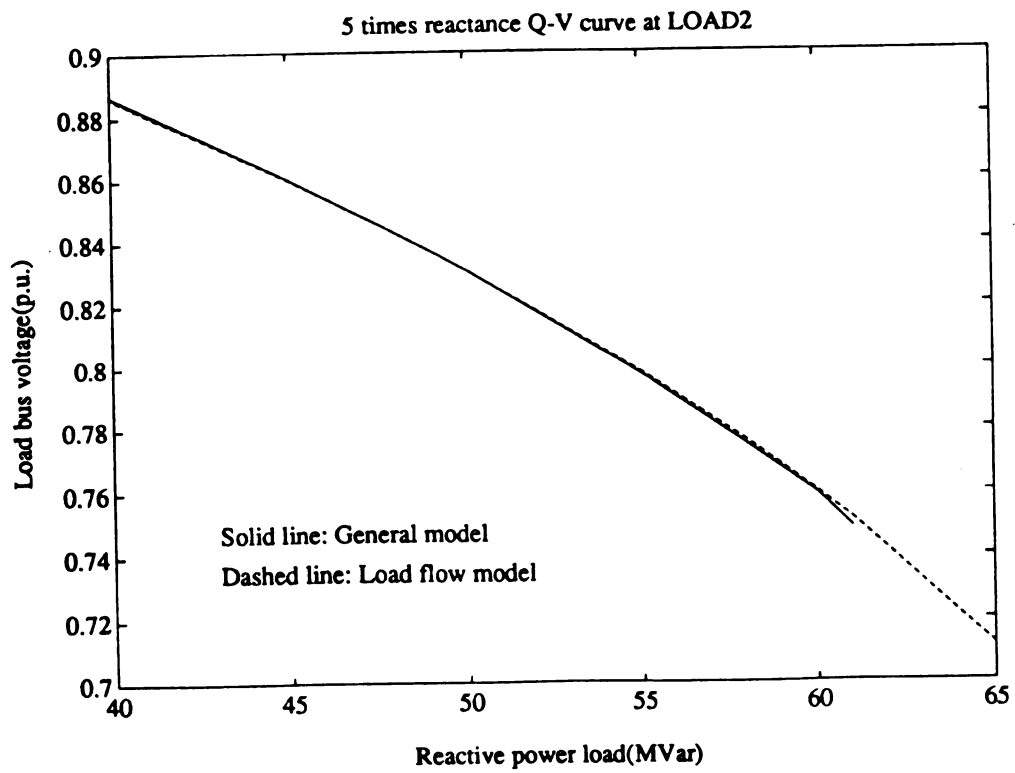
Figure 4.27a Algebraic bifurcation simulation (Q-V curve)
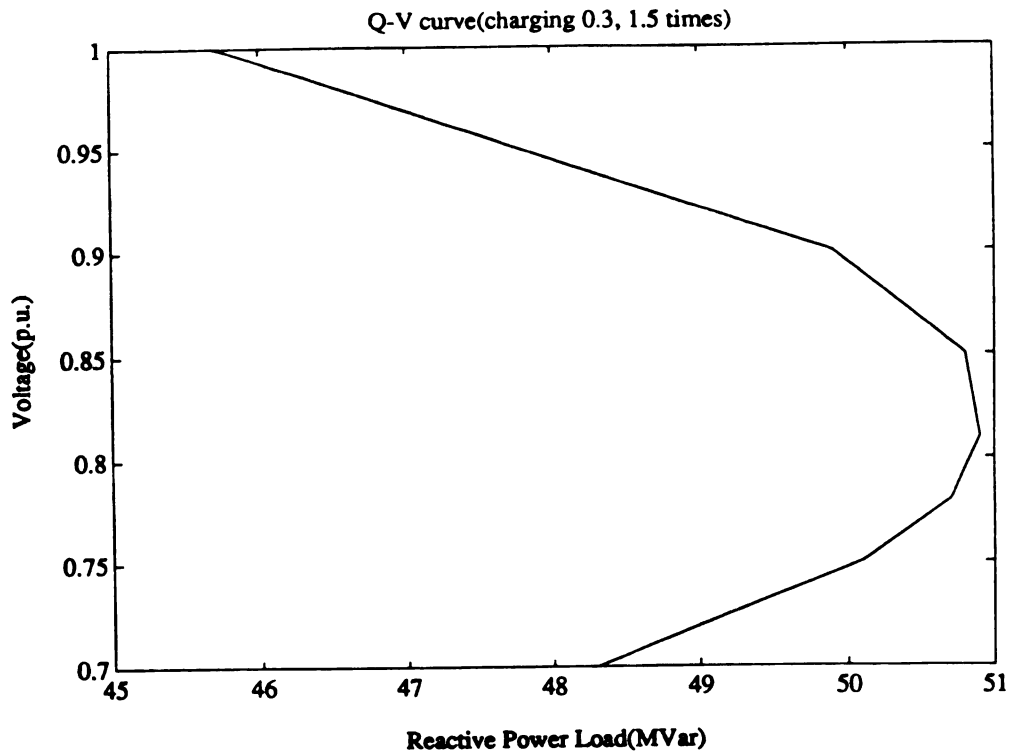


Figure 4.27b Q-V curve (2 times shunt capacitance, 1.5 times series reactance)

librium simulation is performed by increasing the reactive power load at bus LOAD2 and computing it's bus voltage. The Q-V curve for load flow simulation is performed by

(a)    setting bus LOAD2 as a fictitious PV bus with infinite positive and negative reactive generation,

(b)    changing the voltage set point of the fictitious PV bus, and

(c)    computing the reactive generation at that fictitious PV bus.

The negative reactive generation is the reactive power which can be supplied by the system to this fictitious PV bus. The knee of the Q-V curve ($\frac{\partial Q}{\partial V} = 0$) is the point where the maximum reactive power can be supplied by the system to the fictitious PV bus. The Q-V curve for the load flow simulation in Figure 4.27a shows that at 65 MVar the low voltage at bus LOAD2 does not cause a change sign of the Q-V curve. It indicates that the low voltage at bus LOAD2 does not result in large line losses and large capacitive withdrawal of the shunt capacitance. Since the low voltage occurs before the maximum reactive power supply of the system (the knee of the Q-V curve), the system will not experience a voltage collapse at 65 MVars based on either the load flow or general power system model. This confirms the results of Table 4.10 where bifurcation has not occurred at 60 MVars. The slope of the Q-V curve and the bifurcation test results in Table 4.10 indicate the system is close to satisfying the condition for bifurcation. To establish that the test system is not very vulnerable to load flow bifurcation, the test results in Table 4.10 and the Q-V curve are sufficient. However, if the line reactances are multiplied by 1.5 and the shunt susceptances are multiplied by 2, the system should be more vulnerable to voltage collapse. This is confirmed by the Q-V curve for this case given in Figure 4.27b. The knee of the Q-V curve occurs at 0.81 and with a minimum of 51 MVars rather than 65 MVars. Thus, adding shunt reactive supply by increasing line charging did not overcome the effects of increased $I^2X$ losses on branches and increased shunt capacitive reactive with-

drawal.

An extensive set of tests were performed to determine if the system could be modified so that the knee of the Q-V curve would occur at voltage above $V_{min}=.88$ and the reactive margin $Q_{min} = min_V (Q(V_k))$ would decrease. Although increasing the series reactance and shunt susceptances of the transmission lines caused $V_{min}$ to increase and $Q_{min}$ to decrease for load flow computed Q-V curves, the equilibrium program could not even compute one point on some of these curves. An improved equilibrium program is needed to investigate algebraic bifurcation on a general power system model with reactive demand supply problems. Without this improved equilibrium point program, our research had to be content with studying an example system that did not have severe reactive demand supply problems.

## 4.3 Dynamic/Algebraic Voltage Instability Simulations

Because of the large reactance of the transformer compared with the transmission lines, generator terminal buses in a power system can generally be assumed to be isolated from the rest of the system. A system based on this assumption is developed. If there is an increase of reactive power load close to the terminal bus, it will be shown that the generator dynamics will become unstable and cause dynamic voltage instability after the field current limit is reached and the field current limiter disables the exciter control. The simulation shows a rapid decline of the terminal bus voltage immediately occurs after the generator loses the capability of controlling voltage. The air gap saturation and the saturation of the exciter system are shown to contribute to the field current reaching it's upper limit. Complete computer simulation results are in Appendix C.

The twelve bus system (Figure 4.19) is the test system in this section. The generator and exciter data is given in Table 4.11a and 4.11b. The data is taken from [23]. The reactance of L5 is increased by ten times to ensure the buses GEN3 and TERM3 are a voltage con-

Table 4.11a Generator data for the twelve bus system

| | GEN1 | GEN2 | GEN3 |
|---|---|---|---|
| Rated MVA | 250 | 192 | 125 |
| Rated KV | 18 | 18 | 15.5 |
| Rated PF | 0.85 | 0.85 | 0.85 |
| SCR | 1.05 | 0.64 | 0.9 |
| $\tau'_{d0}$ | 9.2 | 5.9 | 8.97 |
| $x'_d$ | 0.195 | 0.232 | 0.174 |
| $x_d$ | 0.995 | 1.651 | 1.22 |
| $x_q$ | 0.568 | 1.59 | 1.16 |
| $x_p$ | 0.16 | 0.102 | 0.078 |
| $S_{G1.0}$ | 0.0769 | 0.105 | 0.1026 |
| $S_{G1.2}$ | 0.282 | 0.477 | 0.432 |
| D | 2.0 | 2.0 | 2.0 |
| A | 0.8178 | 0.85 | 0.8397 |
| B | 2.3167 | 4.67 | 3.9928 |
| $W_R$ | 1603 | 634 | 596 |

Table 4.11b Exciter data for the twelve bus system

| | GEN1 | GEN2 | GEN3 |
|---|---|---|---|
| $\tau_R$ | 0.06 | 0.06 | 0.06 |
| $K_R$ | 1.0 | 1.0 | 1.0 |
| $\tau_A$ | 0.02 | 0.2 | 0.2 |
| $K_A$ | 25 | 25 | 25 |
| $V_{Rmax}$ | 5.99 | 1.0 | 1.0 |
| $V_{Rmin}$ | -5.99 | -1.0 | -1.0 |
| $\tau_E$ | 0.1 | 0.5685 | 0.6758 |
| $K_E$ | -0.02 | -0.0505 | -0.0601 |
| $S_{E0.75max}$ | 0.127 | 0.0778 | 0.0924 |
| $S_{E1.0max}$ | 0.3 | 0.303 | 0.3604 |
| $A_{EX}$ | 0.0096 | 0.0013 | 0.0016 |
| $B_{EX}$ | 1.1461 | 1.3733 | 1.6349 |
| $E_{fdmax}$ | 3.10257 | 3.79307 | 2.3393 |
| $\tau_F$ | 0.48 | 0.35 | 0.35 |
| $K_F$ | 0.0317 | 0.091 | 0.108 |

trol area that is isolated from the rest of the system. The base case data for the simulation of the twelve bus system is in Tables of Appendix C.3. For each simulation, the reactive power load at the bus TERM3 is increased. The equilibrium point of the general power system model is computed. The system jacobian matrix, dynamic/algebraic, and algebraic/dynamic bifurcation test matrices, algebraic bifurcation test matrix, and flux decay bifurcation test matrix and the corresponding eigenvalues and eigenvectors are calculated. The stability of the dynamic states is then being tested. If there is an eigenvalue which has positive real part, a time simulation is performed. It will be shown that reverse actions, such as a decrease of the terminal bus voltage results a decrease of the reactive power generation at a generator bus, may occur in some cases.

This case is a generalization of the dynamic voltage instability observed in the two bus system when the high side transformer and load bus voltage solution of the load flow and equilibrium manifolds converged. The generalization allows for the connection of the generator internal and terminal buses to a power system. The bifurcation occurs due to bifurcation of the generator flux decay and the real and reactive power balance equations at terminal bus since the transformer isolates the generator from the rest of the system and the load at TERM3 is increased.

The reactive power load at the bus TERM3 is 5 MVar in the base case. It is increased to 10 MVar in the first simulation. Table 4.12 shows the equilibrium point of this simulation. The first column and the second column are the number of the snapshot of the transient stability simulation and the time duration at which this snapshot is taken. "11" means the eleventh snapshot and -49.9995 means the eleventh snapshot is taking at 49.9995 seconds and the system solutions have converged to a steady state solution. The third, fourth, and fifth columns are the steady state solutions for the buses GEN1, GEN2, and GEN3 respectively. There are eleven columns for the A-C bus voltage magnitude and A-C bus voltage angle in the last two rows. The first two columns represent the number of snapshot and

Table 4.12 The equilibrium point of 10 MVar load at bus TERM3

```
GENERATOR ANGLE IN DEGREES -NUMBER BUS/GEN NAME NO NUMBER BUS/GEN NAME NO
11 -49.9995 10.4736 45.1464 19.3101

GENERATOR FIELD VOLTAGE -NUMBER BUS/GEN NAME NO NUMBER BUS/GEN NAME NO
11 -49.9995 1.0706 1.5243 1.2870

GEN. FLUX LINKAGE (Q-AXIS) -NUMBER BUS/GEN NAME NO NUMBER BUS/GEN NAME NO
11 -49.9995 0.9861 0.8227 0.9992

GEN. ELECTRICAL POWER - (MW) -NUMBER BUS/GEN NAME NO NUMBER BUS/GEN NAME NO
11 -49.9995 82.5440 123.0011 31.9911

GENERATOR EXCITER SATURATION -NUMBER BUS/GEN NAME NO NUMBER BUS/GEN NAME NO
11 -49.9995 0.0431 0.0146 0.0388

GENERATOR MEGAVAR OUTPUT -NUMBER BUS/GEN NAME NO NUMBER BUS/GEN NAME NO
11 -49.9995 -11.2795 -1.7768 13.7459

GENERATOR FIELD CURRENT -NUMBER BUS/GEN NAME NO NUMBER BUS/GEN NAME NO
11 -49.9995 0.9983 1.3775 1.1563

GENERATOR TERMINAL CURRENT -NUMBER BUS/GEN NAME NO NUMBER BUS/GEN NAME NO
11 -49.9995 0.8331 1.2301 0.3482

GEN. TERM. CURR. ANGLE DEGREES-NUMBER BUS/GEN NAME NO NUMBER BUS/GEN NAME NO
11 -49.9995 7.6718 2.6678 -17.5473

A-C BUS VOLTAGE MAGNITUDE -NUMBER BUS/GEN NAME NO NUMBER BUS/GEN NAME NO
11 -49.9995 1.0000 1.0000 0.9998 1.0078 1.0041 0.9955 0.9924 0.9850 0.9899

A-C BUS VOLTAGE ANGLE DEGREES -NUMBER BUS/GEN NAME NO NUMBER BUS/GEN NAME NO
11 -49.9995 -0.1094 1.8402 5.7049 -2.8605 -2.5509 -4.9643 -5.0428 -6.1330 -5.3102
```

Table 4.13    The eigenvalues of the dynamic/algebraic bifurcation test matrix and the flux decay bifurcation test matrix for 10 MVar load at bus TERM3

```
eigda =                              vtt =

-26.4462 +52.1804i                   1.0000 0.0442 0.0069
-26.4462 -52.1804i                  -0.6955 1.0000 1.0000
-3.8967 +14.9033i                   -0.3321 0.6017 -0.4808
-3.8967 -14.9033i
-3.9132 +14.9901i
-3.9132 -14.9901i                    eigtt =
-15.1523
-16.4814                             1.0e+03 *
-16.5558
-0.3525 + 1.7338i                   -0.1470
-0.3525 - 1.7338i                   -1.1285
-0.1340 + 1.0660i                   -0.5760
-0.1340 - 1.0660i
-0.0342 + 0.9736i
-0.0342 - 0.9736i
-0.0835 + 0.0705i
-0.0835 - 0.0705i
-0.0487 + 0.5929i
-0.0487 - 0.5929i
-0.0108 + 0.5914i
-0.0108 - 0.5914i
```

time duration. The third to the fifth column represent the voltage magnitudes and voltage angles of buses TERM1 to TERM3. The next three columns are for the buses HST1 to HST3. The last three columns are for buses LOAD1 to LOAD3. All the angles are in degrees. The real power is in megawatts. The reactive power is in megavars. The voltage magnitude and current are in per unit. Table 4.12 indicates that the system is operated in a normal condition. No saturation or upper limit violation occurs. The high voltages at buses HST1 and HST2 are caused by large line charging of long transmission lines.

In Table 4.13, the "eigda" represents the eigenvalues of the dynamic/algebraic bifurcation test matrix and the "eigtt" represents the eigenvalues of the flux decay bifurcation test matrix. The negative real parts of the eigenvalues indicates that the system is dynamically stable in this simulation. It will be shown in the simulations that the condition number remains small and will not change dramatically as we change the reactive power load at bus TERM3. It indicates that there is no supply and demand problems in this series of simulation. It is due to the isolation of the generator from the rest of the system and the increase of the reactive power load at bus TERM3 is picked up by the bus GEN3. A complete simulation result which includes condition number of the algebraic bifurcation test matrix and eigenvalues and eigenvectors for the dynamic/algebraic bifurcation test matrix and flux decay bifurcation test matrix are in Tables of Appendix C.3.

Table 4.14 is the equilibrium point of the system when the reactive power load at bus TERM3 is increased to 50 MVar. The field voltage of the bus GEN3 is increased from 1.287 at 10 MVar to 1.6919 and there are small changes in the field voltages of GEN1 and GEN2. It is due to the large reactance of the transformer that isolates the buses GEN3 and TERM3 from the rest of the system. The bus GEN3 has to pick up almost all the reactive power load increase at the bus TERM3. The flux linkage (internal bus voltage $E'_q$) of the bus GEN3 is also increased to support the reactive power generation. The voltage profile of the system is normal and there is no saturation or field current limit violation. The real

117

## Table 4.14 The equilibrium point of 50 MVar load at bus TERM3

```
GENERATOR ANGLE IN DEGREES -NUMBER BUS/GEN NAME NO NUMBER BUS/GEN NAME NO
11 -49.9995 6.6330 41.2437 12.3914

GENERATOR FIELD VOLTAGE -NUMBER BUS/GEN NAME NO NUMBER BUS/GEN NAME NO
11 -49.9995 1.0719 1.5263 1.6919

GEN. FLUX LINKAGE (Q-AXIS) -NUMBER BUS/GEN NAME NO NUMBER BUS/GEN NAME NO
11 -49.9995 0.9864 0.8236 1.0554

GEN. ELECTRICAL POWER - (MW) -NUMBER BUS/GEN NAME NO NUMBER BUS/GEN NAME NO
11 -49.9995 82.5348 123.0010 32.0007

GENERATOR EXCITER SATURATION -NUMBER BUS/GEN NAME NO NUMBER BUS/GEN NAME NO
11 -49.9995 0.0431 0.0147 0.0984

GENERATOR MEGAVAR OUTPUT -NUMBER BUS/GEN NAME NO NUMBER BUS/GEN NAME NO
11 -49.9995 -10.9684 -1.4629 53.2513

GENERATOR FIELD CURRENT -NUMBER BUS/GEN NAME NO NUMBER BUS/GEN NAME NO
11 -49.9995 0.9994 1.3791 1.4841

GENERATOR TERMINAL CURRENT -NUMBER BUS/GEN NAME NO NUMBER BUS/GEN NAME NO
11 -49.9995 0.8326 1.2301 0.6236

GEN. TERM. CURR. ANGLE DEGREES-NUMBER BUS/GEN NAME NO NUMBER BUS/GEN NAME NO
11 -49.9995 3.6286 -1.3086 -57.0667

A-C BUS VOLTAGE MAGNITUDE -NUMBER BUS/GEN NAME NO NUMBER BUS/GEN NAME NO
11 -49.9995 1.0000 1.0000 0.9962 1.0076 1.0039 0.9947 0.9922 0.9845 0.9894

A-C BUS VOLTAGE ANGLE DEGREES -NUMBER BUS/GEN NAME NO NUMBER BUS/GEN NAME NO
11 -49.9995 -3.9413 -1.9900 1.9319 -6.6926 -6.3820 -8.7883 -8.8752 -9.9605 -9.1373
```

Table 4.15 The eigenvalues of the dynamic/algebraic bifurcation test matrix and the flux decay bifurcation test matrix for 50 MVar load at bus TERM3

```
eigda =

-26.4473 +52.1806i
-26.4473 -52.1806i
-3.9097 +14.8996i
-3.9097 -14.8996i
-3.9365 +14.9897i
-3.9365 -14.9897i
-16.4719
-16.5512
-15.1482
-0.3374 + 1.7360i
-0.3374 - 1.7360i
-0.1189 + 1.0689i
-0.1189 - 1.0689i
-0.0402 + 1.0036i
-0.0402 - 1.0036i
-0.0835 + 0.0673i
-0.0835 - 0.0673i
-0.0646 + 0.6331i
-0.0646 - 0.6331i
-0.0257 + 0.6015i
-0.0257 - 0.6015i
```

```
vtt =

-0.6029 0.0333 -0.6322
1.0000 1.0000 -0.2536
-0.4735 0.0371 1.0000

eigtt =

-171.1429
-852.9462
-114.6348
```

part of the eigenvalues of the dynamic/algebraic bifurcation test matrix and the flux decay bifurcation test matrix are all negative. Notice that the eigenvalues of the flux decay bifurcation test matrix have smaller magnitudes compared with the data in Table 4.13. It indicates that the flux decay eigenvalues are moving toward the right half plane as we increase the reactive power load at the bus TERM3.

Table 4.16 shows the equilibrium point of the system as the reactive power load at bus TERM3 is increased to 100 MVar. The field voltage at the bus GEN3 has been increased to 2.1685. The voltage at the terminal bus can not be held close to its preset value and drops to 0.9765 because of the air gap saturation and the excitation system saturation. The eigenvalues in Table 4.17 indicates that the dynamic states are still stable but the flux decay eigenvalues are closer to the origin compared with the data in Table 4.15.

The result of the increase of the reactive power load at the bus TERM3 to be 110 MVar is shown in Table 4.18 and 4.19. The field voltage and reactive power generation of the bus GEN3 are further increased. The voltage magnitude at bus TERM3 is decreased to suck more reactive power from the bus GEN3 to supply its reactive power load increase. The low voltage at bus TERM3 is also caused by the large air gap saturation and exciter saturation. The negative real part of the dynamic/algebraic and flux decay eigenvalues in Table 4.19 indicate that the system is stable.

It can be seen in Table 4.20 that the field current is very close to it's upper limit as we increase the reactive power load to 120 MVar. The terminal bus voltage has dropped to 95 percent of its base case value. It will be shown in the following cases that the terminal bus voltage will decrease tremendously as we increase the reactive power load. It is because the generator can no longer control its terminal bus voltage. Although the upper limit of the field current is not exceeded, it is heavily saturated. The negative real eigenvalues of the dynamic/algebraic test matrix in Table 4.21 indicates that the system is stable.

## Table 4.16 The equilibrium point of 100 MVar load at bus TERM3

```
GENERATOR ANGLE IN DEGREES -NUMBER BUS/GEN NAME NO NUMBER BUS/GEN NAME NO
11 -49.9995 -22.0389 12.2170 -18.1092

GENERATOR FIELD VOLTAGE -NUMBER BUS/GEN NAME NO NUMBER BUS/GEN NAME NO
11 -49.9995 1.0789 1.5374 2.1685

GEN. FLUX LINKAGE (Q-AXIS) -NUMBER BUS/GEN NAME NO NUMBER BUS/GEN NAME NO
11 -49.9995 0.9877 0.8289 1.1037

GEN. ELECTRICAL POWER - (MW) -NUMBER BUS/GEN NAME NO NUMBER BUS/GEN NAME NO
11 -49.9995 82.6329 123.0139 31.9007

GENERATOR EXCITER SATURATION -NUMBER BUS/GEN NAME NO NUMBER BUS/GEN NAME NO
11 -49.9995 0.0433 0.0149 0.3166

GENERATOR MEGAVAR OUTPUT -NUMBER BUS/GEN NAME NO NUMBER BUS/GEN NAME NO
11 -49.9995 -9.2917 0.2288 100.6401

GENERATOR FIELD CURRENT -NUMBER BUS/GEN NAME NO NUMBER BUS/GEN NAME NO
11 -49.9995 1.0056 1.3881 1.8765

GENERATOR TERMINAL CURRENT -NUMBER BUS/GEN NAME NO NUMBER BUS/GEN NAME NO
11 -49.9995 0.8316 1.2301 1.0810

GEN. TERM. CURR. ANGLE DEGREES-NUMBER BUS/GEN NAME NO NUMBER BUS/GEN NAME NO
11 -49.9995 -26.1684 -30.7394 -98.8884

A-C BUS VOLTAGE MAGNITUDE -NUMBER BUS/GEN NAME NO NUMBER BUS/GEN NAME NO
11 -49.9995 1.0000 1.0000 0.9765 1.0066 1.0029 0.9908 0.9912 0.9818 0.9868

A-C BUS VOLTAGE ANGLE DEGREES -NUMBER BUS/GEN NAME NO NUMBER BUS/GEN NAME NO
11 -49.9995 -32.5838 -30.6328 -26.4567 -35.3410 -35.0296 -37.4042 -37.5278 -38.5924 -37.7648
```

### Table 4.17  The eigenvalues of the dynamic/algebraic bifurcation test matrix and the flux decay bifurcation test matrix for 100 MVar load at bus TERM3

```
eigda =

-26.4522 +52.1819i
-26.4522 -52.1819i
-3.9206 +14.9177i
-3.9206 -14.9177i
-4.0319 +14.9750i
-4.0319 -14.9750i
-16.4550
-16.5434
-15.1372
-0.3148 + 1.7424i
-0.3148 - 1.7424i
-0.0353 + 1.1019i
-0.0353 - 1.1019i
-0.1296 + 1.0323i
-0.1296 - 1.0323i
-0.0835 + 0.0649i
-0.0835 - 0.0649i
-0.0664 + 0.6648i
-0.0664 - 0.6648i
-0.0265 + 0.6128i
-0.0265 - 0.6128i
```

```
vtt =

-0.9917 0.0350 -0.2730
1.0000 1.0000 -0.6262
-0.0815 0.0113 1.0000


eigtt =

-152.8097
-815.9868
-42.9767
```

## Table 4.18 The equilibrium point of 110 MVar load at bus TERM3

```
GENERATOR ANGLE IN DEGREES -NUMBER BUS/GEN NAME NO NUMBER BUS/GEN NAME NO
11 -49.9995 -41.6573 -7.5377 -37.8437

GENERATOR FIELD VOLTAGE -NUMBER BUS/GEN NAME NO NUMBER BUS/GEN NAME NO
11 -49.9995 1.0818 1.5420 2.2561

GEN. FLUX LINKAGE (Q-AXIS) -NUMBER BUS/GEN NAME NO NUMBER BUS/GEN NAME NO
11 -49.9995 0.9882 0.8310 1.1094

GEN. ELECTRICAL POWER - (MW) -NUMBER BUS/GEN NAME NO NUMBER BUS/GEN NAME NO
11 -49.9995 82.6391 123.0167 31.8963

GENERATOR EXCITER SATURATION -NUMBER BUS/GEN NAME NO NUMBER BUS/GEN NAME NO
11 -49.9995 0.0433 0.0149 0.3948

GENERATOR MEGAVAR OUTPUT -NUMBER BUS/GEN NAME NO NUMBER BUS/GEN NAME NO
11 -49.9995 -8.6070 0.9225 109.6247

GENERATOR FIELD CURRENT -NUMBER BUS/GEN NAME NO NUMBER BUS/GEN NAME NO
11 -49.9995 1.0081 1.3917 1.9561

GENERATOR TERMINAL CURRENT -NUMBER BUS/GEN NAME NO NUMBER BUS/GEN NAME NO
11 -49.9995 0.8309 1.2302 1.1786

GEN. TERM. CURR. ANGLE DEGREES-NUMBER BUS/GEN NAME NO NUMBER BUS/GEN NAME NO
11 -49.9995 -46.2405 -50.6628 -119.7442

A-C BUS VOLTAGE MAGNITUDE -NUMBER BUS/GEN NAME NO NUMBER BUS/GEN NAME NO
11 -49.9995 1.0000 1.0000 0.9686 1.0062 1.0024 0.9892 0.9908 0.9807 0.9858

A-C BUS VOLTAGE ANGLE DEGREES -NUMBER BUS/GEN NAME NO NUMBER BUS/GEN NAME NO
11 -49.9995 -52.1862 -50.2332 -45.9373 -54.9448 -54.6319 -56.9922 -57.1326 -58.1876 -57.3587
```

## Table 4.19 The eigenvalues of the dynamic/algebraic bifurcation test matrix and the flux decay bifurcation test matrix for 110 MVar load at bus TERM3

```
eigda =

-26.4541 +52.1825i
-26.4541 -52.1825i
-3.9191 +14.9197i
-3.9191 -14.9197i
-4.0663 +14.9742i
-4.0663 -14.9742i
-16.4498
-16.5413
-15.1337
-0.3087 + 1.7447i
-0.3087 - 1.7447i
-0.0293 + 1.1227i
-0.0293 - 1.1227i
-0.1404 + 1.0285i
-0.1404 - 1.0285i
-0.0835 + 0.0646i
-0.0835 - 0.0646i
-0.0662 + 0.6691i
-0.0662 - 0.6691i
-0.0257 + 0.6150i
-0.0257 - 0.6150i
```

```
vtt =

1.0000 0.0359 -0.2668
-0.9899 1.0000 -0.6454
0.0652 0.0097 1.0000


eigtt =

-151.3925
-803.2924
-36.6830
```

## Table 4.20 The equilibrium point of 120 MVar load at bus TERM3

```
GENERATOR ANGLE IN DEGREES -NUMBER BUS/GEN NAME NO NUMBER BUS/GEN NAME NO
11 -49.9995 -81.3496 -47.4235 -77.6249

GENERATOR FIELD VOLTAGE -NUMBER BUS/GEN NAME NO NUMBER BUS/GEN NAME NO
11 -49.9995 1.0857 1.5481 2.3393

GEN. FLUX LINKAGE (Q-AXIS) -NUMBER BUS/GEN NAME NO NUMBER BUS/GEN NAME NO
11 -49.9995 0.9889 0.8337 1.1130

GEN. ELECTRICAL POWER - (MW) -NUMBER BUS/GEN NAME NO NUMBER BUS/GEN NAME NO
11 -49.9995 82.7351 123.0285 31.7987

GENERATOR EXCITER SATURATION -NUMBER BUS/GEN NAME NO NUMBER BUS/GEN NAME NO
11 -49.9995 0.0434 0.0150 0.4876

GENERATOR MEGAVAR OUTPUT -NUMBER BUS/GEN NAME NO NUMBER BUS/GEN NAME NO
11 -49.9995 -7.6940 1.8459 118.2906

GENERATOR FIELD CURRENT -NUMBER BUS/GEN NAME NO NUMBER BUS/GEN NAME NO
11 -49.9995 1.0115 1.3967 2.0380

GENERATOR TERMINAL CURRENT -NUMBER BUS/GEN NAME NO NUMBER BUS/GEN NAME NO
11 -49.9995 0.8310 1.2304 1.2783

GEN. TERM. CURR. ANGLE DEGREES-NUMBER BUS/GEN NAME NO NUMBER BUS/GEN NAME NO
11 -49.9995 -86.5553 -90.7772 -160.4985

A-C BUS VOLTAGE MAGNITUDE -NUMBER BUS/GEN NAME NO NUMBER BUS/GEN NAME NO
11 -49.9995 1.0000 1.0000 0.9580 1.0057 1.0019 0.9872 0.9902 0.9793 0.9844

A-C BUS VOLTAGE ANGLE DEGREES -NUMBER BUS/GEN NAME NO NUMBER BUS/GEN NAME NO
11 -49.9995 -91.8678 -89.9176 -85.4970 -94.6310 -94.3190 -96.6641 -96.8218 -97.8672 -97.0354
```

## Table 4.21 The eigenvalues of the dynamic/algebraic bifurcation test matrix and the flux decay bifurcation test matrix for 120 MVar load at bus TERM3

```
eigda =                          vtt =

-26.4567 +52.1834i               1.0000 0.0370 -0.2646
-26.4567 -52.1834i              -0.9762 1.0000 -0.6620
-3.9179 +14.9206i                0.0539 0.0086 1.0000
-3.9179 -14.9206i
-4.1042 +14.9738i
-4.1042 -14.9738i                eigtt =
-16.4432
-16.5388                        -149.7845
-15.1296                        -786.6969
-0.3014 + 1.7477i               -31.9402
-0.3014 - 1.7477i
-0.0251 + 1.1456i
-0.0251 - 1.1456i
-0.1518 + 1.0259i
-0.1518 - 1.0259i
-0.0835 + 0.0642i
-0.0835 - 0.0642i
-0.0659 + 0.6726i
-0.0659 - 0.6726i
-0.0245 + 0.6175i
-0.0245 - 0.6175i
```

## Table 4.22 The equilibrium point of 135 MVar load at bus TERM3

```
GENERATOR ANGLE IN DEGREES -NUMBER BUS/GEN NAME NO NUMBER BUS/GEN NAME NO
11 -49.9995 -378.5388 -346.0558 -372.2955

GENERATOR FIELD VOLTAGE -NUMBER BUS/GEN NAME NO NUMBER BUS/GEN NAME NO
11 -49.9995 1.1185 1.6006 2.3393

GEN. FLUX LINKAGE (Q-AXIS) -NUMBER BUS/GEN NAME NO NUMBER BUS/GEN NAME NO
11 -49.9995 0.9949 0.8562 1.0562

GEN. ELECTRICAL POWER - (MW) -NUMBER BUS/GEN NAME NO NUMBER BUS/GEN NAME NO
11 -49.9995 82.7741 123.0988 31.8060

GENERATOR EXCITER SATURATION -NUMBER BUS/GEN NAME NO NUMBER BUS/GEN NAME NO
11 -49.9995 0.0442 0.0159 0.4876

GENERATOR MEGAVAR OUTPUT -NUMBER BUS/GEN NAME NO NUMBER BUS/GEN NAME NO
11 -49.9995 0.2228 9.9667 123.5647

GENERATOR FIELD CURRENT -NUMBER BUS/GEN NAME NO NUMBER BUS/GEN NAME NO
11 -49.9995 1.0401 1.4404 2.2099

GENERATOR TERMINAL CURRENT -NUMBER BUS/GEN NAME NO NUMBER BUS/GEN NAME NO
11 -49.9995 0.8278 1.2344 1.4658

GEN. TERM. CURR. ANGLE DEGREES-NUMBER BUS/GEN NAME NO NUMBER BUS/GEN NAME NO
11 -49.9995 -29.0325 -31.5311 -96.8258

A-C BUS VOLTAGE MAGNITUDE -NUMBER BUS/GEN NAME NO NUMBER BUS/GEN NAME NO
11 -49.9995 0.9999 1.0001 0.8692 1.0013 0.9973 0.9694 0.9855 0.9671 0.9726

A-C BUS VOLTAGE ANGLE DEGREES -NUMBER BUS/GEN NAME NO NUMBER BUS/GEN NAME NO
11 -49.9995 -28.8783 -26.9001 -20.9484 -31.6552 -31.3244 -33.5055 -33.8568 -34.7921 -33.9472
```

## Table 4.23 The eigenvalues of the dynamic/algebraic bifurcation test matrix and the flux decay bifurcation test matrix for 135 MVar load at bus TERM3 (without exciter in)

```
eigda =

-26.4792 +52.1911i
-26.4792 -52.1911i
-3.9046 +14.9230i
-3.9046 -14.9230i
-16.4891
-15.1344
-0.3244 + 1.7196i
-0.3244 - 1.7196i
-0.1269 + 1.1085i
-0.1269 - 1.1085i
-0.0838 + 0.6805i
-0.0838 - 0.6805i
-0.0199 + 0.6710i
-0.0199 - 0.6710i
-0.0836 + 0.0629i
-0.0836 - 0.0629i
0.2956
```

```
vtt =

 1.0000 0.0469 -0.2255
-0.9066 1.0000 -0.6684
-0.0013 -0.0004 1.0000


ett =

-137.9121 0 0
0 -659.2447 0
0 0 0.2214
```

Table 4.24 shows the changes of the ratio of the condition number of the jacobian matrix and the algebraic bifurcation test matrix before the exciter on GEN3 is disabled. There are less than 15 percent change for the algebraic bifurcation test matrix and 10 percent change for the jacobian matrix as reactive load at TERM3 is increased. It indicates that no reactive power supply and demand problem occurs. This is confirmed by plotting the Q-V curve for the reactive load increase at TERM3 in Figure 4.31.

Table 4.24 Ratio of the condition number (Algebraic)

| Load | $cond(D_{load})/cond(D_{10})$ | $cond(J_{load})/cond(J_{10})$ |
|------|------|------|
| 10 | 1.0 | 1.0 |
| 50 | 0.9365 | 1.0376 |
| 100 | 0.8758 | 1.0671 |
| 110 | 0.8661 | 1.0714 |
| 120 | 0.8574 | 1.0763 |
| 130 | 0.8642 | 1.0848 |
| 135 | 0.8886 | 1.0935 |

None of the real part of the eigenvalues calculated in this simulation are zero or approaching zero, which means there is no oscillation problem as reactive load increases.

As the reactive power load at bus TERM3 is increased to 135 MVar, the field current upper limit is hit. Since the simulation program does not have the capability to disable the exciter on line, the program converged to a steady state solution. Notice that this equilibrium point is the steady state solution with the exciter. Eigenvalues of the dynamic/algebraic test matrix and flux decay test matrix are computed with $K_{A3}=0$ to represent the loss of the excitation problem. Note that the equilibrium point is computed with AN exciter implemented but the dynamic algebraic test is computed assuming there is no exciter because it is assumed that the state does not change when the machine is operating at the field current

limit before and after the exciter is disabled. The results are shown in Table 4.23. It shows that there is a positive real eigenvalue in both of the dynamic/algebraic and the flux decay test matrices. It indicates that the system becomes unstable. The eigenvector in Appendix C.3 corresponding to this unstable eigenvalue shows that the flux decay state $E'_q$ of GEN3 has the major contribution in this unstable mode. The time simulation of the system without the exciter at GEN3 is calculated for a step reactive load increase of 135 MVars at bus TERM3. Figure 4.28 shows that the internal bus voltage of GEN3 continuously decreases after the disturbance. The field current in Figure 4.29 increases dramatically in the first four seconds and is evidence of the increase in reactive power on GEN3. At 9.8 second, a sharp decrease of the field current occurs and the simulation program stops due to numerical problems. The terminal bus voltage at bus TERM3 in Figure 4.30 is decreased slowly to 0.2 and then experiences a dip to 0.145 at 9.8 seconds in the simulation. The time simulation confirms the voltage instability does occur. This dynamic voltage instability occurs due to action of the uncontrolled generator flux decay dynamics which force the collapse to occur by reducing induced voltage behind transient reactance, the field current, and the reactive power generated by the machine.

If the exciter is not disabled after the field current upper limit is hit and the reactive power load at bus TERM3 is increased, we may still obtain a converged steady state solution but with a reverse action of generator control. Figure 4.32a describes the actions of generator control in the simulation and is a Q-V curve at the generator terminal bus. Note that the Q-V curve indicated by circles in Figure 4.32a is nearly identical to the Q-V curve of Figure 4.31. The circle represents the cases before the reverse action occurs. A decrease in the terminal bus voltage will cause an increase in the reactive power generation to support the reactive load increase. This control action tries to stabilize the system and maintain the terminal bus voltage close to it's preset value. The x-mark represents the cases after the reverse action occurs. A decrease in the terminal bus voltage will cause a decrease in the reactive generation. Thus, the diagonal element of $S_{Q_L V}^{-1}$ are associated with the terminal

Reactive load increase at TERM3(no exciter)
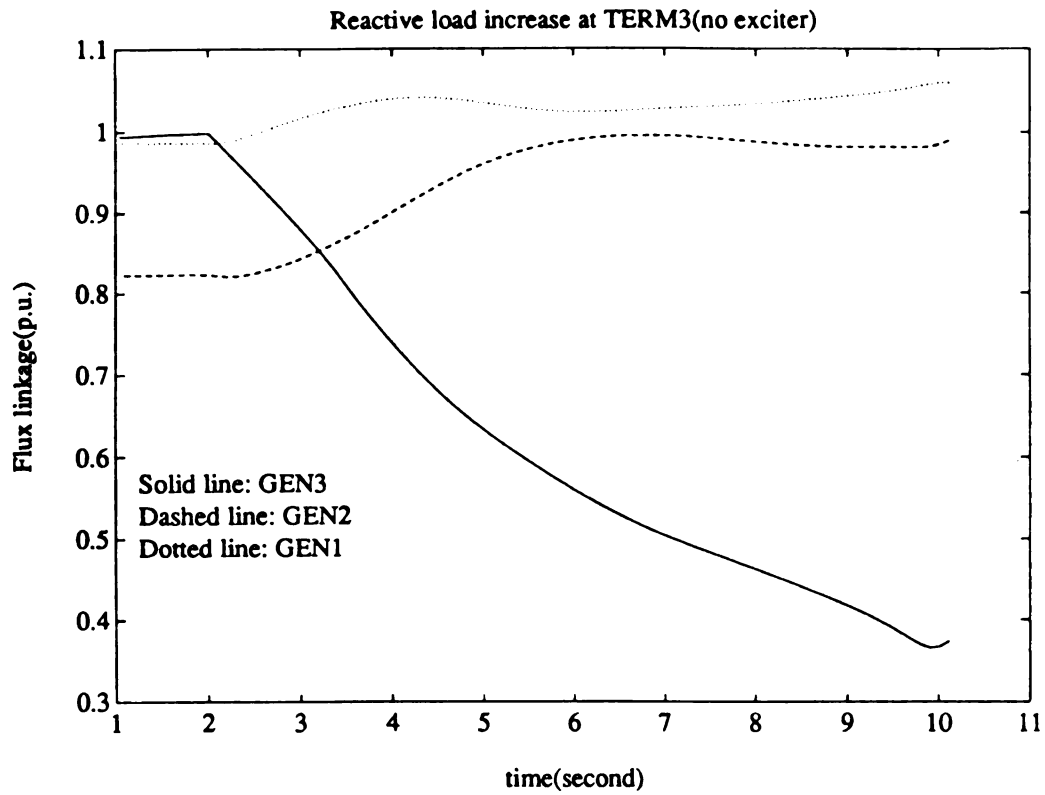


Figure 4.28 Time simulation of $E'_q$ at 135 MVar (without exciter in)

Reactive load increase at TERM3(no exciter)
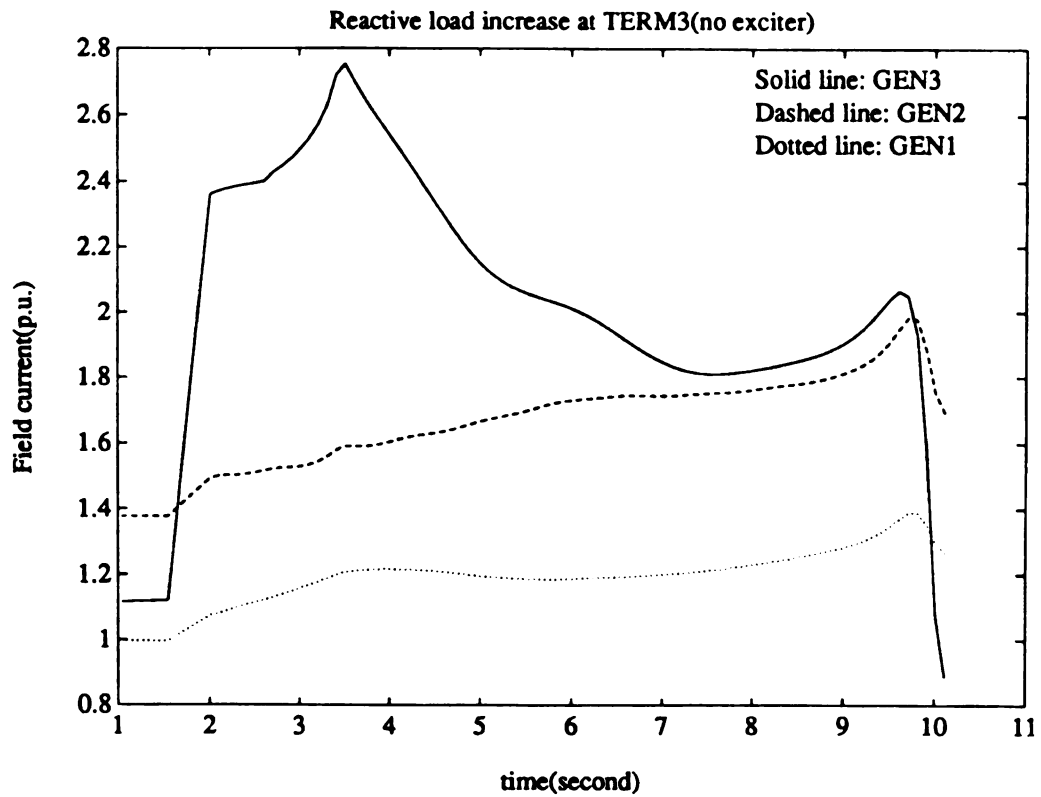


Figure 4.29 Time simulation of $I_{fd}$ at 135 MVar (without exciter in)
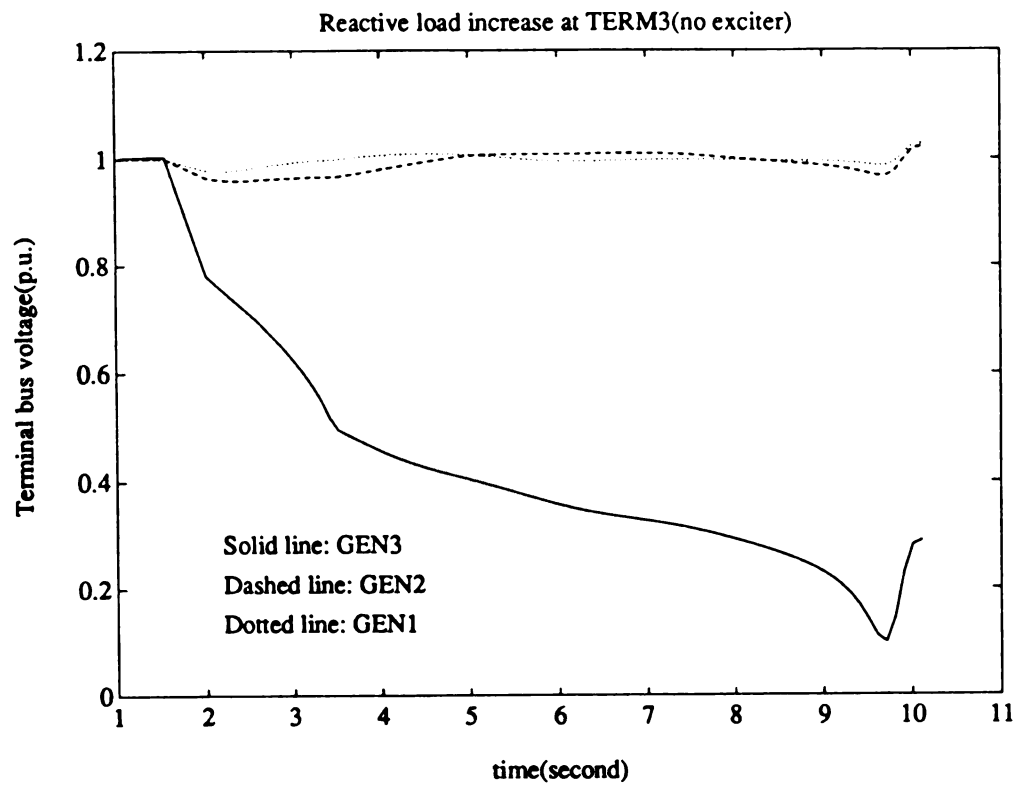
Figure 4.30 Time simulation of $V_T$ at 135 MVar (without exciter in)
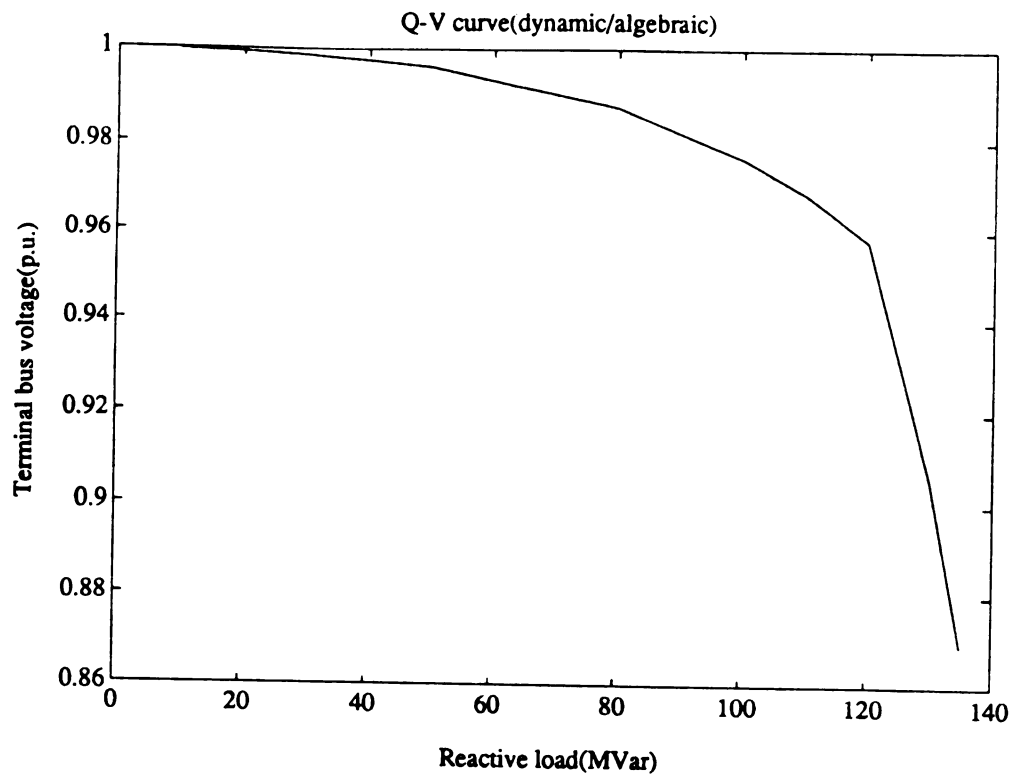
Figure 4.31 Q-V curve at bus TERM3

bus of GEN3 must be negative at points marked by X's where reverse action occurs. Figure 4.32b describes the actions of the reactive generation for a reactive load increase. The dashed line shows the reverse action, an increase in the reactive power load will decrease the reactive power generation. In this case, the diagonal element of $S_{Q_GQ_L}$ associated with the terminal bus of GEN3 is negative. The fact that $S_{Q_GQ_L}$ and $S_{Q_LV}^{-1}$ have negative elements indicate that the closed loop system loses PQ and PV controllability at the points by X's in Figure 4.32a. The points below the knee of the Q-V curve (marked by X's) in Figure 4.32a are also understood to be unstable from the load flow based Q-V curve methods for assessing proximity to voltage collapse. Although Figure 4.32a indicates that a bifurcation point has been reached for system operating at points below the knee of the curve.

The dynamic/ algebraic and algebraic dynamic tests at points below the knee of the Q-V curve indicate the system is still stable but is approaching instability as reactive load increases toward the knee.

This kind of voltage instability is caused by a change sign of $S_{VE}$ and can be explained by root locus. Figure 4.33a is a simplified exciter/flux decay model for a generator. The terminal bus voltage $V_T$ which is controlled by the exciter and the network is fed back to the exciter. Since the network effects can be estimated by the sensitivity matrix $S_{VE}$, Figure 4.33a can be linearized and represented by Figure 4.33b. It is shown in [1] that $S_{VE}$ is positive in the normal operating conditions. Before the reverse action occurs, $S_{VE}$ is positive and the gain is positive. The root locus is shown in Figure 4.33c. The shape of the root locus will change depending on the location of poles and zeros. For a non self excited excitation system, the flux decay pole is generally real and is the closest pole to the $j\omega$ axis. If the reverse action occurs, the sign change of $S_{VE}$ will cause a sign change of the gain. For the negative gain, since the number of poles minus the number of zeros is two, the asymptote is on the real axis which means the root locus has to stay on the real axis for negative gain. Since the flux decay pole is always the closest pole to the $j\omega$ axis, it indicates that

The normal and reverse actions of the reactive generation

circle: normal action

X-mark: reverse action

Reactive generation
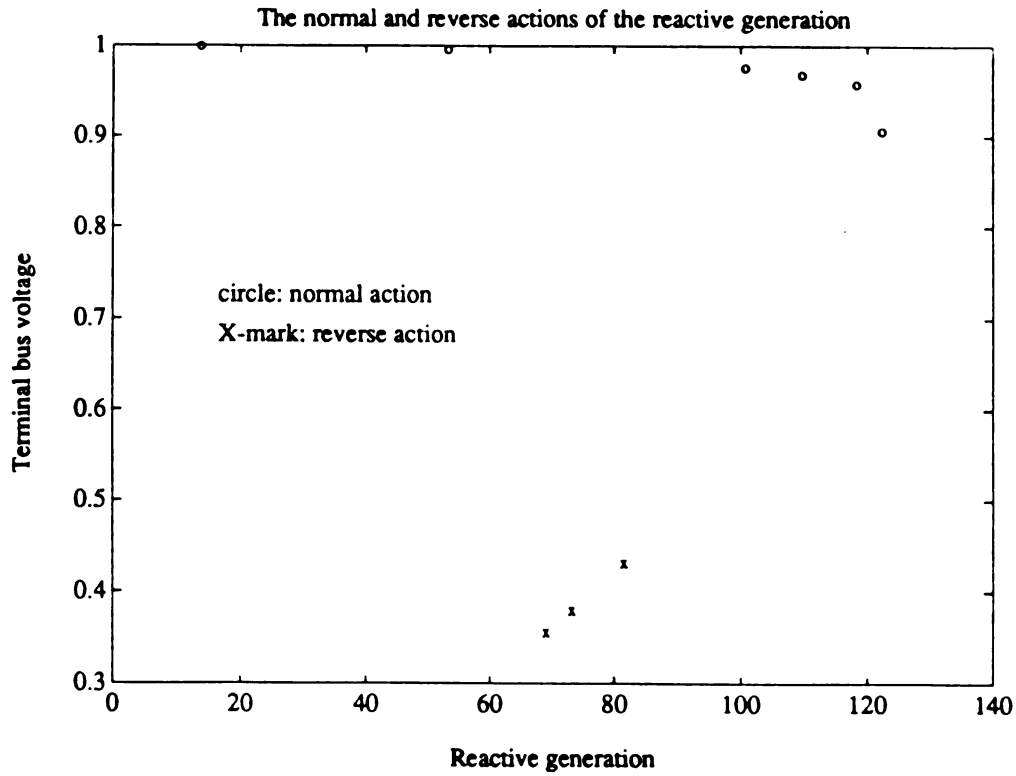
Figure 4.32a The reverse action of the reactive power generation

The reverse action of reactive generation/load

Solid line: Stable case

Dashed line: Unstable case

Reactive power load(MVar)
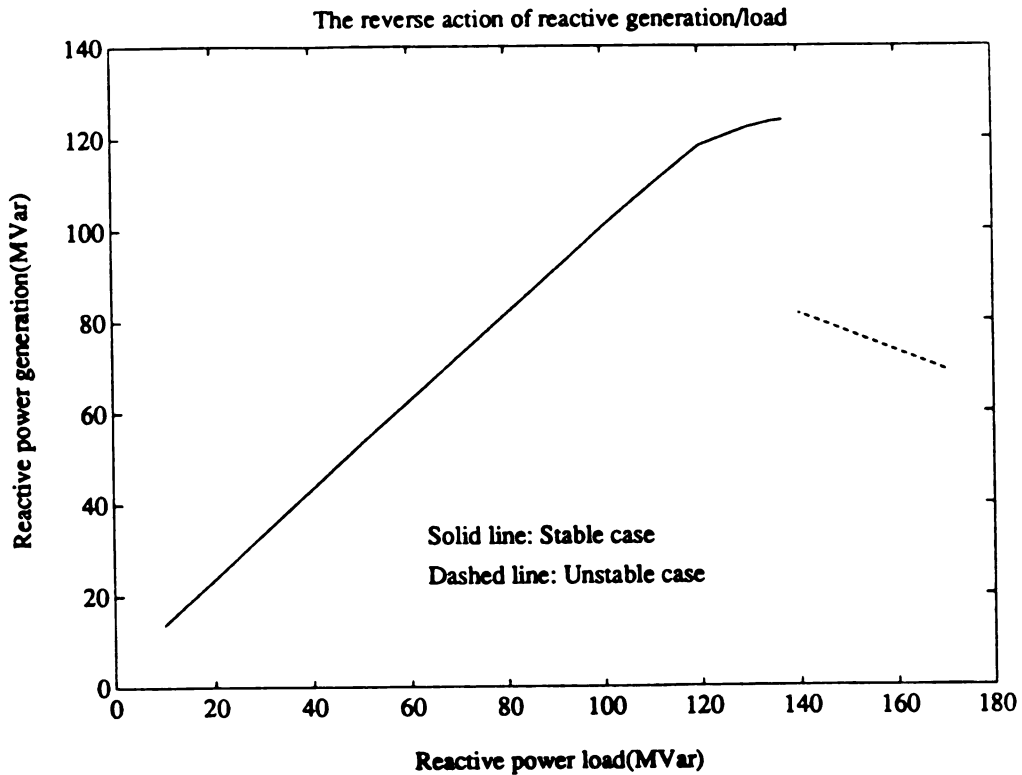
Figure 4.32b The reverse action of the reactive load/generation
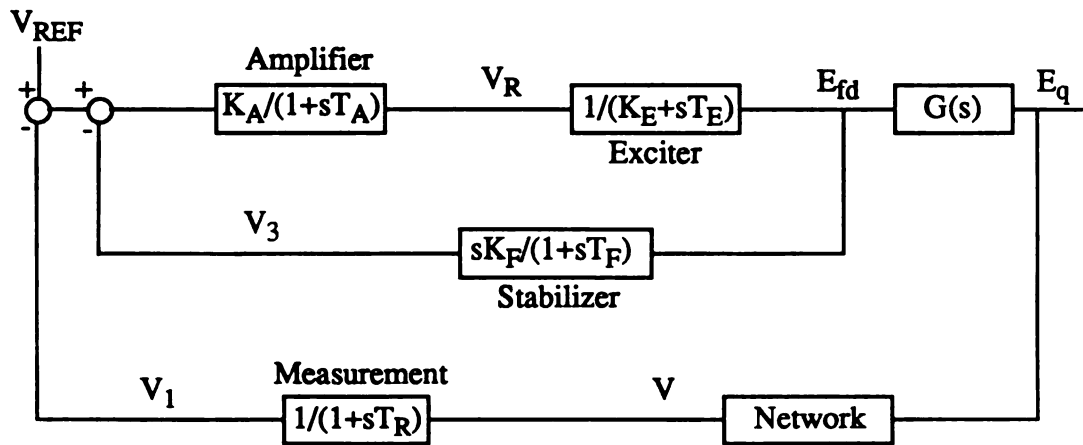
Figure 4.33a Simplified exciter/flux decay model
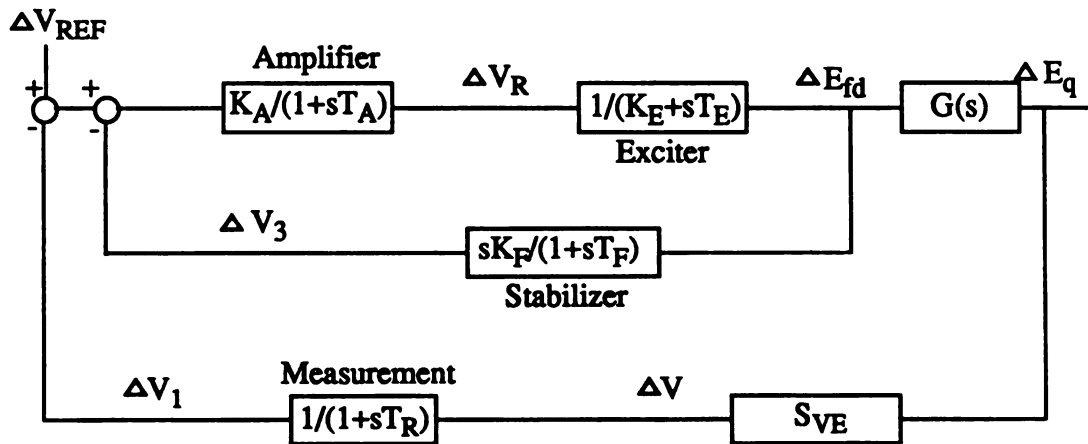


Figure 4.33b Simplified exciter/flux decay model ($S_{VE}$)
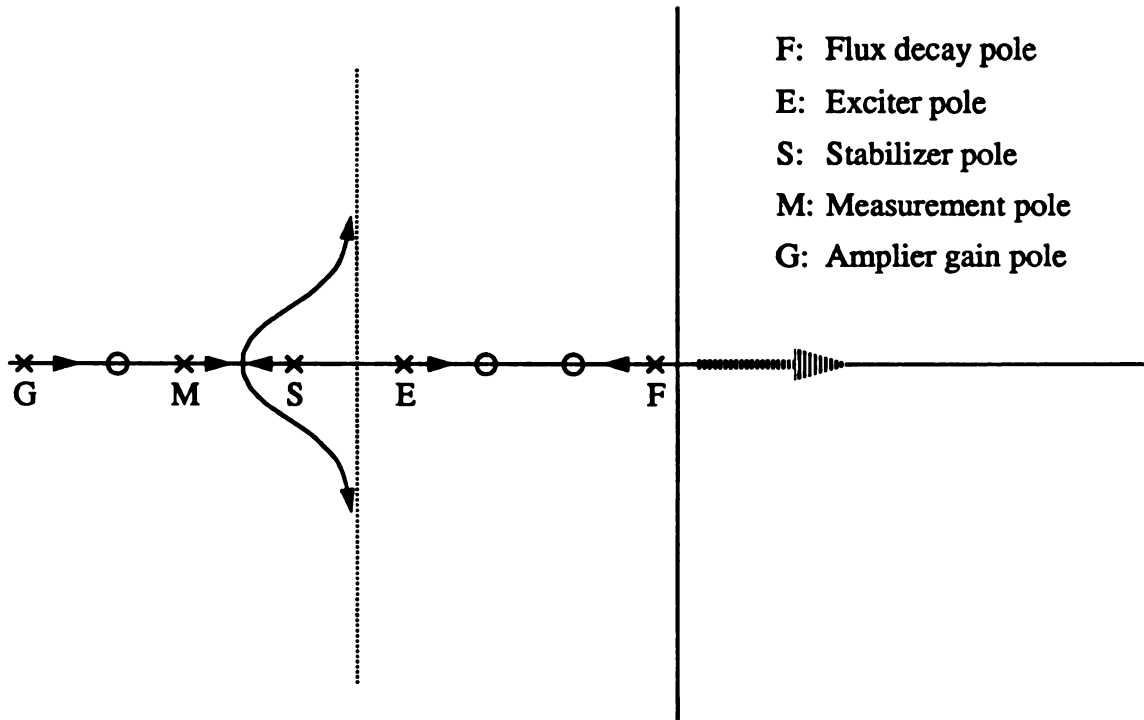
Figure 4.33c Root Locus for A Generator/exciter model(positive gain)
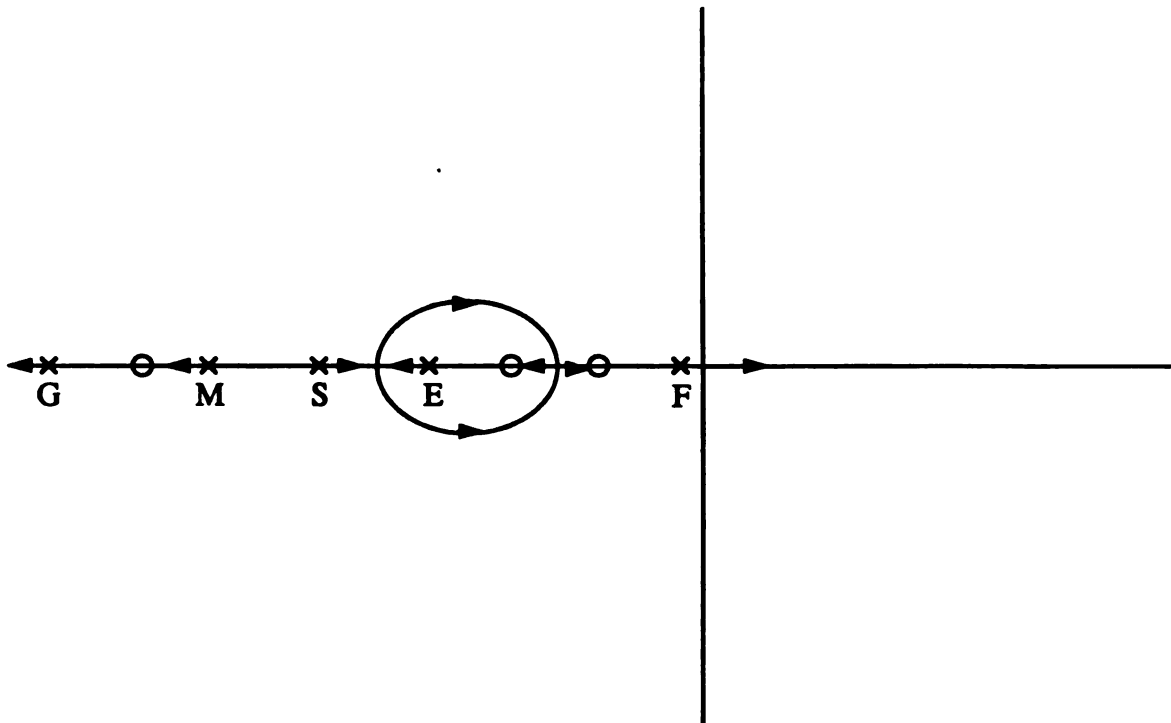


Figure 4.33d Root Locus for A Generator/exciter model(negative gain)

the dynamic instability is caused by the instability of flux decay equations if the reverse action occurred. The gain of the exciter loop becomes more negative and approaches minus infinity as the system approaches the knee of the Q-V curve from below this knee. The decrease in negative gain causes the flux decay pole to move to the right half plane in Figure 4.33d. This explains the loss of dynamic algebraic stability as the knee of the Q-V curve is approached from below the knee.

## 4.4    Algebraic/Dynamic Voltage Instability Simulations

The results in Section 4.3 indicate that the system bifurcation observed in a two bus system composed of a generator and it's terminal can occur in an N bus system if the generator internal and terminal bus of a particular generator are a voltage control area with a weak boundary and the reactive load at the terminal bus is increased. The system experiences a dynamic/algebraic bifurcation after the field current limit is hit and the exciter is disabled. The dynamic/algebraic bifurcation causes the field current and voltage behind transient reactance to approach zero that forces the system into voltage collapse. This result is identical to that on the two bus system. Furthermore, the system has a stable equilibrium point at low voltage when the exciter is not disabled just as in the two bus system model given in [21]. However, if reactive load is increased, the system could experience sustained oscillations.

This simple extension of the two bus system result to the more general 12 bus model is now followed by a slightly more complex case. Lines L2 and L4 reactances are increased so that buses GEN3, TERM3, and LOAD2 are a voltage control area. The reactive load at LOAD2 is increased. In this case, it is hoped that an algebraic bifurcation (reactive demand supply problem) will occur as the network attempts to serve the reactive load at LOAD2. This algebraic bifurcation will hopefully lead to a dynamic/algebraic bifurcation and a dynamic voltage collapse at GEN3. The system has been shown to be not very vul-

nerable to reactive demand supply problems from results in Section 4.2. Thus, the results in this section do not indicate that a reactive demand supply problem (algebraic bifurcation) develops but a dynamic/algebraic bifurcation occurs after the field current limit is reached and the exciter is disabled. This section is titled Algebraic/Dynamic Voltage Instability Simulation because of the assumption that a system can experience dynamic/algebraic voltage instability and algebraic voltage instability simultaneously in an actual power system when the reactive demand supply problem leads to a dynamic voltage instability problem. It is believed that this is a very common type of voltage instability on actual power systems that are vulnerable to reactive demand supply problems.

The algebraic bifurcation test, system bifurcation test, and Q-V curve indicates the system never experiences a reactive demand supply problem (load flow bifurcation) before the field current limit on GEN3 is reached. However, it will be shown that an oscillation problem may develop as the reactive power load is increased and the field current of GEN3 is below but approaches it's upper limit. The real part of the eigenvalues of the dynamic/algebraic bifurcation test matrix approaches zero as LOAD2 reactive load increases. If the exciter is disabled at the point where the field current is very close to it's upper limit, eigenvalues of dynamic /algebraic test is positive. This indicates a dynamic voltage instability has occurred which results in field current and voltage behind transient reactance approaching zero. An attempt was made to simulate the voltage collapse problem using the EPRI Extended Transient Mid Term Stability Program. The simulation program provides the "error in solving differential equations" error message. It indicates that the current simulation program is not suitable for the voltage instability simulation. A new program that includes the air gap saturation, field current limit, line drop compensation with much more robust algorithm needs to be developed to investigate the voltage instability of a power system.

Figure 4.34 is the Q-V curve at bus LOAD2 for the general model and load flow model.
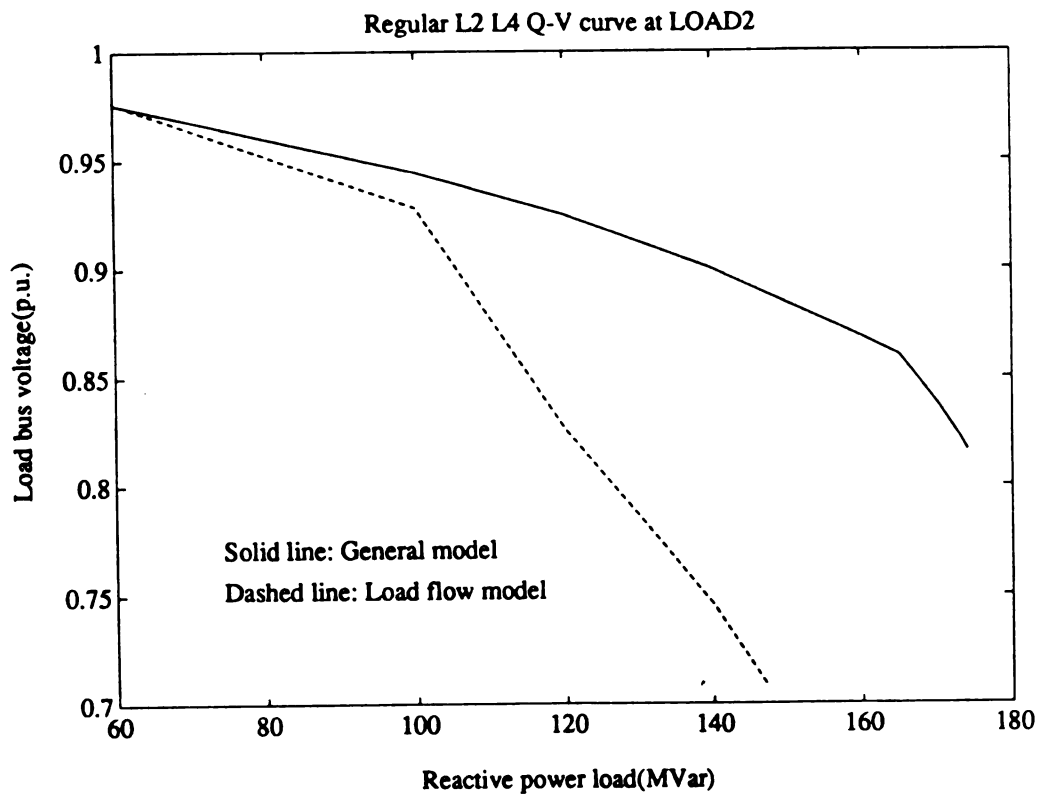
Figure 4.34 Q-V curve for algebraic/dynamic simulation

The solid line shows that the field current limit is hit before the Q-V curve reaches the knee for the Q-V curve produced using the general power system model. The result indicates that the system did not reach the knee of the Q-V curve before the field current limit is reached at reactive load of 170 MVars. The equilibrium program did not converge at reactive load above 170 MVars. The load flow model (Dashed line) diverges earlier than the general model in this case because the reactive generation limit defined in the load flow model is conservative as shown in Figure 4.35. Since the increase of the reactive power load has to be picked up by TERM3 in the load flow model, the small reactive reserve at generator connected to TERM3 is quickly exhausted and causes large voltage decrease (Dashed line).

The reactive generation limit of the load flow model is decided by the capability curve. The capability curve of a synchronous machine shows the limits placed on the electrical watts and VARs (a) by the permissible temperature rise of the windage, and (b) by the mechanical system connected to the shaft, and (c) assuming operation at rated terminal voltage. Figure 4.35 shows a typical capability curve for a generator, plotted on the S plane, where P is the vertical axis and Q is the horizontal axis. Operation within the boundaries of the curve is safe from the standpoints of heating and stability. The maximum reactive generation is decided by the level of real power generation. Since the real power generation is fixed in the load flow model, the maximum reactive power generation could be decided by the capability curve at that specific real power generation level.

The actual load flow reactive generation limit is specified as some approximation to the field current limit in the transient stability model. The field current limit which is the rotor heat limit, is specified at the intersection of the stator heat limit and rotor heat limit. This intersection point is point B in Figure 4.35 . This point B is specified in terms of the stator heat limit $|S|$ and the power factor of the generator. The stator current phasor can be calculated from this information, and the voltage at the internal bus can be calculated. Since the

+P axis

$$C = \frac{3V_1B}{x_d}$$

A

$CE_f$

B

$Cjl_1 x_d$

Rated P of
prime mover

Stability limit

$\delta_{max}$

$\delta$

Generator

0

Motor

$CV_1$

+Q axis

$\delta_{max}$

Stability limit

Stator heat limit

Rated |S| of
sync. machine

$CK'l_{f\,max}$

Rotor heat limit

$$\frac{3V_{1B}^2}{x_d}$$

(Assumes $V_1 = V_{1B}$)
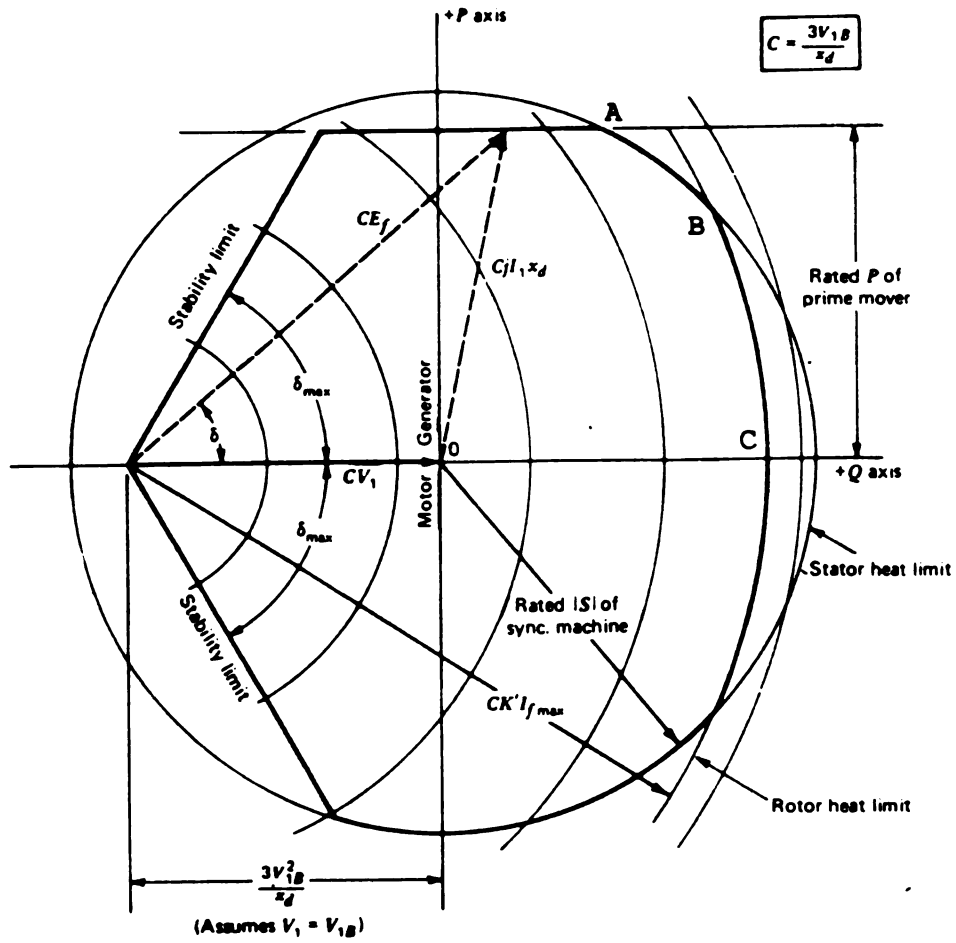
Figure 4.35 Generator capability curve

magnitude of the generator internal voltage is proportional to the field current, the maximum field current can be calculated. It should be noted that this is the continuous rating level and that the field current can exceed this continuous rating level for short period as long as the field current capability curve shown in Figure 2.3 is not exceeded. Generally, the reactive generation limit in a load flow is taken as points A, B, or C in Figure 4.35 depending on the application and operating condition. If point A, is chosen, the generator can produce its maximum real power generation without exceeding the stator heat limit or rotor heat limit. However, the generator could produce far more reactive generation if the generator operated at a real power generation level far below the maximum real power generation level. Point A is a conservative choice for reactive generation limit. If the reactive generation limit was chosen to be at point B, the continuous rating rotor field current limit, the stator heat limit would be exceeded if the generator produced real power above that at point B, $P_B = S \times Pf_B$ . If point C is chosen, the stator heat limit and rotor heat limit would be exceeded if real power is generated and the stator heat limit would be exceeded for real power generation levels above $P_B$. Note that although the transient stability model can exceed the rotor heat limit for short periods without having to modify the excitation control, the load flow must utilize the rotor heat limit since a load flow is a model of the steady state operating condition of the generator. If the rotor heat limit were ever exceeded in the steady state operating condition, physical damage to the generator would result. The load flow reactive generation limit on a generator is often chosen at point A since the rotor heat limit and stator heat limit will never be exceeded. The reactive generation limit was always chosen as point A in this case. Sometimes, point B can be used to specify the rotor heating limit as long as the generator is operating far below $P_B$. Point C might be used for a synchronous condenser. It should be noted that the transient stability model can produce more reactive power in steady state based on the rotor heat limit in Figure 4.35 than the reactive power limit based on point A in Figure 4.35 . Furthermore, the transient stability model can produce more reactive power than the rotor heat limit as long as the

field current level and duration not above the field current capability curve of Figure 2.3. Thus, the load flow would appear to be conservative. The load flow's conservatism in predictingproximity to voltage collapse depends on

(a)    how effective the generator excitation control is in controlling the voltage at some point in the network called the control point.

(b)    how the load flow approximates the actual control point determined from the load drop compensator.

The voltage control point is decided by the setting of line drop compensation in the power system. The voltage control point can be at a point between internal bus and terminal bus, terminal bus and high side transformer bus, or out in the network. The voltage control point out in the network is generally less vulnerable as long as the control is maintained but the control will be lost more quickly. Conversely, the voltage control point close to the generator internal bus is more vulnerable (less effective in controlling voltage) but the control is lost more slowly. There are generally two possible control points in the load flow model, which are the generator terminal bus and high side transformer bus. If the actual voltage control point is chosen to the generator internal bus than is modeled in the load flow, the load flow modeling would make the system appear less vulnerable to voltage problems as long as the voltage control is active since network voltage is more effectively controlled than in the transient stability model. However, the generator would generally lose its reactive generation reserve in the load flow due to the more effective control of network than in the transient stability model. Losing the control of voltage due to exhaustion of reactive generation reserves in the load flow and not in the ttransient stability model makes the load flow far more vulnerable to loss of voltage stability than the transient stability model.

The reactive power load at bus LOAD2 is increased from 100 MVar to 170 MVar. Table 4.25 shows the change of the ratio of condition numbers. The changes of the condition

Table 4.25 Ratio of the condition number (algebraic/dynamic)

| load (MVar) | cond($D_{load}$)/cond($D_{100}$) | cond($J_{load}$)/cond($J_{100}$) |
|---|---|---|
| 100 | 1.0 | 1.0 |
| 120 | 0.9727 | 1.0271 |
| 140 | 0.9513 | 1.0650 |
| 160 | 0.9385 | 1.1000 |
| 170 | 0.9481 | 1.1194 |

Table 4.26 The eigenvalues of the algebraic/dynamic bifurcation test matrix and the flux decay bifurcation test matrix for 100 MVar load at bus LOAD2

```
eigda =

-26.4918 +52.2103i
-26.4918 -52.2103i
 -3.8952 +14.9051i
 -3.8952 -14.9051i
 -3.9486 +14.9862i
 -3.9486 -14.9862i
-15.2041
-16.4660
-16.5489
 -0.3457 +  1.6967i
 -0.3457 -  1.6967i
 -0.0397 +  1.1176i
 -0.0397 -  1.1176i
 -0.0841 +  0.0200i
 -0.0841 -  0.0200i
 -0.0598 +  0.9093i
 -0.0598 -  0.9093i
 -0.0716 +  0.6173i
 -0.0716 -  0.6173i
 -0.0479 +  0.5770i
 -0.0479 -  0.5770i
```

```
vtt =

1.0000  0.0009 -0.5571
-0.7446  1.0000 -0.1589
0.6679  0.0009  1.0000


eigtt =

1.0e+04 *

-0.0146
-2.3122
-0.0094
```

eigenvalues and eigenvectors of the dynamic/algebraic bifurcation test matrix and flux decay bifurcation test matrix at 100 MVar reactive power load. The real parts of the eigenvalues are negative which indicate the system is dynamically stable.

Table 4.27 shows the eigenvalues of the dynamic/algebraic model for the load at 120 MVar. All the eigenvalues have negative real parts. A pair of complex eigenvalues (with arrow sign in Table 4.27) will be shown to approach the $j\omega$ axis as the reactive load is further increased. Another pair of complex eigenvalues (with dashed arrow sign in Table 4.27) will be shown to become real eigenvalues and stay negative as reactive load is increased toward 170 MVars. These results are similar to those in Section 4.3 and is explained in Section 4.3.

Table 4.28 shows the eigenvalues of the dynamic/algebraic model for the reactive power load at 140 MVar. No positive real part of the eigenvalue indicates the system is dynamically stable. Comparing with Table 4.27, the complex eigenvalues with arrow sign in Table 4.28 are closer to $j\omega$ axis than the ones in Table 4.27 and the complex eigenvalues with dashed arrow sign in Table 4.27 become real eigenvalues in Table 4.28.

Table 4.29 shows the dynamic/algebraic model eigenvalues for 160 MVar. The real parts of the complex eigenvalues with arrow sign changed from 0.0196 in Table 4.28 to 0.0078 in Table 4.29 which indicates this pair of complex eigenvalues are moving further toward $j\omega$ axis. One of the eigenvalues with dashed arrow sign becomes more negative and the other one moves toward the origin. All the eigenvalues have negative real parts and thus the system is stable. Notice that the flux decay eigenvalues are moving toward the right half plane as the reactive power load is increased. It indicates that the instability of flux decay dynamics may occur.

Table 4.30 shows the dynamic model eigenvalues at 170 MVar which is the last converged case of this simulation. All the real parts of the eigenvalues stay negative. Figure 4.36,

Table 4.27 The eigenvalues of the algebraic/dynamic bifurcation test matrix and the flux decay bifurcation test matrix for 120 MVar load at bus LOAD2

```
eigda =                                    vtt =

-26.4999 +52.2134i                          1.0000 0.0031 -0.3339
-26.4999 -52.2134i                         -0.5743 1.0000 -0.2918
 -3.8978 +14.9056i                          0.2355 0.0020 1.0000
 -3.8978 -14.9056i
 -3.9807 +14.9862i
 -3.9807 -14.9862i                         eigtt =
-15.1974
-16.4610                                    1.0e+03 *
-16.5452
 -0.3373 +  1.7019i                         -0.1335
 -0.3373 -  1.7019i                         -6.7572
 -0.0305 +  1.1269i                         -0.0630
 -0.0305 -  1.1269i
 -0.0841 +  0.0140i
 -0.0841 -  0.0140i
 -0.0662 +  0.9187i
 -0.0662 -  0.9187i
 -0.0727 +  0.6324i
 -0.0727 -  0.6324i
 -0.0512 +  0.5827i
 -0.0512 -  0.5827i
```

Table 4.28 The eigenvalues of the algebraic/dynamic bifurcation test matrix and the flux decay bifurcation test matrix for 140 MVar load at bus LOAD2

```
eigda =                                    vtt =

-26.5105 +52.2176i                          1.0000 0.0062 -0.2789
-26.5105 -52.2176i                         -0.5335 1.0000 -0.3489
 -3.8992 +14.9057i                          0.1256 0.0027 1.0000
 -3.8992 -14.9057i
 -4.0274 +14.9877i
 -4.0274 -14.9877i                         eigtt =
-15.1892
-16.4542                                    1.0e+03 *
-16.5408
 -0.3255 +  1.7086i                         -0.1274
 -0.3255 -  1.7086i                         -3.5600
 -0.0196 +  1.1414i                         -0.0436
 -0.0196 -  1.1414i
 -0.0925
 -0.0758
 -0.0550 +  0.5882i
 -0.0550 -  0.5882i
 -0.0743 +  0.6454i
 -0.0743 -  0.6454i
 -0.0770 +  0.9271i
 -0.0770 -  0.9271i
```

**Table 4.29 The eigenvalues of the algebraic/dynamic bifurcation test matrix and the flux decay bifurcation test matrix for 160 MVar load at bus LOAD2**

```
eigda =

-26.5260 +52.2235i
-26.5260 -52.2235i
 -3.9004 +14.9037i
 -3.9004 -14.9037i
 -4.0921 +14.9912i
 -4.0921 -14.9912i
-16.4447
-15.1758
-16.5354
 -0.3094 +  1.7191i
 -0.3094 -  1.7191i
 -0.0078 +  1.1638i
 -0.0078 -  1.1638i
 -0.0668
 -0.1015
 -0.0593 +  0.5943i
 -0.0593 -  0.5943i
 -0.0760 +  0.6557i
 -0.0760 -  0.6557i
 -0.0932 +  0.9364i
 -0.0932 -  0.9364i
```

```
vtt =

 1.0000 0.0107 -0.2629
-0.5245 1.0000 -0.3896
 0.0815 0.0034 1.0000


eigtt =

 1.0e+03 *

 -0.1213
 -2.1531
 -0.0316
```

**Table 4.30 The eigenvalues of the algebraic/dynamic bifurcation test matrix and the flux decay bifurcation test matrix for 170 MVar load at bus LOAD2**

```
eigda =

-26.5444 +52.2305i
-26.5444 -52.2305i
 -3.9033 +14.8989i
 -3.9033 -14.8989i
 -4.1104 +14.9864i
 -4.1104 -14.9864i
-16.4349
-15.1595
-16.5306
 -0.2952 +  1.7320i
 -0.2952 -  1.7320i
 -0.0016 +  1.1890i
 -0.0016 -  1.1890i
 -0.0636
 -0.1048
 -0.0630 +  0.6004i
 -0.0630 -  0.6004i
 -0.0770 +  0.6552i
 -0.0770 -  0.6552i
 -0.1122 +  0.9430i
 -0.1122 -  0.9430i
```

```
vtt =

 1.0000 0.0156 -0.2700
-0.5389 1.0000 -0.4010
 0.0836 0.0051 1.0000


eigtt =

 1.0e+03 *

 -0.1158
 -1.5233
 -0.0302
```

4.37, and 4.38 show the time simulation of the internal bus voltage, field current, and terminal bus voltage. These figures state that the system is stable at this load level.

Figure 4.39, 4.40, and 4.41 are the time simulation of the internal bus voltage, field current, and terminal bus voltage when the exciter is disabled but the reactive load is reduced to 150 MVars. These figures show that there is no system instability occursat this load level which is consistent with the eigenvalue results in Table 4.32.

The dynamic/algebraic matrix eigenvalues with the solid arrow for the reactive load from 100 MVar to 170 MVar are collected in Table 4.33. It shows that this pair of eigenvalues approaches the $j\omega$ axis. It indicates that an oscillation problem may occur if the reactive load at LOAD2 is further increased. The eigenvectors in Appendix C.4 associated with this pair of eigenvalues show that this pair of eigenvalues are heavily related to the internal bus angle of GEN2 and the field voltage of all three generators especially GEN2. This indicates that the oscillation may develop before the field current limit is reached if the reactive power load is further increased. Since the oscillation problem is closely related to the internal bus angle and field voltage, the oscillation could cause field current limit violation, and excitation system disablement. If we use the same equilibrium point at 170 MVar and assume the exciter is disabled, the eigenvalues of the flux decay bifurcation test and the reduced dynamic/algebraic bifurcation test matrices, shown in Table 4.31, have one positive real eigenvalue which indicate the system is unstable. A time simulation was attempted. Unfortunately the simulation program did not provide any results if the exciter was disabled. It is caused by the inability of the simulation program to solve the differential equations close to the bifurcation point.

The results indicate that the excitation system would be disabled either due to field current limit violation due either to the average level of the field current or the development of the oscillation. Once the excitation system is disabeld, the system is unstable. Although the Extended Transient Mid Term Stability Program wap not robust enough to simulate the

144
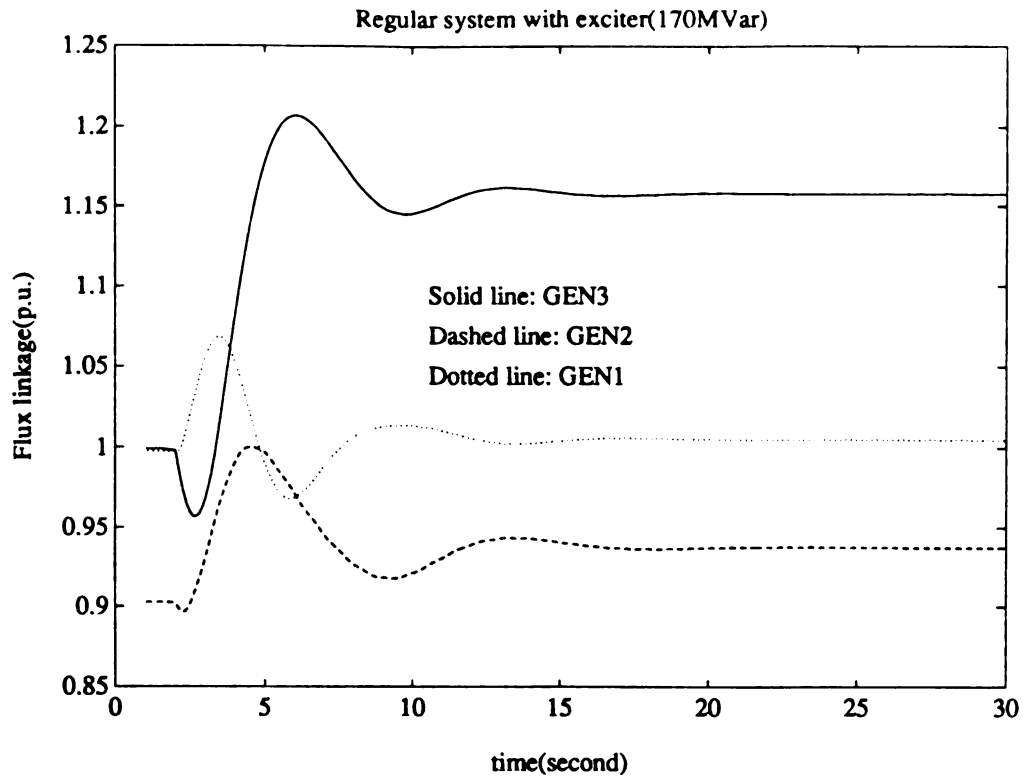


Figure 4.36  Time simulation of the internal bus voltage (170 MVar)
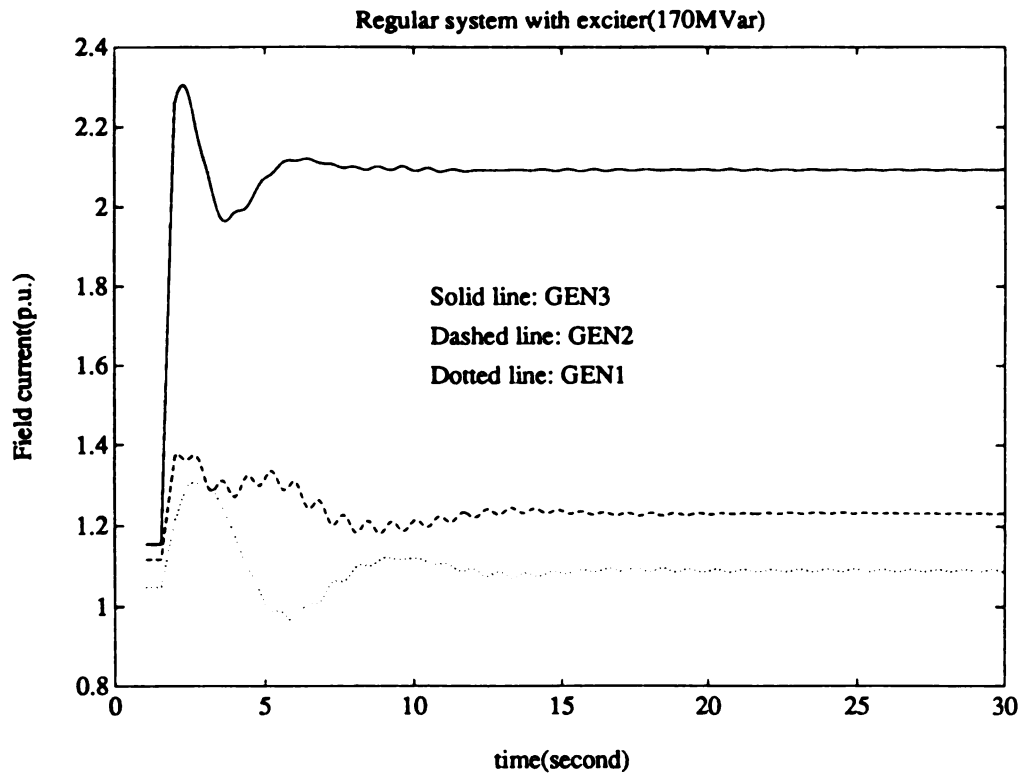
Figure 4.37 Time simulation of the field current (170 MVar)
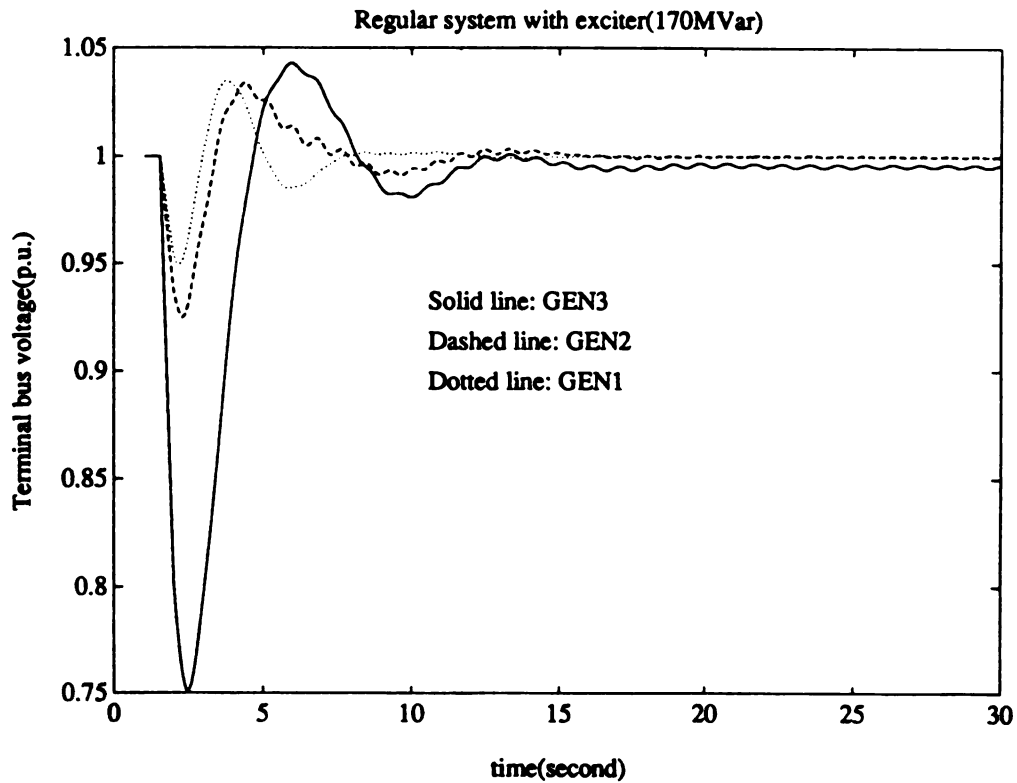


Figure 4.38 Time simulation of the terminal bus voltage (170 MVar)

Figure 4.39 Time simulation of the internal bus voltage (150 MVar)



Figure 4.40 Time simulation of the field current (150 MVar)

Figure 4.41 Time simulation of the terminal bus voltage (150 MVar)

Table 4.31 The eigenvalues of the algebraic/dynamic bifurcation test matrix and the
flux decay bifurcation test matrix for 170 MVar load at bus LOAD2 (saturation)

```
eigda =                                    vtt =

-26.5444 +52.2305i                          1.0000  0.0155 -0.2002
-26.5444 -52.2305i                         -0.4906  1.0000 -0.4246
-3.8928 +14.9079i                          -0.0017 -0.0002  1.0000
-3.8928 -14.9079i
-16.4681
-15.1809                                   ett =
-0.3277 +  1.6990i
-0.3277 -  1.6990i                          1.0e+03 *
-0.0478 +  1.1154i
-0.0478 -  1.1154i                         -0.1140
-0.0683 +  0.6982i                         -1.5191
-0.0683 -  0.6982i                          0.0002
-0.0630 +  0.6124i
-0.0630 -  0.6124i
-0.1048
-0.0636
 0.2004          ◄━━
```

Table 4.32 The eigenvalues of the algebraic/dynamic bifurcation test matrix and the
flux decay bifurcation test matrix for 150 MVar load at bus LOAD2 (saturation)

```
eigda -                                    vtt -

-26.4666 +52.2684i                          1.0000  0.0025 -0.0674
-26.4666 -52.2684i                         -0.1803  1.0000 -0.1320
-3.8998 +14.9699i                          -0.0006  0.0000  1.0000
-3.8998 -14.9699i
-16.5234
-15.6538                                   ett -
-0.3235 +  1.3987i
-0.3235 -  1.3987i                          1.0e+03 *
-0.2121 +  1.0817i
-0.2121 -  1.0817i                         -0.0935  0  0
-0.0688                                      0 -2.4353  0
-0.0932 +  0.7924i                           0  0 -0.0001
-0.0932 -  0.7924i
-0.0632 +  0.6368i
-0.0632 -  0.6368i
-0.0340 +  0.6039i
-0.0340 -  0.6039i
```

number for both system jacobian and algebraic bifurcation test matrices are less that 11 percent which indicate both matrices are not approaching singularity. Table 4.26 shows the system, it is anticipated that the field current, internal generator and terminal voltage would approach zero as in Section 4.3.

A more robust algorithm is needed for the Extended Transient Mid Term Stability Program if it is to be able to simulate the actual voltage collapse problems and calculate contigency equilibria for voltage collapse problems. Such an algorithm may exist in version 2.0 of the Extended Transient Mid Term Stability Program, that was not available at the time this research was conducted.

Table 4.33 Eigenvalues for different load levels

| Load (MVar) | Eigenvalues |
|---|---|
| 100 | $-0.0397 \pm 1.1176i$ |
| 120 | $-0.0305 \pm 1.1269i$ |
| 140 | $-0.0196 \pm 1.1414i$ |
| 160 | $-0.0078 \pm 1.1638i$ |
| 170 | $-0.0016 \pm 1.1890i$ |

# CHAPTER 5

# REVIEW AND TOPICS FOR FUTURE RESEARCH

## 5.1    Review

A precisely modelled power system which includes the generator dynamics and real and reactive power balance equations was developed in this thesis. It has been shown that the voltage instability problems may occur in the dynamics of the generator before the jacobian matrix of the real and reactive power balance equations become singular. It indicates that the load flow based voltage instability methods can not predict the voltage instability problems which occur in the generator dynamics. Furthermore, the thesis also showed that the equilibrium point calculated by using the general power system model was different from the one calculated by using load flow model in the case that both models were using the same system configuration and initial value. The difference of the equilibrium point of the general power system model and the load flow model increases as the system was stressed. The reasons for the divergence of the load flow model from the general power system model are as follows:

    (a)    the load flow simulation uses reactive power generation to regulate bus voltage and the general power system model uses the field current to regulate bus voltage,

    (b)    the general power system model takes into account the air gap saturation

which affects the closed loop gain of the exciter control loop, but the load flow model does not,

(c)   the load flow model assumes $K_A$ is infinite but $K_A$ is a finite value in the general power system model; the exciter loop gain $K_{EX}$ is proportional to the exciter amplifier gain and inversely proportional to air gap saturation,

(d)   generators in the load flow model regulate either their high side transformer bus voltage or terminal bus voltage but the general power system model which takes line drop compensation into account allows any point between the generator internal bus and some fictitious point out in the network to be regulated.

Voltage instability problems were classified into two different categories in this thesis. These two kinds of voltage instability are results of very different types and locations of stress. Load flow voltage instability is caused by the inability of the transmission system to supply the reactive load when there is no reactive power supply at that load voltage control area. System voltage instability is caused by either the instability of the generator dynamics or the coupling between the generator dynamic states and algebraic states in a stressed network.

This thesis provided different types of tests for different voltage instability. The <u>algebraic bifurcation test</u> was used for testing for load flow voltage instability. The test condition for algebraic bifurcation test is a test for loss of causality[27]. Transient stability simulation packages that iteratively update dynamic states using the differential equations and update states of the network using the algebraic equations may not obtain unique solutions and will generally terminate due to numerical failure as singularity of matrix D is approached. It has been shown that the algebraic bifurcation(loss of causality) does not necessarily cause a system bifurcation, but can result in a system bifurcation. An algebraic bifurcation that does not cause a static system bifurcation can result in chaos[21] and possibly other

unacceptable behavior which may or may not be associated with voltage collapse.

The algebraic/dynamic system bifurcation test was shown to be always valid for testing the singularity of the system jacobian matrix J. The algebraic/dynamic system bifurcation test can detect the system bifurcations of the algebraic equations like

(a) linearly dependent rows in matrix $[C_1 \, D_1 \, D_2]$, or

(b) linearly dependent rows in matrix $[D_3 \, D_4]$ and $[C_1 \, D_1 \, D_2]$.

which can not be detected by the algebraic bifurcation test. The algebraic/dynamic test can also be used to test for voltage instability of the generator dynamics.

The dynamic/algebraic system bifurcation test represents the system matrix of the nonlinear constrained differential equation model linearized at an equilibrium point and thus define the eigenvalues of the equivalent unconstrained dynamical system. The dynamic/algebraic system bifurcation test can be used to test the stability of the dynamic states if the matrix D is nonsingular. The singularity of this test indicates that the system jacobian matrix J is singular and that a bifurcation may have occurred in the dynamical system where the algebraic constraints have unique solutions and thus can be eliminated. If the algebraic equations can have bifurcation ( D is regular ), the dynamic algebraic test is not defined.

The flux decay bifurcation test can indicate whether the voltage instability is related to dynamic voltage instability associated with flux decay dynamics. The derivation of the flux decay bifurcation test pointed out how the air gap saturation, line drop compensation, field current limit, sensitivity matrices, and reactive power generation would influence the stability of flux decay dynamics.

A computer program was developed to compute the system jacobian and eigenvalues and eigenvectors of the dynamic states. The computer program was applied to a two bus sys-

tem and a twelve bus system to determine the stability of the system. The results were compared with time simulations to confirm their validity. A series of experiments were designed and conducted as follows:

Experiment 1: A two bus system with flux decay dynamics and real and reactive power balance equations was investigated. The only system bifurcation which could occur in this two bus system where exciters were disabled was when the high and low voltage solutions merge. The system bifurcation resulted in a loss of stability where both generator internal and terminal voltage dropped to extremely small value. An algebraic bifurcation due to linear dependence in the linearized jacobian of real and reactive power balance equations also occurs and does not cause system bifurcation, but is an unstable equilibrium of the transient stability model. This unstable equilibrium point is associated loss of voltage stability or possible chaotic behavior.

Experiment 2: Algebraic bifurcation of the general power system model and load flow bifurcation of a twelve bus system model were studied. A load bus was isolated from the rest of the system by increasing the reactance of lines that connect the load bus to the rest of the system. In the load flow bifurcation case, it was shown that weak boundaries developed and became drains to block the reactive power supply to the load bus. Thus a reactive power demand supply type of voltage instability problem developed at a bus despite the fact that there is ample reactive generation reserves on all the generators in the system. Algebraic bifurcation of the equivalent general power system model was studied. The algebraic bifurcation test results were shown theoretically and computationally to be confirmed by a Q-V

curve. The test results showed that the twelve bus system was not vulnerable to algebraic bifurcation and reactive demand and supply problem. The system was modified to be more susceptible to reactive demand and supply problem. However, the EPRI Transient Mid Term Stability Program would not converge to an equilibrium point when the system was susceptible to reactive demand supply problems.

Experiment 3: A generator and its terminal bus were isolated from the rest of the system by increasing the transformers reactance that connected the generator to the rest of the twelve bus system. The purpose of this particular case was to establish whether the results obtained for the two bus system composed of generator internal bus and terminal bus were valid in a general system. The conclusion is that the results on the two bus system could be used to describe the dynamic/ algebraic bifurcation that can occur due to the bifurcation of load flow manifold, flux decay manifold, and control manifold of the generator. The system experienced a dynamic/algebraic voltage collapse bifurcation when the excitation system was disabled at the reactive load level where the field current was at the continuous rating limit. A time simulation indicated that there was a rapid decline of terminal bus voltage, field current, and reactive power output. The flux decay bifurcation test and the dynamic/algebraic bifurcation test confirmed the eigenvalue analysis and transient stability simulation results that indicated there was a dynamic voltage problem.

Experiment 4: The two bus voltage control area case of a generator internal and terminal buses was extended to a three bus voltage control area

composed of a generator, terminal, and load bus in this experiment. The test for voltage collapse was performed by increasing reactive load at the load bus rather than at the generator terminal bus as in the previous experiment. The results indicated an oscillation developed before the field current limit was reached. The system never approached an algebraic system bifurcation based on a Q-V curve and based on the algebraic bifurcation test. The system never approached dynamic/algebraic bifurcation as reactive load and the field current limit was reached. After the continuous field current limit was hit and the excitation system was disabled, the system experienced a dynamic/algebraic bifurcation. The Transient Stability Program failed to simulate this unstable response.

## 5.2    Topic for Future Research

An equilibrium program which can compute the equilibrium point of a precisely modeled power system needs to be developed. This thesis uses the steady state solution of a precisely modeled transient midterm stability program to compute the equilibrium point. This method is very time consuming and does not guarantee obtaining converged solutions. Since the correct equilibrium point is the basis of the voltage instability analysis and the computation of the equilibrium points have to be repeated many times for different operating conditions, a fast and precise equilibrium program which can handle large scale system databases is a must.

Voltage instability usually occurs at the equilibrium point which is close to bifurcation point. The transient mid term transient stability program also had difficulty performing time simulations when the system was close to loss of voltage stability. A robust numerical algorithm for simulating transient mid term trajectories needs to be developed. If this

algorithm were available, the trajectories of the dynamic states could then be simulated and the system behavior close to voltage instability could be more fully explored.

A theory that describes the bifurcations and singularities of constrained differential equations is not complete. The analysis of voltage stability at the bifurcation point for a large system would be a very interesting topic if that theory was available.

Since dynamic voltage instability is caused by instability the flux decay and excitation control system , new excitation system controls are needed. Nonlinear or adaptive control theory could be applied to develop a control that can prevent a dynamic/algebraic voltage instability and algebraic voltage instability.

A secondary voltage control that slowly adjusts voltage setpoints could also be developed. The secondary voltage control should help prevent both algebraic and dynamic algebraic voltage collapse by preventing field current limit violations on appropriate generators.

**APPENDICES**

# APPENDIX A

# MODEL LINEARIZATION

The general power system model developed in chapter 2 is linearized in this appendix. The subscripts i and j are removed in the cases where there is no difference of the linearization for both controllable buses and uncontrollable buses. The definition of variables and parameters are defined in the LIST OF SYMBOLS.

## A.1 Mechanical Dynamics

$$\Delta\dot{\omega}_i = \left(\frac{1}{M_i}\right)(-D_i\Delta\omega_i - \Delta P_i^e)$$

$$\Delta\dot{\omega}_i = \left(\frac{1}{M_j}\right)(-D_j\Delta\omega_j - \Delta P_j^e)$$

$$\Delta\dot{\delta}_i = \Delta\omega_i$$

$$\Delta\dot{\delta}_j = \Delta\omega_j$$

## A.2 Saturation Function $S_D$

$$E_p = \left(\left(V_d - \frac{V_d x_p}{x_{qs}}\right)^2 + \left(V_q + \frac{(E'_q - V_q)x_p}{x'_{ds}}\right)^2\right)^{\frac{1}{2}}$$

$$= \left( \left( V_T \sin (\delta - \theta_T) - \frac{V_T \sin (\delta - \theta_T) x_p (x_d + x_q S_D)}{x_d x_q + x_q S_D x_p} \right)^2 + \right.$$

$$\left. \left( V_T \cos (\delta - \theta_T) + \frac{(E'_q - V_T \cos (\delta - \theta_T)) x_p (1 + S_D)}{x'_d + S_D x_p} \right)^2 \right)^{\frac{1}{2}}$$

Let

$$V'_{d0} = V_{d0} - \frac{V_{d0} x_p}{x_{qs0}} \qquad \text{and} \qquad V'_{q0} = V_{q0} + \frac{(E'_{q0} - V_{q0}) x_p}{x'_{ds0}}$$

$$E_{p0} = \left( \left( V_{d0} - \frac{V_{d0} x_p}{x_{qs0}} \right)^2 + \left( V_{q0} + \frac{(E'_{q0} - V_{q0}) x_p}{x'_{ds0}} \right)^2 \right)^{\frac{1}{2}}$$

then

$$\Delta E_p = \left( \frac{1}{E_{p0}} \right) \left( \hat{A} \left( \frac{\Delta V_T}{V_{T0}} \right) + \hat{B} \left( \frac{\Delta E'_q}{E'_{q0}} \right) + \hat{C} \Delta \delta + \hat{D} \Delta \theta_T + \hat{E} \Delta S_D \right)$$

where

$$\hat{A} = V'^2_{d0} + V'_{q0} V_{T0} \cos (\delta_0 - \theta_{T0}) \left( \frac{x'_d - x_p}{x'_d + S_{d0} x_p} \right)$$

$$\hat{B} = \frac{V'_{q0} E'_{q0} x_p (1 + S_D)}{x'_d + S_{d0} x_p}$$

$$\hat{C} = V'_{d0} V_{T0} \cos (\delta_0 - \theta_{T0}) \left( \frac{x_d (x_q - x_p)}{x_d x_q + x_q S_{d0} x_p} \right) +$$

$$V'_{q0} V_{T0} \sin (\delta_0 - \theta_{T0}) \left( \frac{-x'_d + x_p}{x'_d + S_{d0} x_p} \right)$$

$$\hat{D} = V'_{d0} V_{T0} \cos (\delta_0 - \theta_{T0}) \left( \frac{x_d (-x_q + x_p)}{x_d x_q + x_q S_{d0} x_p} \right) +$$

$$V'_{q0} V_{T0} \sin (\delta_0 - \theta_{T0}) \left( \frac{x'_d - x_p}{x'_d + S_{d0} x_p} \right)$$

$$\hat{E} = V'_{d0}\left(\frac{-V_{T0}\sin(\delta_0-\theta_{T0})\,x_d x_q x_p\,(x_q-x_p)}{(x_d x_q + x_q S_{d0}x_p)^2}\right) +$$

$$V'_{q0}\left(\frac{(E'_{q0}-V_{T0}\cos(\delta_0-\theta_{T0}))\,x_p\,(x'_d-x_p)}{(x'_d+S_{d0}x_p)^2}\right)$$

$$\Delta S_D = \frac{2B\,(E_{p0}-A)\,\Delta E_p}{E_{p0}^2}$$

$$= \frac{2B\,(E_{p0}-A)}{E_{p0}^3}\left(\hat{A}\left(\frac{\Delta V_T}{V_{T0}}\right)+\hat{B}\left(\frac{\Delta E'_q}{E'_{q0}}\right)+\hat{C}\Delta\delta+\hat{D}\Delta\theta_T+\hat{E}\Delta S_D\right)$$

Solve for $\Delta S_D$

$$\Delta S_D = \frac{2B\,(E_{p0}-A)}{E_{p0}^3-2B\,(E_{p0}-A)\,\hat{E}}\left(\hat{A}\left(\frac{\Delta V_T}{V_{T0}}\right)+\hat{B}\left(\frac{\Delta E'_q}{E'_{q0}}\right)+\hat{C}\Delta\delta+\hat{D}\Delta\theta_T\right)$$

$$= \bar{A}\left(\frac{\Delta V_T}{V_{T0}}\right)+\bar{B}\left(\frac{\Delta E'_q}{E'_{q0}}\right)+\bar{C}\Delta\delta+\bar{D}\Delta\theta_T$$

## A.3  Flux Decay Dynamics

The flus decay equations for controllable internal buses are

$$\Delta\dot{E}'_{qi} = \left(\frac{1+S_{Di}}{\tau_{d0i}}\right)\left(\frac{-(x_{di}+S_{Di0}x_{pi})E'_{qi0}}{x'_{di}+S_{Di0}x_{pi}}\right)\Delta E'_{qi}+\left(\frac{1}{\tau_{d0i}E'_{qi0}}\right)\Delta E_{fdi}+$$

$$\frac{(1+S_{Di})V_{Ti0}(x_{di}-x'_{di})\cos(\delta_{i0}-\theta_{Ti0})}{\tau_{d0i}(x'_{di}+S_{Di0}x_{pi})E'_{qi0}}\Delta V_{Ti}-$$

$$\frac{(1+S_{Di})V_{Ti0}(x_{di}-x'_{di})\sin(\delta_{i0}-\theta_{Ti0})}{\tau_{d0i}(x'_{di}+S_{Di0}x_{pi})E'_{qi0}}\Delta\delta_i+$$

$$\frac{(1+S_{Di})V_{Ti0}(x_{di}-x'_{di})\sin(\delta_{i0}-\theta_{Ti0})}{\tau_{d0i}(x'_{di}+S_{Di0}x_{pi})E'_{qi0}}\Delta\theta_{Ti}+$$

$$
\left( \frac{- (x_{di} + S_{Di0} x_{pi}) E'_{qi0} + V_{Ti0} (x_{di} - x'_{di}) \cos (\delta_{i0} - \theta_{Ti0})}{x'_{di} + S_{Di0} x_{pi}} + \right.
$$

$$
\frac{(1 + S_{Di0}) (-x_{pi} E'_{qi0} (x'_{di} - x_{di}))}{(x'_{di} + S_{Di0} x_{pi})^2} +
$$

$$
\left. \frac{(1 + S_{Di0}) x_{pi} (-V_{Ti0} (x_{di} - x'_{di}) \cos (\delta_{i0} - \theta_{Ti0}))}{(x'_{di} + S_{Di0} x_{pi})^2} \right)
$$

Since the field voltages are assumed to be held constant for uncontrollable internal buses, the linearization of flus decay equations for uncontrollable buses become

$$
\Delta \dot{E}'_{qj} = \left( \frac{1 + S_{Dj}}{\tau_{d0j}} \right) \left( \frac{- (x_{dj} + S_{Dj0} x_{pj}) E'_{qj0}}{x'_{dj} + S_{Dj0} x_{pj}} \right) \Delta E'_{qj} +
$$

$$
\frac{(1 + S_{Dj}) V_{Tj0} (x_{dj} - x'_{dj}) \cos (\delta_{j0} - \theta_{Tj0})}{\tau_{d0j} (x'_{dj} + S_{Dj0} x_{pj}) E'_{qj0}} \Delta V_{Tj} -
$$

$$
\frac{(1 + S_{Dj}) V_{Tj0} (x_{dj} - x'_{dj}) \sin (\delta_{j0} - \theta_{Tj0})}{\tau_{d0j} (x'_{dj} + S_{Dj0} x_{pj}) E'_{qj0}} \Delta \delta_j +
$$

$$
\frac{(1 + S_{Dj}) V_{Tj0} (x_{dj} - x'_{dj}) \sin (\delta_{j0} - \theta_{Tj0})}{\tau_{d0j} (x'_{dj} + S_{Dj0} x_{pj}) E'_{qj0}} \Delta \theta_{Tj} +
$$

$$
\left( \frac{- (x_{dj} + S_{Dj0} x_{pj}) E'_{qj0} + V_{Tj0} (x_{dj} - x'_{dj}) \cos (\delta_{j0} - \theta_{Tj0})}{x'_{dj} + S_{Dj0} x_{pj}} + \right.
$$

$$
\frac{(1 + S_{Dj0}) (-x_{pj} E'_{qj0} (x'_{dj} - x_{dj}))}{(x'_{dj} + S_{Dj0} x_{pj})^2} +
$$

$$
\left. \frac{(1 + S_{Dj0}) x_{pj} (-V_{Tj0} (x_{dj} - x'_{dj}) \cos (\delta_{j0} - \theta_{Tj0}))}{(x'_{dj} + S_{Dj0} x_{pj})^2} \right) \frac{\Delta S_{Dj}}{\tau_{d0j} E'_{qj0}}
$$

## A.4   Excitation System Dynamics

## A.4.1 Line Drop Compensation

If the line drop compensator is considered, the fictitious bus voltage will be

$$V_c = |V_T\angle(\theta_T - \delta) + jI_T x_c|$$

where

$$I_T = I_{ad} + I_{aq}$$

$$= \frac{E'_q - V_T\cos(\delta - \theta_T)}{jx'_{ds}} + \frac{V_T\sin(\delta - \theta_T)}{x_{qs}}$$

$$V_T\angle(\theta_T - \delta) + jI_T x_c = V_T\cos(\delta - \theta_T) - jV_T\sin(\delta - \theta_T) +$$

$$j\left(\frac{(1+S_D)(E'_q - V_T\cos(\delta - \theta_T))}{j(x'_d + S_D x_p)} + \frac{(x_d + x_q S_D)(V_T\sin(\delta - \theta_T))}{x_d x_q + x_p x_q S_D}\right)x_c$$

$$V_c = \left(\left(V_T\cos(\delta - \theta_T) + \frac{(1+S_D)(E'_q - V_T\cos(\delta - \theta_T))x_c}{(x'_d + S_D x_p)}\right)^2 + \right.$$

$$\left.\left(\frac{(x_d + x_q S_D)(V_T\sin(\delta - \theta_T))x_c}{x_d x_q + x_p x_q S_D} - V_T\sin(\delta - \theta_T)\right)^2\right)^{\frac{1}{2}}$$

## A.4.2 Linearization of Excitation System Dynamics

Let $\quad V_c = \sqrt{\hat{V}_1^2 + \hat{V}_2^2}$

The linearized differential equation for the voltage $V_1$ out of measurement device will be

$$\Delta\dot{V}_1 = \left(\frac{1}{\tau_R}\right)\left(-\Delta V_1 + \frac{\partial}{\partial E'_q}V_c\frac{E'_{q0}\Delta E'_q}{E'_{q0}} + \frac{\partial}{\partial V_T}V_c\frac{V_{T0}\Delta V_T}{V_{T0}} + \right.$$

$$\left.\frac{\partial}{\partial\delta}V_c\Delta\delta + \frac{\partial}{\partial\theta_T}V_c\Delta\theta_T + \frac{\partial}{\partial S_D}V_c\Delta S_D\right)$$

where

$$\frac{\partial V_c}{\partial E'_q} = V_{c0}^{-1} \hat{V}_{10} \left( \frac{1 + S_{D0}}{x'_d + S_{D0} x_p} \right)$$

$$\frac{\partial V_c}{\partial V_T} = V_{c0}^{-1} \left( \hat{V}_{10} \left( \cos(\delta_0 - \theta_{T0}) - \frac{(1 + S_{D0}) \cos(\delta_0 - \theta_{T0}) x_c}{x'_d + S_{D0} x_p} \right) + \hat{V}_{20} \left( \frac{(x_d + x_q S_{D0}) \sin(\delta_0 - \theta_{T0}) x_c}{x_d x_q + x_p x_q S_{D0}} - \sin(\delta_0 - \theta_{T0}) \right) \right)$$

$$\frac{\partial V_c}{\partial \delta} = V_{c0}^{-1} \left( \hat{V}_{10} \left( -V_{T0} \sin(\delta_0 - \theta_{T0}) + \frac{(1 + S_{D0}) V_{T0} \sin(\delta_0 - \theta_{T0}) x_c}{x'_d + S_{D0} x_p} \right) + \hat{V}_{20} \left( \frac{(x_d + x_q S_{D0}) V_{T0} \cos(\delta_0 - \theta_{T0}) x_c}{x_d x_q + x_p x_q S_{D0}} - V_{T0} \cos(\delta_0 - \theta_{T0}) \right) \right)$$

$$\frac{\partial V_c}{\partial \theta_T} = V_{c0}^{-1} \left( \hat{V}_{10} \left( V_{T0} \sin(\delta_0 - \theta_{T0}) - \frac{(1 + S_{D0}) V_{T0} \sin(\delta_0 - \theta_{T0}) x_c}{x'_d + S_{D0} x_p} \right) + \hat{V}_{20} \left( \frac{(-(x_d + x_q S_{D0})) V_{T0} \cos(\delta_0 - \theta_{T0}) x_c}{x_d x_q + x_p x_q S_{D0}} + V_{T0} \cos(\delta_0 - \theta_{T0}) \right) \right)$$

$$\frac{\partial V_c}{\partial S_D} = V_{c0}^{-1} \left( \hat{V}_{10} \left( \frac{(E'_q - V_T \cos(\delta - \theta_T)) (x'_d - x_p) x_c}{(x'_d + S_{D0} x_p)^2} \right) + \hat{V}_{20} \left( \frac{V_{T0} \sin(\delta_0 - \theta_{T0}) x_q x_d x_c (x_q - x_p)}{(x_d x_q + x_p x_q S_{D0})^2} \right) \right)$$

The linearization of the rest of excitation system states is

$$\Delta \dot{V}_{3i} = \left( \frac{1}{\tau_{Fi}} \right) \left( -\Delta V_{3i} + \frac{K_{Fi} \Delta V_{Ri}}{\tau_{Ei}} - \frac{K_{Fi} (\dot{S}_{Ei}(E_{fdi0}) E_{fdi0} + S_{Ei}(E_{fdi0}) + K_{Ei}) \Delta E_{fdi}}{\tau_{Ei}} \right)$$

$$\Delta \dot{V}_{Ri} = \frac{K_{Ai}(-\Delta V_{1i} - \Delta V_{3i}) - \Delta V_{Ri}}{\tau_{Ai}}$$

$$\Delta \dot{E}_{fdi} = \frac{\Delta V_{Ri} - (\dot{S}_{Ei}(E_{fdi0}) E_{fdi0} + S_{Ei}(E_{fdi0}) + K_{Ei}) \Delta E_{fdi}}{\tau_{Ei}}$$

## A.5 Power Flow

Real and reactive power balance equations for generator, terminal, high side transformer, and load buses are linearized.

### A.5.1 Real Power Linearization for Generator and Terminal Buses

$$\Delta P^e = \frac{\partial P^e}{\partial E'_q}\left(\frac{\Delta E'_q}{E'_{q0}}\right) + \frac{\partial P^e}{\partial V_T}\left(\frac{\Delta V_T}{V_{T0}}\right) + \frac{\partial P^e}{\partial \delta} \Delta \delta + \frac{\partial P^e}{\partial \theta_T} \Delta \theta_T + \frac{\partial P^e}{\partial S_D} \Delta S_D$$

where

$$\frac{\partial P^e}{\partial E'_q} = \frac{E'_{q0} V_{T0} \sin(\delta_0 - \theta_{T0})(1 + S_{D0})}{x'_d + S_{D0} x_p}$$

$$\frac{\partial P^e}{\partial V_T} = \frac{E'_{q0} V_{T0} \sin(\delta_0 - \theta_{T0})(1 + S_{D0})}{x'_d + S_{D0} x_p} +$$

$$V_{T0}^2 \left(\frac{x_d + x_q S_{D0}}{x_d x_q + x_q S_{D0} x_p} - \frac{1 + S_{D0}}{x'_d + S_{D0} x_p}\right) \sin(2(\delta_0 - \theta_{T0}))$$

$$\frac{\partial P^e}{\partial \delta} = \frac{E'_{q0} V_{T0} \cos(\delta_0 - \theta_{T0})(1 + S_{D0})}{x'_d + S_{D0} x_p} +$$

$$V_{T0}^2 \left(\frac{x_d + x_q S_{D0}}{x_d x_q + x_q S_{D0} x_p} - \frac{1 + S_{D0}}{x'_d + S_{D0} x_p}\right) \cos(2(\delta_0 - \theta_{T0}))$$

$$\frac{\partial P^e}{\partial \theta_T} = \frac{-E'_{q0}V_{T0}\cos(\delta_0 - \theta_{T0})(1 + S_{D0})}{x'_d + S_{D0}x_p} -$$

$$V_{T0}^2 \left( \frac{x_d + x_q S_{D0}}{x_d x_q + x_q S_{D0} x_p} - \frac{1 + S_{D0}}{x'_d + S_{D0}x_p} \right) \cos(2(\delta_0 - \theta_{T0}))$$

$$\frac{\partial P^e}{\partial S_D} = \frac{E'_{q0}V_{T0}\sin(\delta_0 - \theta_{T0})(x'_d - x_p)}{(x'_d + S_{D0}x_p)^2} +$$

$$\frac{V_{T0}^2 \sin(2(\delta_0 - \theta_{T0}))}{2} \left( \frac{x_d x_q (x_q - x_p)}{(x_d x_q + x_q S_{D0} x_p)^2} - \frac{x'_d - x_p}{(x'_d + S_{D0}x_p)^2} \right)$$

$$\Delta P_T^e - \Delta P_T^d = -V_T V_H Y_{TH}\sin(\theta_T - \theta_H - \gamma_{TH})\Delta\theta_T +$$

$$V_T V_H Y_{TH}\sin(\theta_T - \theta_H - \gamma_{TH})\Delta\theta_H +$$

$$(V_T V_H Y_{TH}\cos(\theta_T - \theta_H - \gamma_{TH}) + 2V_T Y_{TH}\cos\gamma_{TH})\Delta V_T +$$

$$V_T V_H Y_{TH}\cos(\theta_T - \theta_H - \gamma_{TH})\Delta V_H$$

### A.5.2 Reactive Power Linearization for Generator Buses

$$\Delta Q^e = \frac{\partial Q^e}{\partial E'_q}\left( \frac{\Delta E'_q}{E'_{q0}} \right) + \frac{\partial Q^e}{\partial V_T}\left( \frac{\Delta V_T}{V_{T0}} \right) + \frac{\partial Q^e}{\partial \delta}\Delta\delta + \frac{\partial Q^e}{\partial \theta_T}\Delta\theta_T + \frac{\partial Q^e}{\partial S_D}\Delta S_D$$

$$\frac{\partial Q^e}{\partial E'_q} = \frac{(2E'_{q0}V_{T0}\sin(\delta_0 - \theta_{T0}) - E'_{q0}V_{T0}\cos(\delta_0 - \theta_{T0}))(1 + S_{D0})}{x'_d + S_{D0}x_p} +$$

$$\frac{2(x_d x_q + x_q x_p S_{D0})E'_{q0}(E'_{q0} - V_{T0}\sin(\delta_0 - \theta_{T0}))(1 + S_{D0})^2}{(x'_d + S_{D0}x_p)^2(x_d + S_{D0}x_q)}$$

$$\frac{\partial Q^e}{\partial V_T} = \frac{(1 + S_{D0})(2E'_{q0}V_{T0}\sin(\delta_0 - \theta_{T0}) - 2V_{T0}^2\sin^2(\delta_0 - \theta_{T0}))}{x'_d + S_{D0}x_p} -$$

$$\frac{(1+S_{D0})\,E'_{q0}V_{T0}\cos(\delta_0-\theta_{T0})}{x'_d+S_{D0}x_p}+$$

$$\frac{2\,(x_dx_q+x_qx_pS_{D0})\,(1+S_{D0})^2\,(-E'_{q0}V_{T0}\sin(\delta_0-\theta_{T0})+V_{T0}^2\sin^2(\delta_0-\theta_{T0}))}{(x'_d+S_{D0}x_p)^2\,(x_d+S_{D0}x_q)}$$

$$\frac{\partial Q^e}{\partial\delta}=\frac{(1+S_{D0})\,(2E'_{q0}V_{T0}\cos(\delta_0-\theta_{T0})-V_{T0}^2\sin(2(\delta_0-\theta_{T0})))}{x'_d+S_{D0}x_p}+$$

$$\frac{(1+S_{D0})\,(E'_{q0}V_{T0}\sin(\delta_0-\theta_{T0}))}{x'_d+S_{D0}x_p}+$$

$$\frac{(x_dx_q+x_qx_pS_{D0})\,(1+S_{D0})^2\,(-2E'_{q0}V_{T0}\cos(\delta_0-\theta_{T0})+V_{T0}^2\sin(2(\delta_0-\theta_{T0})))}{(x'_d+S_{D0}x_p)^2\,(x_d+S_{D0}x_q)}$$

$$\frac{\partial Q^e}{\partial\theta_T}=\frac{(1+S_{D0})\,(-2E'_{q0}V_{T0}\cos(\delta_0-\theta_{T0})+V_{T0}^2\sin(2(\delta_0-\theta_{T0})))}{x'_d+S_{D0}x_p}-$$

$$\frac{(1+S_{D0})\,(E'_{q0}V_{T0}\sin(\delta_0-\theta_{T0}))}{x'_d+S_{D0}x_p}+$$

$$\frac{(x'_d+S_{D0}x_p)\,(1+S_{D0})^2\,(2E'_{q0}V_{T0}\cos(\delta_0-\theta_{T0})-V_{T0}^2\sin(2(\delta_0-\theta_{T0})))}{(x'_d+S_{D0}x_p)^2\,(x_d+S_{D0}x_q)}$$

Let

$$K=-E'_{q0}V_{T0}\cos(\delta_0-\theta_{T0})-V_{T0}^2\sin^2(\delta_0-\theta_{T0})+2E'_{q0}V_{T0}\sin(\delta_0-\theta_{T0})$$

$$K'=-2E'_{q0}V_{T0}\sin(\delta_0-\theta_{T0})+V_{T0}^2\sin^2(\delta_0-\theta_{T0})+E'^2_{q0}$$

$$\frac{\partial Q^e}{\partial S_D}=\frac{(x'_d-x_p)\,K}{(x'_d+S_{D0}x_p)^2}+$$

$$\frac{(2(1+S_{D0})\,(x_dx_q+x_qx_pS_{D0})+(1+S_{D0})^2x_px_q)\,K'}{(x'_d+S_{D0}x_p)^2\,(x_d+S_{D0}x_q)}-$$

$$\frac{(1+S_{D0})^2 \left(2x_q(x_d+S_{D0}x_q)+x_q(x'_d+S_{D0}x_p)\right)\left((x_dx_q+x_qx_pS_{D0})\right)K}{(x'_d+S_{D0}x_p)^3(x_d+S_{D0}x_q)^2}$$

### A.5.3 Reactive Power Linearization for Terminal Buses

$$\Delta Q_T^e = \frac{\partial Q_T^e}{\partial E'_q}\left(\frac{\Delta E'_q}{E'_{q0}}\right) + \frac{\partial Q_T^e}{\partial V_T}\left(\frac{\Delta V_T}{V_{T0}}\right) + \frac{\partial Q_T^e}{\partial \delta}\Delta\delta + \frac{\partial Q_T^e}{\partial \theta_T}\Delta\theta_T + \frac{\partial Q_T^e}{\partial S_D}\Delta S_D$$

$$\frac{\partial Q_T^e}{\partial E'_q} = \frac{E'_{q0}V_{T0}\cos(\delta_0-\theta_{T0})(1+S_{D0})}{x'_d+S_{D0}x_p}$$

$$\frac{\partial Q_T^e}{\partial V_T} = \frac{E'_{q0}V_{T0}\cos(\delta_0-\theta_{T0})(1+S_{D0})-2V_{T0}^2\cos^2(\delta_0-\theta_{T0})(1+S_{D0})}{x'_d+S_{D0}x_p} -$$

$$\frac{2V_{T0}^2\sin^2(\delta_0-\theta_{T0})(x_d+S_{D0}x_q)}{(x_dx_q+x_qS_Dx_p)}$$

$$\frac{\partial Q_T^e}{\partial \delta} = \frac{-E'_{q0}V_{T0}\sin(\delta_0-\theta_{T0})(1+S_{D0})}{x'_d+S_{D0}x_p} -$$

$$V_{T0}^2\sin(2(\delta_0-\theta_{T0}))\left(\frac{-(1+S_{D0})}{x'_d+S_{D0}x_p}+\frac{x_d+S_{D0}x_q}{x_dx_q+x_qS_Dx_p}\right)$$

$$\frac{\partial Q_T^e}{\partial \theta_T} = \frac{E'_{q0}V_{T0}\sin(\delta_0-\theta_{T0})(1+S_{D0})}{x'_d+S_{D0}x_p} -$$

$$V_{T0}^2\sin(2(\delta_0-\theta_{T0}))\left(\frac{(1+S_{D0})}{x'_d+S_{D0}x_p}-\frac{x_d+S_{D0}x_q}{x_dx_q+x_qS_Dx_p}\right)$$

$$\frac{\partial Q_T^e}{\partial S_D} = \frac{E'_{q0}V_{T0}\sin(\delta_0-\theta_{T0})(x'_d-x_p)}{(x'_d+S_{D0}x_p)^2} -$$

$$V_{T0}^2\left(\frac{\cos^2(\delta_0-\theta_{T0})(x'_d-x_p)}{(x'_d+S_{D0}x_p)^2}+\frac{\sin^2(\delta_0-\theta_{T0})x_qx_d(x_q-x_d)}{(x_dx_q+x_qS_Dx_p)^2}\right)$$

$$\Delta Q_T^e - \Delta Q_T^d = V_T V_H Y_{TH} \cos(\theta_T - \theta_H - \gamma_{TH}) \Delta \theta_T +$$

$$-V_T V_H Y_{TH} \cos(\theta_T - \theta_H - \gamma_{TH}) \Delta \theta_H +$$

$$(V_T V_H Y_{TH} \sin(\theta_T - \theta_H - \gamma_{TH}) - 2V_T^2 Y_{TH} s.$$

$$V_T V_H Y_{TH} \sin(\theta_T - \theta_H - \gamma_{TH}) \Delta V_H$$

## A.5.4 Real Power Linearization for The Network

$$-\Delta P_{Hi}^d = \left( \sum_{s=1}^{l} V_{Hi0} V_{Hs0} Y_{HiHs} \cos(\theta_{Hi0} - \theta_{Hs0} - \gamma_{HiHs}) + \right.$$

$$\sum_{j=1}^{m} V_{Hi0} V_{Hj0} Y_{HiHj} \cos(\theta_{Hi0} - \theta_{Hj0} - \gamma_{HiHj}) +$$

$$V_{Hi0} V_{Ti0} Y_{HiTj} \cos(\theta_{Hi0} - \theta_{Ti0} - \gamma_{HiTi})$$

$$\left. \sum_{k=1}^{n} V_{Hi0} V_{k0} Y_{Hik} \cos(\theta_{Hi0} - \theta_{k0} - \gamma_{Hik}) \right) \Delta V_{Hi} +$$

$$\left( \sum_{s=1}^{l} V_{Hi0} V_{Hs0} Y_{HiHs} \cos(\theta_{Hi0} - \theta_{Hs0} - \gamma_{HiHs}) \Delta V_{Hs} \right) +$$

$$\left( \sum_{j=1}^{m} V_{Hi0} V_{Hj0} Y_{HiHj} \cos(\theta_{Hi0} - \theta_{Hj0} - \gamma_{HiHj}) \Delta V_{Hj} \right) +$$

$$\left( \sum_{k=1}^{n} V_{Hi0} V_{k0} Y_{Hik} \cos(\theta_{Hi0} - \theta_{k0} - \gamma_{Hik}) \Delta V_k \right) +$$

$$\left( - \sum_{s=1(s \neq i)}^{l} V_{Hi0} V_{Hs0} Y_{HiHs} \sin(\theta_{Hi0} - \theta_{Hs0} - \gamma_{HiHs}) - \right.$$

$$\sum_{j=1}^{m} V_{Hi0} V_{Hj0} Y_{HiHj} \sin(\theta_{Hi0} - \theta_{Hj0} - \gamma_{HiHj}) -$$

$$V_{Hi0}V_{k0}Y_{Hik}\sin{(\theta_{Hi0}-\theta_{k0}-\gamma_{Hik})} -$$

$$\sum_{k=1}^{n} V_{Hi0}V_{k0}Y_{Hik}\sin{(\theta_{Hi0}-\theta_{k0}-\gamma_{Hik})} \Bigg)\Delta\theta_{Hi} +$$

$$\left(\sum_{s=1\,(s\neq i)}^{l} V_{Hi0}V_{Hs0}Y_{HiHs}\sin{(\theta_{Hi0}-\theta_{Hs0}-\gamma_{HiHs})}\,\Delta\theta_{Hs}\right) +$$

$$\left(\sum_{j=1}^{m} V_{Hi0}V_{Hj0}Y_{HiHj}\sin{(\theta_{Hi0}-\theta_{Hj0}-\gamma_{HiHj})}\,\Delta\theta_{Hj}\right) +$$

$$\left(\sum_{k=1}^{n} V_{Hi0}V_{k0}Y_{Hik}\sin{(\theta_{Hi0}-\theta_{k0}-\gamma_{Hik})}\,\Delta\theta_{k}\right) +$$

$$V_{Hi0}V_{Ti0}Y_{HiTi}\cos{(\theta_{Hi0}-\theta_{Ti0}-\gamma_{HiTi})}\,\Delta V_{Ti} +$$

$$V_{Hi0}V_{Ti0}Y_{HiTi}\sin{(\theta_{Hi0}-\theta_{Ti0}-\gamma_{HiTi})}\,\Delta\theta_{Ti0}$$

$$-\Delta P_{Hj}^{d} = \left(\sum_{i=1}^{l} V_{Hj0}V_{Hi0}Y_{HjHi}\cos{(\theta_{Hj0}-\theta_{Hi0}-\gamma_{HjHi})} +\right.$$

$$\sum_{s=1}^{m} V_{Hj0}V_{Hs0}Y_{HjHs}\cos{(\theta_{Hj0}-\theta_{Hs0}-\gamma_{HjHs})} +$$

$$V_{Hj0}V_{Tj0}Y_{HjTj}\cos{(\theta_{Hi0}-\theta_{Ti0}-\gamma_{HiTi})} +$$

$$\left.\sum_{k=1}^{n} V_{Hj0}V_{k0}Y_{Hjk}\cos{(\theta_{Hj0}-\theta_{k0}-\gamma_{Hjk})} \right)\Delta V_{Hj} +$$

$$\sum_{i=1}^{l} V_{Hj0}V_{Hi0}Y_{HjHi}\cos{(\theta_{Hj0}-\theta_{Hi0}-\gamma_{HjHi})}\,\Delta V_{Hi} +$$

$$\sum_{s=1}^{m} V_{Hj0}V_{Hs0}Y_{HjHs}\cos{(\theta_{Hj0}-\theta_{Hs0}-\gamma_{HjHs})}\,\Delta V_{Hs} +$$

$$\sum_{k=1}^{n} V_{Hj0}V_{k0}Y_{Hjk}\cos{(\theta_{Hj0}-\theta_{k0}-\gamma_{Hjk})}\,\Delta V_{k} +$$

$$
\left( -\sum_{i=1}^{l} V_{Hj0} V_{Hi0} Y_{HjHi} \sin\left(\theta_{Hj0} - \theta_{Hi0} - \gamma_{HjHi}\right) - \right.
$$

$$
\sum_{s=1\,(s \neq i)}^{m} V_{Hj0} V_{Hs0} Y_{HjHs} \sin\left(\theta_{Hj0} - \theta_{Hs0} - \gamma_{HjHs}\right) -
$$

$$
V_{Hj0} V_{Tj0} Y_{HjTj} \sin\left(\theta_{Hj0} - \theta_{Tj0} - \gamma_{HjTj}\right) -
$$

$$
\left. \sum_{k=1}^{n} V_{Hj0} V_{k0} Y_{Hjk} \sin\left(\theta_{Hj0} - \theta_{k0} - \gamma_{Hjk}\right) \right) \Delta\theta_{Hj} +
$$

$$
\sum_{i=1}^{l} V_{Hj0} V_{Hi0} Y_{HjHi} \sin\left(\theta_{Hj0} - \theta_{Hi0} - \gamma_{HjHi}\right) \Delta\theta_{Hi} +
$$

$$
\sum_{s=1\,(s \neq i)}^{m} V_{Hj0} V_{Hs0} Y_{uiuj} \sin\left(\theta_{Hj0} - \theta_{Hs0} - \gamma_{HjHs}\right) \Delta\theta_{Hs} +
$$

$$
\sum_{k=1}^{n} V_{Hj0} V_{0k} Y_{Hjk} \sin\left(\theta_{Hj0} - \theta_{k0} - \gamma_{Hjk}\right) \Delta\theta_{k} +
$$

$$
V_{Hj0} V_{Tj0} Y_{HjTj} \cos\left(\theta_{Hj0} - \theta_{Tj0} - \gamma_{HjTj}\right) \Delta V_{Tj} +
$$

$$
V_{Hj0} V_{Tj0} Y_{HjTj} \sin\left(\theta_{Hi0} - \theta_{Ti0} - \gamma_{HiTi}\right) \Delta\theta_{Ti}
$$

$$
-\Delta P_{k}^{d} = \left( \sum_{i=1}^{l} V_{k0} V_{Hi0} Y_{kHi} \cos\left(\theta_{k0} - \theta_{Hi0} - \gamma_{kHi}\right) + \right.
$$

$$
\sum_{j=1}^{m} V_{k0} V_{Hj0} Y_{kHj} \cos\left(\theta_{k0} - \theta_{Hj0} - \gamma_{kHj}\right) +
$$

$$
\left. \sum_{s=1}^{n} V_{k0} V_{s0} Y_{ks} \cos\left(\theta_{k0} - \theta_{s0} - \gamma_{ks}\right) \right) \Delta V_{k} +
$$

$$
\sum_{i=1}^{l} V_{k0} V_{Hi0} Y_{kHi} \cos\left(\theta_{k0} - \theta_{Hi0} - \gamma_{kHi}\right) \Delta V_{Hi} +
$$

$$
\sum_{j=1}^{m} V_{k0} V_{Hj0} Y_{kHj} \cos\left(\theta_{k0} - \theta_{Hj0} - \gamma_{kHj}\right) \Delta V_{Hj} +
$$

$$\sum_{s=1}^{n} V_{k0} V_{s0} Y_{ks} \cos (\theta_{k0} - \theta_{s0} - \gamma_{ks}) \Delta V_s +$$

$$\left( -\sum_{i=1}^{l} V_{k0} V_{Hi0} Y_{kHi} \sin (\theta_{k0} - \theta_{Hi0} - \gamma_{kHi}) - \right.$$

$$\sum_{j=1}^{m} V_{k0} V_{Hj0} Y_{kHj} \sin (\theta_{k0} - \theta_{Hj0} - \gamma_{kHj}) -$$

$$\left. \sum_{s=1 (k \neq s)}^{n} V_{k0} V_{s0} Y_{ks} \sin (\theta_{k0} - \theta_{s0} - \gamma_{ks}) \right) \Delta \theta_k +$$

$$\sum_{i=1}^{l} V_{k0} V_{Hi0} Y_{kHi} \sin (\theta_{k0} - \theta_{Hi0} - \gamma_{kHi}) \Delta \theta_{Hi} +$$

$$\sum_{j=1}^{m} V_{k0} V_{Hj0} Y_{kHj} \sin (\theta_{k0} - \theta_{Hj0} - \gamma_{kHj}) \Delta \theta_{Hj} +$$

$$\sum_{s=1 (k \neq s)}^{n} V_{k0} V_{s0} Y_{ks} \sin (\theta_{k0} - \theta_{s0} - \gamma_{ks}) \Delta \theta_s$$

## A.5.5    Reactive Power Linearization for The Network

$$-\Delta Q_{Hi}^{d} = \left( \sum_{s=1}^{l} V_{Hi0} V_{Hs0} Y_{HiHs} \sin (\theta_{Hi0} - \theta_{Hs0} - \gamma_{HiHs}) + \right.$$

$$\sum_{j=1}^{m} V_{Hi0} V_{Hj0} Y_{HiHj} \sin (\theta_{Hi0} - \theta_{Hj0} - \gamma_{HiHj}) +$$

$$V_{Hi0} V_{Ti0} Y_{HiTj} \sin (\theta_{Hi0} - \theta_{Ti0} - \gamma_{HiTi}) +$$

$$\left. \sum_{k=1}^{n} V_{Hi0} V_{k0} Y_{Hik} \sin (\theta_{Hi0} - \theta_{k0} - \gamma_{Hik}) \right) \Delta V_{Hi} +$$

$$\left( \sum_{s=1}^{l} V_{Hi0} V_{Hs0} Y_{HiHs} \sin (\theta_{Hi0} - \theta_{Hs0} - \gamma_{HiHs}) \Delta V_{Hs} \right) +$$

$$\left(\sum_{j=1}^{m} V_{Hi0}V_{Hj0}Y_{HiHj}\sin\left(\theta_{Hi0}-\theta_{Hj0}-\gamma_{HiHj}\right)\Delta V_{Hj}\right)+$$

$$\left(\sum_{k=1}^{n} V_{Hi0}V_{k0}Y_{Hik}\sin\left(\theta_{Hi0}-\theta_{k0}-\gamma_{Hik}\right)\Delta V_{k}\right)+$$

$$\left(\sum_{s=1\,(s\neq i)}^{l} V_{Hi0}V_{Hs0}Y_{HiHs}\cos\left(\theta_{Hi0}-\theta_{Hs0}-\gamma_{HiHs}\right)+\right.$$

$$\sum_{j=1}^{m} V_{Hi0}V_{Hj0}Y_{HiHj}\cos\left(\theta_{Hi0}-\theta_{Hj0}-\gamma_{HiHj}\right)+$$

$$V_{Hi0}V_{k0}Y_{Hik}\cos\left(\theta_{Hi0}-\theta_{k0}-\gamma_{Hik}\right)+$$

$$\left.\sum_{k=1}^{n} V_{Hi0}V_{k0}Y_{Hik}\cos\left(\theta_{Hi0}-\theta_{k0}-\gamma_{Hik}\right)\right)\Delta\theta_{Hi}-$$

$$\left(\sum_{s=1\,(s\neq i)}^{l} V_{Hi0}V_{Hs0}Y_{HiHs}\cos\left(\theta_{Hi0}-\theta_{Hs0}-\gamma_{HiHs}\right)\Delta\theta_{Hs}\right)-$$

$$\left(\sum_{j=1}^{m} V_{Hi0}V_{Hj0}Y_{HiHj}\cos\left(\theta_{Hi0}-\theta_{Hj0}-\gamma_{HiHj}\right)\Delta\theta_{Hj}\right)-$$

$$\left(\sum_{k=1}^{n} V_{Hi0}V_{k0}Y_{Hik}\cos\left(\theta_{Hi0}-\theta_{k0}-\gamma_{Hik}\right)\Delta\theta_{k}\right)+$$

$$V_{Hi0}V_{Ti0}Y_{HiTi}\sin\left(\theta_{Hi0}-\theta_{Ti0}-\gamma_{HiTi}\right)\Delta V_{Ti}-$$

$$V_{Hi0}V_{Ti0}Y_{HiTi}\cos\left(\theta_{Hi0}-\theta_{Ti0}-\gamma_{HiTi}\right)\Delta\theta_{Ti0}$$

$$-\Delta Q_{Hj}^{d}=\left(\sum_{i=1}^{l} V_{Hj0}V_{Hi0}Y_{HjHi}\sin\left(\theta_{Hj0}-\theta_{Hi0}-\gamma_{HjHi}\right)+\right.$$

$$\sum_{s=1}^{m} V_{Hj0}V_{Hs0}Y_{HjHs}\sin\left(\theta_{Hj0}-\theta_{Hs0}-\gamma_{HjHs}\right)+$$

$$V_{Hj0}V_{Tj0}Y_{HjTj}\sin\left(\theta_{Hj0}-\theta_{Tj0}-\gamma_{HjTj}\right)+$$

$$\left. \sum_{k=1}^{n} V_{Hj0}V_{k0}Y_{Hjk}\sin\left(\theta_{Hj0}-\theta_{k0}-\gamma_{Hjk}\right)\right)\Delta V_{Hj}+$$

$$\sum_{i=1}^{l} V_{Hj0}V_{Hi0}Y_{HjHi}\sin\left(\theta_{Hj0}-\theta_{Hi0}-\gamma_{HjHi}\right)\Delta V_{Hi}+$$

$$\sum_{s=1}^{m} V_{Hj0}V_{Hs0}Y_{HjHs}\sin\left(\theta_{Hj0}-\theta_{Hs0}-\gamma_{HjHs}\right)\Delta V_{Hs}+$$

$$\sum_{k=1}^{n} V_{Hj0}V_{k0}Y_{Hjk}\sin\left(\theta_{Hj0}-\theta_{k0}-\gamma_{Hjk}\right)\Delta V_{k}+$$

$$\left(\sum_{i=1}^{l} V_{Hj0}V_{Hi0}Y_{HjHi}\cos\left(\theta_{Hj0}-\theta_{Hi0}-\gamma_{HjHi}\right)\ +\right.$$

$$\sum_{s=1(s\neq i)}^{m} V_{Hj0}V_{Hs0}Y_{HjHs}\cos\left(\theta_{Hj0}-\theta_{Hs0}-\gamma_{HjHs}\right)+$$

$$V_{Hj0}V_{Tj0}Y_{HjTj}\cos\left(\theta_{Hj0}-\theta_{Tj0}-\gamma_{HjTj}\right)+$$

$$\left.\sum_{k=1}^{n} V_{Hj0}V_{k0}Y_{Hjk}\cos\left(\theta_{Hj0}-\theta_{k0}-\gamma_{Hjk}\right)\right)\Delta\theta_{Hj}-$$

$$\sum_{i=1}^{l} V_{Hj0}V_{Hi0}Y_{HjHi}\cos\left(\theta_{Hj0}-\theta_{Hi0}-\gamma_{HjHi}\right)\Delta\theta_{Hi}-$$

$$\sum_{s=1(s\neq i)}^{m} V_{Hj0}V_{Hs0}Y_{uiuj}\cos\left(\theta_{Hj0}-\theta_{Hs0}-\gamma_{HjHs}\right)\Delta\theta_{Hs}-$$

$$\sum_{k=1}^{n} V_{Hj0}V_{0k}Y_{Hjk}\cos\left(\theta_{Hj0}-\theta_{k0}-\gamma_{Hjk}\right)\Delta\theta_{k}+$$

$$V_{Hj0}V_{Tj0}Y_{HjTj}\sin\left(\theta_{Hj0}-\theta_{Tj0}-\gamma_{HjTj}\right)\Delta V_{Tj}-$$

$$V_{Hj0}V_{Tj0}Y_{HjTj}\cos\left(\theta_{Hj0}-\theta_{Tj0}-\gamma_{HjTj}\right)\Delta\theta_{Tj}$$

$$-\Delta Q_{k}^{d}=\left(\sum_{i=1}^{l} V_{k0}V_{Hi0}Y_{kHi}\sin\left(\theta_{k0}-\theta_{Hi0}-\gamma_{kHi}\right)+\right.$$

$$\sum_{j=1}^{m} V_{k0} V_{Hj0} Y_{kHj} \sin (\theta_{k0} - \theta_{Hj0} - \gamma_{kHj}) +$$

$$\sum_{s=1}^{n} V_{k0} V_{s0} Y_{ks} \cos (\theta_{k0} - \theta_{s0} - \gamma_{ks}) \bigg) \Delta V_k +$$

$$\sum_{i=1}^{l} V_{k0} V_{Hi0} Y_{kHi} \sin (\theta_{k0} - \theta_{Hi0} - \gamma_{kHi}) \Delta V_{Hi} +$$

$$\sum_{j=1}^{m} V_{k0} V_{Hj0} Y_{kHj} \sin (\theta_{k0} - \theta_{Hj0} - \gamma_{kHj}) \Delta V_{Hj} +$$

$$\sum_{s=1}^{n} V_{k0} V_{s0} Y_{ks} \cos (\theta_{k0} - \theta_{s0} - \gamma_{ks}) \Delta V_s +$$

$$\bigg( \sum_{i=1}^{l} V_{k0} V_{Hi0} Y_{kHi} \cos (\theta_{k0} - \theta_{Hi0} - \gamma_{kHi}) +$$

$$\sum_{j=1}^{m} V_{k0} V_{Hj0} Y_{kHj} \cos (\theta_{k0} - \theta_{Hj0} - \gamma_{kHj}) +$$

$$\sum_{s=1 \, (k \neq s)}^{n} V_{k0} V_{s0} Y_{ks} \cos (\theta_{k0} - \theta_{s0} - \gamma_{ks}) \bigg) \Delta \theta_k -$$

$$\sum_{i=1}^{l} V_{k0} V_{Hi0} Y_{kHi} \cos (\theta_{k0} - \theta_{Hi0} - \gamma_{kHi}) \Delta \theta_{Hi} -$$

$$\sum_{j=1}^{m} V_{k0} V_{Hj0} Y_{kHj} \cos (\theta_{k0} - \theta_{Hj0} - \gamma_{kHj}) \Delta \theta_{Hj} -$$

$$\sum_{s=1 \, (k \neq s)}^{n} V_{k0} V_{s0} Y_{ks} \cos (\theta_{k0} - \theta_{s0} - \gamma_{ks}) \Delta \theta_s$$

# APPENDIX B

## SENSITIVITY MATRIX DEVELOPMENT AND
## MATHEMATICAL BACKGROUND

### B.1    Sensitivity Matrix Development

Sensitivity matrices were used to show how the reactive power generation, air gap saturation, field current limit, and excitation system control will influence the flux decay stability of a power system in chapter 3.

The development of sensitivity matrices is based on the real and reactive power balance equations

$$P_G = g_1(\delta, \theta, E, V)$$

$$P_L = g_2(\delta, \theta, E, V)$$

$$Q_G = g_3(\delta, \theta, E, V)$$

$$Q_L = g_4(\delta, \theta, E, V)$$

where

$E, \delta$:                    voltage magnitude and phase angle of generator internal

bus,

$V, \theta$ voltage magnitude and phase angle of terminal, high side transformer, and load buses,

$g_1 (\delta, \theta, E, V)$ : the vector of the real power balance equations at generator buses,

$g_2 (\delta, \theta, E, V)$ : the vector of the real power balance equations at terminal, high side transformer, and load buses,

$g_3 (\delta, \theta, E, V)$ : the vector of the reactive power balance equations at generator buses, and

$g_4 (\delta, \theta, E, V)$ : the vector of the reactive power balance equations at terminal, high side transformer, and load buses.

The jacobian matrix for the real and reactive power balance equations is

$$
J = \begin{bmatrix} \dfrac{\partial P_G}{\partial \delta} & \dfrac{\partial P_G}{\partial \theta} & \dfrac{\partial P_G}{\partial E} & \dfrac{\partial P_G}{\partial V} \\[2mm] \dfrac{\partial P_L}{\partial \delta} & \dfrac{\partial P_L}{\partial \theta} & \dfrac{\partial P_L}{\partial E} & \dfrac{\partial P_L}{\partial V} \\[4mm] \dfrac{\partial Q_G}{\partial \delta} & \dfrac{\partial Q_G}{\partial \theta} & \dfrac{\partial Q_G}{\partial E} & \dfrac{\partial Q_G}{\partial V} \\[2mm] \dfrac{\partial Q_L}{\partial \delta} & \dfrac{\partial Q_L}{\partial \theta} & \dfrac{\partial Q_L}{\partial E} & \dfrac{\partial Q_L}{\partial V} \end{bmatrix} = \begin{bmatrix} A_1 \, B_1 & C_1 \, D_1 \\ A_2 \, B_2 & C_2 \, D_2 \\[2mm] A_3 \, B_3 & C_3 \, D_3 \\ A_4 \, B_4 & C_4 \, D_4 \end{bmatrix}
$$

and

$$
\begin{bmatrix} \Delta P_G \\ \Delta P_L \\ \Delta Q_G \\ \Delta Q_L \end{bmatrix} = \begin{bmatrix} A_1 \, B_1 & C_1 \, D_1 \\ A_2 \, B_2 & C_2 \, D_2 \\ A_3 \, B_3 & C_3 \, D_3 \\ A_4 \, B_4 & C_4 \, D_4 \end{bmatrix} \begin{bmatrix} \Delta \delta \\ \Delta \theta \\ \Delta E \\ \Delta V \end{bmatrix} \tag{B.1}
$$

Set

$$\begin{bmatrix} \Delta P_G \\ \Delta P_L \end{bmatrix} = \bar{0}$$

Solve for

$$\begin{bmatrix} \Delta \delta \\ \Delta \theta \end{bmatrix} = - \begin{bmatrix} A_1 & B_1 \\ A_2 & B_2 \end{bmatrix}^{-1} \begin{bmatrix} C_1 & D_1 \\ C_2 & D_2 \end{bmatrix} \begin{bmatrix} \Delta E \\ \Delta V \end{bmatrix}$$

and substitute back to equation(B.1) to obtain a reduced model

$$\begin{bmatrix} \Delta Q_G \\ \Delta Q_L \end{bmatrix} = \hat{J} \begin{bmatrix} \Delta E \\ \Delta V \end{bmatrix}$$

where

$$\hat{J} = \begin{bmatrix} \hat{C}_3 & \hat{D}_3 \\ \hat{C}_4 & \hat{D}_4 \end{bmatrix} = \begin{bmatrix} C_3 & D_3 \\ C_4 & D_4 \end{bmatrix} - \begin{bmatrix} A_3 & B_3 \\ A_4 & B_4 \end{bmatrix} \begin{bmatrix} A_1 & B_1 \\ A_2 & B_2 \end{bmatrix}^{-1} \begin{bmatrix} C_1 & D_1 \\ C_2 & D_2 \end{bmatrix}$$

The sensitivity model has the form

$$\Delta V = S_{Q_L V}^{-1} \Delta Q_L + S_{VE} \Delta E$$

$$\Delta Q_G = S_{Q_G E} \Delta E + S_{Q_G Q_L} \Delta Q_L$$

where

$$S_{Q_L V} = D_4 - \begin{bmatrix} A_4 & B_4 \end{bmatrix} \begin{bmatrix} A_1 & B_1 \\ A_2 & B_2 \end{bmatrix}^{-1} \begin{bmatrix} D_1 \\ D_2 \end{bmatrix}$$

$$S_{VE} = -S_{Q_L V} \left( C_4 - \begin{bmatrix} A_4 & B_4 \end{bmatrix} \begin{bmatrix} A_1 & B_1 \\ A_2 & B_2 \end{bmatrix}^{-1} \begin{bmatrix} C_1 \\ C_2 \end{bmatrix} \right)$$

$$S_{Q_G Q_L} = -\left( D_3 - \begin{bmatrix} A_3 & B_3 \end{bmatrix} \begin{bmatrix} A_1 & B_1 \\ A_2 & B_2 \end{bmatrix}^{-1} \begin{bmatrix} D_1 \\ D_2 \end{bmatrix} \right)$$

$$S_{Q_G E} = \left( C_3 - \begin{bmatrix} A_3 & B_3 \end{bmatrix} \begin{bmatrix} A_1 & B_1 \\ A_2 & B_2 \end{bmatrix}^{-1} \begin{bmatrix} C_1 \\ C_2 \end{bmatrix} \right) - S_{Q_G Q_L} S_{Q_L V} S_{VE}$$

The sensitivity matrix $S_{Q_G E}$ has the following properties

(a)     positive diagonal elements and negative off-diagonal elements, and

(b)     the magnitude of the negative off-diagonal elements would increase and the positive diagonal elements would decrease as the network is getting stress.

It is shown in chapter 3 that these properties explain that one of the reason of flux decay dynamics being instability is caused by the stressed distribution system.

Schlueter and Costi [1,9] discussed the derivation and characteristics of sensitivity matrices in much more detailed.

## B.2     Condition Number

Theorem 4.8 [26]:

For any invertible $n \times n$ matrix A and any matrix norm, the condition number of A indicates the relative distance of A from the nearest noninvertible $n \times n$ matrix, Specially,

$$\frac{1}{cond\,(A)} = min\left\{\frac{\|A-B\|}{\|A\|}\middle| B \text{ is not invertible}\right\}$$

## B.3    Nonsingularity of Matrix A

This section shows that the submatrix A of the jacobian matrix of a general power system model is always nonsingular. A general power system model is

Differential Equation Model

$$\dot{x}(t) = f(x(t),y(t),\lambda(t)) \qquad\qquad \lambda(t) \in [\lambda_a,\lambda_b]$$

Algebraic Equation Model

$$0 = g(x(t),y(t),\lambda(t))$$

where

$x(t)$    state vector of the generator dynamics,

$y(t)$    state vector of bus voltage and angle of terminal buses, high side transformer buses, and load buses, and

$\lambda(t)$    state vector of the slow varying operating parameter.

The jacobian matrix is

$$J = \begin{bmatrix} \dfrac{\partial f}{\partial x} & \dfrac{\partial f}{\partial y} \\ \dfrac{\partial g}{\partial x} & \dfrac{\partial g}{\partial y} \end{bmatrix} = \begin{bmatrix} A & B \\ C & D \end{bmatrix}$$

The sub matrix can be represented by

$$A = \begin{bmatrix} A_{MF} & A_I \\ 0 & A_E \end{bmatrix}$$

where

$A_{MF}$:  linearized mechanical and flux decay dynamics,

$A_E$:  linearized exciter dynamics, and

$A_I$:  interface of $A_{MF}$ and $A_E$.

We first show matrix $A_E$ is nonsingular. $A_E$ can be represented by

$$A_E = \begin{bmatrix} Z_{22} & 0 & 0 & 0 \\ 0 & Z_{24} & Z_{25} & Z_{26} \\ Z_{27} & Z_{28} & Z_{29} & 0 \\ 0 & 0 & Z_{30} & Z_{31} \end{bmatrix}$$

where

$$Z_{22} = diag\left(\frac{-1}{\tau_{Ri}}\right)_{l \times l}$$

$$Z_{24} = diag\left(\frac{-1}{\tau_{Fi}}\right)_{l \times l}$$

$$Z_{25} = diag\left(\frac{K_{Fi}}{\tau_{Fi}\tau_{Ei}}\right)_{l \times l}$$

$$Z_{26} = diag\left(-\frac{K_{Fi}(\dot{S}_{Ei}(E_{cfdi0})E_{cfdi0} + S_{Ei}(E_{cfdi0}) + K_{Ei})}{\tau_{Fi}\tau_{Ei}}\right)_{l \times l}$$

$$Z_{27} = diag\left(\frac{-K_{Ai}}{\tau_{Ai}}\right)_{l \times l}$$

$$Z_{28} = diag\left(\frac{-K_{Ai}}{\tau_{Ai}}\right)_{l \times l}$$

$$Z_{29} = diag\left(\frac{-1}{\tau_{Ai}}\right)_{l \times l}$$

$$Z_{30} = diag\left(\frac{1}{\tau_{Ei}}\right)_{l \times l}$$

$$Z_{31} = diag\left(-\frac{(\dot{S}_{Ei}(E_{cfdi0})E_{cfdi0} + S_{Ei}(E_{cfdi0}) + K_{Ei})}{\tau_{Ei}}\right)_{l \times l}$$

Since $Z_{22}$ is a diagonal matrix and has no zero diagonal element, $detZ_{22} \neq 0$.

$$detA_E = detZ_{22} \times det\begin{vmatrix} Z_{24} & Z_{25} & Z_{26} \\ Z_{28} & Z_{29} & 0 \\ 0 & Z_{30} & Z_{31} \end{vmatrix}$$

The term

$$\dot{S}_{Ei}(E_{cfdi0})E_{cfdi0} + S_{Ei}(E_{cfdi0}) + K_{Ei} > 0 \qquad \text{(B.3.1)}$$

because $\dot{S}_{Ei}(E_{cfdi0})E_{cfdi0} > 0$ and $S_{Ei}(E_{cfdi0}) > 0$ and

(a)  if $K_{Ei} > 0$, equation B.3.1 is true, and

(b)  if $K_{Ei} < 0$, equation (b.3.1) is still true because in the normal condition as long as the generator is supplying reactive power (field voltage is large), the magnitudes of the first two positive elements will dominate the whole term. In the heavy load condition, the field voltage and the saturation function are larger than the normal condition, (B.3.1) is true.

Since (b.3.1) is always true, $Z_{31}$ is nonsingular. the determinant of $A_E$ can be represented in the following form

$$detA_E = detZ_{22} \times det(Z_{31}) \times det\left(\begin{bmatrix} Z_{24} & Z_{25} \\ Z_{28} & Z_{29} \end{bmatrix} - \begin{bmatrix} Z_{26} \\ 0 \end{bmatrix}\begin{bmatrix} Z_{31}^{-1} \end{bmatrix}\begin{bmatrix} 0 & Z_{30} \end{bmatrix}\right) =$$

$$detZ_{22} \times detZ_{31} \times det\left(\begin{bmatrix} Z_{24} & Z_{25} - Z_{26}Z_{31}^{-1}Z_{30} \\ Z_{28} & Z_{29} \end{bmatrix}\right) =$$

$$det Z_{22} \times det Z_{31} \times det \begin{bmatrix} Z_{24} & 0 \\ Z_{28} & Z_{29} \end{bmatrix}$$

Since $Z_{24}$ and $Z_{29}$ are nonsingular,

$$det A_E = det Z_{22} \times det Z_{31} \times det Z_{24} \times det Z_{29} \neq 0$$

the matrix $A_E$ is nonsingular.

We now show the matrix $A_{MF}$ is nonsingular. The matrix $A_{MF}$ can be represented by

$$A_{MF} = \begin{bmatrix} Z_1 & 0 & Z_2 & 0 & Z_3 & 0 \\ 0 & Z_6 & 0 & Z_7 & 0 & Z_8 \\ Z_{11} & 0 & 0 & 0 & 0 & 0 \\ 0 & Z_{12} & 0 & 0 & 0 & 0 \\ 0 & 0 & Z_{13} & 0 & Z_{14} & 0 \\ 0 & 0 & 0 & Z_{18} & 0 & Z_{19} \end{bmatrix}$$

where

$$Z_1 = diag \left( \frac{-D_i}{M_i} \right)_{l \times l}$$

$$Z_2 = diag \left( \frac{-E_{i0} V_{Ti0} \cos(\delta_{i0} - \theta_{Ti0})}{M_i x'_{di}} - \right.$$

$$\left. \frac{V^2_{Ti0} \cos(2(\delta_{i0} - \theta_{Ti0}))(x'_{di} - x_{qi})}{M_i x'_{di} x_{qi}} \right)_{l \times l}$$

$$Z_3 = diag \left( \frac{-E_{i0} V_{Ti0} \sin(\delta_{i0} - \theta_{Ti0})}{M_i x'_{di}} \right)_{l \times l}$$

$$Z_6 = diag \left( \frac{-D_j}{M_j} \right)_{m \times m}$$

$$Z_7 = diag \left( \frac{-E_{j0} V_{Tj0} \cos(\delta_{j0} - \theta_{Tj0})}{M_j x'_{dj}} - \right.$$

$$\left. \frac{V_{Tj0}^2 \cos\left(2\left(\delta_{j0} - \theta_{Tj0}\right)\right)\left(x'_{dj} - x_{qj}\right)}{M_j x'_{dj} x_{qj}} \right)_{m \times m}$$

$$Z_8 = diag\left(\frac{-E_{j0} V_{Tj0} \sin\left(\delta_{j0} - \theta_{Tj0}\right)}{M_j x'_{dj}}\right)_{m \times m}$$

$$Z_{11} = I_{l \times l}$$

$$Z_{12} = I_{m \times m}$$

$$Z_{13} = diag\left(\frac{-V_{Ti0} \sin\left(\delta_{i0} - \theta_{Ti0}\right)\left(x_{di} - x'_{di}\right)}{E_{i0} \tau_{d0i} x'_{di}}\right)_{l \times l}$$

$$Z_{14} = diag\left(\frac{-x_{di}}{\tau_{d0i} x'_{di}}\right)_{l \times l}$$

$$Z_{18} = diag\left(\frac{-V_{Tj0} \sin\left(\delta_{j0} - \theta_{Tj0}\right)\left(x_{dj} - x'_{dj}\right)}{E_{j0} \tau_{d0j} x'_{dj}}\right)_{m \times m}$$

$$Z_{19} = diag\left(\frac{-x_{dj}}{\tau_{d0j} x'_{dj}}\right)_{m \times m}$$

Since the matrices $Z_1$ and $Z_6$ are nonsingular,

$$det A_{MF} =$$

$$det\begin{bmatrix} Z_1 & 0 \\ 0 & Z_6 \end{bmatrix} \times det\left(\begin{bmatrix} 0 & 0 & 0 & 0 \\ 0 & 0 & 0 & 0 \\ Z_{13} & 0 & Z_{14} & 0 \\ 0 & Z_{18} & 0 & Z_{19} \end{bmatrix} - \begin{bmatrix} Z_{11} & 0 \\ 0 & Z_{12} \\ 0 & 0 \\ 0 & 0 \end{bmatrix}\begin{bmatrix} Z_1^{-1} & 0 \\ 0 & Z_6^{-1} \end{bmatrix}\begin{bmatrix} Z_2 & 0 & Z_3 & 0 \\ 0 & Z_7 & 0 & Z_8 \end{bmatrix}\right) =$$

$$det\begin{bmatrix} Z_1 & 0 \\ 0 & Z_6 \end{bmatrix} \times det\left(\begin{bmatrix} -Z_{11}Z_1^{-1}Z_2 & 0 & -Z_{11}Z_1^{-1}Z_3 & 0 \\ 0 & -Z_{12}Z_6^{-1}Z_7 & 0 & -Z_{12}Z_6^{-1}Z_8 \\ Z_{13} & 0 & Z_{14} & 0 \\ 0 & Z_{18} & 0 & Z_{19} \end{bmatrix}\right)$$

Since matrices $Z_{14}$ and $Z_{19}$ are nonsingular diagonal matrices,

$$det\left(\begin{bmatrix} -Z_{11}Z_1^{-1}Z_2 & 0 & -Z_{11}Z_1^{-1}Z_3 & 0 \\ 0 & -Z_{12}Z_6^{-1}Z_7 & 0 & -Z_{12}Z_6^{-1}Z_8 \\ Z_{13} & 0 & Z_{14} & 0 \\ 0 & Z_{18} & 0 & Z_{19} \end{bmatrix}\right) =$$

$$det\begin{bmatrix} Z_{14} & 0 \\ 0 & Z_{19} \end{bmatrix} det\left(\begin{bmatrix} -Z_{11}Z_1^{-1}Z_2 & 0 \\ 0 & -Z_{12}Z_6^{-1}Z_7 \end{bmatrix} - \begin{bmatrix} -Z_{11}Z_1^{-1}Z_3Z_{14}^{-1}Z_{13} & 0 \\ 0 & -Z_{12}Z_6^{-1}Z_8Z_{19}^{-1}Z_{18} \end{bmatrix}\right)$$

$$= det\begin{bmatrix} Z_{14} & 0 \\ 0 & Z_{19} \end{bmatrix} det\begin{bmatrix} -Z_{11}Z_1^{-1}(Z_2 + Z_3Z_{14}^{-1}Z_{13}) & 0 \\ 0 & -Z_{12}Z_6^{-1}(Z_7 + Z_8Z_{19}^{-1}Z_{18}) \end{bmatrix}$$

If the matrices $-Z_{11}Z_1^{-1}(Z_2 + Z_3Z_{14}^{-1}Z_{13})$ and $-Z_{12}Z_6^{-1}(Z_7 + Z_8Z_{19}^{-1}Z_{18})$ are nonsingular, the matrix $A_{MF}$ is nonsingular.

Let $\eta_i = \delta_i - \theta_{Ti}$,

$$Z_2 + Z_3Z_{14}^{-1}Z_{13} =$$

$$diag\left(\frac{-E_{qi}V_{Ti}x_{qi}\cos\eta_i - V_{Ti}^2(x_{di} - x'_{di})x_{qi}\sin^2\eta_i - V_{Ti}^2(x'_{di} - x_{qi})\cos(2\eta_i)}{M_i x'_{di} x_{qi}}\right) =$$

$$diag\left(\frac{-V_{Ti}\cos\eta_i K_1 + V_{Ti}^2\sin^2\eta_i K_2}{M_i x'_{di} x_{qi}}\right)$$

where

$$K_1 = E_{qi}x_{qi} - E_{qi}\cos\eta_i(x_{qi} - x'_{di}) \text{ and}$$

$$K_2 = x'_{di}(x_{qi} + 1) - x_{qi}(x'_{di} + 1)$$

Since $E_{qi} > E_{qi}$ and $x_{qi} > \cos\eta_i(x_{qi} - x'_{di})$, $K_1 > 0$ which implies

$$-V_{Ti}\cos\eta_i K_1 \leq 0 \qquad\qquad\qquad\qquad\text{(B.3.2)}$$

Normally, $x'_d \ll x_d$ *or* $x_q$, $K_2 < 0$ which implies

$$V_{Ti}^2 \sin^2\eta_i K_2 \leq 0 \qquad\qquad\qquad\qquad\text{(B.3.3)}$$

But (B.3.2) and (B.3.3) can not be equal at the same time,

$$Z_2 + Z_3 Z_{14}^{-1} Z_{13} < 0$$

for all $\eta$ which implies

$$det\,(Z_2 + Z_3 Z_{14}^{-1} Z_{13}) \neq 0$$

The same procedure can be applied to the matrix $Z_7 + Z_8 Z_{19}^{-1} Z_{18}$ and shows t is matrix is nonsingular. The matrix $A_{MF}$ is nonsingular.

# APPENDIX C

## SIMULATION RESULTS

### C.1    Load flow voltage instability

Table C.1.1 to Table C.1.5 are the outputs from EPRI load flow program. The reactances of L2 and L3 are increased by 2, 3, 4, 4.1 times. Refer to the discussion in section 4.2.2.

# Table C.1.1 Load flow simulation for the regular line reactances

19 BUSES TEST SYSTEM FOR VOLTAGE COLAPSE TRANSIENT STABILITY MODEL
BASE CASE REACTIVE POWER LOAD AT LOAD2 IS 50,real power(real load)
REACTIVE GENERATION GROUP NO. 1, LIGHR REAL POWER LOAD

POWER FLOW REPORT    PAGE NO.  1
ZONE ( ) OF AREA ( )
4/26/1990 15: 1:52

| NAME-BASE ACTUAL KV | P.U. ANGLE | GENERATION MW | MVAR | LOAD MW | MVAR | SHUNT MW | MVAR | ID | TO BUS NAME | LINE FLOWS MW | MVAR | LINE LOSSES MW | MVAR | PCT OVL |
|---|---|---|---|---|---|---|---|---|---|---|---|---|---|---|
| HST1  230 / 230.8 KV | 1.0034 -2.8 | 0.0 | 0.0 | 0.0 | 0.0 | 0.0 | 0.0 | | | | | | | |
| | | | | | | | | 1 | LOAD1 230 | 24.1 | 4.5 | 0.10 | -19.86 | |
| | | | | | | | | 1 | LOAD3 230 | 60.9 | -12.4 | 1.45 | -28.75 | |
| | | | | | | | | 1 | TERM1 18.0 | -85.0 | 7.9 | 0.00 | 4.24 | |
| HST2  230 / 229.1 KV | 0.9962 -1.0 | 0.0 | 0.0 | 0.0 | 0.0 | 0.0 | 0.0 | | | | | | | |
| | | | | | | | | 1 | LOAD1 230 | 76.5 | 0.3 | 0.51 | -10.34 | |
| | | | | | | | | 1 | LOAD2 230 | 86.5 | -2.5 | 2.46 | -16.82 | |
| | | | | | | | | 1 | TERM2 18.0 | -163.0 | 2.3 | 0.00 | 16.74 | |
| HST3  230 / 227.0 KV | 0.9870 -7.2 | 0.0 | 0.0 | 0.0 | 0.0 | 0.0 | 0.0 | | | | | | | |
| | | | | | | | | 1 | LOAD2 230 | 41.2 | 21.3 | 0.27 | -14.38 | |
| | | | | | | | | 1 | LOAD3 230 | 30.8 | -0.6 | 0.17 | -14.27 | |
| | | | | | | | | 1 | TERM3 15.5 | -72.0 | -20.7 | 0.00 | 3.32 | |
| LOAD1  230 / 226.7 KV | 0.9856 -4.1 | 0.0 | 0.0 | 100.0 | 35.0 | 0.0 | 0.0 | | | | | | | |
| | | | | | | | | 1 | HST1 230 | -24.0 | -24.4 | 0.10 | -19.86 | |
| | | | | | | | | 1 | HST2 230 | -76.0 | -10.6 | 0.51 | -10.34 | |
| LOAD2  230 / 220.3 KV | 0.9576 -9.1 | 0.0 | 0.0 | 125.0 | 50.0 | 0.0 | 0.0 | | | | | | | |
| | | | | | | | | 1 | HST2 230 | -84.0 | -14.3 | 2.46 | -16.82 | |
| | | | | | | | | 1 | HST3 230 | -41.0 | -35.7 | 0.27 | -14.38 | |
| LOAD3  230 / 224.4 KV | 0.9755 -8.8 | 0.0 | 0.0 | 90.0 | 30.0 | 0.0 | 0.0 | | | | | | | |
| | | | | | | | | 1 | HST1 230 | -59.4 | -16.3 | 1.45 | -28.75 | |
| | | | | | | | | 1 | HST3 230 | -30.6 | -13.7 | 0.17 | -14.27 | |
| TERM1  18.0 / 18.0 KV | 1.0000 0.0 | 85.0 | -3.7 | 0.0 | 0.0 | 0.0 | 0.0 | 1 | HST1 230 | 85.0 | -3.7 | 0.00 | 4.24 | |
| | | | | | | TAP | 18.0/ 230.0 | | | | | | | |
| TERM2  18.0 / 18.0 KV | 1.0000 4.9 | 163.0 | 14.5R | 0.0 | 0.0 | 0.0 | 0.0 | 1 | HST2 230 | 163.0 | 14.5 | 0.00 | 16.74 | |
| | | | | | | TAP | 18.0/ 230.0 | | | | | | | |
| TERM3  15.5 / 15.5 KV | 1.0000 -4.8 | 72.0 | 24.1R | 0.0 | 0.0 | 0.0 | 0.0 | 1 | HST3 230 | 72.0 | 24.1 | 0.00 | 3.32 | |
| | | | | | | TAP | 15.5/ 230.0 | | | | | | | |

END OF REPORT FOR THIS CASE

## Table C.1.2 Load flow simulation for two times line reactances

19 BUSES TEST SYSTEM FOR VOLTAGE COLAPSE TRANSIENT STABILITY MODEL

BASE CASE REACTIVE POWER LOAD AT LOAD2 IS 50,real power(real load)

2 times, REACTIVE GENERATION GROUP NO. 1, LIGHR REAL POWER LOAD

POWER FLOW REPORT    PAGE NO. 1

ZONE ( ) OF AREA ( )

4/26/1990 15: 7:54

| NAME-BASE / ACTUAL KV | P.U. ANGLE | GENERATION MW | GENERATION MVAR | LOAD MW | LOAD MVAR | SHUNT MW | SHUNT MVAR | ID | TO BUS NAME | LINE FLOWS MW | LINE FLOWS MVAR | LINE LOSSES MW | LINE LOSSES MVAR | PCT OVL |
|---|---|---|---|---|---|---|---|---|---|---|---|---|---|---|
| HST1 230 / 230.3 KV | 1.0014 / -2.9 | 0.0 | 0.0 | 0.0 | 0.0 | 0.0 | 0.0 | 1 | LOAD1 230 | 12.5 | 7.9 | 0.06 | -20.05 | |
| | | | | | | | | 1 | LOAD3 230 | 72.8 | -12.3 | 2.07 | -25.79 | |
| | | | | | | | | 1 | TERM1 18.0 | -85.3 | 4.4 | 0.00 | 4.26 | |
| HST2 230 / 227.9 KV | 0.9910 / 0.3 | 0.0 | 0.0 | 0.0 | 0.0 | 0.0 | 0.0 | 1 | LOAD1 230 | 88.3 | -1.7 | 0.68 | -8.76 | |
| | | | | | | | | 1 | LOAD2 230 | 74.7 | 7.6 | 1.99 | -8.09 | |
| | | | | | | | | 1 | TERM2 18.0 | -163.0 | -5.9 | 0.00 | 16.93 | |
| HST3 230 / 226.1 KV | 0.9833 / -9.1 | 0.0 | 0.0 | 0.0 | 0.0 | 0.0 | 0.0 | 1 | LOAD2 230 | 52.7 | 25.2 | 0.40 | -9.15 | |
| | | | | | | | | 1 | LOAD3 230 | 19.3 | 1.9 | 0.08 | -14.64 | |
| | | | | | | | | 1 | TERM3 15.5 | -72.0 | -27.1 | 0.00 | 3.53 | |
| LOAD1 230 / 225.7 KV | 0.9814 / -3.5 | 0.0 | 0.0 | 100.0 | 35.0 | 0.0 | 0.0 | 1 | HST1 230 | -12.4 | -28.0 | 0.06 | -20.05 | |
| | | | | | | | | 1 | HST2 230 | -87.6 | -7.0 | 0.68 | -8.76 | |
| LOAD2 230 / 212.5 KV | 0.9239 / -14.5 | 0.0 | 0.0 | 125.0 | 50.0 | 0.0 | 0.0 | 1 | HST2 230 | -72.7 | -15.7 | 1.99 | -8.09 | |
| | | | | | | | | 1 | HST3 230 | -52.3 | -34.3 | 0.40 | -9.15 | |
| LOAD3 230 / 223.4 KV | 0.9711 / -10.0 | 0.0 | 0.0 | 90.0 | 30.0 | 0.0 | 0.0 | 1 | HST1 230 | -70.7 | -13.4 | 2.07 | -25.79 | |
| | | | | | | | | 1 | HST3 230 | -19.3 | -16.6 | 0.08 | -14.64 | |
| TERM1 18.0 / 18.0 KV | 1.0000 / 0.0 | 85.3 | -0.2 | 0.0 | 0.0 TAP | 18.0/ 230.0 | 0.0 | 1 | HST1 230 | 85.3 | -0.2 | 0.00 | 4.26 | |
| TERM2 18.0 / 18.0 KV | 1.0000 / 0.0 | 163.0 | 22.8R | 0.0 | 0.0 TAP | 18.0/ 230.0 | 0.0 | 1 | HST2 230 | 163.0 | 22.8 | 0.00 | 16.93 | |
| TERM3 15.5 / 15.5 KV | 1.0000 / -6.7 | 72.0 | 30.6R | 0.0 | 0.0 TAP | 15.5/ 230.0 | 0.0 | 1 | HST3 230 | 72.0 | 30.6 | 0.00 | 3.53 | |

END OF REPORT FOR THIS CASE

# Table C.1.3 Load flow simulation for three times line reactances

```
19 BUSES TEST SYSTEM FOR VOLTAGE COLAPSE TRANSIENT STABILITY MODEL                POWER FLOW REPORT      PAGE NO.   1
BASE CASE  REACTIVE POWER LOAD AT LOAD2 IS 50,real power(real load)               ZONE ( ) OF AREA (   )
3 times, REACTIVE GENERATION GROUP NO. 1, LIGHR REAL POWER LOAD                   4/26/1990 15:17:23
```

| NAME-BASE ACTUAL KV | P.U. ANGLE | GENERATION MW | MVAR | LOAD MW | MVAR | SHUNT MW | MVAR | ID | TO BUS NAME | | LINE FLOWS MW | MVAR | LINE LOSSES MW | MVAR | PCT OVL |
|---|---|---|---|---|---|---|---|---|---|---|---|---|---|---|---|
| HST1 230  229.8 KV | 0.9991  -2.9 | 0.0 | 0.0 | 0.0 | 0.0 | 0.0 | 0.0 | 1 | LOAD1 | 230 | 5.1 | 10.4 | 0.05 | -19.95 | |
| | | | | | | | | 1 | LOAD3 | 230 | 80.7 | -11.0 | 2.56 | -23.38 | |
| | | | | | | | | 1 | TERM1 | 18.0 | -85.8 | 0.6 | 0.00 | 4.33 | |
| HST2 230  226.9 KV | 0.9864  1.0 | 0.0 | 0.0 | 0.0 | 0.0 | 0.0 | 0.0 | 1 | LOAD1 | 230 | 95.7 | -2.9 | 0.80 | -7.57 | |
| | | | | | | | | 1 | LOAD2 | 230 | 67.3 | 15.9 | 1.80 | 0.60 | |
| | | | | | | | | 1 | TERM2 | 18.0 | -163.0 | -13.0 | 0.00 | 17.18 | |
| HST3 230  224.8 KV | 0.9773  -10.3 | 0.0 | 0.0 | 0.0 | 0.0 | 0.0 | 0.0 | 1 | LOAD2 | 230 | 60.1 | 34.0 | 0.57 | -0.69 | |
| | | | | | | | | 1 | LOAD3 | 230 | 11.9 | 3.0 | 0.04 | -14.67 | |
| | | | | | | | | 1 | TERM3 | 15.5 | -72.0 | -36.9 | 0.00 | 3.95 | |
| LOAD1 230  224.8 KV | 0.9775  -3.0 | 0.0 | 0.0 | 100.0 | 35.0 | 0.0 | 0.0 | 1 | HST1 | 230 | -5.1 | -30.4 | 0.05 | -19.95 | |
| | | | | | | | | 1 | HST2 | 230 | -94.9 | -4.6 | 0.80 | -7.57 | |
| LOAD2 230  201.0 KV | 0.8740  -20.4 | 0.0 | 0.0 | 125.0 | 50.0 | 0.0 | 0.0 | 1 | HST2 | 230 | -65.5 | -15.3 | 1.80 | 0.60 | |
| | | | | | | | | 1 | HST3 | 230 | -59.5 | -34.7 | 0.57 | -0.69 | |
| LOAD3 230  222.0 KV | 0.9654  -10.9 | 0.0 | 0.0 | 90.0 | 30.0 | 0.0 | 0.0 | 1 | HST1 | 230 | -78.1 | -12.3 | 2.56 | -23.38 | |
| | | | | | | | | 1 | HST3 | 230 | -11.9 | -17.7 | 0.04 | -14.67 | |
| TERM1 18.0  18.0 KV | 1.0000  0.0 | 85.8 | 3.7 | 0.0  TAP | 0.0 | 0.0  18.0/ 230.0 | 0.0 | 1 | HST1 | 230 | 85.8 | 3.7 | 0.00 | 4.33 | |
| TERM2 18.0  18.0 KV | 1.0000  7.0 | 163.0 | 30.2R | 0.0  TAP | 0.0 | 0.0  18.0/ 230.0 | 0.0 | 1 | HST2 | 230 | 163.0 | 30.2 | 0.00 | 17.18 | |
| TERM3 15.5  15.5 KV | 1.0000  -7.9 | 72.0 | 40.9R | 0.0  TAP | 0.0 | 15.5/ 230.0 | 0.0 | 1 | HST3 | 230 | 72.0 | 40.9 | 0.00 | 3.95 | |

END OF REPORT FOR THIS CASE

## Table C.1.4 Load flow simulation for four times line reactances

19 BUSES TEST SYSTEM FOR VOLTAGE COLAPSE TRANSIENT STABILITY MODEL  POWER FLOW REPORT   PAGE NO. 1
BASE CASE  REACTIVE POWER LOAD AT LOAD2 IS 50, real power(real load)   ZONE ( ) OF AREA ( )
4 times, REACTIVE GENERATION GROUP NO. 1, LIGHR REAL POWER LOAD   4/26/1990 15:26:56

| NAME-BASE ACTUAL KV | P.U. ANGLE | GENERATION MW | MVAR | LOAD MW | MVAR | SHUNT MW | MVAR | ID TO BUS NAME | LINE FLOWS MW | MVAR | LINE LOSSES MW | MVAR | PCT OVL |
|---|---|---|---|---|---|---|---|---|---|---|---|---|---|
| HST1 230 228.8 KV | 0.9948 -2.9 | 0.0 | 0.0 | 0.0 | 0.0 | 0.0 | 0.0 | | | | | | |
| | | | | | | | | 1 LOAD1 230 | -1.2 | 12.5 | 0.06 | -19.68 | |
| | | | | | | | | 1 LOAD3 230 | 87.9 | -5.9 | 3.10 | -20.39 | |
| | | | | | | | | 1 TERM1 18.0 | -86.7 | -6.6 | 0.00 | 4.48 | |
| HST2 230 225.5 KV | 0.9804 1.7 | 0.0 | 0.0 | 0.0 | 0.0 | 0.0 | 0.0 | | | | | | |
| | | | | | | | | 1 LOAD1 230 | 102.2 | -3.6 | 0.92 | -6.36 | |
| | | | | | | | | 1 LOAD2 230 | 60.8 | 25.8 | 1.78 | 11.38 | |
| | | | | | | | | 1 TERM2 18.0 | -163.0 | -22.2 | 0.00 | 17.60 | |
| HST3 230 220.9 KV | 0.9603 -11.5 | 0.0 | 0.0 | 0.0 | 0.0 | 0.0 | 0.0 | | | | | | |
| | | | | | | | | 1 LOAD2 230 | 66.8 | 48.6 | 0.83 | 12.96 | |
| | | | | | | | | 1 LOAD3 230 | 5.2 | 1.2 | 0.02 | -14.34 | |
| | | | | | | | | 1 TERM3 15.5 | -72.0 | -49.7 | 0.00 | 4.78 | |
| LOAD1 230 223.5 KV | 0.9718 -2.7 | 0.0 | 0.0 | 100.0 | 35.0 | 0.0 | 0.0 | | | | | | |
| | | | | | | | | 1 HST1 230 | 1.3 | -32.2 | 0.06 | -19.68 | |
| | | | | | | | | 1 HST2 230 | -101.3 | -2.8 | 0.92 | -6.36 | |
| LOAD2 230 182.8 KV | 0.7946 -27.4 | 0.0 | 0.0 | 125.0 | 50.0 | 0.0 | 0.0 | | | | | | |
| | | | | | | | | 1 HST2 230 | -59.0 | -14.4 | 1.78 | 11.38 | |
| | | | | | | | | 1 HST3 230 | -66.0 | -35.6 | 0.83 | 12.96 | |
| LOAD3 230 218.8 KV | 0.9513 -11.7 | 0.0 | 0.0 | 90.0 | 30.0 | 0.0 | 0.0 | | | | | | |
| | | | | | | | | 1 HST1 230 | -84.8 | -14.5 | 3.10 | -20.39 | |
| | | | | | | | | 1 HST3 230 | -5.2 | -15.5 | 0.02 | -14.34 | |
| TERM1 18.0 18.0 KV | 1.0000 0.0 | 86.7 | 11.1 | 0.0 | 0.0 | 0.0 TAP | 0.0 18.0/ 230.0 | 1 HST1 230 | 86.7 | 11.1 | 0.00 | 4.48 | |
| TERM2 18.0 18.0 KV | 1.0000 7.7 | 163.0 | 39.8R | 0.0 | 0.0 | 0.0 TAP | 0.0 18.0/ 230.0 | 1 HST2 230 | 163.0 | 39.8 | 0.00 | 17.60 | |
| TERM3 15.5 15.4 KV | 0.9911 -9.0 | 72.0 | 54.5H | 0.0 | 0.0 | 0.0 TAP | 0.0 15.5/ 230.0 | 1 HST3 230 | 72.0 | 54.5 | 0.00 | 4.78 | |

END OF REPORT FOR THIS CASE

## Table C.1.5 Load flow simulation for three times line reactances

19 BUSES TEST SYSTEM FOR VOLTAGE COLAPSE TRANSIENT STABILITY MODEL

BASE CASE REACTIVE POWER LOAD AT LOAD2 IS 50, real power(real load)

4.1 times, REACTIVE GENERATION GROUP NO. 1, LIGHR REAL POWER LOAD

POWER FLOW REPORT   PAGE NO. 1

ZONE ( ) OF AREA ( )

4/26/1990 15:41:54

| NAME-BASE ACTUAL KV | P.U. ANGLE | GENERATION MW | MVAR | LOAD MW | MVAR | SHUNT MW | MVAR | ID | TO BUS NAME | LINE FLOWS MW | MVAR | LINE LOSSES MW | MVAR | PCT OVL |
|---|---|---|---|---|---|---|---|---|---|---|---|---|---|---|
| HST1 230 227.0 KV | 0.9868 -3.0 | 0.0 | 0.0 | 0.0 | 0.0 | 0.0 | 0.0 | 1 | LOAD1 230 | -1.2 | 13.1 | 0.07 | -19.31 | |
| | | | | | | | | 1 | LOAD3 230 | 88.7 | 6.8 | 3.38 | -17.87 | |
| | | | | | | | | 1 | TERM1 18.0 | -87.5 | -19.9 | 0.00 | 4.84 | |
| HST2 230 223.5 KV | 0.9719 1.8 | 0.0 | 0.0 | 0.0 | 0.0 | 0.0 | 0.0 | 1 | LOAD1 230 | 102.2 | -3.4 | 0.94 | -5.97 | |
| | | | | | | | | 1 | LOAD2 230 | 60.3 | 38.5 | 2.18 | 22.83 | |
| | | | | | | | | 1 | TERM2 18.0 | -163.0 | -35.2 | 0.00 | 18.40 | |
| HST3 230 211.7 KV | 0.9206 -11.6 | 0.0 | 0.0 | 0.0 | 0.0 | 0.0 | 0.0 | 1 | LOAD2 230 | 66.5 | 57.6 | 1.02 | 23.67 | |
| | | | | | | | | 1 | LOAD3 230 | 4.5 | -8.1 | 0.00 | -13.38 | |
| | | | | | | | | 1 | TERM3 15.5 | -71.5 | -49.5 | 0.00 | 5.14 | |
| LOAD1 230 221.5 KV | 0.9632 -2.7 | 0.0 | 0.0 | 100.0 | 35.0 | 0.0 | 0.0 | 1 | HST1 230 | 1.3 | -32.4 | 0.07 | -19.31 | |
| | | | | | | | | 1 | HST2 230 | -101.3 | -2.6 | 0.94 | -5.97 | |
| LOAD2 230 163.4 KV | 0.7106 -31.8 | 0.0 | 0.0 | 125.0 | 50.0 | 0.0 | 0.0 | 1 | HST2 230 | -58.1 | -15.6 | 2.18 | 22.83 | |
| | | | | | | | | 1 | HST3 230 | -65.5 | -33.9 | 1.02 | 23.67 | |
| LOAD3 230 211.9 KV | 0.9212 -11.9 | 0.0 | 0.0 | 90.0 | 30.0 | 0.0 | 0.0 | 1 | HST1 230 | -85.3 | -24.7 | 3.38 | -17.87 | |
| | | | | | | | | 1 | HST3 230 | -4.5 | -5.3 | 0.00 | -13.38 | |
| TERM1 18.0 18.0 KV | 1.0000 0.0 | 87.5 | 24.8 | 0.0 TAP | 0.0 | 0.0 18.0/ 230.0 | 0.0 | 1 | HST1 230 | 87.5 | 24.8 | 0.00 | 4.84 | |
| TERM2 18.0 18.0 KV | 1.0000 7.8 | 163.0 | 100.0H | 0.0 TAP | 0.0 | 0.0 18.0/ 230.0 | 0.0 | 1 | HST2 230 | 163.0 | 53.6 | 0.00 | 18.40 | |
| TERM3 15.5 14.8 KV | 0.9527 -8.9 | 72.0 | 54.5H | 0.0 TAP | 0.0 | 0.0 15.5/ 230.0 | 0.0 | 1 | HST3 230 | 71.5 | 54.7 | 0.00 | 5.14 | |

END OF REPORT FOR THIS CASE

## C.2    Algebraic Voltage Instability

Table C.2.1 to C.2.6 are converged equilibrium poimts of the simulation in section 4.2.3.

Table C.2.7 to C.2.12 are the output from the eigenvalue program.

| | |
|---|---|
| detjj: | determinant of the system jacobian matrix |
| detd: | determinant of the algebraic bifurcation test matrix |
| detda: | determinant of the dynamic/algebraic bifurcation matrix |
| detad: | determinant of the algebraic/dynamic bifurcation matrix |
| condjj: | condition number of the system jacobian matrix |
| condd: | condition number of the algebraic bifurcation test matrix |
| condda: | condition number of the dynamic/algebraic bifurcation test matrix |
| condad: | condition number of the algebraic/dynamic bifurcation test matrix |
| vtt: | eigenvector of the flux decay matrix |
| eigtt: | eigenvalue of the flux decay matrix |
| eigjj: | eigenvalue of the system jacobian matrix |
| vjj: | eigenvector of the system jacobian matrix |
| eigd: | eigenvalue of the algebraic bifurcation test matrix |
| vd: | eigenvector of the algebraic bifurcation test matrix |
| eigda: | eigenvalue of the dynamic/algebraic bifurcation test matrix |
| vda: | eigenvector of the dynamic/algebraic bifurcation test matrix |

eigad:   eigenvalue of the algebraic/dynamic bifurcation test matrix

vad:   eigenvector of the algebraic/dynamic bifurcation test matrix

Only those variables that are necessary for the discussion will be shown in the tables.

## Table C.2.1 Equilibrium point (algebraic 40 MVar)

```
1 9 BUS TEST SYSTEM(NO LINE DROP COMPENSATION) PAGE NUMBER 7
D1-2.0, D2-2.0, D3-2.0, KA-50, RC-0.0, XC-0.0 DATE 4/26/90
LOAD2-40, Load flow test(reactances are 5 times biger) TIME 23.52.10

GENERATOR ANGLE IN DEGREES -NUMBER BUS/GEN NAME NO NUMBER BUS/GEN NAME NO
11 -49.9995 480.1023 521.9312 478.4626

GENERATOR FIELD VOLTAGE -NUMBER BUS/GEN NAME NO NUMBER BUS/GEN NAME NO
11 -49.9995 1.0488 1.5377 1.3202

GEN. FLUX LINKAGE (Q-AXIS) -NUMBER BUS/GEN NAME NO NUMBER BUS/GEN NAME NO
11 -49.9995 0.9932 0.8697 1.0167

GEN. ELECTRICAL POWER - (MW) -NUMBER BUS/GEN NAME NO NUMBER BUS/GEN NAME NO
11 -49.9995 32.5898 112.8315 22.1943

GENERATOR EXCITER SATURATION -NUMBER BUS/GEN NAME NO NUMBER BUS/GEN NAME NO
11 -49.9995 0.0426 0.0149 0.0418

GENERATOR MEGAVAR OUTPUT -NUMBER BUS/GEN NAME NO NUMBER BUS/GEN NAME NO
11 -49.9995 -8.1783 7.1539 18.5161

GENERATOR FIELD CURRENT -NUMBER BUS/GEN NAME NO NUMBER BUS/GEN NAME NO
11 -49.9995 0.9757 1.3729 1.1799

GENERATOR TERMINAL CURRENT -NUMBER BUS/GEN NAME NO NUMBER BUS/GEN NAME NO
11 -49.9995 0.3350 1.1315 0.2906

GEN. TERM. CURR. ANGLE DEGREES-NUMBER BUS/GEN NAME NO NUMBER BUS/GEN NAME NO
11 -49.9995 130.0460 119.7484 69.7633

A-C BUS VOLTAGE MAGNITUDE -NUMBER BUS/GEN NAME NO NUMBER BUS/GEN NAME NO
11 -49.9995 1.0001 1.0001 1.0005 1.0048 0.9972 0.9898 0.9895 0.8869 0.9844

A-C BUS VOLTAGE ANGLE DEGREES -NUMBER BUS/GEN NAME NO NUMBER BUS/GEN NAME NO
11 -49.9995 115.9183 123.3732 109.3142 114.8294 119.3184 108.5745 116.2736 98.6373 109.4202
```

## Table C.2.2 Equilibrium point (algebraic 45 MVar)

```
1 9 BUS TEST SYSTEM(NO LINE DROP COMPENSATION) PAGE NUMBER 7
D1-2.0, D2-2.0, D3-2.0, KA-50, RC-0.0, XC-0.0 DATE 4/26/90
LOAD2-45, Load flow test(reactances are 5 times biger) TIME 23.26. 5

GENERATOR ANGLE IN DEGREES -NUMBER BUS/GEN NAME NO NUMBER BUS/GEN NAME NO
11 -49.9995 271.2339 312.5252 269.0554

GENERATOR FIELD VOLTAGE -NUMBER BUS/GEN NAME NO NUMBER BUS/GEN NAME NO
11 -49.9995 1.0555 1.5583 1.3726

GEN. FLUX LINKAGE (Q-AXIS) -NUMBER BUS/GEN NAME NO NUMBER BUS/GEN NAME NO
11 -49.9995 0.9944 0.8774 1.0238

GEN. ELECTRICAL POWER - (MW) -NUMBER BUS/GEN NAME NO NUMBER BUS/GEN NAME NO
11 -49.9995 32.8513 112.9162 21.9617

GENERATOR EXCITER SATURATION -NUMBER BUS/GEN NAME NO NUMBER BUS/GEN NAME NO
11 -49.9995 0.0427 0.0152 0.0469

GENERATOR MEGAVAR OUTPUT -NUMBER BUS/GEN NAME NO NUMBER BUS/GEN NAME NO
11 -49.9995 -6.4683 10.5992 23.7105

GENERATOR FIELD CURRENT -NUMBER BUS/GEN NAME NO NUMBER BUS/GEN NAME NO
11 -49.9995 0.9821 1.3930 1.2236

GENERATOR TERMINAL CURRENT -NUMBER BUS/GEN NAME NO NUMBER BUS/GEN NAME NO
11 -49.9995 0.3344 1.1349 0.3242

GEN. TERM. CURR. ANGLE DEGREES-NUMBER BUS/GEN NAME NO NUMBER BUS/GEN NAME NO
11 -49.9995 -81.8151 -90.8223 -146.6501

A-C BUS VOLTAGE MAGNITUDE -NUMBER BUS/GEN NAME NO NUMBER BUS/GEN NAME NO
11 -49.9995 1.0000 1.0000 1.0001 1.0038 0.9954 0.9865 0.9880 0.8603 0.9818

A-C BUS VOLTAGE ANGLE DEGREES -NUMBER BUS/GEN NAME NO NUMBER BUS/GEN NAME NO
11 -49.9995 -92.9684 -85.4633 -99.6677 -94.0672 -89.5291 -100.4023 -92.5988 -110.7306 -99.5299
```

## Table C.2.3 Equilibrium point (algebraic 50 MVar)

```
1 9 BUS TEST SYSTEM(NO LINE DROP COMPENSATION) PAGE NUMBER 7
D1=2.0, D2=2.0, D3=2.0, KA=50, RC=0.0, XC=0.0 DATE 4/25/90
LOAD2=50, Load flow test(reactances are 5 times biger) TIME 8. 3.57

GENERATOR ANGLE IN DEGREES -NUMBER BUS/GEN NAME NO NUMBER BUS/GEN NAME NO
11 -119.9527 4.0186 44.7801 1.4807

GENERATOR FIELD VOLTAGE -NUMBER BUS/GEN NAME NO NUMBER BUS/GEN NAME NO
11 -119.9527 1.0631 1.5818 1.4313

GEN. FLUX LINKAGE (Q-AXIS) -NUMBER BUS/GEN NAME NO NUMBER BUS/GEN NAME NO
11 -119.9527 0.9956 0.8857 1.0315

GEN. ELECTRICAL POWER - (MW) -NUMBER BUS/GEN NAME NO NUMBER BUS/GEN NAME NO
11 -119.9527 32.8573 112.9999 22.0002

GENERATOR EXCITER SATURATION -NUMBER BUS/GEN NAME NO NUMBER BUS/GEN NAME NO
11 -119.9527 0.0429 0.0156 0.0536

GENERATOR MEGAVAR OUTPUT -NUMBER BUS/GEN NAME NO NUMBER BUS/GEN NAME NO
11 -119.9527 -4.6168 14.4625 29.4330

GENERATOR FIELD CURRENT -NUMBER BUS/GEN NAME NO NUMBER BUS/GEN NAME NO
11 -119.9527 0.9891 1.4154 1.2719

GENERATOR TERMINAL CURRENT -NUMBER BUS/GEN NAME NO NUMBER BUS/GEN NAME NO
11 -119.9527 0.3318 1.1392 0.3675

GEN. TERM. CURR. ANGLE DEGREES-NUMBER BUS/GEN NAME NO NUMBER BUS/GEN NAME NO
11 -119.9527 7.8302 0.1097 -60.1378

A-C BUS VOLTAGE MAGNITUDE -NUMBER BUS/GEN NAME NO NUMBER BUS/GEN NAME NO
11 -119.9527 1.0000 1.0000 1.0000 1.0029 0.9935 0.9831 0.9864 0.8312 0.9792

A-C BUS VOLTAGE ANGLE DEGREES -NUMBER BUS/GEN NAME NO NUMBER BUS/GEN NAME NO
11 -119.9527 -0.1681 7.4031 -6.9146 -1.2681 3.3266 -7.6531 0.2286 -18.4519 -6.7644
```

## Table C.2.4 Equilibrium point (algebraic 55 MVar)

```
1 9 BUS TEST SYSTEM(NO LINE DROP COMPENSATION) PAGE NUMBER 7
D1=2.0, D2=2.0, D3=2.0, KA=50, RC=0.0, XC=0.0 DATE 4/25/90
LOAD2=55, Load flow test(reactances are 5 times biger) TIME 11. 9. 6

GENERATOR ANGLE IN DEGREES -NUMBER BUS/GEN NAME NO NUMBER BUS/GEN NAME NO
11 -49.9995 -345.4698 -305.3192 -348.5387

GENERATOR FIELD VOLTAGE -NUMBER BUS/GEN NAME NO NUMBER BUS/GEN NAME NO
11 -49.9995 1.0718 1.6086 1.4973

GEN. FLUX LINKAGE (Q-AXIS) -NUMBER BUS/GEN NAME NO NUMBER BUS/GEN NAME NO
11 -49.9995 0.9971 0.8949 1.0400

GEN. ELECTRICAL POWER - (MW) -NUMBER BUS/GEN NAME NO NUMBER BUS/GEN NAME NO
11 -49.9995 33.0882 113.1236 21.8248

GENERATOR EXCITER SATURATION -NUMBER BUS/GEN NAME NO NUMBER BUS/GEN NAME NO
11 -49.9995 0.0431 0.0161 0.0623

GENERATOR MEGAVAR OUTPUT -NUMBER BUS/GEN NAME NO NUMBER BUS/GEN NAME NO
11 -49.9995 -2.3933 19.0317 35.9617         .

GENERATOR FIELD CURRENT -NUMBER BUS/GEN NAME NO NUMBER BUS/GEN NAME NO
11 -49.9995 0.9974 1.4419 1.3262

GENERATOR TERMINAL CURRENT -NUMBER BUS/GEN NAME NO NUMBER BUS/GEN NAME NO
11 -49.9995 0.3320 1.1456 0.4192

GEN. TERM. CURR. ANGLE DEGREES-NUMBER BUS/GEN NAME NO NUMBER BUS/GEN NAME NO
11 -49.9995 14.4675 8.4112 -55.6365

A-C BUS VOLTAGE MAGNITUDE -NUMBER BUS/GEN NAME NO NUMBER BUS/GEN NAME NO
11 -49.9995 0.9999 0.9999 0.9996 1.0017 0.9912 0.9790 0.9845 0.7980 0.9759

A-C BUS VOLTAGE ANGLE DEGREES -NUMBER BUS/GEN NAME NO NUMBER BUS/GEN NAME NO
11 -49.9995 10.3333 17.9748 3.4834 9.2241 13.8841 2.7473 10.7532 -8.6329 3.6667
```

## Table C.2.5 Equilibrium point (algebraic 58 MVar)

```
1 9 BUS TEST SYSTEM(NO LINE DROP COMPENSATION) PAGE NUMBER 7
D1-2.0, D2-2.0, D3-2.0, KA-50, RC-0.0, XC-0.0 DATE 4/25/90
LOAD2-58, Load flow test(reactances are 5 times biger) TIME 11.38.37

GENERATOR ANGLE IN DEGREES -NUMBER BUS/GEN NAME NO NUMBER BUS/GEN NAME NO
11 -49.9995 -614.1379 -574.3732 -617.4922

GENERATOR FIELD VOLTAGE -NUMBER BUS/GEN NAME NO NUMBER BUS/GEN NAME NO
11 -49.9995 1.0787 1.6278 1.5435

GEN. FLUX LINKAGE (Q-AXIS) -NUMBER BUS/GEN NAME NO NUMBER BUS/GEN NAME NO
11 -49.9995 0.9981 0.9009 1.0458

GEN. ELECTRICAL POWER - (MW) -NUMBER BUS/GEN NAME NO NUMBER BUS/GEN NAME NO
11 -49.9995 33.1591 113.2174 21.7917

GENERATOR EXCITER SATURATION -NUMBER BUS/GEN NAME NO NUMBER BUS/GEN NAME NO
11 -49.9995 0.0433 0.0164 0.0694

GENERATOR MEGAVAR OUTPUT -NUMBER BUS/GEN NAME NO NUMBER BUS/GEN NAME NO
11 -49.9995 -0.8631 22.2199 40.4071

GENERATOR FIELD CURRENT -NUMBER BUS/GEN NAME NO NUMBER BUS/GEN NAME NO
11 -49.9995 1.0031 1.4603 1.3631

GENERATOR TERMINAL CURRENT -NUMBER BUS/GEN NAME NO NUMBER BUS/GEN NAME NO
11 -49.9995 0.3319 1.1506 0.4564

GEN. TERM. CURR. ANGLE DEGREES-NUMBER BUS/GEN NAME NO NUMBER BUS/GEN NAME NO
11 -49.9995 103.1594 98.2279 32.4044

A-C BUS VOLTAGE MAGNITUDE -NUMBER BUS/GEN NAME NO NUMBER BUS/GEN NAME NO
11 -49.9995 0.9999 0.9999 0.9993 1.0009 0.9897 0.9763 0.9833 0.7755 0.9737

A-C BUS VOLTAGE ANGLE DEGREES -NUMBER BUS/GEN NAME NO NUMBER BUS/GEN NAME NO
11 -49.9995 -258.3309 -250.6364 -265.2353 -259.4433 -254.7369 -265.9724 -257.8909 82.2170 -265.0356
```

## Table C.2.6 Equilibrium point (algebraic 60 MVar)

```
1 9 BUS TEST SYSTEM(NO LINE DROP COMPENSATION) PAGE NUMBER 7
D1-2.0, D2-2.0, D3-2.0, KA-50, RC-0.0, XC-0.0 DATE 4/25/90
LOAD2-60, Load flow test(reactances are 5 times biger) TIME 10.35.28

GENERATOR ANGLE IN DEGREES -NUMBER BUS/GEN NAME NO NUMBER BUS/GEN NAME NO
11 -49.9995 -829.4944 -789.9480 -832.7736

GENERATOR FIELD VOLTAGE -NUMBER BUS/GEN NAME NO NUMBER BUS/GEN NAME NO
11 -49.9995 1.0829 1.6420 1.5771

GEN. FLUX LINKAGE (Q-AXIS) -NUMBER BUS/GEN NAME NO NUMBER BUS/GEN NAME NO
11 -49.9995 0.9988 0.9054 1.0499

GEN. ELECTRICAL POWER - (MW) -NUMBER BUS/GEN NAME NO NUMBER BUS/GEN NAME NO
11 -49.9995 32.8113 113.2591 22.1776

GENERATOR EXCITER SATURATION -NUMBER BUS/GEN NAME NO NUMBER BUS/GEN NAME NO
11 -49.9995 0.0434 0.0167 0.0750

GENERATOR MEGAVAR OUTPUT -NUMBER BUS/GEN NAME NO NUMBER BUS/GEN NAME NO
11 -49.9995 0.1422 24.5224 43.5964

GENERATOR FIELD CURRENT -NUMBER BUS/GEN NAME NO NUMBER BUS/GEN NAME NO
11 -49.9995 1.0068 1.4733 1.3899

GENERATOR TERMINAL CURRENT -NUMBER BUS/GEN NAME NO NUMBER BUS/GEN NAME NO
11 -49.9995 0.3281 1.1539 0.4853

GEN. TERM. CURR. ANGLE DEGREES-NUMBER BUS/GEN NAME NO NUMBER BUS/GEN NAME NO
11 -49.9995 -113.8827 -118.1580 175.5071

A-C BUS VOLTAGE MAGNITUDE -NUMBER BUS/GEN NAME NO NUMBER BUS/GEN NAME NO
11 -49.9995 1.0000 1.0001 0.9995 1.0005 0.9888 0.9747 0.9825 0.7598 0.9725

A-C BUS VOLTAGE ANGLE DEGREES -NUMBER BUS/GEN NAME NO NUMBER BUS/GEN NAME NO
11 -49.9995 -113.6344 -105.8894 -120.4918 -114.7355 -109.9946 -121.2430 -113.1653 -133.3874 -120.3143
```

Table C.2.7 Output for algebraic 40 MVar

```
eigjj =

 -26.2673 +52.3641i
 -26.2673 -52.3641i
  49.1836
  46.1034
  39.8293
 -12.5990 +25.4489i
 -12.5990 -25.4489i
 -10.3545 +20.6654i
 -10.3545 -20.6654i
  25.4839
  23.8411
  21.2110
 -15.7823
 -16.6154
 -16.5977
  -4.9845 +14.1162i
  -4.9845 -14.1162i
  -4.1796 +15.0659i
  -4.1796 -15.0659i
  -3.9324 +14.9901i
  -3.9324 -14.9901i
  11.5052
  10.6917
   8.1602 +  1.1839i
   8.1602 -  1.1839i
   1.6114
  -0.5621 +  1.5609i
  -0.5621 -  1.5609i
  -0.2152 +  1.2145i
  -0.2152 -  1.2145i
   0.7097
  -0.0925 +  0.9092i
  -0.0925 -  0.9092i
   0.3103
   0.0545
  -0.0635 +  0.5736i
  -0.0635 -  0.5736i
  -0.0025 +  0.6056i
  -0.0025 -  0.6056i


eigd =

  49.1836
  46.1038
  39.8328
 -12.4443 +25.6610i
 -12.4443 -25.6610i
 -10.1708 +20.6557i
 -10.1708 -20.6557i
  -5.1331 +14.1894i
  -5.1331 -14.1894i
  25.4946
  23.8789
  21.2135
   8.1761 +  1.2309i
   8.1761 -  1.2309i
   1.7777
  11.4941
  11.0223
   0.9511


eigad =

  1.0e+02 *

  -0.2224 +  6.1202i
  -0.2224 -  6.1202i
  -2.4305 +  3.9095i
  -2.4305 -  3.9095i
   2.1554 +  3.1553i
   2.1554 -  3.1553i
   0.3776 +  0.5585i
   0.3776 -  0.5585i
```

# Table C.2.7 (cont'd)

```
0.4905
0.4502
0.3510
0.3313
0.0003
0.0449
0.1206
0.0676 + 0.0058i
0.0676 - 0.0058i
0.1296
```

```
detjj =

 -6.8110e+30

detd =

 1.6769e+21

detda =

 -4.0616e+09

detad =

 1.1185e+29

condjj =

 1.6309e+06

condd =

 66.7979

condda =


 7.7767e+05

condad =

 2.9371e+06

vtt =

 1.0000 0.0495 -0.0046
 -0.7183 1.0000 1.0000
 -0.3687 0.3889 -0.5528

eigtt =

 1.0e+03 *

 -0.1555
 -1.1772
 -0.4878
```

## Table C.2.8 Output for algebraic 45 MVar

```
eigjj =

 -26.2712 +52.3659i
 -26.2712 -52.3659i
 48.9269
 45.8832
 39.7197
 -12.5574 +25.3325i
 -12.5574 -25.3325i
 25.4149
 23.8081
 20.9556
 -10.2499 +20.5509i
 -10.2499 -20.5509i
 -15.7839
 -16.6157
 -16.5981
 -4.1703 +15.0971i
 -4.1703 -15.0971i
 -3.9369 +14.9893i
 -3.9369 -14.9893i
 -4.8887 +13.9539i
 -4.8887 -13.9539i
 11.3732
 10.2916
 8.1280 + 1.1738i
 8.1280 - 1.1738i
 1.4979
 -0.5685 + 1.5554i
 -0.5685 - 1.5554i
 -0.2225 + 1.2151i
 -0.2225 - 1.2151i
 0.7014
 -0.0988 + 0.9158i
 -0.0988 - 0.9158i
 0.3112
 0.0538
 -0.0643 + 0.5805i
 -0.0643 - 0.5805i
 -0.0042 + 0.6081i
 -0.0042 - 0.6081i


eigd =

 48.9268
 45.8835
 -12.4006 +25.5487i
 -12.4006 -25.5487i
 39.7233
 -10.0677 +20.5369i
 -10.0677 -20.5369i
 -5.0251 +14.0573i
 -5.0251 -14.0573i
 25.4254
 23.8462
 20.9590
 1.7386
 8.1361 + 1.2217i
 8.1361 - 1.2217i
 11.4645
 10.5266
 0.8296


eigad =

1.0e+02 *

 -0.2195 + 5.5645i
 -0.2195 - 5.5645i
 -2.1702 + 3.5788i
 -2.1702 - 3.5788i
 1.8949 + 2.7997i
```

# Table C.2.8 (cont'd)

```
1.8949 - 2.7997i
0.3774 + 0.5602i
0.3774 - 0.5602i
0.4878
0.4485
0.3498
0.3302
0.0003
0.0414
0.1167
0.0668 + 0.0054i
0.0668 - 0.0054i
0.1284
```

detjj =

-5.7086e+30

detd =

1.2554e+21

detda =

-4.5473e+09

detad =

5.0494e+28

condjj =

1.6453e+06

condd =

77.7386

condda =

7.8439e+05

condad =

2.3740e+06

vtt =

```
 1.0000 0.0540 -0.0256
-0.6724 1.0000 1.0000
-0.4136 0.2844 -0.6042
```

eigtt =

1.0e+03 *

```
-0.1518
-1.0892
-0.3871
```

## Table C.2.9 Output for algebraic 50 MVar

```
eigjj =

 -26.2756 +52.3680i
 -26.2756 -52.3680i
  48.6824
  45.6562
  39.6142
 -12.5173 +25.2151i
 -12.5173 -25.2151i
  25.3522
  23.7724
 -10.1363 +20.4312i
 -10.1363 -20.4312i
  20.7064
 -15.7855
 -16.6162
 -16.5986
  -4.1544 +15.1244i
  -4.1544 -15.1244i
  -3.9425 +14.9887i
  -3.9425 -14.9887i
  -4.7854 +13.7813i
  -4.7854 -13.7813i
  11.2511
   9.8822
   8.0822 + 1.1644i
   8.0822 - 1.1644i
  -0.5770 + 1.5467i
  -0.5770 - 1.5467i
   1.3701
  -0.2325 + 1.2162i
  -0.2325 - 1.2162i
   0.6834
  -0.1077 + 0.9253i
  -0.1077 - 0.9253i
   0.3129
   0.0532
  -0.0649 + 0.5877i
  -0.0649 - 0.5877i
  -0.0062 + 0.6105i
  -0.0062 - 0.6105i


eigd =

  48.6823
  45.6565
  39.6177
 -12.3580 +25.4353i
 -12.3580 -25.4353i
  -9.9559 +20.4128i
  -9.9559 -20.4128i
  -4.9025 +13.9110i
  -4.9025 -13.9110i
  25.3624
  23.8107
  20.7105
   8.0811 + 1.2114i
   8.0811 - 1.2114i
  11.3876
   1.7030
  10.0815
   0.6667


eigad =

  1.0e+02 *

  -0.2232 + 5.1216i
  -0.2232 - 5.1216i
  -1.9220 + 3.2899i
  -1.9220 - 3.2899i
   1.6527 + 2.4796i
   1.6527 - 2.4796i
   0.3778 + 0.5636i
```

# Table C.2.9 (cont'd)

```
0.3778 - 0.5636i
 0.4851
 0.4468
 0.3487
 0.3291
 0.0003
 0.1278
 0.0370
 0.0660 + 0.0049i
 0.0660 - 0.0049i
 0.1125


detjj =

 -4.6493e+30

detd =

 8.6008e+20

detda =

 -5.4056e+09

detad =

 2.2694e+28

condjj =

 1.6577e+06

condd =

 98.1072


condda =

 7.9004e+05

condad =

 1.9277e+06

vtt =

 1.0000 0.0615 -0.0553
 -0.5948 1.0000 1.0000
 -0.4797 0.2343 -0.5970

eigtt =

 1.0e+03 *

 -0.1471
 -1.0789
 -0.3113
```

# Table C.2.10 Output for algebraic 55 MVar

```
eigjj =

 -26.2808 +52.3704i
 -26.2808 -52.3704i
  48.4166
  45.3777
  39.4845
 -12.4688 +25.0779i
 -12.4688 -25.0779i
  25.2769
  23.7165
 -10.0005 +20.2782i
 -10.0005 -20.2782i
  20.4420
 -15.7873
 -16.6169
 -16.5992
  -4.1316 +15.1476i
  -4.1316 -15.1476i
  -3.9496 +14.9880i
  -3.9496 -14.9880i
  -4.6618 +13.5796i
  -4.6618 -13.5796i
  11.1177
   9.4755
   8.0079 + 1.1449i
   8.0079 - 1.1449i
  -0.5884 + 1.5312i
  -0.5884 - 1.5312i
   1.2337
  -0.2493 + 1.2178i
  -0.2493 - 1.2178i
   0.6399
  -0.1212 + 0.9380i
  -0.1212 - 0.9380i
   0.3179
   0.0522
  -0.0657 + 0.5954i
  -0.0657 - 0.5954i
  -0.0084 + 0.6133i
  -0.0084 - 0.6133i




eigd =

  48.4165
  45.3779
  39.4880
 -12.3069 +25.3025i
 -12.3069 -25.3025i
  -9.8223 +20.2552i
  -9.8223 -20.2552i
  -4.7522 +13.7310i
  -4.7522 -13.7310i
  25.2868
  23.7555
  20.4469
  11.2804
   7.9968 + 1.1882i
   7.9968 - 1.1882i
   0.4393
   9.6582
   1.6724




eigad =

 1.0e+02 *

 -0.2367 + 4.7664i
 -0.2367 - 4.7664i
 -1.6787 + 3.0171i
 -1.6787 - 3.0171i
  1.4255 + 2.1747i
```

# Table C.2.10 (cont'd)

```
1.4255 - 2.1747i
0.3784 + 0.5688i
0.3784 - 0.5688i
0.4821
0.4447
0.3473
0.3277
0.0002
0.0316
0.1272
0.0650 + 0.0040i
0.0650 - 0.0040i
0.1082


detjj =

-3.5278e+30


detd =

4.7215e+20


detda =

-7.4718e+09


detad =

9.5557e+27


condjj =

1.6780e+06


condd =

150.5746


condda =

7.9943e+05


condad =

1.5734e+06


vtt =

1.0000 0.0733 -0.0932
-0.4550 1.0000 1.0000
-0.5731 0.2158 -0.5289


eigtt =

1.0e+03 *

-0.1411
-1.2327
-0.2568
```

# Table C.2.11 Output for algebraic 58 MVar

```
eigjj =

 -26.2849  +52.3723i
 -26.2849  -52.3723i
  48.2570
  45.1980
  39.4003
 -12.4391  +24.9916i
 -12.4391  -24.9916i
  25.2325
  23.6762
  -9.9074  +20.1714i
  -9.9074  -20.1714i
  20.2775
 -15.7886
 -16.6174
 -16.5996
  -4.1159  +15.1588i
  -4.1159  -15.1588i
  -3.9550  +14.9876i
  -3.9550  -14.9876i
  -4.5740  +13.4444i
  -4.5740  -13.4444i
  11.0307
   9.2492
   7.9455  +  1.1235i
   7.9455  -  1.1235i
  -0.5966  +  1.5154i
  -0.5966  -  1.5154i
   1.1557
  -0.2653  +  1.2185i
  -0.2653  -  1.2185i
  -0.1328  +  0.9484i
  -0.1328  -  0.9484i
   0.5897
   0.3246
   0.0515
  -0.0662  +  0.6006i
  -0.0662  -  0.6006i
  -0.0098  +  0.6150i
  -0.0098  -  0.6150i


eigd =

 -12.2753  +25.2190i
 -12.2753  -25.2190i
  48.2570
  45.1983
  39.4038
  -9.7308  +20.1454i
  -9.7308  -20.1454i
  -4.6458  +13.6060i
  -4.6458  -13.6060i
  25.2423
  23.7155
  20.2827
   0.2617
   1.6573
  11.2040
   7.9291  +  1.1630i
   7.9291  -  1.1630i
   9.4251


eigad =

  1.0e+02 *

  -0.2506  +  4.5797i
  -0.2506  -  4.5797i
  -1.5289  +  2.8475i
  -1.5289  -  2.8475i
   1.2909  +  1.9859i
   1.2909  -  1.9859i
   0.3793  +  0.5740i
```

# Table C.2.11 (cont's)

```
0.3793 - 0.5740i
0.4803
0.4434
0.3465
0.3267
0.0002
0.0276
0.1269
0.0644 + 0.0032i
0.0644 - 0.0032i
0.1056


detjj =

 -2.8610e+30


detd =

 2.4987e+20


detda =

 -1.1450e+10


detad =

 5.3121e+27


condjj =

 1.6936e+06


condd =

 254.1842


condda =

 8.0650e+05


condad =

 1.3904e+06


vtt =

 0.0840 1.0000 -0.1177
 1.0000 -0.3165 1.0000
 0.2176 -0.6403 -0.4592


eigtt =

 1.0e+03 *

 -1.6489
 -0.1360
 -0.2318
```

Table C.2.12 Output for algebraic 60 MVar

```
eigjj =

-26.2875 +52.3735i
-26.2875 -52.3735i
 48.1655
 45.0979
 39.3536
-12.4227 +24.9388i
-12.4227 -24.9388i
 25.2130
 23.6544
-9.8454 +20.1084i
-9.8454 -20.1084i
 20.1756
-15.7892
-16.6178
-16.5999
-4.1059 +15.1647i
-4.1059 -15.1647i
-3.9591 +14.9875i
-3.9591 -14.9875i
-4.5119 +13.3553i
-4.5119 -13.3553i
 10.9728
 9.1219
 7.8968 + 1.1046i
 7.8968 - 1.1046i
-0.6017 + 1.5008i
-0.6017 - 1.5008i
 1.1104
-0.2791 + 1.2187i
-0.2791 - 1.2187i
-0.1423 + 0.9572i
-0.1423 - 0.9572i
 0.5411
 0.3323
 0.0511
-0.0664 + 0.6041i
-0.0664 - 0.6041i
-0.0108 + 0.6159i
-0.0108 - 0.6159i


eigd =

-12.2575 +25.1679i
-12.2575 -25.1679i
 48.1654
 45.0982
 39.3571
-9.6699 +20.0804i
-9.6699 -20.0804i
-4.5715 +13.5220i
-4.5715 -13.5220i
 25.2226
 23.6938
 20.1811
 0.1268
 1.6488
 11.1513
 7.8780 + 1.1410i
 7.8780 - 1.1410i
 9.2936


eigad =

1.0e+02 *

-0.2622 + 4.4738i
-0.2622 - 4.4738i
-1.4301 + 2.7334i
-1.4301 - 2.7334i
 1.2042 + 1.8604i
 1.2042 - 1.8604i
 0.3803 + 0.5790i
 0.3803 - 0.5790i
```

# Table C.2.12 (cont'd)

```
0.4793
0.4427
0.3460
0.3261
0.0002
0.0247
0.1267
0.0640 + 0.0025i
0.0640 - 0.0025i
0.1040
```

```
detjj =

   -2.4574e+30

detd =

   1.1225e+20

detda =

   -2.1893e+10

detad =

   3.5268e+27

condjj =

   1.6994e+06

condd =

   526.8583

condda =

   8.0890e+05

condad =

   1.2736e+06

vtt =

   0.0937  1.0000  -0.1321
   1.0000 -0.1928   1.0000
   0.2258 -0.6827  -0.4044

eigtt =

   1.0e+03 *

   -2.8355
   -0.1323
   -0.2186
```

## C.3 Dynamic/Algebraic Voltage Instability

Table C.3.1 to Table C.3.6 are the converged equilibrium point of the simulation in section 4.3. Table C.3.7 to C.3.12 are the output from the eigenvalue program. Table C.3.13 is the case where field current is saturated.

## Table C.3.1 Equilibrium point (dynamic/algebraic 10 MVar)

```
1 9 BUS TEST SYSTEM(NO LINE DROP COMPENSATION) PAGE NUMBER 7
D1=2.0, D2=2.0, D3=2.0, KA=25, RC=0.0, XC=0.0 DATE 5/ 2/90
LOAD2=50, REAL POWER LOAD - regular, no load at LOAD1 and LOAD3 TIME 22.30.13

GENERATOR ANGLE IN DEGREES -NUMBER BUS/GEN NAME NO NUMBER BUS/GEN NAME NO
11 -49.9995 10.4736 45.1464 19.3101

GENERATOR FIELD VOLTAGE -NUMBER BUS/GEN NAME NO NUMBER BUS/GEN NAME NO
11 -49.9995 1.0706 1.5243 1.2870

GEN. FLUX LINKAGE (Q-AXIS) -NUMBER BUS/GEN NAME NO NUMBER BUS/GEN NAME NO
11 -49.9995 0.9861 0.8227 0.9992

GEN. ELECTRICAL POWER - (MW) -NUMBER BUS/GEN NAME NO NUMBER BUS/GEN NAME NO
11 -49.9995 82.5440 123.0011 31.9911

GENERATOR EXCITER SATURATION -NUMBER BUS/GEN NAME NO NUMBER BUS/GEN NAME NO
11 -49.9995 0.0431 0.0146 0.0388

GENERATOR MEGAVAR OUTPUT -NUMBER BUS/GEN NAME NO NUMBER BUS/GEN NAME NO
11 -49.9995 -11.2795 -1.7768 13.7459

GENERATOR FIELD CURRENT -NUMBER BUS/GEN NAME NO NUMBER BUS/GEN NAME NO
11 -49.9995 0.9983 1.3775 1.1563

GENERATOR TERMINAL CURRENT -NUMBER BUS/GEN NAME NO NUMBER BUS/GEN NAME NO
11 -49.9995 0.8331 1.2301 0.3482

GEN. TERM. CURR. ANGLE DEGREES-NUMBER BUS/GEN NAME NO NUMBER BUS/GEN NAME NO
11 -49.9995 7.6718 2.6678 -17.5473

A-C BUS VOLTAGE MAGNITUDE -NUMBER BUS/GEN NAME NO NUMBER BUS/GEN NAME NO
11 -49.9995 1.0000 1.0000 0.9998 1.0078 1.0041 0.9955 0.9924 0.9850 0.9899

A-C BUS VOLTAGE ANGLE DEGREES -NUMBER BUS/GEN NAME NO NUMBER BUS/GEN NAME NO
11 -49.9995 -0.1094 1.8402 5.7049 -2.8605 -2.5509 -4.9643 -5.0428 -6.1330 -5.3102
```

## Table C.3.2 Equilibrium point (dynamic/algebraic 50 MVar)

```
1 9 BUS TEST SYSTEM(NO LINE DROP COMPENSATION) PAGE NUMBER 7
D1=2.0, D2=2.0, D3=2.0, KA=25, RC=0.0, XC=0.0 DATE 5/ 3/90
term3=50, REAL POWER LOAD - regular TIME 7.45.22

GENERATOR ANGLE IN DEGREES -NUMBER BUS/GEN NAME NO NUMBER BUS/GEN NAME NO
11 -49.9995 6.6330 41.2437 12.3914

GENERATOR FIELD VOLTAGE -NUMBER BUS/GEN NAME NO NUMBER BUS/GEN NAME NO
11 -49.9995 1.0719 1.5263 1.6919

GEN. FLUX LINKAGE (Q-AXIS) -NUMBER BUS/GEN NAME NO NUMBER BUS/GEN NAME NO
11 -49.9995 0.9864 0.8236 1.0554

GEN. ELECTRICAL POWER - (MW) -NUMBER BUS/GEN NAME NO NUMBER BUS/GEN NAME NO
11 -49.9995 82.5348 123.0010 32.0007

GENERATOR EXCITER SATURATION -NUMBER BUS/GEN NAME NO NUMBER BUS/GEN NAME NO
11 -49.9995 0.0431 0.0147 0.0984

GENERATOR MEGAVAR OUTPUT -NUMBER BUS/GEN NAME NO NUMBER BUS/GEN NAME NO
11 -49.9995 -10.9684 -1.4629 53.2513

GENERATOR FIELD CURRENT -NUMBER BUS/GEN NAME NO NUMBER BUS/GEN NAME NO
11 -49.9995 0.9994 1.3791 1.4841

GENERATOR TERMINAL CURRENT -NUMBER BUS/GEN NAME NO NUMBER BUS/GEN NAME NO
11 -49.9995 0.8326 1.2301 0.6236

GEN. TERM. CURR. ANGLE DEGREES-NUMBER BUS/GEN NAME NO NUMBER BUS/GEN NAME NO
11 -49.9995 3.6286 -1.3086 -57.0667

A-C BUS VOLTAGE MAGNITUDE -NUMBER BUS/GEN NAME NO NUMBER BUS/GEN NAME NO
11 -49.9995 1.0000 1.0000 0.9962 1.0076 1.0039 0.9947 0.9922 0.9845 0.9894

A-C BUS VOLTAGE ANGLE DEGREES -NUMBER BUS/GEN NAME NO NUMBER BUS/GEN NAME NO
11 -49.9995 -3.9413 -1.9900 1.9319 -6.6926 -6.3820 -8.7883 -8.8752 -9.9605 -9.1373
```

## Table C.3.3 Equilibrium point (dynamic/algebraic 100 MVar)

```
1 9 BUS TEST SYSTEM(NO LINE DROP COMPENSATION) PAGE NUMBER 7
D1-2.0, D2-2.0, D3-2.0, KA-25, RC-0.0, XC-0.0 DATE 5/ 3/90
term3-100, REAL POWER LOAD - regular TIME 8.14.13

GENERATOR ANGLE IN DEGREES -NUMBER BUS/GEN NAME NO NUMBER BUS/GEN NAME NO
11 -49.9995 -22.0389 12.2170 -18.1092

GENERATOR FIELD VOLTAGE -NUMBER BUS/GEN NAME NO NUMBER BUS/GEN NAME NO
11 -49.9995 1.0789 1.5374 2.1685

GEN. FLUX LINKAGE (Q-AXIS) -NUMBER BUS/GEN NAME NO NUMBER BUS/GEN NAME NO
11 -49.9995 0.9877 0.8289 1.1037

GEN. ELECTRICAL POWER - (MW) -NUMBER BUS/GEN NAME NO NUMBER BUS/GEN NAME NO
11 -49.9995 82.6329 123.0139 31.9007

GENERATOR EXCITER SATURATION -NUMBER BUS/GEN NAME NO NUMBER BUS/GEN NAME NO
11 -49.9995 0.0433 0.0149 0.3166

GENERATOR MEGAVAR OUTPUT -NUMBER BUS/GEN NAME NO NUMBER BUS/GEN NAME NO
11 -49.9995 -9.2917 0.2288 100.6401

GENERATOR FIELD CURRENT -NUMBER BUS/GEN NAME NO NUMBER BUS/GEN NAME NO
11 -49.9995 1.0056 1.3881 1.8765

GENERATOR TERMINAL CURRENT -NUMBER BUS/GEN NAME NO NUMBER BUS/GEN NAME NO
11 -49.9995 0.8316 1.2301 1.0810

GEN. TERM. CURR. ANGLE DEGREES-NUMBER BUS/GEN NAME NO NUMBER BUS/GEN NAME NO
11 -49.9995 -26.1684 -30.7394 -98.8884

A-C BUS VOLTAGE MAGNITUDE -NUMBER BUS/GEN NAME NO NUMBER BUS/GEN NAME NO
11 -49.9995 1.0000 1.0000 0.9765 1.0066 1.0029 0.9908 0.9912 0.9818 0.9868

A-C BUS VOLTAGE ANGLE DEGREES -NUMBER BUS/GEN NAME NO NUMBER BUS/GEN NAME NO
11 -49.9995 -32.5838 -30.6328 -26.4567 -35.3410 -35.0296 -37.4042 -37.5278 -38.5924 -37.7648
```

## Table C.3.4 Equilibrium point (dynamic/algebraic 110 MVar)

```
1 9 BUS TEST SYSTEM(NO LINE DROP COMPENSATION) PAGE NUMBER 7
D1-2.0, D2-2.0, D3-2.0, KA-25, RC-0.0, XC-0.0 DATE 5/ 4/90
term3-110, REAL POWER LOAD - regular TIME 9.39.11

GENERATOR ANGLE IN DEGREES -NUMBER BUS/GEN NAME NO NUMBER BUS/GEN NAME NO
11 -49.9995 -41.6573 -7.5377 -37.8437

GENERATOR FIELD VOLTAGE -NUMBER BUS/GEN NAME NO NUMBER BUS/GEN NAME NO
11 -49.9995 1.0818 1.5420 2.2561

GEN. FLUX LINKAGE (Q-AXIS) -NUMBER BUS/GEN NAME NO NUMBER BUS/GEN NAME NO
11 -49.9995 0.9882 0.8310 1.1094

GEN. ELECTRICAL POWER - (MW) -NUMBER BUS/GEN NAME NO NUMBER BUS/GEN NAME NO
11 -49.9995 82.6391 123.0167 31.8963

GENERATOR EXCITER SATURATION -NUMBER BUS/GEN NAME NO NUMBER BUS/GEN NAME NO
11 -49.9995 0.0433 0.0149 0.3948

GENERATOR MEGAVAR OUTPUT -NUMBER BUS/GEN NAME NO NUMBER BUS/GEN NAME NO
11 -49.9995 -8.6070 0.9225 109.6247

GENERATOR FIELD CURRENT -NUMBER BUS/GEN NAME NO NUMBER BUS/GEN NAME NO
11 -49.9995 1.0081 1.3917 1.9561

GENERATOR TERMINAL CURRENT -NUMBER BUS/GEN NAME NO NUMBER BUS/GEN NAME NO
11 -49.9995 0.8309 1.2302 1.1786

GEN. TERM. CURR. ANGLE DEGREES-NUMBER BUS/GEN NAME NO NUMBER BUS/GEN NAME NO
11 -49.9995 -46.2405 -50.6628 -119.7442

A-C BUS VOLTAGE MAGNITUDE -NUMBER BUS/GEN NAME NO NUMBER BUS/GEN NAME NO
11 -49.9995 1.0000 1.0000 0.9686 1.0062 1.0024 0.9892 0.9908 0.9807 0.9858

A-C BUS VOLTAGE ANGLE DEGREES -NUMBER BUS/GEN NAME NO NUMBER BUS/GEN NAME NO
11 -49.9995 -52.1862 -50.2332 -45.9373 -54.9448 -54.6319 -56.9922 -57.1326 -58.1876 -57.3587
```

## Table C.3.5 Equilibrium point (dynamic/algebraic 120 MVar)

```
1 9 BUS TEST SYSTEM(NO LINE DROP COMPENSATION) PAGE NUMBER 7
D1=2.0, D2=2.0, D3=2.0, KA=25, RC=0.0, XC=0.0 DATE 5/ 3/90
term3=120, REAL POWER LOAD = regular TIME 8.41.23

GENERATOR ANGLE IN DEGREES -NUMBER BUS/GEN NAME NO NUMBER BUS/GEN NAME NO
11 -49.9995 -81.3496 -47.4235 -77.6249

GENERATOR FIELD VOLTAGE -NUMBER BUS/GEN NAME NO NUMBER BUS/GEN NAME NO
11 -49.9995 1.0857 1.5481 2.3393

GEN. FLUX LINKAGE (Q-AXIS) -NUMBER BUS/GEN NAME NO NUMBER BUS/GEN NAME NO
11 -49.9995 0.9889 0.8337 1.1130

GEN. ELECTRICAL POWER - (MW) -NUMBER BUS/GEN NAME NO NUMBER BUS/GEN NAME NO
11 -49.9995 82.7351 123.0285 31.7987

GENERATOR EXCITER SATURATION -NUMBER BUS/GEN NAME NO NUMBER BUS/GEN NAME NO
11 -49.9995 0.0434 0.0150 0.4876

GENERATOR MEGAVAR OUTPUT -NUMBER BUS/GEN NAME NO NUMBER BUS/GEN NAME NO
11 -49.9995 -7.6940 1.8459 118.2906

GENERATOR FIELD CURRENT -NUMBER BUS/GEN NAME NO NUMBER BUS/GEN NAME NO
11 -49.9995 1.0115 1.3967 2.0380

GENERATOR TERMINAL CURRENT -NUMBER BUS/GEN NAME NO NUMBER BUS/GEN NAME NO
11 -49.9995 0.8310 1.2304 1.2783

GEN. TERM. CURR. ANGLE DEGREES-NUMBER BUS/GEN NAME NO NUMBER BUS/GEN NAME NO
11 -49.9995 -86.5553 -90.7772 -160.4985

A-C BUS VOLTAGE MAGNITUDE -NUMBER BUS/GEN NAME NO NUMBER BUS/GEN NAME NO
11 -49.9995 1.0000 1.0000 0.9580 1.0057 1.0019 0.9872 0.9902 0.9793 0.9844

A-C BUS VOLTAGE ANGLE DEGREES -NUMBER BUS/GEN NAME NO NUMBER BUS/GEN NAME NO
11 -49.9995 -91.8678 -89.9176 -85.4970 -94.6310 -94.3190 -96.6641 -96.8218 -97.8672 -97.0354
```

## Table C.3.6 Equilibrium point (dynamic/algebraic 135 MVar)

```
1 9 BUS TEST SYSTEM(NO LINE DROP COMPENSATION) PAGE NUMBER 7
D1=2.0, D2=2.0, D3=2.0, KA=25, RC=0.0, XC=0.0 DATE 5/ 4/90
term3=135, REAL POWER LOAD = regular TIME 9.59.34

GENERATOR ANGLE IN DEGREES -NUMBER BUS/GEN NAME NO NUMBER BUS/GEN NAME NO
11 -49.9995 -378.5388 -346.0558 -372.2955

GENERATOR FIELD VOLTAGE -NUMBER BUS/GEN NAME NO NUMBER BUS/GEN NAME NO
11 -49.9995 1.1185 1.6006 2.3393

GEN. FLUX LINKAGE (Q-AXIS) -NUMBER BUS/GEN NAME NO NUMBER BUS/GEN NAME NO
11 -49.9995 0.9949 0.8562 1.0562

GEN. ELECTRICAL POWER - (MW) -NUMBER BUS/GEN NAME NO NUMBER BUS/GEN NAME NO
11 -49.9995 82.7741 123.0988 31.8060

GENERATOR EXCITER SATURATION -NUMBER BUS/GEN NAME NO NUMBER BUS/GEN NAME NO
11 -49.9995 0.0442 0.0159 0.4876

GENERATOR MEGAVAR OUTPUT -NUMBER BUS/GEN NAME NO NUMBER BUS/GEN NAME NO
11 -49.9995 0.2228 9.9667 123.5647

GENERATOR FIELD CURRENT -NUMBER BUS/GEN NAME NO NUMBER BUS/GEN NAME NO
11 -49.9995 1.0401 1.4404 2.2099

GENERATOR TERMINAL CURRENT -NUMBER BUS/GEN NAME NO NUMBER BUS/GEN NAME NO
11 -49.9995 0.8278 1.2344 1.4658

GEN. TERM. CURR. ANGLE DEGREES-NUMBER BUS/GEN NAME NO NUMBER BUS/GEN NAME NO
11 -49.9995 -29.0325 -31.5311 -96.8258

A-C BUS VOLTAGE MAGNITUDE -NUMBER BUS/GEN NAME NO NUMBER BUS/GEN NAME NO
11 -49.9995 0.9999 1.0001 0.8692 1.0013 0.9973 0.9694 0.9855 0.9671 0.9726

A-C BUS VOLTAGE ANGLE DEGREES -NUMBER BUS/GEN NAME NO NUMBER BUS/GEN NAME NO
11 -49.9995 -28.8783 -26.9001 -20.9484 -31.6552 -31.3244 -33.5055 -33.8568 -34.7921 -33.9472
```

## Table C.3.7 Output for dynamic/algebraic 10 MVar

```
eigjj =

-26.2805 +52.3698i
-26.2805 -52.3698i
 50.9883
 47.7837
 40.6818
-12.9438 +26.1431i
-12.9438 -26.1431i
-11.2838 +21.8219i
-11.2838 -21.8219i
 25.1042
 22.0818
 20.3194
-15.8215
-16.5987
-16.6157
 -5.6622 +14.9675i
 -5.6622 -14.9675i
 -3.9241 +15.0083i
 -3.9241 -15.0083i
 -4.0810 +14.9315i
 -4.0810 -14.9315i
 12.2866 + 0.9257i
 12.2866 - 0.9257i
  8.0250 + 1.1106i
  8.0250 - 1.1106i
  1.9009
 -0.5395 + 1.5576i
 -0.5395 - 1.5576i
 -0.1966 + 1.2337i
 -0.1966 - 1.2337i
  0.9130
 -0.1214 + 0.9171i
 -0.1214 - 0.9171i
  0.2535
  0.0692
  0.0153 + 0.5815i
  0.0153 - 0.5815i
 -0.0418 + 0.5857i
 -0.0418 - 0.5857i
```

```
eigd =

 50.9884
 47.7842
 40.6840
-12.8059 +26.3081i
-12.8059 -26.3081i
-11.1218 +21.8468i
-11.1218 -21.8468i
 -5.7241 +14.9101i
 -5.7241 -14.9101i
 25.1119
 22.0913
 20.3424
 12.4410 + 1.0534i
 12.4410 - 1.0534i
  8.0781 + 1.1657i
  8.0781 - 1.1657i
  1.3527
  1.9337
```

```
eigda =

-26.4462 +52.1804i
-26.4462 -52.1804i
 -3.8967 +14.9033i
 -3.8967 -14.9033i
 -3.9132 +14.9901i
 -3.9132 -14.9901i
-15.1523
-16.4814
-16.5558
 -0.3525 + 1.7338i
 -0.3525 - 1.7338i
 -0.1340 + 1.0660i
 -0.1340 - 1.0660i
 -0.0342 + 0.9736i
 -0.0342 - 0.9736i
 -0.0835 + 0.0705i
 -0.0835 - 0.0705i
 -0.0487 + 0.5929i
 -0.0487 - 0.5929i
 -0.0108 + 0.5914i
 -0.0108 - 0.5914i
```

```
eigad =

1.0e+03 *

-0.0535 + 3.8961i
-0.0535 - 3.8961i
-0.2283 + 0.5119i
-0.2283 - 0.5119i
 0.2267 + 0.4487i
 0.2267 - 0.4487i
 0.0388 + 0.0557i
 0.0388 - 0.0557i
 0.0511
 0.0452
 0.0357
 0.0321
 0.0000
 0.0146
 0.0058
 0.0070 + 0.0004i
 0.0070 - 0.0004i
 0.0125
```

```
vda =

Columns 1 through 4

0.0000 - 0.0000i 0.0000 + 0.0000i 0.0000 + 0.0000i 0.0000 - 0.0000i
0.0000 + 0.0000i 0.0000 - 0.0000i 0.0000 - 0.0000i 0.0000 + 0.0000i
0.0000 + 0.0000i 0.0000 - 0.0000i 0.0000 + 0.0000i 0.0000 - 0.0000i
0.0000 + 0.0000i 0.0000 - 0.0000i 0.0000 - 0.0000i 0.0000 + 0.0000i
```

## Table C.3.7 (cont'd)

```
0.0000 - 0.0000i 0.0000 + 0.0000i 0.0000 + 0.0000i 0.0000 - 0.0000i
0.0000 - 0.0000i 0.0000 + 0.0000i 0.0000 - 0.0000i 0.0000 + 0.0000i
-0.0002 + 0.0003i -0.0002 - 0.0003i 0.0000 + 0.0000i 0.0000 - 0.0000i
0.0000 + 0.0000i 0.0000 - 0.0000i -0.0013 + 0.0008i -0.0013 - 0.0008i
0.0000 + 0.0000i 0.0000 - 0.0000i -0.0005 + 0.0003i -0.0005 - 0.0003i
0.0001 + 0.0000i 0.0001 - 0.0000i 0.0000 + 0.0002i 0.0000 - 0.0002i
0.0000 + 0.0000i 0.0000 - 0.0000i -0.0001 + 0.0007i -0.0001 - 0.0007i
0.0000 + 0.0000i 0.0000 - 0.0000i -0.0001 + 0.0006i -0.0001 - 0.0006i
-0.0048 - 0.0105i -0.0048 + 0.0105i 0.0000 - 0.0002i 0.0000 + 0.0002i
0.0000 - 0.0000i 0.0000 + 0.0000i -0.0021 - 0.0306i -0.0021 + 0.0306i
0.0000 - 0.0000i 0.0000 + 0.0000i -0.0023 - 0.0249i -0.0023 + 0.0249i
1.0000 + 0.0000i 1.0000 - 0.0000i 0.0054 - 0.0000i 0.0054 + 0.0000i
0.0000 + 0.0003i 0.0000 - 0.0003i 1.0000 + 0.0000i 1.0000 - 0.0000i
0.0000 + 0.0003i 0.0000 - 0.0003i 0.8175 - 0.0177i 0.8175 + 0.0177i
-0.0764 - 0.1537i -0.0764 + 0.1537i -0.0008 - 0.0035i -0.0008 + 0.0035i
0.0000 - 0.0000i 0.0000 + 0.0000i -0.0288 - 0.1106i -0.0288 + 0.1106i
0.0000 - 0.0000i 0.0000 + 0.0000i -0.0214 - 0.0756i -0.0214 + 0.0756i
```

Columns 5 through 8

```
0.0000 - 0.0000i 0.0000 + 0.0000i 0.0000 0.0000
0.0000 + 0.0000i 0.0000 - 0.0000i -0.0001 0.0000
0.0000 - 0.0000i 0.0000 + 0.0000i 0.0000 0.0000
0.0000 + 0.0000i 0.0000 - 0.0000i 0.0000 0.0000
0.0000 - 0.0000i 0.0000 + 0.0000i 0.0000 0.0000
0.0000 + 0.0000i 0.0000 - 0.0000i 0.0000 0.0000
0.0000 - 0.0000i 0.0000 + 0.0000i 0.0049 -0.0003
0.0011 - 0.0006i 0.0011 + 0.0006i 0.0004 0.0013
-0.0006 + 0.0003i -0.0006 - 0.0003i 0.0001 0.0004
0.0000 + 0.0000i 0.0000 - 0.0000i 0.0454 -0.0025
0.0001 - 0.0003i 0.0001 + 0.0003i 0.0222 0.0566
-0.0001 + 0.0003i -0.0001 - 0.0003i 0.0190 0.0352
0.0000 - 0.0000i 0.0000 + 0.0000i -0.0524 0.0030
0.0017 + 0.0246i 0.0017 - 0.0246i -0.0144 -0.0336
-0.0021 - 0.0303i -0.0021 + 0.0303i -0.0123 -0.0209
0.0000 + 0.0000i 0.0000 - 0.0000i 1.0000 -0.0623
-0.8089 - 0.0005i -0.8089 + 0.0005i 0.3852 1.0000
1.0000 + 0.0000i 1.0000 - 0.0000i 0.3307 0.6233
0.0000 - 0.0000i 0.0000 + 0.0000i -0.6839 0.0390
0.0230 + 0.0889i 0.0230 - 0.0889i -0.0448 -0.1069
-0.0240 - 0.0925i -0.0240 + 0.0925i -0.0323 -0.0560
```

Columns 9 through 12

```
0.0000 0.0060 + 0.0009i 0.0060 - 0.0009i -0.0656 + 0.0176i
0.0000 -0.0115 - 0.0061i -0.0115 + 0.0061i 0.2602 + 0.0205i
0.0000 -0.0039 + 0.0030i -0.0039 - 0.0030i -0.0883 - 0.0402i
0.0000 -0.0002 - 0.0034i -0.0002 + 0.0034i 0.0238 + 0.0585i
0.0000 -0.0021 + 0.0071i -0.0021 - 0.0071i -0.0113 - 0.2427i
0.0000 0.0021 + 0.0018i 0.0021 - 0.0018i -0.0269 + 0.0862i
0.0000 -0.0194 - 0.0544i -0.0194 + 0.0544i 0.0353 + 0.0297i
-0.0009 -0.0312 + 0.0073i -0.0312 - 0.0073i -0.0100 - 0.1786i
0.0006 -0.0135 + 0.0066i -0.0135 - 0.0066i -0.0718 + 0.0094i
-0.0003 -0.0265 - 0.0415i -0.0265 + 0.0415i 0.0160 + 0.0057i
-0.0367 -0.0278 - 0.0110i -0.0278 + 0.0110i -0.0215 - 0.0984i
0.0565 -0.0229 - 0.0086i -0.0229 + 0.0086i -0.0528 - 0.0015i
0.0003 0.0264 + 0.0398i 0.0264 - 0.0398i -0.0155 - 0.0055i
0.0217 0.0272 + 0.0092i 0.0272 - 0.0092i 0.0235 + 0.0926i
-0.0334 0.0224 + 0.0071i 0.0224 - 0.0071i 0.0501 - 0.0002i
-0.0068 0.0177 + 0.1734i 0.0177 - 0.1734i -0.0547 - 0.0208i
-0.6487 0.1156 + 0.1518i 0.1156 - 0.1518i -0.0640 + 0.6060i
1.0000 0.0969 + 0.1233i 0.0969 - 0.1233i 0.3005 + 0.1113i
0.0043 1.0000 + 0.0000i 1.0000 - 0.0000i -0.3384 + 0.3874i
0.0690 0.1269 - 0.1416i 0.1269 + 0.1416i 1.0000 + 0.0000i
-0.0895 0.0859 - 0.0994i 0.0859 + 0.0994i 0.1069 - 0.4289i
```

Columns 13 through 16

```
-0.0656 - 0.0176i -0.0358 - 0.0408i -0.0358 + 0.0408i -0.0835 + 0.0705i
0.2602 - 0.0205i -0.0099 + 0.1768i -0.0099 - 0.1768i -0.0761 + 0.0669i
-0.0883 + 0.0402i 0.0830 - 0.0673i 0.0830 + 0.0673i -0.0815 + 0.0703i
0.0238 - 0.0585i -0.0405 + 0.0382i -0.0405 - 0.0382i 1.0000 - 0.0000i
-0.0113 + 0.2427i 0.1818 + 0.0038i 0.1818 - 0.0038i 0.9269 - 0.0189i
-0.0269 - 0.0862i -0.0721 - 0.0827i -0.0721 + 0.0827i 0.9849 - 0.0099i
0.0353 - 0.0297i 0.0078 + 0.0532i 0.0078 - 0.0532i 0.0003 - 0.0013i
-0.0100 + 0.1786i 0.0694 - 0.0812i 0.0694 + 0.0812i 0.0121 + 0.0051i
-0.0718 - 0.0094i -0.0386 - 0.1254i -0.0386 + 0.1254i -0.0012 + 0.0002i
```

## Table C.3.7 (cont'd)

```
0.0160 - 0.0057i 0.0090 + 0.0136i 0.0090 - 0.0136i 0.0006 - 0.0007i
-0.0215 + 0.0984i 0.0419 - 0.0593i 0.0419 + 0.0593i -0.0007 + 0.0004i
-0.0528 + 0.0015i -0.0281 - 0.1028i -0.0281 + 0.1028i 0.0001 - 0.0001i
-0.0155 + 0.0055i -0.0086 - 0.0131i -0.0086 + 0.0131i -0.0007 + 0.0007i
0.0235 - 0.0926i -0.0379 + 0.0572i -0.0379 - 0.0572i 0.0007 - 0.0004i
0.0501 + 0.0002i 0.0295 + 0.0963i 0.0295 - 0.0963i -0.0001 + 0.0001i
-0.0547 + 0.0208i -0.0363 - 0.0484i -0.0363 + 0.0484i 0.0122 + 0.0022i
-0.0640 - 0.6060i -0.3494 + 0.2802i -0.3494 - 0.2802i 0.0033 - 0.0026i
0.3005 - 0.1113i -0.0125 + 0.6579i -0.0125 - 0.6579i -0.0002 + 0.0004i
-0.3384 - 0.3874i -0.5452 + 0.0951i -0.5452 - 0.0951i 0.2750 + 0.0050i
1.0000 - 0.0000i 0.5146 + 0.6245i 0.5146 - 0.6245i -0.0770 - 0.0151i
0.1069 + 0.4289i 1.0000 - 0.0000i 1.0000 + 0.0000i 0.0067 - 0.0012i
```

Columns 17 through 20

```
-0.0835 - 0.0705i 0.0104 - 0.1895i 0.0104 + 0.1895i 0.0524 - 0.0326i
-0.0761 - 0.0669i 0.1035 + 0.1340i 0.1035 - 0.1340i -0.1307 + 0.1853i
-0.0815 - 0.0703i -0.1859 + 0.3890i -0.1859 - 0.3890i -0.0492 - 0.1270i
1.0000 + 0.0000i -0.3188 + 0.0087i -0.3188 - 0.0087i -0.0535 - 0.0895i
0.9269 + 0.0189i 0.2103 - 0.1918i 0.2103 + 0.1918i 0.3092 + 0.2267i
0.9849 + 0.0099i 0.6773 + 0.2579i 0.6773 - 0.2579i -0.2161 + 0.0793i
0.0003 + 0.0013i 0.0273 + 0.0226i 0.0273 - 0.0226i -0.0042 + 0.0169i
0.0121 - 0.0051i -0.1317 + 0.0919i -0.1317 - 0.0919i -0.1388 - 0.2071i
-0.0012 - 0.0002i -0.0585 - 0.1206i -0.0585 + 0.1206i 0.0799 + 0.0368i
0.0006 + 0.0007i 0.0041 + 0.0051i 0.0041 - 0.0051i -0.0003 + 0.0027i
-0.0007 - 0.0004i -0.0345 - 0.0030i -0.0345 + 0.0030i -0.0113 - 0.0546i
0.0001 + 0.0001i -0.0073 - 0.0674i -0.0073 + 0.0674i 0.0384 + 0.0158i
-0.0007 - 0.0007i -0.0039 - 0.0050i -0.0039 + 0.0050i 0.0004 - 0.0026i
0.0007 + 0.0004i 0.0326 + 0.0023i 0.0326 - 0.0023i 0.0115 + 0.0512i
-0.0001 - 0.0001i 0.0080 + 0.0635i 0.0080 - 0.0635i -0.0364 - 0.0143i
0.0122 - 0.0022i -0.0236 - 0.0109i -0.0236 + 0.0109i -0.0036 - 0.0111i
0.0033 + 0.0026i 0.1984 + 0.0492i 0.1984 - 0.0492i 0.0182 + 0.3362i
-0.0002 - 0.0004i -0.0223 + 0.4007i -0.0223 - 0.4007i -0.2137 - 0.1311i
0.2750 - 0.0050i -0.3053 + 0.1503i -0.3053 - 0.1503i -0.1326 - 0.0606i
-0.0770 + 0.0151i 0.1186 - 0.5940i 0.1186 + 0.5940i 1.0000 + 0.0000i
0.0067 + 0.0012i 1.0000 + 0.0000i 1.0000 - 0.0000i -0.3513 + 0.5191i
```

Column 21

```
0.0524 + 0.0326i
-0.1307 - 0.1853i
-0.0492 + 0.1270i
-0.0535 + 0.0895i
0.3092 - 0.2267i
-0.2161 - 0.0793i
-0.0042 - 0.0169i
-0.1388 + 0.2071i
0.0799 - 0.0368i
-0.0003 - 0.0027i
-0.0113 + 0.0546i
0.0384 - 0.0158i
0.0004 + 0.0026i
0.0115 - 0.0512i
-0.0364 + 0.0143i
-0.0036 + 0.0111i
0.0182 - 0.3362i
-0.2137 + 0.1311i
-0.1326 + 0.0606i
1.0000 - 0.0000i
-0.3513 - 0.5191i
```

detjj =

-1.6291e+31

detd =

3.9878e+21

detda =

-4.0852e+09

# Table C.3.7 (cont'd)

```
detad =

  2.2963e+31


condjj =

  1.4060e+06


condd =

  60.7094


condda =

  6.7747e+05


condad =

  1.3290e+08


vtt =

  1.0000 0.0442 0.0069
 -0.6955 1.0000 1.0000
 -0.3321 0.6017 -0.4808


eigtt =

  1.0e+03 *

 -0.1470
 -1.1285
 -0.5760
```

## Table C.3.8 Output for dynamic/algebraic 50 MVar

eigjj =

```
-26.2812 +52.3701i
-26.2812 -52.3701i
 50.9551
 47.7583
 40.6669
-12.9343 +26.1020i
-12.9343 -26.1020i
-11.3214 +21.6635i
-11.3214 -21.6635i
 25.0956
 22.0582
 20.4673
-15.8216
-16.5962
-16.6131
 -5.6908 +14.9354i
 -5.6908 -14.9354i
 -3.9536 +15.0079i
 -3.9536 -15.0079i
 -4.0934 +14.9407i
 -4.0934 -14.9407i
 12.2942 + 0.9443i
 12.2942 - 0.9443i
  8.0423 + 1.0581i
  8.0423 - 1.0581i
  1.9557
 -0.5412 + 1.5617i
 -0.5412 - 1.5617i
  0.9595
 -0.2020 + 1.2383i
 -0.2020 - 1.2383i
  0.2503
  0.0659
 -0.0450 + 0.6286i
 -0.0450 - 0.6286i
  0.0250 + 0.5912i
  0.0250 - 0.5912i
 -0.1225 + 0.9300i
 -0.1225 - 0.9300i
```

eigd =

```
 50.9553
 47.7590
 40.6690
-12.7930 +26.2697i
-12.7930 -26.2697i
-11.1508 +21.6857i
-11.1508 -21.6857i
 -5.7533 +14.8822i
 -5.7533 -14.8822i
 25.1034
 22.0691
 20.4957
 12.4480 + 1.0687i
 12.4480 - 1.0687i
  8.0977 + 1.1212i
  8.0977 - 1.1212i
  1.3188
  2.0642
```

eigda =

```
-26.4473 +52.1806i
-26.4473 -52.1806i
 -3.9097 +14.8996i
 -3.9097 -14.8996i
 -3.9365 +14.9897i
 -3.9365 -14.9897i
-16.4719
-16.5512
-15.1482
 -0.3374 + 1.7360i
 -0.3374 - 1.7360i
 -0.1189 + 1.0689i
 -0.1189 - 1.0689i
 -0.0402 + 1.0036i
 -0.0402 - 1.0036i
 -0.0835 + 0.0673i
 -0.0835 - 0.0673i
 -0.0646 + 0.6331i
 -0.0646 - 0.6331i
 -0.0257 + 0.6015i
 -0.0257 - 0.6015i
```

eigad =

1.0e+03 *

```
-0.0529 + 2.7439i
-0.0529 - 2.7439i
-0.0701 + 0.4258i
-0.0701 - 0.4258i
 0.0663 + 0.2236i
 0.0663 - 0.2236i
 0.0412 + 0.0612i
 0.0412 - 0.0612i
 0.0511
 0.0451
 0.0357
 0.0317
 0.0000
 0.0146
 0.0058
 0.0070 + 0.0004i
 0.0070 - 0.0004i
 0.0125
```

vda =

Columns 1 through 4

```
0.0000 - 0.0000i  0.0000 + 0.0000i  0.0000 + 0.0000i  0.0000 - 0.0000i
0.0000 + 0.0000i  0.0000 - 0.0000i  0.0000 - 0.0000i  0.0000 + 0.0000i
0.0000 + 0.0000i  0.0000 - 0.0000i  0.0000 + 0.0000i  0.0000 - 0.0000i
0.0000 + 0.0000i  0.0000 - 0.0000i  0.0000 - 0.0000i  0.0000 + 0.0000i
0.0000 - 0.0000i  0.0000 + 0.0000i  0.0000 + 0.0000i  0.0000 - 0.0000i
```

## Table C.3.8 (cont'd)

```
0.0000 - 0.0000i 0.0000 + 0.0000i 0.0000 - 0.0000i 0.0000 + 0.0000i
-0.0002 + 0.0003i -0.0002 - 0.0003i 0.0000 + 0.0000i 0.0000 - 0.0000i
0.0000 + 0.0000i 0.0000 - 0.0000i -0.0013 + 0.0008i -0.0013 - 0.0008i
0.0000 + 0.0000i 0.0000 - 0.0000i -0.0003 + 0.0004i -0.0003 - 0.0004i
0.0001 + 0.0000i 0.0001 - 0.0000i 0.0000 + 0.0002i 0.0000 - 0.0002i
0.0000 + 0.0000i 0.0000 - 0.0000i -0.0001 + 0.0008i -0.0001 - 0.0008i
0.0000 + 0.0000i 0.0000 - 0.0000i 0.0001 + 0.0006i 0.0001 - 0.0006i
-0.0048 - 0.0105i -0.0048 + 0.0105i -0.0001 - 0.0002i -0.0001 + 0.0002i
0.0000 - 0.0000i 0.0000 + 0.0000i -0.0021 - 0.0306i -0.0021 + 0.0306i
0.0000 - 0.0000i 0.0000 + 0.0000i -0.0103 - 0.0212i -0.0103 + 0.0212i
1.0000 - 0.0000i 1.0000 + 0.0000i 0.0055 - 0.0008i 0.0055 + 0.0008i
0.0000 + 0.0003i 0.0000 - 0.0003i 1.0000 + 0.0000i 1.0000 - 0.0000i
0.0000 + 0.0003i 0.0000 - 0.0003i 0.7114 - 0.2926i 0.7114 + 0.2926i
-0.0764 - 0.1537i -0.0764 + 0.1537i -0.0013 - 0.0034i -0.0013 + 0.0034i
0.0000 - 0.0000i 0.0000 + 0.0000i -0.0288 - 0.1105i -0.0288 + 0.1105i
0.0000 - 0.0000i 0.0000 + 0.0000i -0.0442 - 0.0593i -0.0442 + 0.0593i
```

Columns 5 through 8

```
0.0000 - 0.0000i 0.0000 + 0.0000i 0.0000 0.0000
0.0000 + 0.0000i 0.0000 - 0.0000i 0.0000 0.0000
0.0000 - 0.0000i 0.0000 + 0.0000i 0.0000 0.0000
0.0000 + 0.0000i 0.0000 - 0.0000i 0.0000 0.0000
0.0000 - 0.0000i 0.0000 + 0.0000i 0.0000 0.0000
0.0000 + 0.0000i 0.0000 - 0.0000i 0.0000 0.0000
0.0000 - 0.0000i 0.0000 + 0.0000i -0.0003 0.0000
0.0007 - 0.0009i 0.0007 + 0.0009i 0.0013 -0.0010
-0.0006 + 0.0003i -0.0006 - 0.0003i 0.0004 0.0006
0.0000 + 0.0000i 0.0000 - 0.0000i -0.0029 -0.0002
-0.0001 - 0.0003i -0.0001 + 0.0003i 0.0566 -0.0430
-0.0001 + 0.0004i -0.0001 - 0.0004i 0.0431 0.0566
0.0000 - 0.0000i 0.0000 + 0.0000i 0.0034 0.0002
0.0096 + 0.0206i 0.0096 - 0.0206i -0.0336 0.0255
-0.0020 - 0.0304i -0.0020 + 0.0304i -0.0256 -0.0335
0.0006 + 0.0009i 0.0006 - 0.0009i -0.0716 -0.0047
-0.6976 + 0.2662i -0.6976 - 0.2662i 1.0000 -0.7610
1.0000 + 0.0000i 1.0000 - 0.0000i 0.7600 1.0000
0.0005 - 0.0005i 0.0005 + 0.0005i 0.0449 0.0029
0.0493 + 0.0690i 0.0493 - 0.0690i -0.1069 0.0810
-0.0237 - 0.0926i -0.0237 + 0.0926i -0.0687 -0.0899
```

Columns 9 through 12

```
0.0000 0.0060 + 0.0011i 0.0060 - 0.0011i -0.0622 + 0.0158i
-0.0001 -0.0120 - 0.0064i -0.0120 + 0.0064i 0.2487 + 0.0377i
0.0000 -0.0033 + 0.0029i -0.0033 - 0.0029i -0.0873 - 0.0538i
0.0000 0.0000 - 0.0035i 0.0000 + 0.0035i 0.0210 + 0.0559i
0.0000 -0.0022 + 0.0074i -0.0022 - 0.0074i 0.0093 - 0.2337i
0.0000 0.0019 + 0.0015i 0.0019 - 0.0015i -0.0407 + 0.0862i
0.0049 -0.0188 - 0.0545i -0.0188 + 0.0545i 0.0429 + 0.0332i
0.0004 -0.0315 + 0.0080i -0.0315 - 0.0080i -0.0099 - 0.1690i
0.0001 -0.0135 + 0.0073i -0.0135 - 0.0073i -0.0828 + 0.0011i
0.0454 -0.0266 - 0.0411i -0.0266 + 0.0411i 0.0188 + 0.0059i
0.0223 -0.0286 - 0.0100i -0.0286 + 0.0100i -0.0227 - 0.0977i
0.0198 -0.0253 - 0.0071i -0.0253 + 0.0071i -0.0697 - 0.0131i
-0.0524 0.0264 + 0.0394i 0.0264 - 0.0394i -0.0182 - 0.0057i
-0.0144 0.0279 + 0.0082i 0.0279 - 0.0082i 0.0246 + 0.0919i
-0.0128 0.0245 + 0.0056i 0.0245 - 0.0056i 0.0663 + 0.0105i
1.0000 0.0193 + 0.1736i 0.0193 - 0.1736i -0.0650 - 0.0218i
0.3870 0.1244 + 0.1491i 0.1244 - 0.1491i -0.0554 + 0.6076i
0.3425 0.1197 + 0.1167i 0.1197 - 0.1167i 0.3888 + 0.1823i
-0.6841 1.0000 + 0.0000i 1.0000 - 0.0000i -0.3819 + 0.4612i
-0.0450 0.1240 - 0.1487i 0.1240 + 0.1487i 1.0000 + 0.0000i
-0.0337 0.0837 - 0.1136i 0.0837 + 0.1136i 0.2413 - 0.5431i
```

Columns 13 through 16

```
-0.0622 - 0.0158i -0.0377 - 0.0379i -0.0377 + 0.0379i -0.0835 + 0.0673i
0.2487 - 0.0377i 0.0093 + 0.1829i 0.0093 - 0.1829i -0.0762 + 0.0640i
-0.0873 + 0.0538i 0.0690 - 0.0793i 0.0690 + 0.0793i -0.0818 + 0.0672i
0.0210 - 0.0559i -0.0362 + 0.0390i -0.0362 - 0.0390i 1.0000 + 0.0000i
0.0093 + 0.2337i 0.1816 - 0.0166i 0.1816 + 0.0166i 0.9275 - 0.0181i
-0.0407 - 0.0862i -0.0817 - 0.0654i -0.0817 + 0.0654i 0.9873 - 0.0091i
0.0429 - 0.0332i 0.0081 + 0.0574i 0.0081 - 0.0574i 0.0004 - 0.0012i
-0.0099 + 0.1690i 0.0774 - 0.0851i 0.0774 + 0.0851i 0.0123 + 0.0049i
-0.0828 - 0.0011i -0.0420 - 0.1148i -0.0420 + 0.1148i -0.0006 + 0.0001i
0.0188 - 0.0059i 0.0099 + 0.0154i 0.0099 - 0.0154i 0.0006 - 0.0006i
```

# Table C.3.8 (cont'd)

```
-0.0227 + 0.0977i  0.0452 - 0.0641i  0.0452 + 0.0641i  -0.0007 + 0.0004i
-0.0697 + 0.0131i -0.0299 - 0.1058i -0.0299 + 0.1058i  0.0001 - 0.0001i
-0.0182 + 0.0057i -0.0096 - 0.0149i -0.0096 + 0.0149i -0.0007 + 0.0006i
 0.0246 - 0.0919i -0.0409 + 0.0619i -0.0409 - 0.0619i  0.0007 - 0.0004i
 0.0663 - 0.0105i  0.0309 + 0.0990i  0.0309 - 0.0990i -0.0001 + 0.0001i
-0.0650 + 0.0218i -0.0388 - 0.0555i -0.0388 + 0.0555i  0.0122 + 0.0021i
-0.0554 - 0.6076i -0.3809 + 0.2995i -0.3809 - 0.2995i  0.0033 - 0.0025i
 0.3888 - 0.1823i  0.0385 + 0.6783i  0.0385 - 0.6783i  0.0001 + 0.0003i
-0.3819 - 0.4612i -0.5992 + 0.0940i -0.5992 - 0.0940i  0.2744 + 0.0048i
 1.0000 - 0.0000i  0.5372 + 0.6576i  0.5372 - 0.6576i -0.0779 - 0.0144i
 0.2413 + 0.5431i  1.0000 - 0.0000i  1.0000 + 0.0000i  0.0065 - 0.0006i
```

Columns 17 through 20

```
-0.0835 - 0.0673i -0.0025 - 0.3055i -0.0025 + 0.3055i  0.0187 - 0.0441i
-0.0762 - 0.0640i -0.0130 + 0.1816i -0.0130 - 0.1816i -0.1192 + 0.1777i
-0.0818 - 0.0672i -0.0646 + 0.6331i -0.0646 - 0.6331i  0.0280 - 0.0816i
 1.0000 - 0.0000i -0.4771 + 0.0526i -0.4771 - 0.0526i -0.0718 - 0.0342i
 0.9275 + 0.0181i  0.2860 - 0.0087i  0.2860 + 0.0087i  0.2864 + 0.2105i
 0.9873 + 0.0091i  1.0000 + 0.0000i  1.0000 - 0.0000i -0.1334 - 0.0523i
 0.0004 + 0.0012i  0.0340 + 0.0294i  0.0340 - 0.0294i  0.0018 + 0.0137i
 0.0123 - 0.0049i -0.0710 - 0.0168i -0.0710 + 0.0168i -0.1269 - 0.2065i
-0.0006 - 0.0001i -0.0599 - 0.0670i -0.0599 + 0.0670i  0.0372 + 0.0429i
 0.0006 + 0.0006i  0.0063 + 0.0086i  0.0063 - 0.0086i  0.0009 + 0.0021i
-0.0007 - 0.0004i -0.0104 - 0.0242i -0.0104 + 0.0242i -0.0129 - 0.0550i
 0.0001 + 0.0001i -0.0166 - 0.0589i -0.0166 + 0.0589i  0.0223 + 0.0174i
-0.0007 - 0.0006i -0.0059 - 0.0084i -0.0059 + 0.0084i -0.0008 - 0.0021i
 0.0007 + 0.0004i  0.0102 + 0.0226i  0.0102 - 0.0226i  0.0131 + 0.0515i
-0.0001 - 0.0001i  0.0162 + 0.0553i  0.0162 - 0.0553i -0.0211 - 0.0161i
 0.0122 - 0.0021i -0.0352 - 0.0205i -0.0352 + 0.0205i -0.0072 - 0.0070i
 0.0033 + 0.0025i  0.0362 + 0.1507i  0.0362 - 0.1507i  0.0269 + 0.3419i
 0.0001 - 0.0003i  0.0771 + 0.3518i  0.0771 - 0.3518i -0.1333 - 0.1122i
 0.2744 - 0.0048i -0.4755 + 0.2058i -0.4755 - 0.2058i -0.1217 + 0.0063i
-0.0779 + 0.0144i  0.4100 - 0.1284i  0.4100 + 0.1284i  1.0000 + 0.0000i
 0.0065 + 0.0006i  0.8294 - 0.1374i  0.8294 + 0.1374i -0.3293 + 0.2607i
```

Column 21

```
 0.0187 + 0.0441i
-0.1192 - 0.1777i
 0.0280 + 0.0816i
-0.0718 + 0.0342i
 0.2864 - 0.2105i
-0.1334 + 0.0523i
 0.0018 - 0.0137i
-0.1269 + 0.2065i
 0.0372 - 0.0429i
 0.0009 - 0.0021i
-0.0129 + 0.0550i
 0.0223 - 0.0174i
-0.0008 + 0.0021i
 0.0131 - 0.0515i
-0.0211 + 0.0161i
-0.0072 + 0.0070i
 0.0269 - 0.3419i
-0.1333 + 0.1122i
-0.1217 - 0.0063i
 1.0000 - 0.0000i
-0.3293 - 0.2607i
```

detjj =

-2.0475e+31

detd =

4.1246e+21

detda =

-4.9640e+09

# Table C.3.8 (cont'd)

```
detad =

 1.6198e+30

condjj =

 1.4589e+06

condd =

 56.8584

condda =

 7.0325e+05

condad =

 6.8366e+07

vtt =

 -0.6029 0.0333 -0.6322
 1.0000 1.0000 -0.2536
 -0.4735 0.0371 1.0000

eigtt =

 -171.1429
 -852.9462
 -114.6348
```

## Table C.3.9 Output for dynamic/algebraic 100 MVar

eigjj =

```
-26.2854 +52.3721i
-26.2854 -52.3721i
 50.7730
 47.6031
 40.5914
-12.8643 +25.9649i
-12.8643 -25.9649i
-11.1901 +21.0734i
-11.1901 -21.0734i
 25.0576
 21.9705
 20.2247
-15.8216
-16.6106
-16.5913
 -5.6948 +14.7869i
 -5.6948 -14.7869i
 -4.1666 +14.9944i
 -4.1666 -14.9944i
 -4.0085 +14.9888i
 -4.0085 -14.9888i
 12.2683 + 0.9604i
 12.2683 - 0.9604i
  8.0234 + 0.9685i
  8.0234 - 0.9685i
  2.0079
 -0.5451 + 1.5670i
 -0.5451 - 1.5670i
  0.9982
 -0.2075 + 1.2449i
 -0.2075 - 1.2449i
 -0.1431 + 0.9632i
 -0.1431 - 0.9632i
  0.2478
  0.0634
 -0.0341 + 0.6627i
 -0.0341 - 0.6627i
  0.0228 + 0.6012i
  0.0228 - 0.6012i
```

eigd =

```
 50.7732
 47.6038
 40.5936
-12.7191 +26.1411i
-12.7191 -26.1411i
-11.0137 +21.0874i
-11.0137 -21.0874i
 -5.7709 +14.7482i
 -5.7709 -14.7482i
 25.0651
 21.9803
 20.2582
  1.2702
  2.1924
 12.4206 + 1.0800i
 12.4206 - 1.0800i
  8.0821 + 1.0462i
  8.0821 - 1.0462i
```

eigda =

```
-26.4522 +52.1819i
-26.4522 -52.1819i
 -3.9206 +14.9177i
 -3.9206 -14.9177i
 -4.0319 +14.9750i
 -4.0319 -14.9750i
-16.4550
-16.5434
-15.1372
 -0.3148 + 1.7424i
 -0.3148 - 1.7424i
 -0.0353 + 1.1019i
 -0.0353 - 1.1019i
 -0.1296 + 1.0323i
 -0.1296 - 1.0323i
 -0.0835 + 0.0649i
 -0.0835 - 0.0649i
 -0.0664 + 0.6648i
 -0.0664 - 0.6648i
 -0.0265 + 0.6128i
 -0.0265 - 0.6128i
```

eigad =

```
1.0e+03 *

 -0.0519 + 1.3544i
 -0.0519 - 1.3544i
 -0.0438 + 0.4469i
 -0.0438 - 0.4469i
  0.0029 + 0.0853i
  0.0029 - 0.0853i
  0.0784 + 0.0635i
  0.0784 - 0.0635i
  0.0509
  0.0449
  0.0356
  0.0304
  0.0000
  0.0124
  0.0058
  0.0070 + 0.0003i
  0.0070 - 0.0003i
  0.0145
```

vda =

Columns 1 through 4

```
0.0000 - 0.0000i  0.0000 + 0.0000i  0.0000 + 0.0000i  0.0000 - 0.0000i
0.0000 + 0.0000i  0.0000 - 0.0000i  0.0000 - 0.0000i  0.0000 + 0.0000i
0.0000 + 0.0000i  0.0000 - 0.0000i  0.0000 + 0.0000i  0.0000 - 0.0000i
0.0000 + 0.0000i  0.0000 - 0.0000i  0.0000 - 0.0000i  0.0000 + 0.0000i
0.0000 - 0.0000i  0.0000 + 0.0000i  0.0000 + 0.0000i  0.0000 - 0.0000i
```

## Table C.3.9 (cont'd)

```
0.0000 - 0.0000i 0.0000 + 0.0000i 0.0000 - 0.0000i 0.0000 + 0.0000i
-0.0002 + 0.0003i -0.0002 - 0.0003i 0.0000 + 0.0000i 0.0000 - 0.0000i
0.0000 + 0.0000i 0.0000 - 0.0000i -0.0013 + 0.0008i -0.0013 - 0.0008i
0.0000 + 0.0000i 0.0000 - 0.0000i 0.0000 + 0.0003i 0.0000 - 0.0003i
0.0001 + 0.0000i 0.0001 - 0.0000i 0.0000 + 0.0002i 0.0000 - 0.0002i
0.0000 + 0.0000i 0.0000 - 0.0000i 0.0000 + 0.0007i 0.0000 - 0.0007i
0.0000 + 0.0000i 0.0000 - 0.0000i 0.0002 + 0.0004i 0.0002 - 0.0004i
-0.0048 - 0.0105i -0.0048 + 0.0105i -0.0001 - 0.0002i -0.0001 + 0.0002i
0.0000 - 0.0000i 0.0000 + 0.0000i -0.0021 - 0.0305i -0.0021 + 0.0305i
0.0000 - 0.0000i 0.0000 + 0.0000i -0.0119 - 0.0054i -0.0119 + 0.0054i
1.0000 + 0.0000i 1.0000 - 0.0000i 0.0042 - 0.0013i 0.0042 + 0.0013i
0.0000 + 0.0003i 0.0000 - 0.0003i 1.0000 - 0.0000i 1.0000 + 0.0000i
0.0000 + 0.0003i 0.0000 - 0.0003i 0.1954 - 0.3797i 0.1954 + 0.3797i
-0.0763 - 0.1537i -0.0763 + 0.1537i -0.0014 - 0.0025i -0.0014 + 0.0025i
0.0000 - 0.0000i 0.0000 + 0.0000i -0.0288 - 0.1104i -0.0288 + 0.1104i
0.0000 - 0.0000i 0.0000 + 0.0000i -0.0400 - 0.0098i -0.0400 + 0.0098i
```

Columns 5 through 8

```
0.0000 + 0.0000i 0.0000 - 0.0000i 0.0000 0.0000
0.0000 + 0.0000i 0.0000 - 0.0000i 0.0000 0.0000
0.0000 - 0.0000i 0.0000 + 0.0000i 0.0000 0.0000
0.0000 + 0.0000i 0.0000 - 0.0000i 0.0000 0.0000
0.0000 - 0.0000i 0.0000 + 0.0000i 0.0000 0.0000
0.0000 + 0.0000i 0.0000 - 0.0000i 0.0000 0.0000
0.0000 + 0.0000i 0.0000 - 0.0000i -0.0004 0.0000
0.0000 - 0.0006i 0.0000 + 0.0006i 0.0013 -0.0012
-0.0005 + 0.0003i -0.0005 - 0.0003i 0.0005 0.0006
-0.0001 + 0.0001i -0.0001 - 0.0001i -0.0036 0.0000
-0.0002 + 0.0001i -0.0002 - 0.0001i 0.0566 -0.0537
-0.0002 + 0.0006i -0.0002 - 0.0006i 0.0570 0.0571
0.0000 - 0.0001i 0.0000 + 0.0001i 0.0042 0.0000
0.0109 + 0.0051i 0.0109 - 0.0051i -0.0337 0.0318
-0.0018 - 0.0305i -0.0018 + 0.0305i -0.0342 -0.0340
0.0026 + 0.0013i 0.0026 - 0.0013i -0.0888 0.0002
-0.1929 + 0.3435i -0.1929 - 0.3435i 1.0000 -0.9490
1.0000 - 0.0000i 1.0000 + 0.0000i 0.9977 1.0000
0.0004 - 0.0018i 0.0004 + 0.0018i 0.0558 -0.0001
0.0433 + 0.0111i 0.0433 - 0.0111i -0.1070 0.1010
-0.0230 - 0.0931i -0.0230 + 0.0931i -0.0916 -0.0913
```

Columns 9 through 12

```
0.0000 0.0060 + 0.0014i 0.0060 - 0.0014i -0.0540 + 0.0129i
-0.0001 -0.0124 - 0.0067i -0.0124 + 0.0067i 0.1636 + 0.0506i
0.0000 -0.0030 + 0.0024i -0.0030 - 0.0024i -0.0269 - 0.0663i
0.0000 0.0002 - 0.0035i 0.0002 + 0.0035i 0.0133 + 0.0486i
0.0000 -0.0025 + 0.0076i -0.0025 - 0.0076i 0.0411 - 0.1498i
0.0000 0.0017 + 0.0014i 0.0017 - 0.0014i -0.0593 + 0.0263i
0.0049 -0.0179 - 0.0544i -0.0179 + 0.0544i 0.0605 + 0.0444i
0.0004 -0.0319 + 0.0090i -0.0319 - 0.0090i -0.0306 - 0.1483i
0.0001 -0.0141 + 0.0082i -0.0141 - 0.0082i -0.0937 - 0.0501i
0.0455 -0.0267 - 0.0406i -0.0267 + 0.0406i 0.0270 + 0.0047i
0.0226 -0.0300 - 0.0086i -0.0300 + 0.0086i -0.0301 - 0.0954i
0.0220 -0.0300 - 0.0054i -0.0300 + 0.0054i -0.0955 - 0.0689i
-0.0525 0.0266 + 0.0389i 0.0266 - 0.0389i -0.0260 - 0.0044i
-0.0146 0.0292 + 0.0067i 0.0292 - 0.0067i 0.0316 + 0.0892i
-0.0143 0.0288 + 0.0039i 0.0288 - 0.0039i 0.0908 + 0.0628i
1.0000 0.0225 + 0.1742i 0.0225 - 0.1742i -0.1000 - 0.0205i
0.3924 0.1381 + 0.1466i 0.1381 - 0.1466i -0.0071 + 0.6264i
0.3770 0.1648 + 0.1007i 0.1648 - 0.1007i 0.5863 + 0.4795i
-0.6850 1.0000 + 0.0000i 1.0000 - 0.0000i -0.4969 + 0.6801i
-0.0457 0.1212 - 0.1598i 0.1212 + 0.1598i 1.0000 - 0.0000i
-0.0377 0.0866 - 0.1393i 0.0866 + 0.1393i 0.7969 - 0.5753i
```

Columns 13 through 16

```
-0.0540 - 0.0129i -0.0246 - 0.0564i -0.0246 + 0.0564i -0.0835 + 0.0649i
0.1636 - 0.0506i -0.0485 + 0.2933i -0.0485 - 0.2933i -0.0763 + 0.0617i
-0.0269 + 0.0663i 0.0838 + 0.1458i 0.0838 + 0.1458i -0.0820 + 0.0649i
0.0133 - 0.0486i -0.0509 + 0.0302i -0.0509 - 0.0302i 1.0000 + 0.0000i
0.0411 + 0.1498i 0.2856 + 0.0111i 0.2856 - 0.0111i 0.9276 - 0.0174i
-0.0593 - 0.0263i -0.1491 - 0.0625i -0.1491 + 0.0625i 0.9885 - 0.0086i
0.0605 + 0.0444i -0.0158 - 0.0570i -0.0158 - 0.0570i 0.0004 - 0.0012i
-0.0306 + 0.1483i 0.1486 - 0.0106i 0.1486 + 0.0106i 0.0124 + 0.0046i
-0.0937 + 0.0501i -0.0440 - 0.1151i -0.0440 + 0.1151i -0.0001 + 0.0000i
0.0270 - 0.0047i 0.0004 + 0.0204i 0.0004 - 0.0204i 0.0006 - 0.0006i
-0.0301 + 0.0954i 0.0892 - 0.0335i 0.0892 + 0.0335i -0.0007 + 0.0004i
```

# Table C.3.9 (cont'd)

```
-0.0955 + 0.0689i -0.0257 - 0.1141i -0.0257 + 0.1141i 0.0000 - 0.0001i
-0.0260 + 0.0044i -0.0004 - 0.0197i -0.0004 + 0.0197i -0.0007 + 0.0006i
 0.0316 - 0.0892i -0.0835 + 0.0344i -0.0835 - 0.0344i 0.0007 - 0.0004i
 0.0908 - 0.0628i 0.0258 + 0.1070i 0.0258 - 0.1070i -0.0001 + 0.0001i
-0.1000 + 0.0205i -0.0026 - 0.0702i -0.0026 + 0.0702i 0.0125 + 0.0020i
-0.0071 - 0.6264i -0.5738 + 0.0293i -0.5738 - 0.0293i 0.0032 - 0.0024i
 0.5863 - 0.4795i 0.1343 + 0.6976i 0.1343 - 0.6976i 0.0011 + 0.0003i
-0.4969 - 0.6801i -0.5963 - 0.2115i -0.5963 + 0.2115i 0.2738 + 0.0046i
 1.0000 + 0.0000i 0.1495 + 0.9623i 0.1495 - 0.9623i -0.0781 - 0.0135i
 0.7969 + 0.5753i 1.0000 + 0.0000i 1.0000 - 0.0000i 0.0067 - 0.0002i
```

Columns 17 through 20

```
-0.0835 - 0.0649i 0.0416 - 0.3196i 0.0416 + 0.3196i 0.0085 - 0.0566i
-0.0763 - 0.0617i -0.1275 + 0.1600i -0.1275 - 0.1600i -0.1135 + 0.1795i
-0.0820 - 0.0649i -0.0664 + 0.6648i -0.0664 - 0.6648i 0.0474 - 0.0474i
 1.0000 - 0.0000i -0.4822 - 0.0145i -0.4822 + 0.0145i -0.0916 - 0.0178i
 0.9276 + 0.0174i 0.2572 + 0.1661i 0.2572 - 0.1661i 0.2844 + 0.1976i
 0.9885 + 0.0086i 1.0000 - 0.0000i 1.0000 + 0.0000i -0.0738 - 0.0806i
 0.0004 + 0.0012i 0.0227 + 0.0323i 0.0227 - 0.0323i 0.0047 + 0.0141i
 0.0124 - 0.0046i 0.0234 - 0.0898i 0.0234 + 0.0898i -0.1212 - 0.2016i
-0.0001 - 0.0000i -0.0251 - 0.0394i -0.0251 + 0.0394i 0.0205 + 0.0329i
 0.0006 + 0.0006i 0.0046 + 0.0104i 0.0046 - 0.0104i 0.0015 + 0.0022i
-0.0007 - 0.0004i 0.0233 - 0.0309i 0.0233 + 0.0309i -0.0134 - 0.0559i
 0.0000 + 0.0001i -0.0056 - 0.0444i -0.0056 + 0.0444i 0.0162 + 0.0138i
-0.0007 - 0.0006i -0.0043 - 0.0101i -0.0043 + 0.0101i -0.0014 - 0.0022i
 0.0007 + 0.0004i -0.0215 + 0.0296i -0.0215 - 0.0296i 0.0135 + 0.0524i
-0.0001 - 0.0001i 0.0050 + 0.0417i 0.0050 - 0.0417i -0.0150 - 0.0130i
 0.0125 - 0.0020i -0.0311 - 0.0301i -0.0311 + 0.0301i -0.0098 - 0.0063i
 0.0032 + 0.0024i -0.1684 + 0.1545i -0.1684 - 0.1545i 0.0280 + 0.3484i
 0.0011 - 0.0003i 0.0996 + 0.2641i 0.0996 - 0.2641i -0.1335 - 0.0633i
 0.2738 - 0.0046i -0.5212 + 0.0971i -0.5212 - 0.0971i -0.1351 + 0.0349i
-0.0781 + 0.0135i 0.4363 + 0.4168i 0.4363 - 0.4168i 1.0000 + 0.0000i
 0.0067 + 0.0002i 0.5844 + 0.0086i 0.5844 - 0.0086i -0.2542 + 0.1751i
```

Column 21

```
 0.0085 + 0.0566i
-0.1135 - 0.1795i
 0.0474 + 0.0474i
-0.0916 + 0.0178i
 0.2844 - 0.1976i
-0.0738 + 0.0806i
 0.0047 - 0.0141i
-0.1212 + 0.2016i
 0.0205 - 0.0329i
 0.0015 - 0.0022i
-0.0134 + 0.0559i
 0.0162 - 0.0138i
-0.0014 + 0.0022i
 0.0135 - 0.0524i
-0.0150 + 0.0130i
-0.0098 + 0.0063i
 0.0280 - 0.3484i
-0.1335 + 0.0633i
-0.1351 - 0.0349i
 1.0000 - 0.0000i
-0.2542 - 0.1751i
```

detjj =

   -2.3623e+31

detd =

   3.7768e+21

detda =

   -6.2547e+09

detad =

# Table C.3.9 (cont'd)

```
 9.6026e+28

condjj =

 1.5003e+06

condd =

 53.1719

condda =

 7.2324e+05

condad =

 1.7124e+07

vtt =

 -0.9917 0.0350 -0.2730
 1.0000 1.0000 -0.6262
 -0.0815 0.0113 1.0000

eigtt =

 -152.8097
 -815.9868
 -42.9767
```

# Table C.3.10 Output for dynamic/algebraic 110 MVar

eigjj =

```
-26.2872 +52.3729i
-26.2872 -52.3729i
 50.6961
 47.5341
 40.5593
-12.8396 +25.9208i
-12.8396 -25.9208i
-11.1220 +20.8626i
-11.1220 -20.8626i
 25.0429
 21.9409
 20.0631
-15.8216
-16.6102
-16.5899
 -5.6908 +14.7273i
 -5.6908 -14.7273i
 -4.2012 +15.0127i
 -4.2012 -15.0127i
 -4.0142 +14.9834i
 -4.0142 -14.9834i
 12.2529 +  0.9592i
 12.2529 -  0.9592i
  8.0054 +  0.9446i
  8.0054 -  0.9446i
  2.0161
 -0.5464 +  1.5682i
 -0.5464 -  1.5682i
  1.0013
 -0.2087 +  1.2467i
 -0.2087 -  1.2467i
 -0.1508 +  0.9724i
 -0.1508 -  0.9724i
  0.2476
  0.0631
 -0.0321 +  0.6675i
 -0.0321 -  0.6675i
  0.0216 +  0.6030i
  0.0216 -  0.6030i
```

eigd =

```
 50.6964
 47.5348
 40.5615
-12.6936 +26.0994i
-12.6936 -26.0994i
-10.9456 +20.8744i
-10.9456 -20.8744i
 -5.7720 +14.6953i
 -5.7720 -14.6953i
 25.0503
 21.9500
 20.0974
  1.2561
  2.2121
 12.4047 +  1.0780i
 12.4047 -  1.0780i
  8.0648 +  1.0261i
  8.0648 -  1.0261i
```

eigda =

```
-26.4541 +52.1825i
-26.4541 -52.1825i
 -3.9191 +14.9197i
 -3.9191 -14.9197i
 -4.0663 +14.9742i
 -4.0663 -14.9742i
-16.4498
-16.5413
-15.1337
 -0.3087 +  1.7447i
 -0.3087 -  1.7447i
 -0.0293 +  1.1227i
 -0.0293 -  1.1227i
 -0.1404 +  1.0285i
 -0.1404 -  1.0285i
 -0.0835 +  0.0646i
 -0.0835 -  0.0646i
 -0.0662 +  0.6691i
 -0.0662 -  0.6691i
 -0.0257 +  0.6150i
 -0.0257 -  0.6150i
```

eigad =

```
1.0e+03 *

-0.0517 + 1.1797i
-0.0517 - 1.1797i
-0.0426 + 0.4471i
-0.0426 - 0.4471i
 0.0828 + 0.0552i
 0.0828 - 0.0552i
-0.0027 + 0.0774i
-0.0027 - 0.0774i
 0.0508
 0.0448
 0.0355
 0.0300
 0.0000
 0.0124
 0.0058
 0.0069 + 0.0002i
 0.0069 - 0.0002i
 0.0145
```

vda =

Columns 1 through 4

```
0.0000 - 0.0000i  0.0000 + 0.0000i  0.0000 + 0.0000i  0.0000 - 0.0000i
0.0000 + 0.0000i  0.0000 - 0.0000i  0.0000 - 0.0000i  0.0000 + 0.0000i
0.0000 + 0.0000i  0.0000 - 0.0000i  0.0000 + 0.0000i  0.0000 - 0.0000i
0.0000 + 0.0000i  0.0000 - 0.0000i  0.0000 - 0.0000i  0.0000 + 0.0000i
0.0000 - 0.0000i  0.0000 + 0.0000i  0.0000 + 0.0000i  0.0000 - 0.0000i
```

# Table C.3.10 (cont'd)

```
0.0000 - 0.0000i  0.0000 + 0.0000i  0.0000 - 0.0000i  0.0000 + 0.0000i
-0.0002 + 0.0003i -0.0002 - 0.0003i  0.0000 + 0.0000i  0.0000 - 0.0000i
0.0000 + 0.0000i  0.0000 - 0.0000i -0.0013 + 0.0008i -0.0013 - 0.0008i
0.0000 + 0.0000i  0.0000 - 0.0000i  0.0000 + 0.0002i  0.0000 - 0.0002i
0.0001 + 0.0000i  0.0001 - 0.0000i  0.0000 + 0.0002i  0.0000 - 0.0002i
0.0000 + 0.0000i  0.0000 - 0.0000i  0.0000 + 0.0007i  0.0000 - 0.0007i
0.0000 + 0.0000i  0.0000 - 0.0000i  0.0002 + 0.0004i  0.0002 - 0.0004i
-0.0048 - 0.0105i -0.0048 + 0.0105i -0.0001 - 0.0002i -0.0001 + 0.0002i
0.0000 - 0.0000i  0.0000 + 0.0000i -0.0021 - 0.0305i -0.0021 + 0.0305i
0.0000 - 0.0000i  0.0000 + 0.0000i -0.0103 - 0.0039i -0.0103 + 0.0039i
1.0000 - 0.0000i  1.0000 + 0.0000i  0.0041 - 0.0011i  0.0041 + 0.0011i
0.0000 + 0.0003i  0.0000 - 0.0003i  1.0000 + 0.0001i  1.0000 - 0.0001i
0.0000 + 0.0004i  0.0000 - 0.0004i  0.1426 - 0.3302i  0.1426 + 0.3302i
-0.0763 - 0.1537i -0.0763 + 0.1537i -0.0013 - 0.0025i -0.0013 + 0.0025i
0.0000 - 0.0000i  0.0000 + 0.0000i -0.0288 - 0.1104i -0.0288 + 0.1104i
0.0000 - 0.0000i  0.0000 + 0.0000i -0.0342 - 0.0061i -0.0342 + 0.0061i


Columns 5 through 8

0.0000 + 0.0000i  0.0000 - 0.0000i  0.0000   0.0000
0.0000 + 0.0000i  0.0000 - 0.0000i  0.0000   0.0001
0.0000 - 0.0000i  0.0000 + 0.0000i  0.0000   0.0000
0.0000 + 0.0000i  0.0000 - 0.0000i  0.0000   0.0000
0.0000 - 0.0000i  0.0000 + 0.0000i  0.0000   0.0000
0.0000 + 0.0000i  0.0000 - 0.0000i  0.0000   0.0000
0.0000 + 0.0000i  0.0000 - 0.0000i -0.0004   0.0000
0.0000 - 0.0005i  0.0000 + 0.0005i  0.0012   0.0013
-0.0005 + 0.0003i -0.0005 - 0.0003i  0.0005  -0.0006
-0.0001 + 0.0001i -0.0001 - 0.0001i -0.0036  -0.0001
-0.0002 + 0.0001i -0.0002 - 0.0001i  0.0528   0.0566
-0.0002 + 0.0006i -0.0002 - 0.0006i  0.0573  -0.0571
0.0000 - 0.0001i  0.0000 + 0.0001i  0.0042   0.0001
0.0093 + 0.0036i  0.0093 - 0.0036i -0.0314  -0.0335
-0.0017 - 0.0305i -0.0017 + 0.0305i -0.0344   0.0341
0.0029 + 0.0011i  0.0029 - 0.0011i -0.0879  -0.0018
-0.1408 + 0.2936i -0.1408 - 0.2936i  0.9332   1.0000
1.0000 - 0.0000i  1.0000 + 0.0000i  1.0000  -0.9975
0.0003 - 0.0020i  0.0003 + 0.0020i  0.0553   0.0011
0.0363 + 0.0067i  0.0363 - 0.0067i -0.0999  -0.1065
-0.0228 - 0.0932i -0.0228 + 0.0932i -0.0922   0.0914


Columns 9 through 12

0.0000   0.0060 + 0.0015i  0.0060 - 0.0015i -0.0519 - 0.0152i
-0.0001 -0.0125 - 0.0067i -0.0125 + 0.0067i  0.1119 + 0.1130i
0.0000 -0.0029 + 0.0022i -0.0029 - 0.0022i  0.0118 - 0.0605i
0.0000  0.0002 - 0.0035i  0.0002 + 0.0035i -0.0123 + 0.0465i
0.0000 -0.0025 + 0.0076i -0.0025 - 0.0076i  0.0980 - 0.1022i
0.0000  0.0015 + 0.0014i  0.0015 - 0.0014i -0.0541 - 0.0091i
0.0049 -0.0177 - 0.0544i -0.0177 + 0.0544i  0.0294 + 0.0727i
0.0004 -0.0320 + 0.0093i -0.0320 - 0.0093i  0.0471 - 0.1446i
0.0001 -0.0145 + 0.0084i -0.0145 - 0.0084i -0.0468 - 0.0930i
0.0455 -0.0268 - 0.0405i -0.0268 + 0.0405i  0.0222 + 0.0193i
0.0227 -0.0304 - 0.0082i -0.0304 + 0.0082i  0.0227 - 0.0986i
0.0228 -0.0316 - 0.0051i -0.0316 + 0.0051i -0.0400 - 0.1150i
-0.0525 0.0266 + 0.0388i  0.0266 - 0.0388i -0.0215 - 0.0185i
-0.0147 0.0295 + 0.0064i  0.0295 - 0.0064i -0.0182 + 0.0939i
-0.0149 0.0302 + 0.0036i  0.0302 - 0.0036i  0.0393 + 0.1069i
1.0000  0.0234 + 0.1745i  0.0234 - 0.1745i -0.0803 - 0.0757i
0.3940  0.1419 + 0.1461i  0.1419 - 0.1461i -0.3317 + 0.5428i
0.3893  0.1791 + 0.0956i  0.1791 - 0.0956i  0.2500 + 0.7587i
-0.6854 1.0000 + 0.0000i  1.0000 - 0.0000i -0.8280 + 0.3359i
-0.0459 0.1206 - 0.1628i  0.1206 + 0.1628i  0.8532 + 0.5151i
-0.0391 0.0887 - 0.1473i  0.0887 + 0.1473i  1.0000 - 0.0000i


Columns 13 through 16

-0.0519 + 0.0152i -0.0177 - 0.0538i -0.0177 + 0.0538i -0.0835 + 0.0646i
0.1119 - 0.1130i -0.0766 + 0.2837i -0.0766 - 0.2837i -0.0764 + 0.0614i
0.0118 + 0.0605i  0.0948 - 0.1455i  0.0948 + 0.1455i -0.0820 + 0.0646i
-0.0123 - 0.0465i -0.0490 + 0.0239i -0.0490 - 0.0239i  1.0000 - 0.0000i
0.0980 + 0.1022i  0.2807 + 0.0362i  0.2807 - 0.0362i  0.9276 - 0.0173i
-0.0541 + 0.0091i -0.1513 - 0.0715i -0.1513 + 0.0715i  0.9888 - 0.0085i
0.0294 - 0.0727i -0.0168 + 0.0519i -0.0168 - 0.0519i  0.0004 - 0.0012i
0.0471 + 0.1446i  0.1383 + 0.0125i  0.1383 - 0.0125i  0.0124 + 0.0046i
-0.0468 + 0.0930i -0.0418 - 0.1143i -0.0418 + 0.1143i  0.0000 + 0.0000i
0.0222 - 0.0193i -0.0009 + 0.0188i -0.0009 - 0.0188i  0.0006 - 0.0006i
```

## Table C.3.10 (cont'd)

```
0.0227 + 0.0986i 0.0856 - 0.0208i 0.0856 + 0.0208i -0.0007 + 0.0004i
-0.0400 + 0.1150i -0.0250 - 0.1146i -0.0250 + 0.1146i 0.0000 - 0.0001i
-0.0215 + 0.0185i 0.0009 - 0.0181i 0.0009 + 0.0181i -0.0007 + 0.0006i
-0.0182 - 0.0939i -0.0805 + 0.0223i -0.0805 - 0.0223i 0.0007 - 0.0004i
0.0393 - 0.1069i 0.0247 + 0.1075i 0.0247 - 0.1075i -0.0001 + 0.0001i
-0.0803 + 0.0757i 0.0017 - 0.0643i 0.0017 + 0.0643i 0.0125 + 0.0020i
-0.3317 - 0.5428i -0.5277 - 0.0370i -0.5277 + 0.0370i 0.0032 - 0.0024i
0.2500 - 0.7587i 0.1750 + 0.6950i 0.1750 - 0.6950i 0.0015 + 0.0003i
-0.8280 - 0.3359i -0.5362 - 0.2267i -0.5362 + 0.2267i 0.2736 + 0.0046i
0.8532 - 0.5151i 0.0390 + 0.8981i 0.0390 - 0.8981i -0.0780 - 0.0133i
1.0000 + 0.0000i 1.0000 - 0.0000i 1.0000 + 0.0000i 0.0069 - 0.0001i
```

Columns 17 through 20

```
-0.0835 - 0.0646i 0.0471 - 0.3208i 0.0471 + 0.3208i 0.0076 - 0.0586i
-0.0764 - 0.0614i -0.1416 + 0.1554i -0.1416 - 0.1554i -0.1132 + 0.1806i
-0.0820 - 0.0646i -0.0662 + 0.6691i -0.0662 - 0.6691i 0.0492 - 0.0429i
1.0000 + 0.0000i -0.4816 - 0.0227i -0.4816 + 0.0227i -0.0946 - 0.0163i
0.9276 + 0.0173i 0.2507 + 0.1868i 0.2507 - 0.1868i 0.2855 + 0.1960i
0.9888 + 0.0085i 1.0000 - 0.0000i 1.0000 + 0.0000i -0.0663 - 0.0827i
0.0004 + 0.0012i 0.0210 + 0.0325i 0.0210 - 0.0325i 0.0051 + 0.0143i
0.0124 - 0.0046i 0.0369 - 0.0966i 0.0369 + 0.0966i -0.1202 - 0.2003i
0.0000 - 0.0000i -0.0199 - 0.0365i -0.0199 + 0.0365i 0.0187 + 0.0311i
0.0006 + 0.0006i 0.0044 + 0.0106i 0.0044 - 0.0106i 0.0016 + 0.0023i
-0.0007 - 0.0004i 0.0281 - 0.0311i 0.0281 + 0.0311i -0.0134 - 0.0561i
0.0000 + 0.0001i -0.0039 - 0.0432i -0.0039 + 0.0432i 0.0156 + 0.0131i
-0.0007 - 0.0006i -0.0041 - 0.0103i -0.0041 + 0.0103i -0.0015 - 0.0022i
0.0007 + 0.0004i -0.0259 + 0.0299i -0.0259 - 0.0299i 0.0135 + 0.0526i
-0.0001 - 0.0001i 0.0032 + 0.0404i 0.0032 - 0.0404i -0.0143 - 0.0124i
0.0125 - 0.0020i -0.0305 - 0.0312i -0.0305 + 0.0312i -0.0102 - 0.0063i
0.0032 + 0.0024i -0.1963 + 0.1507i -0.1963 - 0.1507i 0.0278 + 0.3497i
0.0015 - 0.0003i 0.1112 + 0.2607i 0.1112 - 0.2607i -0.1386 - 0.0528i
0.2736 - 0.0046i -0.5249 + 0.0814i -0.5249 - 0.0814i -0.1381 + 0.0382i
-0.0780 + 0.0133i 0.4276 + 0.4885i 0.4276 - 0.4885i 1.0000 + 0.0000i
0.0069 + 0.0001i 0.5601 + 0.0329i 0.5601 - 0.0329i -0.2420 + 0.1663i
```

Column 21

```
0.0076 + 0.0586i
-0.1132 - 0.1806i
0.0492 + 0.0429i
-0.0946 + 0.0163i
0.2855 - 0.1960i
-0.0663 + 0.0827i
0.0051 - 0.0143i
-0.1202 + 0.2003i
0.0187 - 0.0311i
0.0016 - 0.0023i
-0.0134 + 0.0561i
0.0156 - 0.0131i
-0.0015 + 0.0022i
0.0135 - 0.0526i
-0.0143 + 0.0124i
-0.0102 + 0.0063i
0.0278 - 0.3497i
-0.1386 + 0.0528i
-0.1381 - 0.0382i
1.0000 - 0.0000i
-0.2420 - 0.1663i
```

detjj =

-2.3599e+31

detd =

3.5874e+21

detda =

-6.5782e+09

detad =

# Table C.3.10 (cont'd)

```
5.6399e+28

condjj =
 1.5064e+06

condd =
 52.5824

condda =
 7.2616e+05

condad =
 1.3045e+07

vtt =
 1.0000 0.0359 -0.2668
 -0.9899 1.0000 -0.6454
 0.0652 0.0097 1.0000

eigtt =
 -151.3925
 -803.2924
 -36.6830
```

## Table C.3.11 Output for dynamic/algebraic 120 MVar

eigjj =

```
-26.2895 +52.3740i
-26.2895 -52.3740i
 50.6033
 47.4511
 40.5218
-12.8088 +25.8672i
-12.8088 -25.8672i
-11.0249 +20.5866i
-11.0249 -20.5866i
 25.0234
 21.9046
 19.8396
-15.8215
-16.6097
-16.5882
 -5.6860 +14.6432i
 -5.6860 -14.6432i
 -4.2433 +15.0329i
 -4.2433 -15.0329i
 -4.0178 +14.9802i
 -4.0178 -14.9802i
 12.2312 + 0.9558i
 12.2312 - 0.9558i
  7.9789 + 0.9153i
  7.9789 - 0.9153i
  2.0248
 -0.5480 + 1.5695i
 -0.5480 - 1.5695i
  1.0022
 -0.2103 + 1.2488i
 -0.2103 - 1.2488i
 -0.1604 + 0.9830i
 -0.1604 - 0.9830i
  0.2476
  0.0626
 -0.0304 + 0.6716i
 -0.0304 - 0.6716i
  0.0202 + 0.6050i
  0.0202 - 0.6050i
```

eigd =

```
 50.6035
 47.4517
 40.5241
-12.6620 +26.0486i
-12.6620 -26.0486i
-10.8491 +20.5961i
-10.8491 -20.5961i
 -5.7734 +14.6215i
 -5.7734 -14.6215i
 25.0307
 21.9129
 19.8742
  1.2392
  2.2303
 12.3822 + 1.0736i
 12.3822 - 1.0736i
  8.0390 + 1.0014i
  8.0390 - 1.0014i
```

eigda =

```
-26.4567 +52.1834i
-26.4567 -52.1834i
 -3.9179 +14.9206i
 -3.9179 -14.9206i
 -4.1042 +14.9738i
 -4.1042 -14.9738i
-16.4432
-16.5388
-15.1296
 -0.3014 + 1.7477i
 -0.3014 - 1.7477i
 -0.0251 + 1.1456i
 -0.0251 - 1.1456i
 -0.1518 + 1.0259i
 -0.1518 - 1.0259i
 -0.0835 + 0.0642i
 -0.0835 - 0.0642i
 -0.0659 + 0.6726i
 -0.0659 - 0.6726i
 -0.0245 + 0.6175i
 -0.0245 - 0.6175i
```

eigad =

1.0e+03 *

```
-0.0514 + 1.0259i
-0.0514 - 1.0259i
-0.0417 + 0.4465i
-0.0417 - 0.4465i
 0.0854 + 0.0475i
 0.0854 - 0.0475i
-0.0062 + 0.0706i
-0.0062 - 0.0706i
 0.0508
 0.0447
 0.0355
 0.0294
 0.0000
 0.0124
 0.0058
 0.0069 + 0.0002i
 0.0069 - 0.0002i
 0.0145
```

vda =

Columns 1 through 4

```
0.0000 - 0.0000i 0.0000 + 0.0000i 0.0000 + 0.0000i 0.0000 - 0.0000i
0.0000 + 0.0000i 0.0000 - 0.0000i 0.0000 - 0.0000i 0.0000 + 0.0000i
0.0000 + 0.0000i 0.0000 - 0.0000i 0.0000 - 0.0000i 0.0000 - 0.0000i
0.0000 + 0.0000i 0.0000 - 0.0000i 0.0000 - 0.0000i 0.0000 + 0.0000i
0.0000 - 0.0000i 0.0000 + 0.0000i 0.0000 + 0.0000i 0.0000 - 0.0000i
```

## Table C.3.11 (cont'd)

```
0.0000 - 0.0000i 0.0000 + 0.0000i 0.0000 - 0.0000i 0.0000 + 0.0000i
-0.0002 + 0.0003i -0.0002 - 0.0003i 0.0000 + 0.0000i 0.0000 - 0.0000i
0.0000 + 0.0000i 0.0000 - 0.0000i -0.0013 + 0.0008i -0.0013 - 0.0008i
0.0000 + 0.0000i 0.0000 - 0.0000i 0.0000 + 0.0002i 0.0000 - 0.0002i
0.0001 + 0.0000i 0.0001 - 0.0000i 0.0000 + 0.0002i 0.0000 - 0.0002i
0.0000 + 0.0000i 0.0000 - 0.0000i 0.0000 + 0.0007i 0.0000 - 0.0007i
0.0000 + 0.0000i 0.0000 - 0.0000i 0.0002 + 0.0004i 0.0002 - 0.0004i
-0.0048 - 0.0105i -0.0048 + 0.0105i -0.0001 - 0.0002i -0.0001 + 0.0002i
0.0000 - 0.0000i 0.0000 + 0.0000i -0.0021 - 0.0305i -0.0021 + 0.0305i
0.0000 - 0.0000i 0.0000 + 0.0000i -0.0091 - 0.0030i -0.0091 + 0.0030i
1.0000 - 0.0000i 1.0000 + 0.0000i 0.0041 - 0.0011i 0.0041 + 0.0011i
0.0000 + 0.0003i 0.0000 - 0.0003i 1.0000 + 0.0000i 1.0000 - 0.0000i
0.0000 + 0.0004i 0.0000 - 0.0004i 0.1095 - 0.2914i 0.1095 + 0.2914i
-0.0763 - 0.1537i -0.0763 + 0.1537i -0.0013 - 0.0024i -0.0013 + 0.0024i
0.0000 - 0.0000i 0.0000 + 0.0000i -0.0288 - 0.1104i -0.0288 + 0.1104i
0.0000 - 0.0000i 0.0000 + 0.0000i -0.0298 - 0.0040i -0.0298 + 0.0040i
```

Columns 5 through 8

```
0.0000 + 0.0000i 0.0000 - 0.0000i 0.0000 0.0000
0.0000 + 0.0000i 0.0000 - 0.0000i 0.0000 0.0001
0.0000 - 0.0000i 0.0000 + 0.0000i 0.0000 0.0000
0.0000 + 0.0000i 0.0000 - 0.0000i 0.0000 0.0000
0.0000 - 0.0000i 0.0000 + 0.0000i 0.0000 0.0000
0.0000 + 0.0000i 0.0000 - 0.0000i 0.0000 0.0000
0.0000 + 0.0000i 0.0000 - 0.0000i -0.0004 0.0000
0.0000 - 0.0004i 0.0000 + 0.0004i 0.0011 0.0013
-0.0005 + 0.0003i -0.0005 - 0.0003i 0.0005 -0.0005
-0.0001 + 0.0001i -0.0001 - 0.0001i -0.0035 -0.0001
-0.0002 + 0.0001i -0.0002 - 0.0001i 0.0486 0.0566
-0.0002 + 0.0006i -0.0002 - 0.0006i 0.0575 -0.0538
0.0000 - 0.0001i 0.0000 + 0.0001i 0.0041 0.0002
0.0079 + 0.0026i 0.0079 - 0.0026i -0.0289 -0.0335
-0.0016 - 0.0306i -0.0016 + 0.0306i -0.0346 0.0322
0.0031 + 0.0010i 0.0031 - 0.0010i -0.0868 -0.0036
-0.1078 + 0.2530i -0.1078 - 0.2530i 0.8578 1.0000
1.0000 - 0.0000i 1.0000 + 0.0000i 1.0000 -0.9370
0.0001 - 0.0021i 0.0001 + 0.0021i 0.0546 0.0023
0.0309 + 0.0042i 0.0309 - 0.0042i -0.0919 -0.1065
-0.0226 - 0.0934i -0.0226 + 0.0934i -0.0927 0.0863
```

Columns 9 through 12

```
0.0000 0.0061 + 0.0016i 0.0061 - 0.0016i -0.0505 - 0.0091i
-0.0001 -0.0125 - 0.0067i -0.0125 + 0.0067i 0.1147 + 0.0866i
0.0000 -0.0028 + 0.0019i -0.0028 - 0.0019i 0.0080 - 0.0500i
0.0000 0.0003 - 0.0035i 0.0003 + 0.0035i -0.0070 + 0.0442i
0.0000 -0.0025 + 0.0076i -0.0025 - 0.0076i 0.0734 - 0.1017i
0.0000 0.0013 + 0.0014i 0.0013 - 0.0014i -0.0438 - 0.0060i
0.0049 -0.0174 - 0.0543i -0.0174 + 0.0543i 0.0354 + 0.0720i
0.0004 -0.0321 + 0.0096i -0.0321 - 0.0096i 0.0309 - 0.1450i
0.0001 -0.0150 + 0.0086i -0.0150 - 0.0086i -0.0456 - 0.0891i
0.0456 -0.0269 - 0.0403i -0.0269 + 0.0403i 0.0250 + 0.0184i
0.0228 -0.0309 - 0.0078i -0.0309 + 0.0078i 0.0134 - 0.0986i
0.0238 -0.0336 - 0.0047i -0.0336 + 0.0047i -0.0423 - 0.1166i
-0.0525 0.0267 + 0.0386i 0.0267 - 0.0386i -0.0241 - 0.0176i
-0.0148 0.0300 + 0.0060i 0.0300 - 0.0060i -0.0094 + 0.0937i
-0.0156 0.0321 + 0.0032i 0.0321 - 0.0032i 0.0410 + 0.1082i
1.0000 0.0246 + 0.1748i 0.0246 - 0:1748i -0.0904 - 0.0743i
0.3958 0.1465 + 0.1456i 0.1465 - 0.1456i -0.2808 + 0.5623i
0.4052 0.1971 + 0.0898i 0.1971 - 0.0898i 0.3066 + 0.7742i
-0.6858 1.0000 + 0.0000i 1.0000 - 0.0000i -0.8351 + 0.4082i
-0.0461 0.1201 - 0.1665i 0.1201 + 0.1665i 0.8638 + 0.4303i
-0.0409 0.0920 - 0.1576i 0.0920 + 0.1576i 1.0000 - 0.0000i
```

Columns 13 through 16

```
-0.0505 + 0.0091i -0.0107 - 0.0504i -0.0107 + 0.0504i -0.0835 + 0.0642i
0.1147 - 0.0866i -0.1037 + 0.2694i -0.1037 - 0.2694i -0.0764 + 0.0610i
0.0080 + 0.0500i 0.1050 - 0.1426i 0.1050 + 0.1426i -0.0821 + 0.0642i
-0.0070 - 0.0442i -0.0466 + 0.0174i -0.0466 - 0.0174i 1.0000 - 0.0000i
0.0734 + 0.1017i 0.2716 + 0.0609i 0.2716 - 0.0609i 0.9276 - 0.0172i
-0.0438 + 0.0060i -0.1508 - 0.0800i -0.1508 + 0.0800i 0.9891 - 0.0084i
0.0354 - 0.0720i -0.0172 + 0.0466i -0.0172 - 0.0466i 0.0004 - 0.0012i
0.0309 + 0.1450i 0.1256 + 0.0349i 0.1256 - 0.0349i 0.0124 + 0.0045i
-0.0456 + 0.0891i -0.0393 - 0.1132i -0.0393 + 0.1132i 0.0000 + 0.0000i
0.0250 - 0.0184i -0.0020 + 0.0171i -0.0020 - 0.0171i 0.0006 - 0.0006i
0.0134 + 0.0986i 0.0805 - 0.0082i 0.0805 + 0.0082i -0.0007 + 0.0004i
```

## Table C.3.11 (cont'd)

```
-0.0423 + 0.1166i -0.0244 - 0.1152i -0.0244 + 0.1152i 0.0000 - 0.0001i
-0.0241 + 0.0176i 0.0020 - 0.0165i 0.0020 + 0.0165i -0.0007 + 0.0006i
-0.0094 - 0.0937i -0.0761 + 0.0101i -0.0761 - 0.0101i 0.0007 - 0.0004i
0.0410 - 0.1082i 0.0237 + 0.1080i 0.0237 - 0.1080i -0.0001 + 0.0001i
-0.0904 + 0.0743i 0.0053 - 0.0581i 0.0053 + 0.0581i 0.0127 + 0.0020i
-0.2808 - 0.5623i -0.4738 - 0.0998i -0.4738 + 0.0998i 0.0031 - 0.0024i
0.3066 - 0.7742i 0.2210 + 0.6933i 0.2210 - 0.6933i 0.0019 + 0.0003i
-0.8351 - 0.4082i -0.4757 + 0.2351i -0.4757 + 0.2351i 0.2734 + 0.0046i
0.8638 - 0.4303i -0.0688 + 0.8209i -0.0688 - 0.8209i -0.0777 - 0.0131i
1.0000 + 0.0000i 1.0000 + 0.0000i 1.0000 - 0.0000i 0.0072 - 0.0001i
```

Columns 17 through 20

```
-0.0835 - 0.0642i 0.0518 - 0.3214i 0.0518 + 0.3214i 0.0068 - 0.0606i
-0.0764 - 0.0610i -0.1538 + 0.1507i -0.1538 - 0.1507i -0.1132 + 0.1821i
-0.0821 - 0.0642i -0.0659 + 0.6726i -0.0659 - 0.6726i 0.0508 - 0.0389i
1.0000 + 0.0000i -0.4808 - 0.0299i -0.4808 + 0.0299i -0.0975 - 0.0149i
0.9276 + 0.0172i 0.2441 + 0.2047i 0.2441 - 0.2047i 0.2871 + 0.1948i
0.9891 + 0.0084i 1.0000 + 0.0000i 1.0000 - 0.0000i -0.0596 - 0.0846i
0.0004 + 0.0012i 0.0194 + 0.0326i 0.0194 - 0.0326i 0.0055 + 0.0146i
0.0124 - 0.0045i 0.0482 - 0.1019i 0.0482 + 0.1019i -0.1191 - 0.1988i
0.0000 - 0.0000i -0.0149 - 0.0340i -0.0149 + 0.0340i 0.0170 + 0.0294i
0.0006 + 0.0006i 0.0041 + 0.0108i 0.0041 - 0.0108i 0.0017 + 0.0023i
-0.0007 - 0.0004i 0.0321 - 0.0312i 0.0321 + 0.0312i -0.0134 - 0.0564i
0.0000 + 0.0001i -0.0022 - 0.0423i -0.0022 + 0.0423i 0.0150 + 0.0125i
-0.0007 - 0.0006i -0.0038 - 0.0105i -0.0038 + 0.0105i -0.0016 - 0.0022i
0.0007 + 0.0004i -0.0297 + 0.0300i -0.0297 - 0.0300i 0.0135 + 0.0528i
-0.0001 - 0.0001i 0.0013 + 0.0395i 0.0013 - 0.0395i -0.0136 - 0.0119i
0.0127 - 0.0020i -0.0299 - 0.0322i -0.0299 + 0.0322i -0.0106 - 0.0064i
0.0031 + 0.0024i -0.2198 + 0.1469i -0.2198 - 0.1469i 0.0275 + 0.3511i
0.0019 - 0.0003i 0.1249 + 0.2620i 0.1249 - 0.2620i -0.1443 - 0.0420i
0.2734 - 0.0046i -0.5272 + 0.0667i -0.5272 - 0.0667i -0.1415 + 0.0412i
-0.0777 + 0.0131i 0.4185 + 0.5486i 0.4185 - 0.5486i 1.0000 - 0.0000i
0.0072 + 0.0001i 0.5413 + 0.0574i 0.5413 - 0.0574i -0.2298 + 0.1584i
```

Column 21

```
0.0068 + 0.0606i
-0.1132 - 0.1821i
0.0508 + 0.0389i
-0.0975 + 0.0149i
0.2871 - 0.1948i
-0.0596 + 0.0846i
0.0055 - 0.0146i
-0.1191 + 0.1988i
0.0170 - 0.0294i
0.0017 - 0.0023i
-0.0134 + 0.0564i
0.0150 - 0.0125i
-0.0016 + 0.0022i
0.0135 - 0.0528i
-0.0136 + 0.0119i
-0.0106 + 0.0064i
0.0275 - 0.3511i
-0.1443 + 0.0420i
-0.1415 - 0.0412i
1.0000 + 0.0000i
-0.2298 - 0.1584i
```

detjj =

-2.3191e+31

detd =

3.3387e+21

detda =

-6.9461e+09

detad =

3.3012e+28

# Table C.3.11 (cont'd)

```
condjj =

 1.5133e+06


condd =

 52.0531


condda =

 7.2942e+05


condad =

 9.9080e+06


vtt =

 1.0000 0.0370 -0.2646
 -0.9762 1.0000 -0.6620
 0.0539 0.0086 1.0000


eigtt =

 -149.7845
 -786.6969
 -31.9402
```

## Table C.3.12 Output for dynamic/algebraic 135 MVar (with exciter)

eigjj =

```
-26.3100 +52.3837i
-26.3100 -52.3837i
49.8143
46.7068
40.1863
-12.6240 +25.5431i
-12.6240 -25.5431i
24.8738
-10.0765 +18.6717i
-10.0765 -18.6717i
21.6456
-16.6080
-15.8202
-16.5817
-5.7156 +13.8081i
-5.7156 -13.8081i
-4.2625 +15.1042i
-4.2625 -15.1042i
-4.0018 +14.9819i
-4.0018 -14.9819i
17.6120
12.0060 + 0.8553i
12.0060 - 0.8553i
7.6532 + 0.7923i
7.6532 - 0.7923i
2.0066
-0.5653 + 1.5718i
-0.5653 - 1.5718i
0.9580
-0.2299 + 1.2577i
-0.2299 - 1.2577i
-0.2269 + 1.0460i
-0.2269 - 1.0460i
0.2525
0.0611
-0.0376 + 0.6607i
-0.0376 - 0.6607i
0.0137 + 0.6165i
0.0137 - 0.6165i
```

eigd =

```
49.8143
46.7072
-12.4724 +25.7372i
-12.4724 -25.7372i
40.1889
-9.9252 +18.6740i
-9.9252 -18.6740i
-5.7988 +13.8735i
-5.7988 -13.8735i
24.8799
21.6507
17.6370
1.1086
2.1907
12.1502 + 0.9725i
12.1502 - 0.9725i
7.7099 + 0.8899i
7.7099 - 0.8899i
```

eigda =

```
-26.4792 +52.1911i
-26.4792 -52.1911i
-3.9388 +14.9116i
-3.9388 -14.9116i
-4.0725 +14.9177i
-4.0725 -14.9177i
-16.5262
-16.3923
-15.0917
-0.2489 + 1.7974i
-0.2489 - 1.7974i
-0.0627 + 1.2692i
-0.0627 - 1.2692i
-0.2073 + 1.0284i
-0.2073 - 1.0284i
-0.0835 + 0.0628i
-0.0835 - 0.0628i
-0.0673 + 0.6597i
-0.0673 - 0.6597i
-0.0173 + 0.6302i
-0.0173 - 0.6302i
```

eigad =

1.0e+02 *

```
-0.4740 + 5.5650i
-0.4740 - 5.5650i
-0.4325 + 4.2767i
-0.4325 - 4.2767i
0.8529 + 0.3876i
0.8529 - 0.3876i
-0.0792 + 0.6333i
-0.0792 - 0.6333i
0.5003
0.4420
0.3508
0.2733
0.0003
0.0726
0.1229
0.0628
0.1413
0.0576
```

vda =

Columns 1 through 4

```
0.0000 - 0.0000i 0.0000 + 0.0000i 0.0000 + 0.0000i 0.0000 - 0.0000i
0.0000 + 0.0000i 0.0000 - 0.0000i 0.0000 - 0.0000i 0.0000 + 0.0000i
0.0000 + 0.0000i 0.0000 - 0.0000i 0.0000 + 0.0000i 0.0000 - 0.0000i
0.0000 + 0.0000i 0.0000 - 0.0000i 0.0000 - 0.0000i 0.0000 + 0.0000i
0.0000 - 0.0000i 0.0000 + 0.0000i 0.0000 + 0.0000i 0.0000 - 0.0000i
```

## Table C.3.12 (cont'd)

```
0.0000 - 0.0000i 0.0000 + 0.0000i 0.0000 - 0.0000i 0.0000 + 0.0000i
-0.0002 + 0.0003i -0.0002 - 0.0003i 0.0000 - 0.0000i 0.0000 - 0.0000i
0.0000 + 0.0000i 0.0000 - 0.0000i -0.0012 + 0.0007i -0.0012 - 0.0007i
0.0000 + 0.0000i 0.0000 - 0.0000i 0.0002 + 0.0004i 0.0002 - 0.0004i
0.0001 + 0.0000i 0.0001 - 0.0000i 0.0001 + 0.0002i 0.0001 - 0.0002i
0.0000 + 0.0000i 0.0000 - 0.0000i 0.0000 + 0.0007i 0.0000 - 0.0007i
0.0000 + 0.0000i 0.0000 - 0.0000i 0.0005 + 0.0005i 0.0005 - 0.0005i
-0.0048 - 0.0105i -0.0048 + 0.0105i -0.0001 - 0.0002i -0.0001 + 0.0002i
0.0000 - 0.0000i 0.0000 + 0.0000i -0.0022 - 0.0305i -0.0022 + 0.0305i
0.0000 - 0.0000i 0.0000 + 0.0000i -0.0171 - 0.0012i -0.0171 + 0.0012i
1.0000 + 0.0000i 1.0000 - 0.0000i 0.0043 - 0.0023i 0.0043 + 0.0023i
0.0000 + 0.0004i 0.0000 - 0.0004i 1.0000 - 0.0000i 1.0000 + 0.0000i
0.0000 + 0.0005i 0.0000 - 0.0005i 0.0639 - 0.5523i 0.0639 + 0.5523i
-0.0763 - 0.1538i -0.0763 + 0.1538i -0.0021 - 0.0024i -0.0021 + 0.0024i
0.0000 - 0.0000i 0.0000 + 0.0000i -0.0289 - 0.1104i -0.0289 + 0.1104i
0.0000 - 0.0000i 0.0000 + 0.0000i -0.0534 + 0.0061i -0.0534 - 0.0061i
```

Columns 5 through 8

```
0.0000 + 0.0000i 0.0000 - 0.0000i 0.0000 0.0000
0.0000 - 0.0000i 0.0000 + 0.0000i 0.0000 0.0000
0.0000 - 0.0000i 0.0000 + 0.0000i 0.0000 0.0000
0.0000 + 0.0000i 0.0000 - 0.0000i 0.0000 0.0000
0.0000 - 0.0000i 0.0000 + 0.0000i 0.0000 0.0000
0.0000 + 0.0000i 0.0000 - 0.0000i 0.0000 0.0000
0.0000 + 0.0000i 0.0000 - 0.0000i -0.0001 -0.0003
-0.0002 - 0.0005i -0.0002 + 0.0005i 0.0013 0.0006
-0.0006 + 0.0003i -0.0006 - 0.0003i -0.0004 0.0006
-0.0001 + 0.0002i -0.0001 - 0.0002i -0.0005 -0.0034
-0.0003 + 0.0002i -0.0003 - 0.0002i 0.0566 0.0290
-0.0003 + 0.0009i -0.0003 - 0.0009i -0.0416 0.0575
0.0001 - 0.0002i 0.0001 + 0.0002i 0.0006 0.0039
0.0118 + 0.0009i 0.0118 - 0.0009i -0.0335 -0.0173
-0.0016 - 0.0307i -0.0016 + 0.0307i 0.0249 -0.0348
0.0038 + 0.0016i 0.0038 - 0.0016i -0.0123 -0.0818
-0.0607 + 0.3809i -0.0607 - 0.3809i 1.0000 0.5111
1.0000 + 0.0000i 1.0000 - 0.0000i -0.7236 1.0000
0.0004 - 0.0027i 0.0004 + 0.0027i 0.0077 0.0518
0.0437 - 0.0047i 0.0437 + 0.0047i -0.1066 -0.0549
-0.0226 - 0.0938i -0.0226 + 0.0938i 0.0667 -0.0930
```

Columns 9 through 12

```
0.0000 0.0057 + 0.0027i 0.0057 - 0.0027i 0.0335 + 0.0104i
-0.0001 -0.0126 - 0.0063i -0.0126 + 0.0063i -0.0685 - 0.0346i
0.0000 -0.0018 - 0.0012i -0.0018 + 0.0012i -0.0139 + 0.0006i
0.0000 0.0010 - 0.0033i 0.0010 + 0.0033i 0.0069 - 0.0267i
0.0000 -0.0025 + 0.0074i -0.0025 - 0.0074i -0.0245 + 0.0552i
0.0000 -0.0005 + 0.0011i -0.0005 - 0.0011i 0.0010 + 0.0109i
0.0049 -0.0151 - 0.0526i -0.0151 + 0.0526i -0.0056 - 0.0791i
0.0004 -0.0336 + 0.0115i -0.0336 - 0.0115i -0.0361 + 0.0976i
0.0003 -0.0219 + 0.0072i -0.0219 - 0.0072i -0.0190 + 0.0775i
0.0459 -0.0281 - 0.0393i -0.0281 + 0.0393i -0.0177 - 0.0320i
0.0238 -0.0357 - 0.0063i -0.0357 + 0.0063i -0.0287 + 0.0673i
0.0337 -0.0554 - 0.0069i -0.0554 + 0.0069i -0.0375 + 0.1191i
-0.0528 0.0278 + 0.0375i 0.0278 - 0.0375i 0.0172 + 0.0307i
-0.0154 0.0345 + 0.0041i 0.0345 - 0.0041i 0.0247 - 0.0648i
-0.0221 0.0528 + 0.0043i 0.0528 - 0.0043i 0.0328 - 0.1122i
1.0000 0.0341 + 0.1797i 0.0341 - 0.1797i 0.0527 + 0.1269i
0.4123 0.1829 + 0.1559i 0.1829 - 0.1559i 0.3224 - 0.3348i
0.5742 0.3350 + 0.1496i 0.3350 - 0.1496i 0.2787 - 0.7770i
-0.6895 1.0000 + 0.0000i 1.0000 - 0.0000i 1.0000 + 0.0000i
-0.0482 0.1288 - 0.1947i 0.1288 + 0.1947i -0.4753 - 0.4346i
-0.0581 0.1559 - 0.2559i 0.1559 + 0.2559i -0.7219 - 0.5615i
```

Columns 13 through 16

```
0.0335 - 0.0104i 0.0211 - 0.0267i 0.0211 + 0.0267i -0.0835 + 0.0628i
-0.0685 + 0.0346i -0.1993 + 0.1336i -0.1993 - 0.1336i -0.0764 + 0.0596i
-0.0139 - 0.0006i 0.1286 - 0.0784i 0.1286 + 0.0784i -0.0824 + 0.0631i
0.0069 + 0.0267i -0.0290 - 0.0147i -0.0290 + 0.0147i 1.0000 + 0.0000i
-0.0245 - 0.0552i 0.1624 + 0.1611i 0.1624 - 0.1611i 0.9273 - 0.0166i
0.0010 - 0.0109i -0.0975 - 0.1054i -0.0975 + 0.1054i 0.9930 - 0.0083i
-0.0056 + 0.0791i -0.0090 + 0.0224i -0.0090 - 0.0224i 0.0005 - 0.0011i
-0.0361 - 0.0976i 0.0356 - 0.1141i 0.0356 + 0.1141i 0.0120 + 0.0041i
-0.0190 - 0.0775i -0.0205 - 0.1111i -0.0205 + 0.1111i 0.0004 - 0.0000i
-0.0177 + 0.0320i -0.0031 + 0.0086i -0.0031 - 0.0086i 0.0006 - 0.0006i
-0.0287 - 0.0673i 0.0347 + 0.0435i 0.0347 - 0.0435i -0.0007 + 0.0004i
```

# Table C.3.12 (cont'd)

```
-0.0375 - 0.1191i -0.0197 - 0.1193i -0.0197 + 0.1193i 0.0001 - 0.0001i
0.0172 - 0.0307i 0.0030 - 0.0083i 0.0030 + 0.0083i -0.0007 + 0.0006i
0.0247 + 0.0648i -0.0342 - 0.0403i -0.0342 + 0.0403i 0.0006 - 0.0004i
0.0328 + 0.1122i 0.0194 + 0.1122i 0.0194 - 0.1122i -0.0001 + 0.0001i
0.0527 - 0.1269i 0.0085 - 0.0286i 0.0085 + 0.0286i 0.0137 + 0.0019i
0.3224 + 0.3348i -0.1158 - 0.3057i -0.1158 + 0.3057i 0.0027 - 0.0023i
0.2787 + 0.7770i 0.1834 + 0.6950i 0.1834 - 0.6950i 0.0030 + 0.0004i
1.0000 - 0.0000i -0.2172 - 0.1637i -0.2172 + 0.1637i 0.2706 + 0.0045i
-0.4753 + 0.4346i -0.4745 + 0.2800i -0.4745 - 0.2800i -0.0748 - 0.0116i
-0.7219 + 0.5615i 1.0000 + 0.0000i 1.0000 - 0.0000i 0.0112 - 0.0001i

Columns 17 through 20

-0.0835 - 0.0628i 0.0483 - 0.3198i 0.0483 + 0.3198i 0.0063 - 0.0624i
-0.0764 - 0.0596i -0.1461 + 0.1605i -0.1461 - 0.1605i -0.1195 + 0.1921i
-0.0824 - 0.0631i -0.0673 + 0.6597i -0.0673 - 0.6597i 0.0577 - 0.0438i
1.0000 - 0.0000i -0.4871 - 0.0235i -0.4871 + 0.0235i -0.0986 - 0.0127i
0.9273 + 0.0166i 0.2631 + 0.1946i 0.2631 - 0.1946i 0.2994 + 0.1979i
0.9930 + 0.0083i 1.0000 - 0.0000i 1.0000 + 0.0000i -0.0669 - 0.0934i
0.0005 + 0.0011i 0.0187 + 0.0322i 0.0187 - 0.0322i 0.0063 + 0.0152i
0.0120 - 0.0041i 0.0092 - 0.0988i 0.0092 + 0.0988i -0.1120 - 0.1906i
0.0004 + 0.0000i 0.0105 - 0.0311i 0.0105 + 0.0311i 0.0110 + 0.0272i
0.0006 + 0.0006i 0.0039 + 0.0103i 0.0039 - 0.0103i 0.0018 + 0.0025i
-0.0007 - 0.0004i 0.0218 - 0.0335i 0.0218 + 0.0335i -0.0132 - 0.0577i
0.0001 + 0.0001i 0.0078 - 0.0502i 0.0078 + 0.0502i 0.0125 + 0.0124i
-0.0007 - 0.0006i -0.0036 - 0.0100i -0.0036 + 0.0100i -0.0017 - 0.0024i
0.0006 + 0.0004i -0.0200 + 0.0320i -0.0200 - 0.0320i 0.0134 + 0.0541i
-0.0001 - 0.0001i -0.0082 + 0.0468i -0.0082 - 0.0468i -0.0113 - 0.0117i
0.0137 - 0.0019i -0.0311 - 0.0302i -0.0311 + 0.0302i -0.0119 - 0.0065i
0.0027 + 0.0023i -0.1602 + 0.1730i -0.1602 - 0.1730i 0.0268 + 0.3583i
0.0030 - 0.0004i 0.0874 + 0.3385i 0.0874 - 0.3385i -0.1240 - 0.0496i
0.2706 - 0.0045i -0.5111 + 0.0666i -0.5111 - 0.0666i -0.1478 + 0.0466i
-0.0748 + 0.0116i 0.4840 + 0.3995i 0.4840 - 0.3995i 1.0000 - 0.0000i
0.0112 + 0.0001i 0.6347 + 0.1997i 0.6347 - 0.1997i -0.2134 + 0.1232i

Column 21

0.0063 + 0.0624i
-0.1195 - 0.1921i
0.0577 + 0.0438i
-0.0986 + 0.0127i
0.2994 - 0.1979i
-0.0669 + 0.0934i
0.0063 - 0.0152i
-0.1120 + 0.1906i
0.0110 - 0.0272i
0.0018 - 0.0025i
-0.0132 + 0.0577i
0.0125 - 0.0124i
-0.0017 + 0.0024i
0.0134 - 0.0541i
-0.0113 + 0.0117i
-0.0119 + 0.0065i
0.0268 - 0.3583i
-0.1240 + 0.0496i
-0.1478 - 0.0466i
1.0000 + 0.0000i
-0.2134 - 0.1232i
```

detjj =

-1.4207e+31

detd =

1.5970e+21

detda =

-8.8961e+09

detad =

5.4416e+27

# Table C.3.12 (cont'd)

```
condjj =

 1.5374e+06

condd =

 53.9462

condda =

 7.4085e+05

condad =

 2.9271e+06

vtt =

 -0.9950 0.0478 -0.3074
 1.0000 1.0000 -0.6522
 -0.0870 0.0167 1.0000

eigtt =

 -140.1835
 -668.6855
 -41.0645
```

## Table C.3.13 Output for dynamic/algebraic 135 MVar (without exciter)

```
eigjj =

-26.3100 +52.3837i
-26.3100 -52.3837i
 49.8143
 46.7068
 40.1863
-12.6242 +25.5426i
-12.6242 -25.5426i
 24.8737
-10.1048 +18.6480i
-10.1048 -18.6480i
 21.6455
-16.6012
-15.8222
 -4.0397 +14.9935i
 -4.0397 -14.9935i
 -5.8019 +13.8856i
 -5.8019 -13.8856i
 17.6090
 12.0060 + 0.8555i
 12.0060 - 0.8555i
  7.6339 + 0.7734i
  7.6339 - 0.7734i
  1.7916
 -0.5340 + 1.5603i
 -0.5340 - 1.5603i
 -0.2013 + 1.2350i
 -0.2013 - 1.2350i
 -0.0865 + 0.7180i
 -0.0865 - 0.7180i
 -0.0001 + 0.6299i
 -0.0001 - 0.6299i
  0.4741 + 0.1452i
  0.4741 - 0.1452i
  0.0596
  0.2686
```

```
eigd =

 49.8143
 46.7072
-12.4724 +25.7372i
-12.4724 -25.7372i
 40.1889
 -9.9252 +18.6740i
 -9.9252 -18.6740i
 -5.7988 +13.8735i
 -5.7988 -13.8735i
 24.8799
 21.6507
 17.6370
  1.1086
  2.1907
 12.1502 + 0.9725i
 12.1502 - 0.9725i
  7.7099 + 0.8899i
  7.7099 - 0.8899i
```

```
eigda =

-26.4792 +52.1911i
-26.4792 -52.1911i
 -3.9046 +14.9230i
 -3.9046 -14.9230i
-16.4891
-15.1344
 -0.3244 + 1.7196i
 -0.3244 - 1.7196i
 -0.1269 + 1.1085i
 -0.1269 - 1.1085i
 -0.0838 + 0.6805i
 -0.0838 - 0.6805i
 -0.0199 + 0.6710i
 -0.0199 - 0.6710i
 -0.0836 + 0.0629i
 -0.0836 - 0.0629i
  0.2956
```

```
eigad =

 1.0e+02 *

-0.5080 + 5.5113i
-0.5080 - 5.5113i
-0.3552 + 4.3830i
-0.3552 - 4.3830i
 1.2416
 0.5481
 0.4958
 0.4296
 0.3503
-0.0391 + 0.1061i
-0.0391 - 0.1061i
-0.0355
 0.0003
 0.1571
 0.0620
 0.0997
 0.0726
 0.1411
```

```
vda =

Columns 1 through 4

 0.0000 - 0.0000i  0.0000 + 0.0000i  0.0000 + 0.0000i  0.0000 - 0.0000i
 0.0000 + 0.0000i  0.0000 - 0.0000i  0.0000 - 0.0000i  0.0000 + 0.0000i
 0.0000 + 0.0000i  0.0000 - 0.0000i  0.0000 + 0.0000i  0.0000 - 0.0000i
 0.0000 + 0.0000i  0.0000 - 0.0000i  0.0000 - 0.0000i  0.0000 + 0.0000i
 0.0000 - 0.0000i  0.0000 + 0.0000i  0.0000 + 0.0000i  0.0000 - 0.0000i
 0.0000 - 0.0000i  0.0000 + 0.0000i  0.0000 - 0.0000i  0.0000 + 0.0000i
-0.0002 + 0.0003i -0.0002 - 0.0003i  0.0000 + 0.0000i  0.0000 - 0.0000i
 0.0000 + 0.0000i  0.0000 - 0.0000i -0.0013 + 0.0007i -0.0013 - 0.0007i
 0.0000 + 0.0000i  0.0000 - 0.0000i  0.0000 + 0.0000i  0.0000 - 0.0000i
 0.0001 + 0.0000i  0.0001 - 0.0000i  0.0000 + 0.0002i  0.0000 - 0.0002i
 0.0000 + 0.0000i  0.0000 - 0.0000i -0.0001 + 0.0007i -0.0001 - 0.0007i
-0.0048 - 0.0105i -0.0048 + 0.0105i  0.0000 - 0.0002i  0.0000 + 0.0002i
 0.0000 - 0.0000i  0.0000 + 0.0000i -0.0021 - 0.0305i -0.0021 + 0.0305i
```

## Table C.3.13 (cont'd)

```
1.0000 - 0.0000i 1.0000 + 0.0000i 0.0040 - 0.0001i 0.0040 + 0.0001i
0.0000 + 0.0004i 0.0000 - 0.0004i 1.0000 - 0.0000i 1.0000 + 0.0000i
-0.0763 - 0.1538i -0.0763 + 0.1538i -0.0006 - 0.0026i -0.0006 + 0.0026i
0.0000 - 0.0000i 0.0000 + 0.0000i -0.0287 - 0.1104i -0.0287 + 0.1104i
```

Columns 5 through 8

```
0.0000 0.0000 0.0061 + 0.0010i 0.0061 - 0.0010i
0.0000 -0.0001 -0.0126 - 0.0065i -0.0126 + 0.0065i
0.0000 0.0000 -0.0028 + 0.0031i -0.0028 - 0.0031i
0.0000 0.0000 -0.0001 - 0.0035i -0.0001 + 0.0035i
0.0000 0.0000 -0.0023 + 0.0077i -0.0023 - 0.0077i
0.0000 0.0000 0.0020 + 0.0012i 0.0020 - 0.0012i
-0.0002 0.0049 -0.0186 - 0.0547i -0.0186 + 0.0547i
0.0013 0.0004 -0.0300 + 0.0089i -0.0300 - 0.0089i
0.0000 -0.0001 -0.0059 + 0.0111i -0.0059 - 0.0111i
-0.0020 0.0457 -0.0263 - 0.0408i -0.0263 + 0.0408i
0.0566 0.0223 -0.0280 - 0.0077i -0.0280 + 0.0077i
0.0023 -0.0527 0.0261 + 0.0391i 0.0261 - 0.0391i
-0.0336 -0.0144 0.0272 + 0.0060i 0.0272 - 0.0060i
-0.0491 1.0000 0.0265 + 0.1720i 0.0265 - 0.1720i
1.0000 0.3864 0.1303 + 0.1328i 0.1303 - 0.1328i
0.0309 -0.6875 1.0000 - 0.0000i 1.0000 + 0.0000i
-0.1069 -0.0450 0.1098 - 0.1521i 0.1098 + 0.1521i
```

Columns 9 through 12

```
-0.0560 + 0.0156i -0.0560 - 0.0156i 0.1022 - 0.2326i 0.1022 + 0.2326i
0.2274 - 0.0045i 0.2274 + 0.0045i -0.2205 - 0.1190i -0.2205 + 0.1190i
-0.0793 - 0.0136i -0.0793 + 0.0136i -0.0838 + 0.6805i -0.0838 - 0.6805i
0.0196 + 0.0483i 0.0196 - 0.0483i -0.3549 - 0.1065i -0.3549 + 0.1065i
-0.0272 - 0.2020i -0.0272 + 0.2020i -0.1330 + 0.3403i -0.1330 - 0.3403i
-0.0041 + 0.0720i -0.0041 - 0.0720i 1.0000 + 0.0000i 1.0000 - 0.0000i
0.0333 + 0.0415i 0.0333 - 0.0415i -0.0132 - 0.0021i -0.0132 + 0.0021i
-0.0223 - 0.1715i -0.0223 + 0.1715i 0.1840 - 0.0968i 0.1840 + 0.0968i
-0.0318 + 0.0111i -0.0318 - 0.0111i 0.0337 + 0.0449i 0.0337 - 0.0449i
0.0173 + 0.0103i 0.0173 - 0.0103i -0.0030 + 0.0055i -0.0030 - 0.0055i
-0.0245 - 0.1009i -0.0245 + 0.1009i 0.0654 + 0.0083i 0.0654 - 0.0083i
-0.0167 - 0.0099i -0.0167 + 0.0099i 0.0030 - 0.0052i 0.0030 + 0.0052i
0.0264 + 0.0948i 0.0264 - 0.0948i -0.0620 - 0.0067i -0.0620 + 0.0067i
-0.0611 - 0.0368i -0.0611 + 0.0368i 0.0021 - 0.0238i 0.0021 + 0.0238i
-0.0552 + 0.6302i -0.0552 - 0.6302i -0.3696 - 0.1160i -0.3696 + 0.1160i
-0.4787 + 0.3510i -0.4787 - 0.3510i -0.2106 - 0.1867i -0.2106 + 0.1867i
1.0000 + 0.0000i 1.0000 - 0.0000i -0.2227 + 0.9730i -0.2227 - 0.9730i
```

Columns 13 through 16

```
-0.0233 - 0.0711i -0.0233 + 0.0711i -0.0836 + 0.0629i -0.0836 - 0.0629i
-0.0880 + 0.2069i -0.0880 - 0.2069i -0.0767 + 0.0599i -0.0767 - 0.0599i
0.1036 - 0.0252i 0.1036 + 0.0252i -0.0821 + 0.0630i -0.0821 - 0.0630i
-0.1069 + 0.0316i -0.1069 - 0.0316i 1.0000 - 0.0000i 1.0000 + 0.0000i
0.3042 + 0.1401i 0.3042 - 0.1401i 0.9299 - 0.0162i 0.9299 + 0.0162i
-0.0330 - 0.1553i -0.0330 + 0.1553i 0.9897 - 0.0088i 0.9897 + 0.0088i
0.0160 + 0.0203i 0.0160 - 0.0203i -0.0002 - 0.0012i -0.0002 + 0.0012i
-0.0996 - 0.1688i -0.0996 + 0.1688i 0.0092 + 0.0036i 0.0092 - 0.0036i
-0.0137 + 0.0019i -0.0137 - 0.0019i 0.0034 + 0.0005i 0.0034 - 0.0005i
0.0042 + 0.0026i 0.0042 - 0.0026i 0.0006 - 0.0006i 0.0006 + 0.0006i
-0.0149 - 0.0610i -0.0149 + 0.0610i -0.0007 + 0.0004i -0.0007 - 0.0004i
-0.0040 - 0.0026i -0.0040 + 0.0026i -0.0007 + 0.0006i -0.0007 - 0.0006i
0.0151 + 0.0571i 0.0151 - 0.0571i 0.0006 - 0.0004i 0.0006 + 0.0004i
-0.0211 - 0.0038i -0.0211 + 0.0038i 0.0137 + 0.0019i 0.0137 - 0.0019i
0.0282 + 0.3815i 0.0282 - 0.3815i 0.0027 - 0.0023i 0.0027 + 0.0023i
-0.1879 + 0.1440i -0.1879 - 0.1440i 0.2704 + 0.0040i 0.2704 - 0.0040i
1.0000 + 0.0000i 1.0000 - 0.0000i -0.0742 - 0.0125i -0.0742 + 0.0125i
```

Column 17

```
-0.0020
-0.0880
0.1236
-0.0067
-0.2976
0.4180
0.1203
0.3874
-0.5088
-0.0045
-0.0263
```

# Table C.3.13 (cont'd)

```
0.0041
0.0244
0.0438
0.1850
0.4949
1.0000
```

detjj =

```
8.4838e+26
```

detd =

```
1.5970e+21
```

detda =

```
5.3124e+05
```

detad =

```
-3.7038e+25
```

condjj =

```
1.5371e+06
```

condd =

```
53.9462
```

condda =

```
7.4053e+05
```

condad =

```
2.9308e+06
```

vtt =

```
1.0000 0.0469 -0.2255
-0.9066 1.0000 -0.6684
-0.0013 -0.0004 1.0000
```

ett =

```
-137.9121 0 0
0 -659.2447 0
0 0 0.2214
```

Tab

4.4

ca

## C.4   Algebraic/Dynamic Voltage Instability

Table C.4.1 to Table C.4.5 are the converged equilibrium point of the simulation in section 4.4. Table C.4.6 to C.4.10 are the output from the eigenvalue program. Table C.4.11 is the case where field current is saturated.

## Table C.4.1 Equilibrium point(algebraic/dynamic 100 MVar)

```
1 9 BUS TEST SYSTEM(NO LINE DROP COMPENSATION) PAGE NUMBER 7
D1-2.0, D2-2.0, D3-2.0, KA-25, RC-0.0, XC-0.0 DATE 5/ 6/90
load2-100, REAL POWER LOAD = regular, real system TIME 21.58. 9

GENERATOR ANGLE IN DEGREES -NUMBER BUS/GEN NAME NO NUMBER BUS/GEN NAME NO
11 -49.9995-1177.6327-1158.5438-1178.7778

GENERATOR FIELD VOLTAGE -NUMBER BUS/GEN NAME NO NUMBER BUS/GEN NAME NO
11 -49.9995 1.1505 1.2844 1.7498

GEN. FLUX LINKAGE (Q-AXIS) -NUMBER BUS/GEN NAME NO NUMBER BUS/GEN NAME NO
11 -49.9995 1.0009 0.9183 1.0624

GEN. ELECTRICAL POWER - (MW) -NUMBER BUS/GEN NAME NO NUMBER BUS/GEN NAME NO
11 -49.9995 81.9070 73.2209 32.2941

GENERATOR EXCITER SATURATION -NUMBER BUS/GEN NAME NO NUMBER BUS/GEN NAME NO
11 -49.9995 0.0451 0.0114 0.1130

GENERATOR MEGAVAR OUTPUT -NUMBER BUS/GEN NAME NO NUMBER BUS/GEN NAME NO
11 -49.9995 9.3730 3.3089 59.8387

GENERATOR FIELD CURRENT -NUMBER BUS/GEN NAME NO NUMBER BUS/GEN NAME NO
11 -49.9995 1.0722 1.1746 1.5360

GENERATOR TERMINAL CURRENT -NUMBER BUS/GEN NAME NO NUMBER BUS/GEN NAME NO
11 -49.9995 0.8221 0.7323 0.6751

GEN. TERM. CURR. ANGLE DEGREES-NUMBER BUS/GEN NAME NO NUMBER BUS/GEN NAME NO
11 -49.9995 -114.2417 -109.8750 -171.9371

A-C BUS VOLTAGE MAGNITUDE -NUMBER BUS/GEN NAME NO NUMBER BUS/GEN NAME NO
11 -49.9995 1.0000 1.0001 0.9953 0.9982 1.0000 0.9783 0.9903 0.9443 0.9664

A-C BUS VOLTAGE ANGLE DEGREES -NUMBER BUS/GEN NAME NO NUMBER BUS/GEN NAME NO
11 -49.9995 -107.6946 -107.2852 -108.9968 -109.0723 -108.5942 -109.5441 -109.9591 -109.9120 -109.9659
```

## Table C.4.2 Equilibrium point(algebraic/dynamic 120 MVar)

```
1 9 BUS TEST SYSTEM(NO LINE DROP COMPENSATION) PAGE NUMBER 7
D1-2.0, D2-2.0, D3-2.0, KA-25, RC-0.0, XC-0.0 DATE 5/ 5/90
load2-120, REAL POWER LOAD = regular, real system TIME 13.37.32

GENERATOR ANGLE IN DEGREES -NUMBER BUS/GEN NAME NO NUMBER BUS/GEN NAME NO
11 -49.9995-2051.0349-2032.4624-2052.9587

GENERATOR FIELD VOLTAGE -NUMBER BUS/GEN NAME NO NUMBER BUS/GEN NAME NO
11 -49.9995 1.1617 1.3131 1.9371

GEN. FLUX LINKAGE (Q-AXIS) -NUMBER BUS/GEN NAME NO NUMBER BUS/GEN NAME NO
11 -49.9995 1.0028 0.9259 1.0831

GEN. ELECTRICAL POWER - (MW) -NUMBER BUS/GEN NAME NO NUMBER BUS/GEN NAME NO
11 -49.9995 81.9194 73.3913 32.5427

GENERATOR EXCITER SATURATION -NUMBER BUS/GEN NAME NO NUMBER BUS/GEN NAME NO
11 -49.9995 0.0454 0.0118 0.1781

GENERATOR MEGAVAR OUTPUT -NUMBER BUS/GEN NAME NO NUMBER BUS/GEN NAME NO
11 -49.9995 13.5463 8.2481 78.8409

GENERATOR FIELD CURRENT -NUMBER BUS/GEN NAME NO NUMBER BUS/GEN NAME NO
11 -49.9995 1.0871 1.2076 1.6889

GENERATOR TERMINAL CURRENT -NUMBER BUS/GEN NAME NO NUMBER BUS/GEN NAME NO
11 -49.9995 0.8247 0.7353 0.8473

GEN. TERM. CURR. ANGLE DEGREES-NUMBER BUS/GEN NAME NO NUMBER BUS/GEN NAME NO
11 -49.9995 89.5024 92.9486 27.6158

A-C BUS VOLTAGE MAGNITUDE -NUMBER BUS/GEN NAME NO NUMBER BUS/GEN NAME NO
11 -49.9995 0.9999 1.0001 0.9900 0.9974 0.9989 0.9675 0.9894 0.9246 0.9645

A-C BUS VOLTAGE ANGLE DEGREES -NUMBER BUS/GEN NAME NO NUMBER BUS/GEN NAME NO
11 -49.9995 -261.0426 -260.6111 -262.3363 -262.4216 -261.9244 -262.8969 -263.2994 -263.1671 -263.2791
```

## Table C.4.3 Equilibrium point(algebraic/dynamic 140 MVar)

```
1 9 BUS TEST SYSTEM(NO LINE DROP COMPENSATION) PAGE NUMBER 7
D1-2.0, D2-2.0, D3-2.0, KA-25, RC-0.0, XC-0.0 DATE 5/ 5/90
load2-140, REAL POWER LOAD - regular, real system TIME 13.55.36

GENERATOR ANGLE IN DEGREES -NUMBER BUS/GEN NAME NO NUMBER BUS/GEN NAME NO
11 -49.9995-3264.8188-3247.0376-3267.9502

GENERATOR FIELD VOLTAGE -NUMBER BUS/GEN NAME NO NUMBER BUS/GEN NAME NO
11 -49.9995 1.1762 1.3488 2.1176

GEN. FLUX LINKAGE (Q-AXIS) -NUMBER BUS/GEN NAME NO NUMBER BUS/GEN NAME NO
11 -49.9995 1.0054 0.9352 1.0997

GEN. ELECTRICAL POWER - (MW) -NUMBER BUS/GEN NAME NO NUMBER BUS/GEN NAME NO
11 -49.9995 83.1457 73.6318 31.6923

GENERATOR EXCITER SATURATION -NUMBER BUS/GEN NAME NO NUMBER BUS/GEN NAME NO
11 -49.9995 0.0458 0.0122 0.2787

GENERATOR MEGAVAR OUTPUT -NUMBER BUS/GEN NAME NO NUMBER BUS/GEN NAME NO
11 -49.9995 19.3959 14.6628 97.6530

GENERATOR FIELD CURRENT -NUMBER BUS/GEN NAME NO NUMBER BUS/GEN NAME NO
11 -49.9995 1.1088 1.2496 1.8409

GENERATOR TERMINAL CURRENT -NUMBER BUS/GEN NAME NO NUMBER BUS/GEN NAME NO
11 -49.9995 0.8414 0.7416 1.0261

GEN. TERM. CURR. ANGLE DEGREES-NUMBER BUS/GEN NAME NO NUMBER BUS/GEN NAME NO
11 -49.9995 -48.2228 -45.8850 -112.5751

A-C BUS VOLTAGE MAGNITUDE -NUMBER BUS/GEN NAME NO NUMBER BUS/GEN NAME NO
11 -49.9995 0.9999 1.0001 0.9801 0.9964 0.9976 0.9521 0.9881 0.8999 0.9616

A-C BUS VOLTAGE ANGLE DEGREES -NUMBER BUS/GEN NAME NO NUMBER BUS/GEN NAME NO
11 -49.9995 -394.8943 -394.4821 -396.4099 -396.2954 -395.8015 -396.9703 -397.1780 -397.1258 -397.1205
```

## Table C.4.4 Equilibrium point(algebraic/dynamic 160 MVar)

```
1 9 BUS TEST SYSTEM(NO LINE DROP COMPENSATION) PAGE NUMBER 7
D1-2.0, D2-2.0, D3-2.0, KA-25, RC-0.0, XC-0.0 DATE 5/ 5/90
load2-160, REAL POWER LOAD - regular, real system TIME 14.10.46

GENERATOR ANGLE IN DEGREES -NUMBER BUS/GEN NAME NO NUMBER BUS/GEN NAME NO
11 -49.9995-5102.7803-5085.8179-5106.4595

GENERATOR FIELD VOLTAGE -NUMBER BUS/GEN NAME NO NUMBER BUS/GEN NAME NO
11 -49.9995 1.1967 1.3968 2.2925

GEN. FLUX LINKAGE (Q-AXIS) -NUMBER BUS/GEN NAME NO NUMBER BUS/GEN NAME NO
11 -49.9995 1.0090 0.9468 1.1112

GEN. ELECTRICAL POWER - (MW) -NUMBER BUS/GEN NAME NO NUMBER BUS/GEN NAME NO
11 -49.9995 83.7227 73.9501 31.6281

GENERATOR EXCITER SATURATION -NUMBER BUS/GEN NAME NO NUMBER BUS/GEN NAME NO
11 -49.9995 0.0464 0.0128 0.4329

GENERATOR MEGAVAR OUTPUT -NUMBER BUS/GEN NAME NO NUMBER BUS/GEN NAME NO
11 -49.9995 27.3257 23.1931 116.2336

GENERATOR FIELD CURRENT -NUMBER BUS/GEN NAME NO NUMBER BUS/GEN NAME NO
11 -49.9995 1.1369 1.3042 1.9989

GENERATOR TERMINAL CURRENT -NUMBER BUS/GEN NAME NO NUMBER BUS/GEN NAME NO
11 -49.9995 0.8553 0.7534 1.2193

GEN. TERM. CURR. ANGLE DEGREES-NUMBER BUS/GEN NAME NO NUMBER BUS/GEN NAME NO
11 -49.9995 -91.4546 -90.3235 -155.6560

A-C BUS VOLTAGE MAGNITUDE -NUMBER BUS/GEN NAME NO NUMBER BUS/GEN NAME NO
11 -49.9995 0.9999 1.0001 0.9645 0.9950 0.9958 0.9307 0.9865 0.8684 0.9578

A-C BUS VOLTAGE ANGLE DEGREES -NUMBER BUS/GEN NAME NO NUMBER BUS/GEN NAME NO
11 -49.9995 -792.8209 -792.3969 -794.3982 -794.2339 -793.7243 -794.9797 -795.1110 -795.0235 -794.9921
```

## Table C.4.5 Equilibrium point(algebraic/dynamic 170 MVar)

```
1 9 BUS TEST SYSTEM(NO LINE DROP COMPENSATION) PAGE NUMBER 7
D1=2.0, D2=2.0, D3=2.0, KA=25, RC=0.0, XC=0.0 DATE 5/ 5/90
load2=170, REAL POWER LOAD = regular, real system TIME 14.47. 8

GENERATOR ANGLE IN DEGREES -NUMBER BUS/GEN NAME NO NUMBER BUS/GEN NAME NO
11 -49.9995-6788.8491-6772.3994-6791.4521

GENERATOR FIELD VOLTAGE -NUMBER BUS/GEN NAME NO NUMBER BUS/GEN NAME NO
11 -49.9995 1.2204 1.4455 2.3393

GEN. FLUX LINKAGE (Q-AXIS) -NUMBER BUS/GEN NAME NO NUMBER BUS/GEN NAME NO
11 -49.9995 1.0130 0.9581 1.1031

GEN. ELECTRICAL POWER - (MW) -NUMBER BUS/GEN NAME NO NUMBER BUS/GEN NAME NO
11 -49.9995 82.4783 74.1971 33.2760

GENERATOR EXCITER SATURATION -NUMBER BUS/GEN NAME NO NUMBER BUS/GEN NAME NO
11 -49.9995 0.0472 0.0135 0.4876

GENERATOR MEGAVAR OUTPUT -NUMBER BUS/GEN NAME NO NUMBER BUS/GEN NAME NO
11 -49.9995 34.8703 31.2340 123.3748

GENERATOR FIELD CURRENT -NUMBER BUS/GEN NAME NO NUMBER BUS/GEN NAME NO
11 -49.9995 1.1618 1.3542 2.0799

GENERATOR TERMINAL CURRENT -NUMBER BUS/GEN NAME NO NUMBER BUS/GEN NAME NO
11 -49.9995 0.8550 0.7685 1.3178

GEN. TERM. CURR. ANGLE DEGREES-NUMBER BUS/GEN NAME NO NUMBER BUS/GEN NAME NO
11 -49.9995 17.2926 17.8892 -43.1107

A-C BUS VOLTAGE MAGNITUDE -NUMBER BUS/GEN NAME NO NUMBER BUS/GEN NAME NO
11 -49.9995 0.9998 1.0002 0.9426 0.9935 0.9942 0.9061 0.9849 0.8378 0.9540

A-C BUS VOLTAGE ANGLE DEGREES -NUMBER BUS/GEN NAME NO NUMBER BUS/GEN NAME NO
11 -49.9995-1038.6335-1038.1355-1039.8147-1040.0276-1039.4691-1040.4576-1040.8798-1040.4736-1040.6694
```

## Table C.4.6 Output for algebraic/dynamic 100 MVar

eigjj =

```
-26.3306 +52.3938i
-26.3306 -52.3938i
 48.8605
 45.7222
 39.8842
-12.9499 +25.7027i
-12.9499 -25.7027i
-10.6054 +20.5482i
-10.6054 -20.5482i
 25.0774
 23.5798
 21.7340
-15.8133
-16.5808
-16.6084
 -5.4912 +14.6526i
 -5.4912 -14.6526i
 -4.1864 +14.9386i
 -4.1864 -14.9386i
 -3.9697 +14.9865i
 -3.9697 -14.9865i
 11.5361 + 0.6927i
 11.5361 - 0.6927i
  8.1440 + 0.1959i
  8.1440 - 0.1959i
  2.0359
 -0.5034 + 1.5763i
 -0.5034 - 1.5763i
 -0.1350 + 1.1938i
 -0.1350 - 1.1938i
  0.8303
 -0.1017 + 0.8999i
 -0.1017 - 0.8999i
  0.3216
  0.0368
 -0.0570 + 0.6165i
 -0.0570 - 0.6165i
 -0.0430 + 0.5721i
 -0.0430 - 0.5721i
```

eigd =

```
 48.8603
 45.7234
 39.8885
-12.7885 +25.8791i
-12.7885 -25.8791i
-10.4184 +20.5590i
-10.4184 -20.5590i
 -5.6040 +14.6142i
 -5.6040 -14.6142i
 25.0820
 23.6173
 21.7496
  1.4243
  1.9648
 11.6231 + 0.8097i
 11.6231 - 0.8097i
  8.2102 + 0.4533i
  8.2102 - 0.4533i
```

eigda =

```
-26.4918 +52.2103i
-26.4918 -52.2103i
 -3.8952 +14.9051i
 -3.8952 -14.9051i
 -3.9486 +14.9862i
 -3.9486 -14.9862i
-15.2041
-16.4660
-16.5489
 -0.3457 + 1.6967i
 -0.3457 - 1.6967i
 -0.0397 + 1.1176i
 -0.0397 - 1.1176i
 -0.0841 + 0.0200i
 -0.0841 - 0.0200i
 -0.0598 + 0.9093i
 -0.0598 - 0.9093i
 -0.0716 + 0.6173i
 -0.0716 - 0.6173i
 -0.0479 + 0.5770i
 -0.0479 - 0.5770i
```

vda =

Columns 1 through 4

```
0.0000 - 0.0000i 0.0000 + 0.0000i 0.0000 + 0.0000i 0.0000 - 0.0000i
0.0000 + 0.0000i 0.0000 - 0.0000i 0.0000 - 0.0000i 0.0000 + 0.0000i
0.0000 + 0.0000i 0.0000 - 0.0000i 0.0000 + 0.0000i 0.0000 - 0.0000i
0.0000 + 0.0000i 0.0000 - 0.0000i 0.0000 - 0.0000i 0.0000 + 0.0000i
0.0000 - 0.0000i 0.0000 + 0.0000i 0.0000 + 0.0000i 0.0000 - 0.0000i
```

## Table C.4.6 (cont'd)

```
0.0000 - 0.0000i 0.0000 + 0.0000i 0.0000 - 0.0000i 0.0000 + 0.0000i
-0.0002 + 0.0003i -0.0002 - 0.0003i 0.0000 + 0.0000i 0.0000 - 0.0000i
0.0000 + 0.0000i 0.0000 - 0.0000i -0.0012 + 0.0007i -0.0012 - 0.0007i
0.0000 + 0.0000i 0.0000 - 0.0000i -0.0001 + 0.0003i -0.0001 - 0.0003i
0.0001 + 0.0000i 0.0001 - 0.0000i 0.0000 + 0.0002i 0.0000 - 0.0002i
0.0000 + 0.0000i 0.0000 - 0.0000i -0.0001 + 0.0007i -0.0001 - 0.0007i
0.0000 + 0.0000i 0.0000 - 0.0000i 0.0001 + 0.0004i 0.0001 - 0.0004i
-0.0048 - 0.0105i -0.0048 + 0.0105i 0.0000 - 0.0002i 0.0000 + 0.0002i
0.0000 - 0.0000i 0.0000 + 0.0000i -0.0021 - 0.0305i -0.0021 + 0.0305i
0.0000 - 0.0000i 0.0000 + 0.0000i -0.0090 - 0.0125i -0.0090 + 0.0125i
1.0000 - 0.0000i 1.0000 + 0.0000i 0.0046 - 0.0006i 0.0046 + 0.0006i
0.0000 + 0.0002i 0.0000 - 0.0002i 1.0000 + 0.0000i 1.0000 - 0.0000i
0.0000 + 0.0002i 0.0000 - 0.0002i 0.4246 - 0.2674i 0.4246 + 0.2674i
-0.0762 - 0.1538i -0.0762 + 0.1538i -0.0011 - 0.0028i -0.0011 + 0.0028i
0.0000 - 0.0000i 0.0000 + 0.0000i -0.0289 - 0.1105i -0.0289 + 0.1105i
0.0000 - 0.0000i 0.0000 + 0.0000i -0.0350 - 0.0333i -0.0350 + 0.0333i


Columns 5 through 8

0.0000 + 0.0000i 0.0000 - 0.0000i 0.0000 0.0000
0.0000 + 0.0000i 0.0000 - 0.0000i -0.0001 0.0000
0.0000 - 0.0000i 0.0000 + 0.0000i 0.0000 0.0000
0.0000 + 0.0000i 0.0000 - 0.0000i 0.0000 0.0000
0.0000 - 0.0000i 0.0000 + 0.0000i 0.0000 0.0000
0.0000 + 0.0000i 0.0000 - 0.0000i 0.0000 0.0000
0.0000 + 0.0000i 0.0000 - 0.0000i 0.0048 -0.0003
0.0003 - 0.0004i 0.0003 + 0.0004i 0.0003 0.0012
-0.0006 + 0.0003i -0.0006 - 0.0003i 0.0001 0.0003
0.0000 + 0.0000i 0.0000 - 0.0000i 0.0456 -0.0026
-0.0001 - 0.0001i -0.0001 + 0.0001i 0.0167 0.0565
-0.0001 + 0.0004i -0.0001 - 0.0004i 0.0156 0.0299
0.0000 - 0.0001i 0.0000 + 0.0001i -0.0525 0.0031
0.0068 + 0.0095i 0.0068 - 0.0095i -0.0108 -0.0336
-0.0020 - 0.0304i -0.0020 + 0.0304i -0.0101 -0.0178
0.0013 + 0.0007i 0.0013 - 0.0007i 1.0000 -0.0643
-0.3265 + 0.2006i -0.3265 - 0.2006i 0.2906 1.0000
1.0000 - 0.0000i 1.0000 + 0.0000i 0.2701 0.5277
0.0003 - 0.0009i 0.0003 + 0.0009i -0.6862 0.0406
0.0315 + 0.0300i 0.0315 - 0.0300i -0.0336 -0.1068
-0.0237 - 0.0927i -0.0237 + 0.0927i -0.0265 -0.0478


Columns 9 through 12

0.0000 0.0055 - 0.0004i 0.0055 + 0.0004i -0.0353 + 0.0095i
0.0000 -0.0106 - 0.0031i -0.0106 + 0.0031i 0.1203 + 0.0071i
0.0000 -0.0036 + 0.0034i -0.0036 - 0.0034i -0.0309 - 0.0191i
0.0000 -0.0008 - 0.0031i -0.0008 + 0.0031i 0.0096 + 0.0312i
0.0000 -0.0005 + 0.0063i -0.0005 - 0.0063i 0.0025 - 0.1077i
0.0000 0.0023 + 0.0016i 0.0023 - 0.0016i -0.0161 + 0.0282i
-0.0001 -0.0198 - 0.0550i -0.0198 + 0.0550i 0.0376 + 0.0382i
-0.0005 -0.0242 + 0.0090i -0.0242 - 0.0090i -0.0393 - 0.1501i
0.0006 -0.0109 + 0.0055i -0.0109 - 0.0055i -0.0456 - 0.0214i
-0.0005 -0.0257 - 0.0413i -0.0257 + 0.0413i 0.0189 + 0.0066i
-0.0239 -0.0231 - 0.0050i -0.0231 + 0.0050i -0.0305 - 0.0966i
0.0567 -0.0190 - 0.0060i -0.0190 + 0.0060i -0.0392 - 0.0304i
0.0006 0.0255 + 0.0396i 0.0255 - 0.0396i -0.0181 - 0.0064i
0.0141 0.0224 + 0.0036i 0.0224 - 0.0036i 0.0322 + 0.0904i
-0.0336 0.0185 + 0.0048i 0.0185 - 0.0048i 0.0378 + 0.0276i
-0.0123 0.0286 + 0.1697i 0.0286 - 0.1697i -0.0729 - 0.0239i
-0.4222 0.1094 + 0.1030i 0.1094 - 0.1030i -0.0221 + 0.6354i
1.0000 0.0888 + 0.0886i 0.0888 - 0.0886i 0.1922 + 0.2445i
0.0077 1.0000 - 0.0000i 1.0000 + 0.0000i -0.4365 + 0.4208i
0.0449 0.0804 - 0.1298i 0.0804 + 0.1298i 1.0000 - 0.0000i
-0.0900 0.0655 - 0.0864i 0.0655 + 0.0864i 0.3393 - 0.2316i


Columns 13 through 16

-0.0353 - 0.0095i -0.0841 + 0.0200i -0.0841 - 0.0200i -0.0059 - 0.0216i
0.1203 - 0.0071i -0.0799 + 0.0195i -0.0799 - 0.0195i -0.1066 + 0.0858i
-0.0309 + 0.0191i -0.0833 + 0.0200i -0.0833 - 0.0200i 0.1130 - 0.0399i
0.0096 - 0.0312i 1.0000 + 0.0000i 1.0000 - 0.0000i -0.0232 + 0.0081i
0.0025 + 0.1077i 0.9518 - 0.0063i 0.9518 + 0.0063i 0.1016 + 0.1105i
-0.0161 - 0.0282i 0.9915 - 0.0027i 0.9915 + 0.0027i -0.0518 - 0.1209i
0.0376 - 0.0382i 0.0006 - 0.0003i 0.0006 + 0.0003i -0.0048 + 0.0319i
-0.0393 + 0.1501i 0.0086 + 0.0013i 0.0086 - 0.0013i 0.0722 + 0.0076i
-0.0456 + 0.0214i -0.0008 + 0.0001i -0.0008 - 0.0001i -0.0311 - 0.1200i
0.0189 - 0.0066i 0.0006 - 0.0002i 0.0006 + 0.0002i 0.0016 + 0.0084i
-0.0305 + 0.0966i -0.0002 + 0.0000i -0.0002 - 0.0000i 0.0486 - 0.0034i
```

## Table C.4.6 (cont'd)

```
-0.0392 + 0.0304i 0.0000 - 0.0000i 0.0000 + 0.0000i -0.0228 - 0.0988i
-0.0181 + 0.0064i -0.0007 + 0.0002i -0.0007 - 0.0002i -0.0015 - 0.0081i
0.0322 - 0.0904i 0.0002 - 0.0000i 0.0002 + 0.0000i -0.0458 + 0.0045i
0.0378 - 0.0276i 0.0000 + 0.0027i 0.0000 - 0.0000i 0.0235 + 0.0927i
-0.0729 + 0.0239i 0.0144 + 0.0006i 0.0144 - 0.0006i -0.0123 - 0.0300i
-0.0221 - 0.6354i 0.0014 - 0.0002i 0.0014 + 0.0002i -0.2892 - 0.0632i
0.1922 - 0.2445i 0.0000 + 0.0000i 0.0000 - 0.0000i 0.0375 + 0.6145i
-0.4365 - 0.4208i 0.2629 + 0.0014i 0.2629 - 0.0014i -0.2976 - 0.0522i
1.0000 + 0.0000i -0.0286 - 0.0025i -0.0286 + 0.0025i -0.0857 + 0.5650i
0.3393 + 0.2316i 0.0007 - 0.0000i 0.0007 + 0.0000i 1.0000 - 0.0000i

Columns 17 through 20

-0.0059 + 0.0216i 0.2355 - 0.1701i 0.2355 + 0.1701i 0.0402 - 0.0792i
-0.1066 - 0.0858i -0.1710 + 0.0976i -0.1710 - 0.0976i -0.2319 + 0.2209i
0.1130 + 0.0399i -0.5062 + 0.2865i -0.5062 - 0.2865i 0.0785 + 0.0553i
-0.0232 - 0.0081i -0.3155 - 0.3449i -0.3155 + 0.3449i -0.1421 - 0.0578i
0.1016 - 0.1105i 0.1877 + 0.2553i 0.1877 - 0.2553i 0.4133 + 0.3675i
-0.0518 + 0.1209i 0.5518 + 0.7559i 0.5518 - 0.7559i -0.1063 - 0.1273i
-0.0048 - 0.0319i 0.0091 + 0.0489i 0.0091 - 0.0489i 0.0044 + 0.0143i
0.0722 - 0.0076i -0.0182 - 0.0621i -0.0182 + 0.0621i -0.1290 - 0.2153i
-0.0311 + 0.1200i -0.0601 - 0.1564i -0.0601 + 0.1564i 0.0257 + 0.0602i
0.0016 - 0.0084i -0.0015 + 0.0095i -0.0015 - 0.0095i 0.0005 + 0.0028i
0.0486 + 0.0034i 0.0127 - 0.0201i 0.0127 + 0.0201i -0.0056 - 0.0553i
-0.0228 + 0.0988i -0.0067 - 0.0710i -0.0067 + 0.0710i 0.0121 + 0.0235i
-0.0015 + 0.0081i 0.0016 - 0.0091i 0.0016 + 0.0091i -0.0004 - 0.0027i
-0.0458 - 0.0045i -0.0116 + 0.0192i -0.0116 - 0.0192i 0.0063 + 0.0521i
0.0235 - 0.0927i 0.0069 + 0.0669i 0.0069 - 0.0669i -0.0115 - 0.0221i
-0.0123 + 0.0300i -0.0146 - 0.0367i -0.0146 + 0.0367i -0.0084 - 0.0092i
-0.2892 + 0.0632i -0.0964 + 0.1014i -0.0964 - 0.1014i -0.0268 + 0.3280i
0.0375 - 0.6145i 0.0295 + 0.4172i 0.0295 - 0.4172i -0.0720 - 0.1394i
-0.2976 + 0.0522i -0.4437 - 0.1661i -0.4437 + 0.1661i -0.1514 - 0.0076i
-0.0857 - 0.5650i 0.3163 + 0.2385i 0.3163 - 0.2385i 1.0000 - 0.0000i
1.0000 + 0.0000i 1.0000 - 0.0000i 1.0000 + 0.0000i -0.3739 + 0.1411i

Column 21

0.0402 + 0.0792i
-0.2319 - 0.2209i
0.0785 + 0.0553i
-0.1421 + 0.0578i
0.4133 - 0.3675i
-0.1063 + 0.1273i
0.0044 - 0.0143i
-0.1290 + 0.2153i
0.0257 - 0.0602i
0.0005 - 0.0028i
-0.0056 + 0.0553i
0.0121 - 0.0235i
-0.0004 + 0.0027i
0.0063 - 0.0521i
-0.0115 + 0.0221i
-0.0084 + 0.0092i
-0.0268 - 0.3280i
-0.0720 + 0.1394i
-0.1514 + 0.0076i
1.0000 + 0.0000i
-0.3739 - 0.1411i


eigad =

1.0e+03 *

-0.0510 + 1.9264i
-0.0510 - 1.9264i
-0.0647 + 0.3978i
-0.0647 - 0.3978i
0.0626 + 0.1919i
0.0626 - 0.1919i
0.0408 + 0.0627i
0.0408 - 0.0627i
0.0488
0.0439
0.0327
0.0349
0.0000
0.0122
```

## Table C.4.6 (cont'd)

```
0.0054
0.0068 + 0.0004i
0.0068 - 0.0004i
0.0134


vad =

Columns 1 through 4

0.0001 + 0.0006i 0.0001 - 0.0006i 0.0085 + 0.0411i 0.0085 - 0.0411i
0.0324 + 0.0080i 0.0324 - 0.0080i -0.0071 - 0.0013i -0.0071 + 0.0013i
0.0000 + 0.0000i 0.0000 - 0.0000i 0.0018 + 0.0026i 0.0018 - 0.0026i
0.0696 - 0.0037i 0.0696 + 0.0037i 1.0000 - 0.0000i 1.0000 + 0.0000i
1.0000 + 0.0000i 1.0000 - 0.0000i -0.1105 + 0.0721i -0.1105 - 0.0721i
0.0002 - 0.0000i 0.0002 + 0.0000i 0.0708 - 0.0255i 0.0708 + 0.0255i
-0.0001 - 0.0012i -0.0001 + 0.0012i -0.0125 - 0.0787i -0.0125 + 0.0787i
-0.0005 - 0.0180i -0.0005 + 0.0180i 0.0103 + 0.0076i 0.0103 - 0.0076i
0.0001 - 0.0000i 0.0001 + 0.0000i -0.0035 - 0.0059i -0.0035 + 0.0059i
0.0002 + 0.0074i 0.0002 - 0.0074i -0.0035 + 0.0218i -0.0035 - 0.0218i
-0.0001 + 0.0029i -0.0001 - 0.0029i 0.0000 - 0.0001i 0.0000 + 0.0001i
0.0000 + 0.0002i 0.0000 - 0.0002i 0.0028 + 0.0150i 0.0028 - 0.0150i
-0.0001 + 0.0001i -0.0001 - 0.0001i 0.0005 + 0.0062i 0.0005 - 0.0062i
0.0000 + 0.0014i 0.0000 - 0.0014i -0.0007 - 0.0005i -0.0007 + 0.0005i
0.0000 + 0.0000i 0.0000 - 0.0000i -0.0002 + 0.0007i -0.0002 - 0.0007i
-0.0001 - 0.0010i -0.0001 + 0.0010i 0.0002 - 0.0029i 0.0002 + 0.0029i
0.0000 - 0.0007i 0.0000 + 0.0007i 0.0001 + 0.0001i 0.0001 - 0.0001i
0.0000 - 0.0000i 0.0000 + 0.0000i -0.0009 - 0.0035i -0.0009 + 0.0035i

Columns 5 through 8

-0.0199 + 0.0840i -0.0199 - 0.0840i -0.0896 + 0.2376i -0.0896 - 0.2376i
0.0201 - 0.0427i 0.0201 + 0.0427i 0.1540 - 0.0421i 0.1540 + 0.0421i
-0.0269 + 0.0065i -0.0269 - 0.0065i -0.0727 - 0.1042i -0.0727 + 0.1042i
1.0000 + 0.0000i 1.0000 - 0.0000i 1.0000 + 0.0000i 1.0000 - 0.0000i
-0.4968 - 0.3535i -0.4968 + 0.3535i -0.3501 - 0.6364i -0.3501 + 0.6364i
0.1415 + 0.2921i 0.1415 - 0.2921i -0.2884 + 0.4165i -0.2884 - 0.4165i
0.0492 - 0.1489i 0.0492 + 0.1489i 0.2087 - 0.3587i 0.2087 + 0.3587i
-0.0756 + 0.0694i -0.0756 - 0.0694i -0.3085 + 0.0520i -0.3085 - 0.0520i
0.0575 - 0.0125i 0.0575 + 0.0125i 0.1127 + 0.1922i 0.1127 - 0.1922i
0.0035 + 0.0105i 0.0035 - 0.0105i 0.0023 + 0.0034i 0.0023 - 0.0034i
0.0001 - 0.0002i 0.0001 + 0.0002i 0.0000 - 0.0001i 0.0000 + 0.0001i
-0.0237 + 0.0228i -0.0237 - 0.0228i -0.0191 - 0.0007i -0.0191 + 0.0007i
-0.0034 + 0.0126i -0.0034 - 0.0126i -0.0064 + 0.0354i -0.0064 - 0.0354i
0.0051 - 0.0062i 0.0051 + 0.0062i 0.0206 - 0.0144i 0.0206 + 0.0144i
-0.0061 - 0.0005i -0.0061 + 0.0005i -0.0124 - 0.0167i -0.0124 + 0.0167i
-0.0010 - 0.0010i -0.0010 + 0.0010i -0.0044 + 0.0030i -0.0044 - 0.0030i
-0.0012 + 0.0008i -0.0012 - 0.0008i -0.0016 - 0.0006i -0.0016 + 0.0006i
0.0045 - 0.0066i 0.0045 + 0.0066i 0.0052 - 0.0068i 0.0052 + 0.0068i

Columns 9 through 12

0.2346 0.2420 -0.9939 0.4225
0.2158 0.0291 -0.8998 0.2693
0.1966 0.0698 -0.9850 0.2055
-0.4241 -0.3856 0.9156 -0.4203
-0.4290 -0.0904 1.0000 -0.3784
-0.3646 -0.1006 0.9222 -0.2207
-0.2415 -0.3144 0.9762 -0.3819
-0.2012 -0.0284 0.9499 -0.3545
-0.1951 -0.0102 0.9668 -0.1785
-0.0007 -0.0011 0.0019 0.0000
0.0000 0.0000 0.0001 0.0000
-0.0028 0.0063 0.0154 -0.0045
0.5748 -0.1471 0.0686 1.0000
1.0000 -0.5768 -0.0084 -0.6227
0.7328 1.0000 0.0130 -0.0699
-0.7482 0.4470 -0.0573 -0.1028
-0.4081 -0.2608 -0.0037 0.2160
-0.3182 -0.3309 -0.0354 -0.2460

Columns 13 through 16

1.0000 0.0171 0.2148 1.0000 - 0.0000i
0.9879 0.1488 -0.0757 -0.3162 - 0.1715i
0.9986 -0.2145 -0.0784 -0.5512 + 0.1410i
0.9989 0.0126 0.1563 0.6012 - 0.0230i
0.9926 0.0671 -0.0255 -0.1875 - 0.0947i
```

## Table C.4.6 (cont'd)

```
0.9985 -0.0634 -0.0462 -0.3261 + 0.0965i
0.9952 0.0115 0.0541 0.1404 - 0.0650i
0.9965 0.0193 -0.0740 -0.2788 + 0.0313i
0.9986 0.0571 -0.0290 -0.0015 + 0.0566i
-0.0002 0.0003 0.0004 0.0001 - 0.0000i
0.0000 0.0000 0.0000 0.0000 - 0.0000i
0.0000 -0.0032 0.0052 -0.0011 + 0.0001i
0.0000 0.3245 0.4209 0.0834 - 0.0223i
-0.0001 0.5382 0.4575 0.0379 - 0.0279i
0.0001 -0.3295 0.6234 0.0065 - 0.0189i
-0.0001 1.0000 0.6012 0.0870 - 0.0354i
0.0002 -0.1934 1.0000 0.0314 - 0.0355i
0.0001 -0.5994 0.9307 0.0468 - 0.0348i

Columns 17 through 18

1.0000 + 0.0000i -0.0982
-0.3162 + 0.1715i 0.1642
-0.5512 - 0.1410i -0.0917
0.6012 + 0.0230i -0.0306
-0.1875 + 0.0947i 0.0347
-0.3261 - 0.0965i -0.0184
0.1404 + 0.0650i 0.0185
-0.2788 - 0.0313i -0.1057
-0.0015 - 0.0566i 0.1111
0.0001 + 0.0000i -0.0004
0.0000 + 0.0000i 0.0000
-0.0011 - 0.0001i 0.0006
0.0834 + 0.0223i -0.3908
0.0379 + 0.0279i 0.1051
0.0065 + 0.0189i 0.0873
0.0870 + 0.0354i -0.2529
0.0314 + 0.0355i 1.0000
0.0468 + 0.0348i -0.8546


detjj =

 -7.7919e+30


detd =

 3.1981e+21


detda =

 -2.4364e+09


detad =

 2.5928e+29


condjj =

 2.2617e+06


condd =

 64.9835


condda =

 1.0843e+06


condad =

 5.3892e+07


vtt =
```

## Table C.4.6 (cont'd)

```
1.0000 0.0009 -0.5571
-0.7446 1.0000 -0.1589
0.6679 0.0009 1.0000


eigtt =

1.0e+04 *

-0.0146
-2.3122
-0.0094
```

## Table C.4.7 Output for algebraic/dynamic 120 MVar

eigjj =

```
-26.3382 +52.3974i
-26.3382 -52.3974i
 48.5461
 44.8936
 39.7860
-12.8916 +25.5713i
-12.8916 -25.5713i
-10.4749 +20.3135i
-10.4749 -20.3135i
 24.9942
 23.4238
 21.5370
-15.8138
-16.5808
-16.6075
 -5.4317 +14.4865i
 -5.4317 -14.4865i
 -3.9957 +14.9810i
 -3.9957 -14.9810i
 -4.2132 +14.9806i
 -4.2132 -14.9806i
 11.3305 + 0.7427i
 11.3305 - 0.7427i
  8.4729
  7.7830
  1.9690
 -0.5044 + 1.5773i
 -0.5044 - 1.5773i
 -0.1370 + 1.1951i
 -0.1370 - 1.1951i
  0.8575
 -0.1080 + 0.9088i
 -0.1080 - 0.9088i
  0.3181
  0.0356
 -0.0549 + 0.6323i
 -0.0549 - 0.6323i
 -0.0459 + 0.5778i
 -0.0459 - 0.5778i
```

eigd =

```
-12.7286 +25.7531i
-12.7286 -25.7531i
 48.5460
 44.8949
 39.7902
-10.2868 +20.3189i
-10.2868 -20.3189i
 -5.5572 +14.4788i
 -5.5572 -14.4788i
 24.9982
 23.4628
 21.5542
  1.4136
  1.9238
 11.4166 + 0.8403i
 11.4166 - 0.8403i
  8.1916 + 0.2313i
  8.1916 - 0.2313i
```

eigda =

```
-26.4999 +52.2134i
-26.4999 -52.2134i
 -3.8978 +14.9056i
 -3.8978 -14.9056i
 -3.9807 +14.9862i
 -3.9807 -14.9862i
-15.1974
-16.4610
-16.5452
 -0.3373 + 1.7019i
 -0.3373 - 1.7019i
 -0.0305 + 1.1269i
 -0.0305 - 1.1269i
 -0.0841 + 0.0140i
 -0.0841 - 0.0140i
 -0.0662 + 0.9187i
 -0.0662 - 0.9187i
 -0.0727 + 0.6324i
 -0.0727 - 0.6324i
 -0.0512 + 0.5827i
 -0.0512 - 0.5827i
```

vda =

Columns 1 through 4

```
0.0000 - 0.0000i  0.0000 + 0.0000i  0.0000 + 0.0000i  0.0000 - 0.0000i
0.0000 + 0.0000i  0.0000 - 0.0000i  0.0000 - 0.0000i  0.0000 + 0.0000i
0.0000 + 0.0000i  0.0000 - 0.0000i  0.0000 + 0.0000i  0.0000 - 0.0000i
0.0000 + 0.0000i  0.0000 - 0.0000i  0.0000 - 0.0000i  0.0000 + 0.0000i
0.0000 - 0.0000i  0.0000 + 0.0000i  0.0000 + 0.0000i  0.0000 - 0.0000i
```

## Table C.4.7 (cont'd)

```
0.0000 - 0.0000i 0.0000 + 0.0000i 0.0000 - 0.0000i 0.0000 + 0.0000i
-0.0002 + 0.0003i -0.0002 - 0.0003i 0.0000 + 0.0000i 0.0000 - 0.0000i
0.0000 + 0.0000i 0.0000 - 0.0000i -0.0012 + 0.0007i -0.0012 - 0.0007i
0.0000 + 0.0000i 0.0000 - 0.0000i -0.0001 + 0.0003i -0.0001 - 0.0003i
0.0001 + 0.0000i 0.0001 - 0.0000i 0.0000 + 0.0002i 0.0000 - 0.0002i
0.0000 + 0.0000i 0.0000 - 0.0000i -0.0001 + 0.0007i -0.0001 - 0.0007i
0.0000 + 0.0000i 0.0000 - 0.0000i 0.0001 + 0.0004i 0.0001 - 0.0004i
-0.0048 - 0.0105i -0.0048 + 0.0105i 0.0000 - 0.0002i 0.0000 + 0.0002i
0.0000 - 0.0000i 0.0000 + 0.0000i -0.0021 - 0.0305i -0.0021 + 0.0305i
0.0000 - 0.0000i 0.0000 + 0.0000i -0.0095 - 0.0089i -0.0095 + 0.0089i
1.0000 - 0.0000i 1.0000 + 0.0000i 0.0045 - 0.0008i 0.0045 + 0.0008i
0.0000 + 0.0003i 0.0000 - 0.0003i 1.0000 - 0.0000i 1.0000 + 0.0000i
0.0000 + 0.0002i 0.0000 - 0.0002i 0.3066 - 0.2912i 0.3066 + 0.2912i
-0.0762 - 0.1538i -0.0762 + 0.1538i -0.0011 - 0.0027i -0.0011 + 0.0027i
0.0000 - 0.0000i 0.0000 + 0.0000i -0.0289 - 0.1105i -0.0289 + 0.1105i
0.0000 - 0.0000i 0.0000 + 0.0000i -0.0344 - 0.0219i -0.0344 + 0.0219i
```

Columns 5 through 8

```
0.0000 + 0.0000i 0.0000 - 0.0000i 0.0000 0.0000
0.0000 + 0.0000i 0.0000 - 0.0000i -0.0001 0.0000
0.0000 - 0.0000i 0.0000 + 0.0000i 0.0000 0.0000
0.0000 + 0.0000i 0.0000 - 0.0000i 0.0000 0.0000
0.0000 - 0.0000i 0.0000 + 0.0000i 0.0000 0.0000
0.0000 + 0.0000i 0.0000 - 0.0000i 0.0000 0.0000
0.0000 + 0.0000i 0.0000 - 0.0000i 0.0048 -0.0003
0.0001 - 0.0004i 0.0001 + 0.0004i 0.0003 0.0012
-0.0006 + 0.0003i -0.0006 - 0.0003i 0.0001 0.0003
0.0000 + 0.0001i 0.0000 - 0.0001i 0.0456 -0.0028
-0.0001 - 0.0000i -0.0001 + 0.0000i 0.0169 0.0566
-0.0001 + 0.0004i -0.0001 - 0.0004i 0.0163 0.0331
0.0000 - 0.0001i 0.0000 + 0.0001i -0.0526 0.0033
0.0071 + 0.0066i 0.0071 - 0.0066i 0.0109 -0.0336
-0.0019 - 0.0304i -0.0019 + 0.0304i -0.0106 -0.0198
0.0017 + 0.0008i 0.0017 - 0.0008i 1.0000 -0.0687
-0.2343 + 0.2162i -0.2343 - 0.2162i 0.2948 1.0000
1.0000 - 0.0000i 1.0000 - 0.0000i 0.2823 0.5821
0.0003 - 0.0012i 0.0003 + 0.0012i -0.6873 0.0435
0.0305 + 0.0194i 0.0305 - 0.0194i -0.0341 -0.1069
-0.0235 - 0.0928i -0.0235 + 0.0928i -0.0278 -0.0529
```

Columns 9 through 12

```
0.0000 0.0054 - 0.0003i 0.0054 + 0.0003i -0.0340 + 0.0094i
0.0000 -0.0105 - 0.0032i -0.0105 + 0.0032i 0.1142 + 0.0068i
0.0000 -0.0035 + 0.0034i -0.0035 - 0.0034i -0.0285 - 0.0191i
0.0000 -0.0008 - 0.0030i -0.0008 + 0.0030i 0.0092 + 0.0299i
0.0000 -0.0006 + 0.0063i -0.0006 - 0.0063i 0.0033 - 0.1014i
0.0000 0.0023 + 0.0016i 0.0023 - 0.0016i -0.0163 + 0.0257i
0.0000 -0.0194 - 0.0547i -0.0194 + 0.0547i 0.0405 + 0.0398i
-0.0005 -0.0243 + 0.0094i -0.0243 - 0.0094i -0.0401 - 0.1471i
0.0006 -0.0111 + 0.0058i -0.0111 - 0.0058i -0.0465 - 0.0255i
-0.0005 -0.0259 - 0.0411i -0.0259 + 0.0411i 0.0204 + 0.0066i
-0.0260 -0.0237 - 0.0046i -0.0237 + 0.0046i -0.0316 - 0.0967i
0.0568 -0.0204 - 0.0057i -0.0204 + 0.0057i -0.0424 - 0.0364i
0.0006 0.0256 + 0.0394i 0.0256 - 0.0394i -0.0196 - 0.0064i
0.0154 0.0230 + 0.0032i 0.0230 - 0.0032i 0.0332 + 0.0904i
-0.0337 0.0198 + 0.0045i 0.0198 - 0.0045i 0.0408 + 0.0332i
-0.0118 0.0310 + 0.1702i 0.0310 - 0.1702i -0.0798 - 0.0236i
-0.4606 0.1149 + 0.1031i 0.1149 - 0.1031i -0.0157 + 0.6406i
1.0000 0.1010 + 0.0866i 0.1010 - 0.0866i 0.2217 + 0.2759i
0.0074 1.0000 - 0.0000i 1.0000 + 0.0000i -0.4595 + 0.4563i
0.0490 0.0801 - 0.1345i 0.0801 + 0.1345i 1.0000 - 0.0000i
-0.0905 0.0672 - 0.0936i 0.0672 + 0.0936i 0.3955 - 0.2352i
```

Columns 13 through 16

```
-0.0340 - 0.0094i -0.0841 + 0.0140i -0.0841 - 0.0140i -0.0044 - 0.0210i
0.1142 - 0.0068i -0.0801 + 0.0137i -0.0801 - 0.0137i -0.1125 + 0.0883i
-0.0285 + 0.0191i -0.0834 + 0.0141i -0.0834 - 0.0141i 0.1139 - 0.0442i
0.0092 - 0.0299i 1.0000 + 0.0000i 1.0000 - 0.0000i -0.0224 + 0.0064i
0.0033 + 0.1014i 0.9529 - 0.0044i 0.9529 + 0.0044i 0.1043 + 0.1149i
-0.0163 - 0.0257i 0.9925 - 0.0019i 0.9925 + 0.0019i -0.0568 - 0.1198i
0.0405 - 0.0398i 0.0006 - 0.0002i 0.0006 + 0.0002i -0.0060 + 0.0314i
-0.0401 + 0.1471i 0.0082 + 0.0009i 0.0082 - 0.0009i 0.0756 + 0.0161i
-0.0465 + 0.0255i -0.0007 + 0.0001i -0.0007 - 0.0001i -0.0310 - 0.1167i
0.0204 - 0.0066i 0.0006 - 0.0001i 0.0006 + 0.0001i 0.0012 + 0.0085i
-0.0316 + 0.0967i -0.0002 + 0.0000i -0.0002 - 0.0000i 0.0512 + 0.0008i
```

# Table C.4.7 (cont'd)

```
-0.0424 + 0.0364i  0.0000 - 0.0000i  0.0000 + 0.0000i -0.0232 - 0.1001i
-0.0196 + 0.0064i -0.0007 + 0.0001i -0.0007 - 0.0001i -0.0011 - 0.0082i
 0.0332 - 0.0904i  0.0002 - 0.0000i  0.0002 + 0.0000i -0.0485 + 0.0006i
 0.0408 - 0.0332i  0.0000 + 0.0000i  0.0000 - 0.0000i  0.0236 + 0.0938i
-0.0798 + 0.0236i  0.0148 + 0.0004i  0.0148 - 0.0004i -0.0108 - 0.0310i
-0.0157 - 0.6406i  0.0013 - 0.0001i  0.0013 + 0.0001i -0.2973 - 0.0925i
 0.2217 - 0.2759i  0.0000 + 0.0000i  0.0000 - 0.0000i  0.0834 + 0.6208i
-0.4595 - 0.4563i  0.2628 + 0.0010i  0.2628 - 0.0010i -0.2943 - 0.0682i
 1.0000 + 0.0000i -0.0271 - 0.0017i -0.0271 + 0.0017i -0.1373 + 0.5787i
 0.3955 + 0.2352i  0.0005 + 0.0000i  0.0005 - 0.0000i  1.0000 + 0.0000i

Columns 17 through 20

-0.0044 + 0.0210i  0.2427 - 0.1300i  0.2427 + 0.1300i  0.0488 - 0.0935i
-0.1125 - 0.0883i -0.1306 + 0.0220i -0.1306 - 0.0220i -0.2388 + 0.2302i
 0.1139 + 0.0442i -0.5473 + 0.2608i -0.5473 - 0.2608i  0.0594 - 0.0289i
-0.0224 - 0.0064i -0.2464 - 0.3556i -0.2464 + 0.3556i -0.1665 - 0.0690i
 0.1043 - 0.1149i  0.0578 + 0.1999i  0.0578 - 0.1999i  0.4277 + 0.3722i
-0.0568 + 0.1198i  0.5053 + 0.8075i  0.5053 - 0.8075i -0.0580 - 0.0968i
-0.0060 - 0.0314i  0.0044 + 0.0449i  0.0044 - 0.0449i  0.0059 + 0.0164i
 0.0756 - 0.0161i  0.0265 - 0.0082i  0.0265 + 0.0082i -0.1274 - 0.2109i
-0.0310 + 0.1167i -0.0517 - 0.1538i -0.0517 + 0.1538i  0.0179 + 0.0498i
 0.0012 - 0.0085i -0.0024 + 0.0087i -0.0024 - 0.0087i  0.0006 + 0.0033i
 0.0512 - 0.0008i  0.0172 - 0.0025i  0.0172 + 0.0025i -0.0055 - 0.0560i
-0.0232 + 0.1001i -0.0077 - 0.0727i -0.0077 + 0.0727i  0.0105 + 0.0199i
-0.0011 + 0.0082i  0.0025 + 0.0084i  0.0025 - 0.0084i -0.0005 - 0.0032i
-0.0485 - 0.0006i -0.0162 + 0.0027i -0.0162 - 0.0027i  0.0062 + 0.0527i
 0.0236 - 0.0938i  0.0075 + 0.0684i  0.0075 - 0.0684i -0.0098 - 0.0187i
-0.0108 + 0.0310i -0.0096 - 0.0362i -0.0096 + 0.0362i -0.0101 - 0.0107i
-0.2973 + 0.0925i -0.1022 - 0.0054i -0.1022 + 0.0054i -0.0275 + 0.3313i
 0.0834 - 0.6208i  0.0790 + 0.4273i  0.0790 - 0.4273i -0.0766 - 0.1120i
-0.2943 + 0.0682i -0.3884 - 0.2021i -0.3884 + 0.2021i -0.1765 - 0.0074i
-0.1373 - 0.5787i  0.0162 + 0.2825i  0.0162 - 0.2825i  1.0000 + 0.0000i
 1.0000 - 0.0000i  1.0000 + 0.0000i  1.0000 - 0.0000i -0.3129 + 0.1202i

Column 21

 0.0488 + 0.0935i
-0.2388 - 0.2302i
 0.0594 + 0.0289i
-0.1665 + 0.0690i
 0.4277 - 0.3722i
-0.0580 + 0.0968i
 0.0059 - 0.0164i
-0.1274 + 0.2109i
 0.0179 - 0.0498i
 0.0006 - 0.0033i
-0.0055 + 0.0560i
 0.0105 - 0.0199i
-0.0005 + 0.0032i
 0.0062 - 0.0527i
-0.0098 + 0.0187i
-0.0101 + 0.0107i
-0.0275 - 0.3313i
-0.0766 + 0.1120i
-0.1765 + 0.0074i
 1.0000 - 0.0000i
-0.3129 - 0.1202i


eigad =

1.0e+03 *

-0.0497 + 1.0003i
-0.0497 - 1.0003i
-0.0516 + 0.4059i
-0.0516 - 0.4059i
 0.0433 + 0.1207i
 0.0433 - 0.1207i
 0.0461 + 0.0743i
 0.0461 - 0.0743i
 0.0485
 0.0431
 0.0322
 0.0348
 0.0000
 0.0122
```

# Table C.4.7 (cont'd)

```
0.0053
0.0068 + 0.0003i
0.0068 - 0.0003i
0.0130
```

vad =

Columns 1 through 4

```
0.0009 + 0.0049i 0.0009 - 0.0049i 0.0069 + 0.0408i 0.0069 - 0.0408i
0.0317 + 0.0154i 0.0317 - 0.0154i -0.0039 - 0.0012i -0.0039 + 0.0012i
0.0000 + 0.0000i 0.0000 - 0.0000i 0.0007 + 0.0015i 0.0007 - 0.0015i
0.2943 - 0.0304i 0.2943 + 0.0304i 1.0000 + 0.0000i 1.0000 - 0.0000i
1.0000 + 0.0000i 1.0000 - 0.0000i -0.0683 + 0.0363i -0.0683 - 0.0363i
0.0018 - 0.0004i 0.0018 + 0.0004i 0.0392 - 0.0104i 0.0392 + 0.0104i
-0.0014 - 0.0094i -0.0014 + 0.0094i -0.0097 - 0.0778i -0.0097 + 0.0778i
-0.0016 - 0.0345i -0.0016 + 0.0345i 0.0063 + 0.0047i 0.0063 - 0.0047i
0.0003 - 0.0001i 0.0003 + 0.0001i -0.0014 - 0.0032i -0.0014 + 0.0032i
0.0009 + 0.0163i 0.0009 - 0.0163i -0.0028 + 0.0224i -0.0028 - 0.0224i
-0.0003 + 0.0056i -0.0003 - 0.0056i -0.0001 - 0.0002i -0.0001 + 0.0002i
0.0002 + 0.0016i 0.0002 - 0.0016i 0.0019 + 0.0140i 0.0019 - 0.0140i
-0.0001 + 0.0008i -0.0001 - 0.0008i 0.0003 + 0.0061i 0.0003 - 0.0061i
0.0001 + 0.0026i 0.0001 - 0.0026i -0.0004 - 0.0003i -0.0004 + 0.0003i
0.0000 + 0.0000i 0.0000 - 0.0000i -0.0003 + 0.0004i -0.0003 - 0.0004i
-0.0002 - 0.0023i -0.0002 + 0.0023i 0.0001 - 0.0030i 0.0001 + 0.0030i
0.0000 - 0.0012i 0.0000 + 0.0012i 0.0001 + 0.0001i 0.0001 - 0.0001i
-0.0001 - 0.0004i -0.0001 + 0.0004i -0.0007 - 0.0033i -0.0007 + 0.0033i
```

Columns 5 through 8

```
-0.0292 + 0.1346i -0.0292 - 0.1346i -0.0775 + 0.1987i -0.0775 - 0.1987i
0.0514 - 0.0654i 0.0514 + 0.0654i 0.1161 - 0.0485i 0.1161 + 0.0485i
-0.0547 - 0.0032i -0.0547 + 0.0032i -0.0664 - 0.0638i -0.0664 + 0.0638i
1.0000 + 0.0000i 1.0000 - 0.0000i 1.0000 + 0.0000i 1.0000 - 0.0000i
-0.5237 - 0.4359i -0.5237 + 0.4359i -0.3984 - 0.5564i -0.3984 + 0.5564i
0.0603 + 0.4043i 0.0603 - 0.4043i -0.1710 + 0.4100i -0.1710 - 0.4100i
0.0815 - 0.2291i 0.0815 + 0.2291i 0.1774 - 0.3078i 0.1774 + 0.3078i
-0.1380 + 0.1122i -0.1380 - 0.1122i -0.2474 + 0.0731i -0.2474 - 0.0731i
0.1095 + 0.0107i 0.1095 - 0.0107i 0.1149 + 0.1223i 0.1149 - 0.1223i
0.0024 + 0.0066i 0.0024 - 0.0066i 0.0026 + 0.0041i 0.0026 - 0.0041i
0.0002 - 0.0005i 0.0002 + 0.0005i 0.0001 - 0.0003i 0.0001 + 0.0003i
-0.0394 + 0.0210i -0.0394 - 0.0210i -0.0327 + 0.0051i -0.0327 - 0.0051i
-0.0038 + 0.0198i -0.0038 - 0.0198i -0.0075 + 0.0300i -0.0075 - 0.0300i
0.0084 - 0.0109i 0.0084 + 0.0109i 0.0166 - 0.0128i 0.0166 + 0.0128i
-0.0112 - 0.0042i -0.0112 + 0.0042i -0.0116 + 0.0137i -0.0116 - 0.0137i
-0.0013 + 0.0003i -0.0013 - 0.0003i -0.0032 + 0.0017i -0.0032 - 0.0017i
-0.0018 + 0.0008i -0.0018 - 0.0008i -0.0017 + 0.0000i -0.0017 - 0.0000i
0.0074 - 0.0082i 0.0074 + 0.0082i 0.0078 - 0.0072i 0.0078 + 0.0072i
```

Columns 9 through 12

```
0.1906 0.2824 0.9827 0.3679
0.2027 0.0675 0.9099 0.2285
0.1776 0.0923 1.0000 0.1636
-0.3385 -0.4352 -0.8788 -0.3606
-0.3940 -0.1537 -0.9823 -0.3230
-0.3344 -0.1362 -0.9396 -0.1803
-0.1854 -0.3549 -0.9483 -0.3237
-0.1903 -0.0689 -0.9603 -0.3099
-0.1816 -0.0341 -0.9854 -0.1404
-0.0004 -0.0012 -0.0018 0.0002
0.0000 -0.0001 -0.0002 -0.0001
-0.0055 0.0091 -0.0263 -0.0067
0.5611 -0.0792 -0.0207 1.0000
1.0000 -0.4967 -0.0153 -0.6178
0.5887 1.0000 -0.0265 -0.0916
-0.7514 0.3758 0.0443 -0.1093
-0.3470 -0.2670 0.0194 0.2136
-0.2715 -0.3504 0.0333 -0.2355
```

Columns 13 through 16

```
1.0000 0.0297 0.1796 1.0000 + 0.0000i
0.9880 0.1200 -0.0661 -0.3000 - 0.1390i
0.9989 -0.1925 -0.0651 -0.5674 + 0.1149i
0.9989 0.0171 0.1333 0.6044 - 0.0187i
0.9927 0.0581 -0.0220 -0.1774 - 0.0774i
```

## Table C.4.7 (cont'd)

```
0.9987 -0.0553 -0.0378 -0.3350 + 0.0787i
0.9953 0.0082 0.0469 0.1478 - 0.0531i
0.9966 0.0310 -0.0696 -0.2812 + 0.0253i
0.9988 0.0455 -0.0256 -0.0045 + 0.0459i
-0.0002 0.0003 0.0004 0.0001 - 0.0000i
0.0000 0.0000 0.0000 0.0000 - 0.0000i
0.0000 -0.0051 0.0083 -0.0018 + 0.0001i
0.0000 0.3593 0.3840 0.0861 - 0.0175i
-0.0001 0.5149 0.4281 0.0418 - 0.0223i
0.0002 -0.3233 0.6029 0.0100 - 0.0156i
-0.0001 1.0000 0.5516 0.0916 - 0.0279i
0.0002 -0.2820 1.0000 0.0407 - 0.0306i
0.0001 -0.4760 0.8592 0.0515 - 0.0274i

Columns 17 through 18

1.0000 - 0.0000i -0.1027
-0.3000 + 0.1390i 0.1876
-0.5674 - 0.1149i -0.1264
0.6044 + 0.0187i -0.0333
-0.1774 + 0.0774i 0.0454
-0.3350 - 0.0787i -0.0275
0.1478 + 0.0531i 0.0197
-0.2812 - 0.0253i -0.1071
-0.0045 - 0.0459i 0.1238
0.0001 + 0.0000i -0.0004
0.0000 + 0.0000i 0.0000
-0.0018 - 0.0001i 0.0000
0.0861 + 0.0175i -0.3763
0.0418 + 0.0223i 0.1533
0.0100 + 0.0156i 0.0219
0.0916 + 0.0279i -0.1620
0.0407 + 0.0306i 1.0000
0.0515 + 0.0274i -0.9890
```

```
detjj =

-7.1532e+30


detd =

2.7013e+21


detda =

-2.6481e+09


detad =

3.4097e+28


condjj =

2.3231e+06


condd =

63.2110


condda =

1.1141e+06


condad =

1.5128e+07


vtt =
```

# Table C.4.7 (cont'd)

```
1.0000 0.0031 -0.3339
-0.5743 1.0000 -0.2918
0.2355 0.0020 1.0000
```

```
eigtt =
```

```
1.0e+03 *
```

```
-0.1335
-6.7572
-0.0630
```

# Table C.4.8 Output for algebraic/dynamic 140 MVar

```
eigjj =

 -26.3481 +52.4022i
 -26.3481 -52.4022i
  48.2581
  43.6372
  39.6573
 -12.8140 +25.4019i
 -12.8140 -25.4019i
  24.8905
  23.1327
  21.2563
 -10.2704 +19.9517i
 -10.2704 -19.9517i
 -15.8155
 -16.5809
 -16.6067
  -5.3659 +14.2441i
  -5.3659 -14.2441i
  -4.0238 +14.9725i
  -4.0238 -14.9725i
  -4.2413 +15.0447i
  -4.2413 -15.0447i
  11.0753 +  0.7659i
  11.0753 -  0.7659i
   8.6791
   7.5169
   1.8834
  -0.5052 +  1.5778i
  -0.5052 -  1.5778i
   0.8780
  -0.1406 +  1.1969i
  -0.1406 -  1.1969i
   0.3163
   0.0342
  -0.1181 +  0.9180i
  -0.1181 -  0.9180i
  -0.0535 +  0.6461i
  -0.0535 -  0.6461i
  -0.0490 +  0.5833i
  -0.0490 -  0.5833i
```

```
eigd =

 -12.6492 +25.5903i
 -12.6492 -25.5903i
  48.2580
  43.6386
  39.6612
 -10.0834 +19.9501i
 -10.0834 -19.9501i
  -5.4933 +14.2838i
  -5.4933 -14.2838i
  24.8936
  23.1728
  21.2755
   1.3797
   1.8751
  11.1611 +  0.8462i
  11.1611 -  0.8462i
   7.7588
   8.5551
```

```
eigda =

 -26.5105 +52.2176i
 -26.5105 -52.2176i
  -3.8992 +14.9057i
  -3.8992 -14.9057i
  -4.0274 +14.9877i
  -4.0274 -14.9877i
 -15.1892
 -16.4542
 -16.5408
  -0.3255 +  1.7086i
  -0.3255 -  1.7086i
  -0.0196 +  1.1414i
  -0.0196 -  1.1414i
  -0.0925
  -0.0758
  -0.0550 +  0.5882i
  -0.0550 -  0.5882i
  -0.0743 +  0.6454i
  -0.0743 -  0.6454i
  -0.0770 +  0.9271i
  -0.0770 -  0.9271i
```

```
vda =

Columns 1 through 4

 0.0000 - 0.0000i 0.0000 + 0.0000i 0.0000 + 0.0000i 0.0000 - 0.0000i
 0.0000 + 0.0000i 0.0000 - 0.0000i 0.0000 - 0.0000i 0.0000 + 0.0000i
 0.0000 + 0.0000i 0.0000 - 0.0000i 0.0000 + 0.0000i 0.0000 - 0.0000i
 0.0000 + 0.0000i 0.0000 - 0.0000i 0.0000 - 0.0000i 0.0000 + 0.0000i
 0.0000 - 0.0000i 0.0000 + 0.0000i 0.0000 + 0.0000i 0.0000 - 0.0000i
 0.0000 - 0.0000i 0.0000 + 0.0000i 0.0000 - 0.0000i 0.0000 + 0.0000i
```

## Table C.4.8 (cont'd)

```
-0.0002 + 0.0003i -0.0002 - 0.0003i 0.0000 + 0.0000i 0.0000 - 0.0000i
0.0000 + 0.0000i 0.0000 - 0.0000i -0.0011 + 0.0007i -0.0011 - 0.0007i
0.0000 + 0.0000i 0.0000 - 0.0000i 0.0000 + 0.0002i 0.0000 - 0.0002i
0.0001 + 0.0000i 0.0001 - 0.0000i 0.0000 + 0.0002i 0.0000 - 0.0002i
0.0000 + 0.0000i 0.0000 - 0.0000i -0.0001 + 0.0007i -0.0001 - 0.0007i
0.0000 + 0.0000i 0.0000 - 0.0000i 0.0001 + 0.0003i 0.0001 - 0.0003i
-0.0048 - 0.0105i -0.0048 + 0.0105i 0.0000 - 0.0002i 0.0000 + 0.0002i
0.0000 - 0.0000i 0.0000 + 0.0000i -0.0021 - 0.0305i -0.0021 + 0.0305i
0.0000 - 0.0000i 0.0000 + 0.0000i -0.0087 - 0.0059i -0.0087 + 0.0059i
1.0000 - 0.0000i 1.0000 + 0.0000i 0.0044 - 0.0008i 0.0044 + 0.0008i
0.0000 + 0.0003i 0.0000 - 0.0003i 1.0000 - 0.0000i 1.0000 + 0.0000i
0.0000 + 0.0003i 0.0000 - 0.0003i 0.2067 - 0.2718i 0.2067 + 0.2718i
-0.0761 - 0.1538i -0.0761 + 0.1538i -0.0011 - 0.0027i -0.0011 + 0.0027i
0.0000 - 0.0000i 0.0000 + 0.0000i -0.0289 - 0.1105i -0.0289 + 0.1105i
0.0000 - 0.0000i 0.0000 + 0.0000i -0.0302 - 0.0132i -0.0302 + 0.0132i
```

Columns 5 through 8

```
0.0000 + 0.0000i 0.0000 - 0.0000i 0.0000 0.0000
0.0000 + 0.0000i 0.0000 - 0.0000i -0.0001 0.0000
0.0000 - 0.0000i 0.0000 + 0.0000i 0.0000 0.0000
0.0000 + 0.0000i 0.0000 - 0.0000i 0.0000 0.0000
0.0000 - 0.0000i 0.0000 + 0.0000i 0.0000 0.0000
0.0000 + 0.0000i 0.0000 - 0.0000i 0.0000 0.0000
0.0000 + 0.0000i 0.0000 - 0.0000i 0.0048 -0.0003
0.0001 - 0.0003i 0.0001 + 0.0003i 0.0003 0.0012
-0.0005 + 0.0003i -0.0005 - 0.0003i 0.0001 0.0004
0.0000 + 0.0001i 0.0000 - 0.0001i 0.0458 -0.0031
-0.0001 + 0.0000i -0.0001 - 0.0000i 0.0173 0.0566
-0.0001 + 0.0005i -0.0001 - 0.0005i 0.0174 0.0374
0.0000 - 0.0001i 0.0000 + 0.0001i -0.0527 0.0036
0.0064 + 0.0043i 0.0064 - 0.0043i -0.0111 -0.0337
-0.0018 - 0.0305i -0.0018 + 0.0305i -0.0113 -0.0224
0.0022 + 0.0008i 0.0022 - 0.0008i 1.0000 -0.0749
-0.1568 + 0.1984i -0.1568 - 0.1984i 0.3002 1.0000
1.0000 + 0.0000i 1.0000 - 0.0000i 0.2992 0.6543
0.0002 - 0.0015i 0.0002 + 0.0015i -0.6886 0.0474
0.0263 + 0.0113i 0.0263 - 0.0113i -0.0348 -0.1069
-0.0232 - 0.0930i -0.0232 + 0.0930i -0.0297 -0.0599
```

Columns 9 through 12

```
0.0000 0.0054 - 0.0002i 0.0054 + 0.0002i -0.0326 + 0.0095i
0.0000 -0.0105 - 0.0034i -0.0105 + 0.0034i 0.1068 + 0.0051i
0.0000 -0.0034 + 0.0035i -0.0034 - 0.0035i -0.0249 - 0.0178i
0.0000 -0.0007 - 0.0030i -0.0007 + 0.0030i 0.0088 + 0.0284i
0.0000 -0.0008 + 0.0063i -0.0008 - 0.0063i 0.0028 - 0.0936i
0.0000 0.0023 + 0.0016i 0.0023 - 0.0016i -0.0152 + 0.0220i
0.0000 -0.0190 - 0.0544i -0.0190 + 0.0544i 0.0442 + 0.0422i
-0.0006 -0.0245 + 0.0099i -0.0245 - 0.0099i -0.0413 - 0.1435i
0.0006 -0.0115 + 0.0061i -0.0115 - 0.0061i -0.0464 - 0.0314i
-0.0005 -0.0261 - 0.0408i -0.0261 + 0.0408i 0.0226 + 0.0067i
-0.0289 -0.0246 - 0.0040i -0.0246 + 0.0040i -0.0331 - 0.0971i
0.0571 -0.0224 - 0.0053i -0.0224 + 0.0053i -0.0454 - 0.0450i
0.0005 0.0258 + 0.0391i 0.0258 - 0.0391i -0.0217 - 0.0065i
0.0171 0.0238 + 0.0026i 0.0238 - 0.0026i 0.0347 + 0.0907i
-0.0340 0.0216 + 0.0041i 0.0216 - 0.0041i 0.0436 + 0.0412i
-0.0111 0.0342 + 0.1709i 0.0342 - 0.1709i -0.0896 - 0.0240i
-0.5107 0.1224 + 0.1032i 0.1224 - 0.1032i -0.0080 + 0.6489i
1.0000 0.1178 + 0.0832i 0.1178 - 0.0832i 0.2604 + 0.3202i
0.0070 1.0000 - 0.0000i 1.0000 + 0.0000i -0.4959 + 0.5037i
0.0543 0.0798 - 0.1409i 0.0798 + 0.1409i 1.0000 + 0.0000i
-0.0911 0.0700 - 0.1034i 0.0700 + 0.1034i 0.4689 - 0.2255i
```

Columns 13 through 16

```
-0.0326 - 0.0095i -0.0925 -0.0758 0.0583 - 0.1040i
0.1068 - 0.0051i -0.0885 -0.0721 -0.2496 + 0.2403i
-0.0249 + 0.0178i -0.0920 -0.0753 0.0425 - 0.0141i
0.0088 - 0.0284i 1.0000 1.0000 -0.1845 - 0.0818i
0.0028 + 0.0936i 0.9569 0.9517 0.4444 + 0.3827i
-0.0152 - 0.0220i 0.9951 0.9929 -0.0305 - 0.0693i
0.0442 - 0.0422i 0.0008 0.0005 0.0065 + 0.0183i
-0.0413 + 0.1435i 0.0072 0.0082 -0.1258 - 0.2072i
-0.0464 + 0.0314i -0.0007 -0.0007 0.0146 + 0.0427i
0.0226 - 0.0067i 0.0007 0.0005 0.0006 + 0.0038i
-0.0331 + 0.0971i -0.0002 -0.0002 -0.0054 - 0.0566i
-0.0454 + 0.0450i 0.0000 0.0000 0.0104 + 0.0175i
```

# Table C.4.8 (cont'd)

```
-0.0217 + 0.0065i -0.0008 -0.0007 -0.0004 - 0.0037i
0.0347 - 0.0907i 0.0002 0.0002 0.0061 + 0.0533i
0.0436 - 0.0412i 0.0000 0.0000 -0.0096 - 0.0165i
-0.0896 + 0.0240i 0.0153 0.0158 -0.0114 - 0.0125i
-0.0080 - 0.6489i 0.0012 0.0011 -0.0282 + 0.3344i
0.2604 - 0.3202i 0.0000 0.0001 -0.0918 - 0.0899i
-0.4959 - 0.5037i 0.2661 0.2673 -0.1987 - 0.0136i
1.0000 - 0.0000i -0.0245 -0.0264 1.0000 + 0.0000i
0.4689 + 0.2255i 0.0003 0.0003 -0.2746 + 0.1202i
```

```
Columns 17 through 20
```

```
0.0583 + 0.1040i 0.2469 - 0.1022i 0.2469 + 0.1022i -0.0012 - 0.0201i
-0.2496 - 0.2403i -0.0826 - 0.0148i -0.0826 + 0.0148i -0.1216 + 0.0885i
0.0425 + 0.0141i -0.5955 + 0.2299i -0.5955 - 0.2299i 0.1134 - 0.0476i
-0.1845 + 0.0818i -0.1998 - 0.3595i -0.1998 + 0.3595i -0.0214 + 0.0031i
0.4444 - 0.3827i -0.0081 + 0.1289i -0.0081 - 0.1289i 0.1056 + 0.1224i
-0.0305 + 0.0693i 0.4564 + 0.8702i 0.4564 - 0.8702i -0.0611 - 0.1172i
0.0065 - 0.0183i 0.0024 + 0.0417i 0.0024 - 0.0417i -0.0073 + 0.0301i
-0.1258 + 0.2072i 0.0390 + 0.0385i 0.0390 - 0.0385i 0.0769 + 0.0298i
0.0146 - 0.0427i -0.0432 + 0.1507i -0.0432 + 0.1507i -0.0304 - 0.1139i
0.0006 - 0.0038i -0.0030 + 0.0082i -0.0030 - 0.0082i 0.0005 + 0.0085i
-0.0054 + 0.0566i 0.0151 + 0.0107i 0.0151 - 0.0107i 0.0528 + 0.0081i
0.0104 - 0.0175i -0.0088 - 0.0742i -0.0088 + 0.0742i -0.0235 - 0.1016i
-0.0004 + 0.0037i 0.0031 - 0.0078i 0.0031 + 0.0078i -0.0004 - 0.0082i
0.0061 - 0.0533i -0.0145 - 0.0098i -0.0145 + 0.0098i -0.0502 - 0.0062i
-0.0096 + 0.0165i 0.0079 + 0.0697i 0.0079 - 0.0697i 0.0232 + 0.0952i
-0.0114 + 0.0125i -0.0063 - 0.0357i -0.0063 + 0.0357i -0.0085 - 0.0313i
-0.0282 - 0.3344i -0.0748 - 0.0796i -0.0748 + 0.0796i -0.2932 - 0.1379i
-0.0918 + 0.0899i 0.1473 + 0.4361i 0.1473 - 0.4361i 0.1455 + 0.6265i
-0.1987 + 0.0136i -0.3490 - 0.2228i -0.3490 + 0.2228i -0.2815 - 0.0879i
1.0000 - 0.0000i -0.1930 + 0.2245i -0.1930 - 0.2245i -0.2174 + 0.5731i
-0.2746 - 0.1202i 1.0000 + 0.0000i 1.0000 - 0.0000i 1.0000 - 0.0000i
```

```
Column 21
```

```
-0.0012 + 0.0201i
-0.1216 - 0.0885i
0.1134 + 0.0476i
-0.0214 - 0.0031i
0.1056 - 0.1224i
-0.0611 + 0.1172i
-0.0073 - 0.0301i
0.0769 - 0.0298i
-0.0304 + 0.1139i
0.0005 - 0.0085i
0.0528 - 0.0081i
-0.0235 + 0.1016i
-0.0004 + 0.0082i
-0.0502 + 0.0062i
0.0232 - 0.0952i
-0.0085 + 0.0313i
-0.2932 + 0.1379i
0.1455 - 0.6265i
-0.2815 + 0.0879i
-0.2174 - 0.5731i
1.0000 + 0.0000i
```

```
eigad =
```

```
1.0e+02 *
```

```
-0.4749 + 6.9429i
-0.4749 - 6.9429i
-0.4694 + 4.1219i
-0.4694 - 4.1219i
0.7469 + 0.6741i
0.7469 - 0.6741i
0.0822 + 0.8494i
0.0822 - 0.8494i
0.4806
0.4193
0.3465
0.3149
0.0002
0.1208
0.0503
```

# Table C.4.8 (cont'd)

```
0.0669 + 0.0014i
0.0669 - 0.0014i
0.1262
```

vad =

Columns 1 through 4

```
0.0047 + 0.0191i  0.0047 - 0.0191i  0.0063 + 0.0403i  0.0063 - 0.0403i
0.0311 + 0.0221i  0.0311 - 0.0221i -0.0026 - 0.0009i -0.0026 + 0.0009i
0.0001 + 0.0001i  0.0001 - 0.0001i  0.0004 + 0.0009i  0.0004 - 0.0009i
0.7964 - 0.1206i  0.7964 + 0.1206i  1.0000 - 0.0000i  1.0000 + 0.0000i
1.0000 - 0.0000i  1.0000 + 0.0000i -0.0484 + 0.0239i -0.0484 - 0.0239i
0.0064 - 0.0019i  0.0064 + 0.0019i  0.0233 - 0.0054i  0.0233 + 0.0054i
-0.0080 - 0.0362i -0.0080 + 0.0362i -0.0085 - 0.0767i -0.0085 + 0.0767i
-0.0028 - 0.0495i -0.0028 + 0.0495i  0.0049 + 0.0032i  0.0049 - 0.0032i
0.0006 - 0.0004i  0.0006 + 0.0004i -0.0007 - 0.0018i -0.0007 + 0.0018i
0.0025 + 0.0305i  0.0025 - 0.0305i -0.0025 + 0.0225i -0.0025 - 0.0225i
-0.0005 + 0.0079i -0.0005 - 0.0079i -0.0001 - 0.0002i -0.0001 + 0.0002i
0.0014 + 0.0061i  0.0014 - 0.0061i  0.0015 + 0.0133i  0.0015 - 0.0133i
0.0001 + 0.0030i  0.0001 - 0.0030i  0.0002 + 0.0061i  0.0002 - 0.0061i
0.0002 + 0.0037i  0.0002 - 0.0037i -0.0003 - 0.0002i -0.0003 + 0.0002i
-0.0002 + 0.0001i -0.0002 - 0.0001i -0.0004 + 0.0003i -0.0004 - 0.0003i
-0.0006 - 0.0042i -0.0006 + 0.0042i  0.0001 - 0.0030i  0.0001 + 0.0030i
0.0000 - 0.0017i  0.0000 + 0.0017i  0.0000 + 0.0001i  0.0000 - 0.0001i
-0.0004 - 0.0015i -0.0004 + 0.0015i -0.0006 - 0.0032i -0.0006 + 0.0032i
```

Columns 5 through 8

```
-0.1245 + 0.1457i -0.1245 - 0.1457i  0.0206 + 0.1980i  0.0206 - 0.1980i
0.0819 - 0.0080i  0.0819 + 0.0080i  0.0801 - 0.1411i  0.0801 + 0.1411i
-0.0208 - 0.0452i -0.0208 + 0.0452i -0.1319 + 0.0164i -0.1319 - 0.0164i
1.0000 + 0.0000i  1.0000 - 0.0000i  1.0000 + 0.0000i  1.0000 - 0.0000i
-0.3280 - 0.4136i -0.3280 + 0.4136i -0.6277 - 0.6030i -0.6277 + 0.6030i
-0.1150 + 0.2501i -0.1150 - 0.2501i  0.0165 + 0.7002i  0.0165 - 0.7002i
0.2286 - 0.2164i  0.2286 + 0.2164i  0.0346 - 0.3488i  0.0346 + 0.3488i
-0.1855 + 0.0139i -0.1855 - 0.0139i -0.2056 + 0.2451i -0.2056 - 0.2451i
0.0409 + 0.0802i  0.0409 - 0.0802i  0.2629 + 0.0000i  0.2629 - 0.0000i
0.0041 + 0.0037i  0.0041 - 0.0037i  0.0005 + 0.0046i  0.0005 - 0.0046i
0.0000 - 0.0006i  0.0000 + 0.0006i  0.0005 + 0.0007i  0.0005 - 0.0007i
-0.0345 + 0.0146i -0.0345 - 0.0146i -0.0808 + 0.0096i -0.0808 - 0.0096i
-0.0171 + 0.0251i -0.0171 - 0.0251i  0.0036 + 0.0260i  0.0036 - 0.0260i
0.0158 - 0.0063i  0.0158 + 0.0063i  0.0084 - 0.0204i  0.0084 + 0.0204i
-0.0042 - 0.0127i -0.0042 + 0.0127i -0.0252 - 0.0080i -0.0252 + 0.0080i
-0.0033 - 0.0007i -0.0033 + 0.0007i  0.0002 + 0.0020i  0.0002 - 0.0020i
-0.0015 + 0.0005i -0.0015 - 0.0005i -0.0032 + 0.0005i -0.0032 - 0.0005i
0.0097 - 0.0077i  0.0097 + 0.0077i  0.0134 - 0.0097i  0.0134 + 0.0097i
```

Columns 9 through 12

```
0.1357  0.3301  0.3042  0.9407
0.1842  0.1148  0.1808  0.9033
0.1569  0.1200  0.1143  1.0000
-0.2348 -0.4844 -0.2915 -0.8016
-0.3481 -0.2258 -0.2592 -0.9305
-0.3046 -0.1801 -0.1318 -0.9458
-0.1158 -0.4002 -0.2560 -0.8831
-0.1737 -0.1205 -0.2585 -0.9517
-0.1675 -0.0636 -0.0953 -0.9922
-0.0001 -0.0012  0.0003 -0.0016
0.0000 -0.0002 -0.0002 -0.0003
-0.0100  0.0116 -0.0089 -0.0417
0.5430  0.0007  1.0000  0.0270
1.0000 -0.4252 -0.6110 -0.0367
0.4500  1.0000 -0.1241 -0.0455
-0.7522  0.3047 -0.1180  0.0274
-0.2886 -0.2700  0.2127  0.0364
-0.2242 -0.3762 -0.2198  0.0365
```

Columns 13 through 16

```
1.0000  0.0556  0.1315  1.0000 - 0.0000i
0.9881  0.0629 -0.0578 -0.2796 - 0.0629i
0.9994 -0.1466 -0.0417 -0.5886 + 0.0524i
0.9990  0.0268  0.1009  0.6088 - 0.0085i
0.9928  0.0409 -0.0196 -0.1640 - 0.0354i
0.9990 -0.0407 -0.0225 -0.3457 + 0.0358i
```

# Table C.4.8 (cont'd)

```
0.9953 0.0024 0.0351 0.1576 - 0.0243i
0.9968 0.0554 -0.0597 -0.2838 + 0.0113i
0.9990 0.0178 -0.0228 -0.0076 + 0.0208i
-0.0002 0.0004 0.0003 0.0001 - 0.0000i
0.0000 0.0001 0.0001 0.0000 - 0.0000i
0.0000 -0.0072 0.0126 -0.0027 + 0.0001i
0.0000 0.4355 0.3412 0.0903 - 0.0078i
-0.0001 0.4659 0.3936 0.0486 - 0.0102i
0.0002 -0.2986 0.5803 0.0170 - 0.0076i
-0.0001 1.0000 0.4941 0.0992 - 0.0125i
0.0003 -0.4777 1.0000 0.0591 - 0.0156i
0.0001 -0.2004 0.7774 0.0590 - 0.0125i

Columns 17 through 18

1.0000 + 0.0000i 0.0839
-0.2796 + 0.0629i -0.1895
-0.5886 - 0.0524i 0.1638
0.6088 + 0.0085i 0.0275
-0.1640 + 0.0354i -0.0547
-0.3457 - 0.0358i 0.0374
0.1576 + 0.0243i -0.0177
-0.2838 - 0.0113i 0.0820
-0.0076 - 0.0208i -0.1223
0.0001 + 0.0000i 0.0002
0.0000 + 0.0000i -0.0001
-0.0027 - 0.0001i 0.0027
0.0903 + 0.0078i 0.2396
0.0486 + 0.0102i -0.2451
0.0170 + 0.0076i 0.0959
0.0992 + 0.0125i -0.1003
0.0591 + 0.0156i -0.7730
0.0590 + 0.0125i 1.0000
```

```
detjj =

 -6.0033e+30


detd =

 2.1031e+21


detda =

 -2.8546e+09


detad =

 8.0480e+27


condjj =

 2.4087e+06


condd =

 61.8176


condda =

 1.1557e+06


condad =

 7.6703e+06


vtt =

 1.0000 0.0062 -0.2789
```

## Table C.4.8 (cont'd)

```
-0.5335 1.0000 -0.3489
0.1256 0.0027 1.0000


eigtt =

 1.0e+03 *

 -0.1274
 -3.5600
 -0.0436
```

## Table C.4.9 Output for algebraic/dynamic 160 MVar

eigjj =

```
-26.3625 +52.4091i
-26.3625 -52.4091i
 47.9863
 41.9016
 39.4275
-12.7188 +25.1943i
-12.7188 -25.1943i
 24.7753
 -9.9658 +19.4280i
 -9.9658 -19.4280i
 22.7029
 20.8268
-15.8168
-16.5812
-16.6064
 -5.2985 +13.9175i
 -5.2985 -13.9175i
 -4.2669 +15.1141i
 -4.2669 -15.1141i
 -4.0509 +14.9680i
 -4.0509 -14.9680i
 10.7543 + 0.7291i
 10.7543 - 0.7291i
  8.8583
  7.2567
  1.7696
 -0.5073 + 1.5778i
 -0.5073 - 1.5778i
  0.8926
 -0.1464 + 1.1995i
 -0.1464 - 1.1995i
  0.3148
  0.0329
 -0.1347 + 0.9301i
 -0.1347 - 0.9301i
 -0.0524 + 0.5896i
 -0.0524 - 0.5896i
 -0.0527 + 0.6570i
 -0.0527 - 0.6570i
```

eigd =

```
-12.5516 +25.3908i
-12.5516 -25.3908i
 47.9862
 41.9035
 39.4309
 -9.7834 +19.4176i
 -9.7834 -19.4176i
 -5.4046 +14.0109i
 -5.4046 -14.0109i
 24.7776
 22.7421
 20.8486
  1.3117
  1.8161
 10.8424 + 0.7974i
 10.8424 - 0.7974i
  7.4401
  8.7768
```

eigda =

```
-26.5260 +52.2235i
-26.5260 -52.2235i
 -3.9004 +14.9037i
 -3.9004 -14.9037i
 -4.0921 +14.9912i
 -4.0921 -14.9912i
-16.4447
-15.1758
-16.5354
 -0.3094 + 1.7191i
 -0.3094 - 1.7191i
 -0.0078 + 1.1638i
 -0.0078 - 1.1638i
 -0.0668
 -0.1015
 -0.0593 + 0.5943i
 -0.0593 - 0.5943i
 -0.0760 + 0.6557i
 -0.0760 - 0.6557i
 -0.0932 + 0.9364i
 -0.0932 - 0.9364i
```

vda =

Columns 1 through 4

```
0.0000 - 0.0000i 0.0000 + 0.0000i 0.0000 + 0.0000i 0.0000 - 0.0000i
0.0000 + 0.0000i 0.0000 - 0.0000i 0.0000 - 0.0000i 0.0000 + 0.0000i
0.0000 + 0.0000i 0.0000 - 0.0000i 0.0000 + 0.0000i 0.0000 - 0.0000i
0.0000 + 0.0000i 0.0000 - 0.0000i 0.0000 - 0.0000i 0.0000 + 0.0000i
0.0000 - 0.0000i 0.0000 + 0.0000i 0.0000 + 0.0000i 0.0000 - 0.0000i
```

## Table C.4.9 (cont'd)

```
0.0000 - 0.0000i 0.0000 + 0.0000i 0.0000 - 0.0000i 0.0000 + 0.0000i
-0.0002 + 0.0003i -0.0002 - 0.0003i 0.0000 + 0.0000i 0.0000 - 0.0000i
0.0000 + 0.0000i 0.0000 - 0.0000i -0.0011 + 0.0007i -0.0011 - 0.0007i
0.0000 + 0.0000i 0.0000 - 0.0000i 0.0000 + 0.0002i 0.0000 - 0.0002i
0.0001 + 0.0000i 0.0001 - 0.0000i 0.0000 + 0.0002i 0.0000 - 0.0002i
0.0000 + 0.0000i 0.0000 - 0.0000i -0.0001 + 0.0007i -0.0001 - 0.0007i
0.0000 + 0.0000i 0.0000 - 0.0000i 0.0001 + 0.0003i 0.0001 - 0.0003i
-0.0048 - 0.0105i -0.0048 + 0.0105i 0.0000 - 0.0002i 0.0000 + 0.0002i
0.0000 - 0.0000i 0.0000 + 0.0000i -0.0021 - 0.0305i -0.0021 + 0.0305i
0.0000 - 0.0000i 0.0000 + 0.0000i -0.0075 - 0.0040i -0.0075 + 0.0040i
1.0000 - 0.0000i 1.0000 + 0.0000i 0.0044 - 0.0008i 0.0044 + 0.0008i
0.0000 + 0.0003i 0.0000 - 0.0003i 1.0000 + 0.0000i 1.0000 - 0.0000i
0.0000 + 0.0003i 0.0000 - 0.0003i 0.1416 - 0.2393i 0.1416 + 0.2393i
-0.0761 - 0.1539i -0.0761 + 0.1539i -0.0011 - 0.0027i -0.0011 + 0.0027i
0.0000 - 0.0000i 0.0000 + 0.0000i -0.0289 - 0.1105i -0.0289 + 0.1105i
0.0000 - 0.0000i 0.0000 + 0.0000i -0.0256 - 0.0081i -0.0256 + 0.0081i
```

Columns 5 through 8

```
0.0000 + 0.0000i 0.0000 - 0.0000i 0.0000 0.0000
0.0000 + 0.0000i 0.0000 - 0.0000i 0.0000 -0.0001
0.0000 - 0.0000i 0.0000 + 0.0000i 0.0000 0.0000
0.0000 + 0.0000i 0.0000 - 0.0000i 0.0000 0.0000
0.0000 - 0.0000i 0.0000 + 0.0000i 0.0000 0.0000
0.0000 + 0.0000i 0.0000 - 0.0000i 0.0000 0.0000
0.0000 + 0.0000i 0.0000 - 0.0000i -0.0004 0.0048
0.0000 - 0.0002i 0.0000 + 0.0002i 0.0011 0.0003
-0.0005 + 0.0003i -0.0005 - 0.0003i 0.0004 0.0001
0.0000 + 0.0001i 0.0000 - 0.0001i -0.0035 0.0459
-0.0001 + 0.0001i -0.0001 - 0.0001i 0.0566 0.0178
-0.0001 + 0.0005i -0.0001 - 0.0005i 0.0434 0.0191
0.0000 - 0.0001i 0.0000 + 0.0001i 0.0040 -0.0529
0.0054 + 0.0028i 0.0054 - 0.0028i -0.0337 -0.0115
-0.0017 - 0.0305i -0.0017 + 0.0305i -0.0261 -0.0124
0.0026 + 0.0007i 0.0026 - 0.0007i -0.0838 1.0000
-0.1057 + 0.1688i -0.1057 - 0.1688i 1.0000 0.3094
1.0000 + 0.0000i 1.0000 - 0.0000i 0.7568 0.3260
0.0001 - 0.0018i 0.0001 + 0.0018i 0.0532 -0.6907
0.0216 + 0.0065i 0.0216 - 0.0065i -0.1070 -0.0359
-0.0227 - 0.0932i -0.0227 + 0.0932i -0.0699 -0.0327
```

Columns 9 through 12

```
0.0000 0.0054 - 0.0001i 0.0054 + 0.0001i -0.0312 + 0.0097i
0.0000 -0.0103 - 0.0035i -0.0103 + 0.0035i 0.0975 + 0.0018i
0.0000 -0.0034 + 0.0034i -0.0034 - 0.0034i -0.0198 - 0.0156i
0.0000 -0.0006 - 0.0030i -0.0006 + 0.0030i 0.0085 + 0.0268i
0.0000 -0.0009 + 0.0062i -0.0009 - 0.0062i 0.0009 - 0.0838i
0.0000 0.0023 + 0.0016i 0.0023 - 0.0016i -0.0133 + 0.0171i
0.0000 -0.0184 - 0.0540i -0.0184 + 0.0540i 0.0490 + 0.0458i
-0.0007 -0.0248 + 0.0105i -0.0248 - 0.0105i -0.0435 - 0.1393i
0.0006 -0.0122 + 0.0064i -0.0122 - 0.0064i -0.0451 - 0.0393i
-0.0004 -0.0264 - 0.0405i -0.0264 + 0.0405i 0.0258 + 0.0070i
-0.0325 -0.0260 - 0.0033i -0.0260 + 0.0033i -0.0350 - 0.0979i
0.0574 -0.0254 - 0.0050i -0.0254 + 0.0050i -0.0480 - 0.0573i
0.0005 0.0261 + 0.0388i 0.0261 - 0.0388i -0.0247 - 0.0067i
0.0193 0.0251 + 0.0019i 0.0251 - 0.0019i 0.0366 + 0.0913i
-0.0343 0.0243 + 0.0038i 0.0243 - 0.0038i 0.0457 + 0.0527i
-0.0098 0.0388 + 0.1719i 0.0388 - 0.1719i -0.1044 - 0.0251i
-0.5755 0.1331 + 0.1040i 0.1331 - 0.1040i 0.0009 + 0.6616i
1.0000 0.1434 + 0.0779i 0.1434 - 0.0779i 0.3161 + 0.3880i
0.0062 1.0000 + 0.0000i 1.0000 - 0.0000i -0.5527 + 0.5693i
0.0613 0.0802 - 0.1502i 0.0802 + 0.1502i 1.0000 + 0.0000i
-0.0919 0.0755 - 0.1180i 0.0755 + 0.1180i 0.5648 - 0.1958i
```

Columns 13 through 16

```
-0.0312 - 0.0097i -0.0668 -0.1015 0.0682 - 0.1135i
0.0975 - 0.0018i -0.0635 -0.0976 -0.2643 + 0.2523i
-0.0198 + 0.0156i -0.0663 -0.1012 0.0290 - 0.0047i
0.0085 - 0.0268i 1.0000 1.0000 -0.2005 - 0.0947i
0.0009 + 0.0838i 0.9507 0.9615 0.4643 + 0.3984i
-0.0133 - 0.0171i 0.9927 0.9973 -0.0127 - 0.0475i
0.0490 - 0.0458i 0.0004 0.0010 0.0068 + 0.0199i
-0.0435 + 0.1393i 0.0080 0.0060 -0.1238 - 0.2035i
-0.0451 + 0.0393i -0.0006 -0.0008 0.0132 + 0.0386i
0.0258 - 0.0070i 0.0004 0.0007 0.0005 + 0.0042i
-0.0350 + 0.0979i -0.0002 -0.0002 -0.0053 - 0.0573i
```

# Table C.4.9 (cont'd)

```
-0.0480 + 0.0573i 0.0000 0.0000 0.0110 + 0.0162i
-0.0247 + 0.0067i -0.0006 -0.0009 -0.0003 - 0.0041i
0.0366 - 0.0913i 0.0002 0.0002 0.0060 + 0.0540i
0.0457 - 0.0527i 0.0000 0.0000 -0.0100 - 0.0154i
-0.1044 + 0.0251i 0.0170 0.0159 -0.0126 - 0.0144i
0.0009 - 0.6616i 0.0008 0.0011 -0.0284 + 0.3379i
0.3161 - 0.3880i 0.0000 0.0000 -0.1154 - 0.0699i
-0.5527 - 0.5693i 0.2697 0.2672 -0.2180 - 0.0221i
1.0000 - 0.0000i -0.0252 -0.0216 1.0000 - 0.0000i
0.5648 + 0.1958i 0.0001 0.0000 -0.2543 + 0.1276i
```

Columns 17 through 20

```
0.0682 + 0.1135i 0.0245 - 0.2575i 0.0245 + 0.2575i 0.0028 - 0.0183i
-0.2643 - 0.2523i -0.0420 + 0.0240i -0.0420 - 0.0240i -0.1340 + 0.0853i
0.0290 + 0.0047i -0.0760 + 0.6557i -0.0760 - 0.6557i 0.1137 - 0.0499i
-0.2005 + 0.0947i -0.3918 + 0.0080i -0.3918 - 0.0080i -0.0197 - 0.0010i
0.4643 - 0.3984i 0.0435 + 0.0591i 0.0435 - 0.0591i 0.1043 + 0.1327i
-0.0127 + 0.0475i 1.0000 - 0.0000i 1.0000 + 0.0000i -0.0647 - 0.1150i
0.0068 - 0.0199i 0.0361 + 0.0139i 0.0361 - 0.0139i -0.0084 + 0.0274i
-0.1238 + 0.2035i 0.0794 - 0.0049i 0.0794 + 0.0049i 0.0744 + 0.0491i
0.0132 - 0.0386i -0.1472 - 0.0251i -0.1472 + 0.0251i -0.0288 - 0.1115i
0.0005 - 0.0042i 0.0057 + 0.0061i 0.0057 - 0.0061i -0.0004 + 0.0081i
-0.0053 + 0.0573i 0.0219 - 0.0020i 0.0219 + 0.0020i 0.0524 + 0.0190i
0.0110 - 0.0162i -0.0720 - 0.0207i -0.0720 + 0.0207i -0.0235 - 0.1036i
-0.0003 + 0.0041i -0.0053 - 0.0060i -0.0053 + 0.0060i 0.0004 - 0.0078i
0.0060 - 0.0540i -0.0207 + 0.0023i -0.0207 - 0.0023i -0.0501 - 0.0166i
-0.0100 + 0.0154i 0.0671 + 0.0204i 0.0671 - 0.0204i 0.0224 + 0.0969i
-0.0126 + 0.0144i -0.0336 - 0.0097i -0.0336 + 0.0097i -0.0054 - 0.0303i
-0.0284 - 0.3379i -0.1291 - 0.0135i -0.1291 + 0.0135i -0.2706 - 0.1999i
-0.1154 + 0.0699i 0.4945 - 0.0429i 0.4945 + 0.0429i 0.2293 + 0.6329i
-0.2180 + 0.0221i -0.3340 + 0.1961i -0.3340 - 0.1961i -0.2548 - 0.1067i
1.0000 + 0.0000i -0.0011 + 0.3466i -0.0011 - 0.3466i -0.3273 + 0.5377i
-0.2543 - 0.1276i 0.3937 - 0.9020i 0.3937 + 0.9020i 1.0000 - 0.0000i
```

Column 21

```
0.0028 + 0.0183i
-0.1340 - 0.0853i
0.1137 + 0.0499i
-0.0197 + 0.0010i
0.1043 - 0.1327i
-0.0647 + 0.1150i
-0.0084 - 0.0274i
0.0744 - 0.0491i
-0.0288 + 0.1115i
-0.0004 - 0.0081i
0.0524 - 0.0190i
-0.0235 + 0.1036i
0.0004 + 0.0078i
-0.0501 + 0.0166i
0.0224 - 0.0969i
-0.0054 + 0.0303i
-0.2706 + 0.1999i
0.2293 - 0.6329i
-0.2548 + 0.1067i
-0.3273 - 0.5377i
1.0000 + 0.0000i
```

eigad =

1.0e+02 *

```
-0.4274 + 5.1559i
-0.4274 - 5.1559i
-0.4694 + 4.1096i
-0.4694 - 4.1096i
0.8182 + 0.4955i
0.8182 - 0.4955i
-0.0305 + 0.6959i
-0.0305 - 0.6959i
0.4767
0.4029
0.3443
0.3041
0.0002
0.0470
```

## Table C.4.9 (cont'd)

```
0.0689
0.1178
0.0627
0.1237
```

vad =

Columns 1 through 4

```
0.0038 + 0.0325i  0.0038 - 0.0325i  0.0063 + 0.0403i  0.0063 - 0.0403i
0.0086 + 0.0127i  0.0086 - 0.0127i -0.0025 - 0.0010i -0.0025 + 0.0010i
0.0001 + 0.0003i  0.0001 - 0.0003i  0.0002 + 0.0005i  0.0002 - 0.0005i
1.0000 + 0.0000i  1.0000 - 0.0000i  1.0000 - 0.0000i  1.0000 + 0.0000i
0.3530 + 0.0720i  0.3530 - 0.0720i -0.0499 + 0.0241i -0.0499 - 0.0241i
0.0095 - 0.0016i  0.0095 + 0.0016i  0.0149 - 0.0035i  0.0149 + 0.0035i
-0.0050 - 0.0615i -0.0050 + 0.0615i -0.0086 - 0.0767i -0.0086 + 0.0767i
0.0043 - 0.0239i  0.0043 + 0.0239i  0.0049 + 0.0033i  0.0049 - 0.0033i
0.0003 - 0.0006i  0.0003 + 0.0006i -0.0005 - 0.0011i -0.0005 + 0.0011i
-0.0023 + 0.0282i -0.0023 - 0.0282i -0.0025 + 0.0225i -0.0025 - 0.0225i
-0.0011 + 0.0037i -0.0011 - 0.0037i -0.0002 + 0.0004i -0.0002 + 0.0004i
0.0008 + 0.0104i  0.0008 - 0.0104i  0.0015 + 0.0131i  0.0015 - 0.0131i
-0.0002 + 0.0049i -0.0002 - 0.0049i  0.0002 + 0.0061i  0.0002 - 0.0061i
-0.0003 + 0.0018i -0.0003 - 0.0018i -0.0003 - 0.0002i -0.0003 + 0.0002i
-0.0003 + 0.0001i -0.0003 - 0.0001i -0.0004 + 0.0002i -0.0004 - 0.0002i
0.0000 - 0.0038i  0.0000 + 0.0038i  0.0001 - 0.0030i  0.0001 + 0.0030i
0.0002 - 0.0008i  0.0002 + 0.0008i  0.0001 + 0.0001i  0.0001 - 0.0001i
-0.0003 - 0.0025i -0.0003 + 0.0025i -0.0006 - 0.0031i -0.0006 + 0.0031i
```

Columns 5 through 8

```
-0.1653 + 0.1264i -0.1653 - 0.1264i -0.2034 - 0.1145i -0.2034 + 0.1145i
0.0696 + 0.0138i  0.0696 - 0.0138i  0.0840 + 0.2068i  0.0840 - 0.2068i
-0.0006 - 0.0397i -0.0006 + 0.0397i  0.0983 - 0.1795i  0.0983 + 0.1795i
1.0000 + 0.0000i  1.0000 - 0.0000i -0.7101 + 0.6987i -0.7101 - 0.6987i
-0.2498 - 0.3428i -0.2498 + 0.3428i  1.0000 - 0.0000i  1.0000 + 0.0000i
-0.1246 + 0.1710i -0.1246 - 0.1710i -0.6803 + 0.6569i -0.6803 + 0.6569i
0.2815 - 0.1793i  0.2815 + 0.1793i  0.2961 + 0.2851i  0.2961 - 0.2851i
-0.1650 - 0.0172i -0.1650 + 0.0172i -0.0885 - 0.4241i -0.0885 + 0.4241i
0.0074 + 0.0686i  0.0074 - 0.0686i -0.2570 + 0.3210i -0.2570 - 0.3210i
0.0045 + 0.0027i  0.0045 - 0.0027i -0.0025 - 0.0028i -0.0025 + 0.0028i
-0.0001 - 0.0008i -0.0001 + 0.0008i -0.0001 + 0.0014i -0.0001 - 0.0014i
-0.0389 + 0.0159i -0.0389 - 0.0159i  0.1004 - 0.0952i  0.1004 + 0.0952i
-0.0250 + 0.0242i -0.0250 - 0.0242i -0.0139 - 0.0251i -0.0139 + 0.0139i
0.0165 - 0.0031i  0.0165 + 0.0031i  0.0139 + 0.0238i  0.0139 - 0.0238i
0.0009 - 0.0135i  0.0009 + 0.0135i  0.0373 - 0.0194i  0.0373 + 0.0194i
-0.0030 - 0.0021i -0.0030 + 0.0021i -0.0031 - 0.0005i -0.0031 + 0.0005i
-0.0015 + 0.0008i -0.0015 - 0.0008i  0.0035 - 0.0031i  0.0035 + 0.0031i
0.0120 - 0.0075i  0.0120 + 0.0075i -0.0077 + 0.0240i -0.0077 - 0.0240i
```

Columns 9 through 12

```
0.0714  0.3903  0.2296 -0.8755
0.1604  0.1761  0.1242 -0.8885
0.1357  0.1572  0.0577 -0.9973
-0.1163 -0.5337 -0.2114  0.6914
-0.2924 -0.3090 -0.1847  0.8503
-0.2764 -0.2386 -0.0719  0.9508
-0.0346 -0.4537 -0.1769  0.7869
-0.1518 -0.1889 -0.1977  0.9323
-0.1524 -0.1031 -0.0437  1.0000
0.0002 -0.0012  0.0005  0.0013
0.0000 -0.0004 -0.0003  0.0006
-0.0168  0.0123 -0.0111  0.0632
0.5213  0.1023  1.0000 -0.0711
1.0000 -0.3815 -0.6012  0.0544
0.3310  1.0000 -0.1814  0.0732
-0.7510  0.2405 -0.1309 -0.0061
-0.2371 -0.2655  0.2170 -0.0553
-0.1814 -0.4132 -0.1933 -0.0494
```

Columns 13 through 16

```
1.0000  0.0939  1.0000  0.1019
0.9882 -0.0498 -0.3898 -0.0318
0.9997 -0.0303 -0.5035 -0.0608
0.9990  0.0751  0.5961  0.0453
0.9928 -0.0178 -0.2244  0.0112
```

# Table C.4.9 (cont'd)

```
0.9993 -0.0150 -0.2814 -0.0174
0.9954 0.0257 0.1171 -0.0060
0.9970 -0.0555 -0.2628 0.0954
0.9992 -0.0200 0.0343 -0.0379
-0.0002 0.0003 0.0001 0.0005
0.0000 0.0001 0.0000 0.0001
0.0000 0.0178 -0.0038 -0.0076
0.0000 0.2936 0.0767 0.5721
-0.0001 0.3542 0.0326 0.3868
0.0002 0.5544 0.0057 -0.2225
-0.0001 0.4295 0.0784 1.0000
0.0003 1.0000 0.0416 -0.8107
0.0002 0.6835 0.0376 0.3108
```

```
Columns 17 through 18
```

```
1.0000 0.0522
-0.1155 -0.1889
-0.7347 0.2106
0.6332 0.0150
-0.0676 -0.0649
-0.4393 0.0464
0.2244 -0.0150
-0.3113 0.0466
-0.0564 -0.1222
0.0001 0.0000
0.0000 -0.0001
-0.0044 0.0091
0.1081 0.0338
0.0748 -0.4045
0.0385 0.2461
0.1290 -0.5052
0.1136 -0.4809
0.0871 1.0000
```

detjj =

-4.5853e+30

detd =

1.4648e+21

detda =

-3.1304e+09

detad =

2.0335e+27

condjj =

2.4879e+06

condd =

60.9866

condda =

1.1942e+06

condad =

4.3957e+06

vtt =

## Table C.4.9 (cont'd)

```
1.0000 0.0107 -0.2629
-0.5245 1.0000 -0.3896
0.0815 0.0034 1.0000
         .

eigtt =

1.0e+03 *

-0.1213
-2.1531
-0.0316
```

## Table C.4.10 Output for algebraic/dynamic 170 MVar

eigjj =

```
-26.3797 +52.4173i
-26.3797 -52.4173i
 47.7826
 40.2813
 38.8520
-12.6302 +24.9980i
-12.6302 -24.9980i
 24.6874
 22.2377      ·
 20.1966
 -9.5934 +18.8025i
 -9.5934 -18.8025i
-15.8158
-16.6073
-16.5818
 -4.2540 +15.1464i
 -4.2540 -15.1464i
 -4.0594 +14.9700i
 -4.0594 -14.9700i
 -5.2398 +13.5730i
 -5.2398 -13.5730i
 10.4425 + 0.5844i
 10.4425 - 0.5844i
  9.0127
  7.0083
  1.6632
 -0.5111 + 1.5761i
 -0.5111 - 1.5761i
  0.8882
 -0.1538 + 1.2009i
 -0.1538 - 1.2009i
 -0.1563 + 0.9406i
 -0.1563 - 0.9406i
  0.3149
  0.0323
 -0.0535 + 0.6566i
 -0.0535 - 0.6566i
 -0.0552 + 0.5960i
 -0.0552 - 0.5960i
```

eigd =

```
-12.4605 +25.2025i
-12.4605 -25.2025i
 47.7826
 40.2851
 38.8534
 -9.4218 +18.7836i
 -9.4218 -18.7836i
 -5.3122 +13.7008i
 -5.3122 -13.7008i
 24.6893
 22.2731
 20.2200
  1.2223
  1.7561
  7.1667
 10.5407 + 0.6607i
 10.5407 - 0.6607i
  8.9260
```

eigda =

```
-26.5444 +52.2305i
-26.5444 -52.2305i
 -3.9033 +14.8989i
 -3.9033 -14.8989i
 -4.1104 +14.9864i
 -4.1104 -14.9864i
-16.4349
-15.1595
-16.5306
 -0.2952 + 1.7320i
 -0.2952 - 1.7320i
 -0.0016 + 1.1890i
 -0.0016 - 1.1890i
 -0.0636
 -0.1048
 -0.0630 + 0.6004i
 -0.0630 - 0.6004i
 -0.0770 + 0.6552i
 -0.0770 - 0.6552i
 -0.1122 + 0.9430i
 -0.1122 - 0.9430i
```

vda =

Columns 1 through 4

```
0.0000 - 0.0000i  0.0000 + 0.0000i  0.0000 + 0.0000i  0.0000 - 0.0000i
0.0000 + 0.0000i  0.0000 - 0.0000i  0.0000 - 0.0000i  0.0000 + 0.0000i
0.0000 + 0.0000i  0.0000 - 0.0000i  0.0000 + 0.0000i  0.0000 - 0.0000i
0.0000 + 0.0000i  0.0000 - 0.0000i  0.0000 - 0.0000i  0.0000 + 0.0000i
0.0000 - 0.0000i  0.0000 + 0.0000i  0.0000 + 0.0000i  0.0000 - 0.0000i
```

## Table C.4.10 (cont'd)

```
0.0000 - 0.0000i 0.0000 + 0.0000i 0.0000 - 0.0000i 0.0000 + 0.0000i
-0.0002 + 0.0003i -0.0002 - 0.0003i 0.0000 + 0.0000i 0.0000 - 0.0000i
0.0000 + 0.0000i 0.0000 - 0.0000i -0.0011 + 0.0007i -0.0011 - 0.0007i
0.0000 + 0.0000i 0.0000 - 0.0000i 0.0000 + 0.0002i 0.0000 - 0.0002i
0.0001 + 0.0000i 0.0001 - 0.0000i 0.0000 + 0.0002i 0.0000 - 0.0002i
0.0000 + 0.0000i 0.0000 - 0.0000i -0.0001 + 0.0008i -0.0001 - 0.0008i
0.0000 + 0.0000i 0.0000 - 0.0000i 0.0001 + 0.0004i 0.0001 - 0.0004i
-0.0048 - 0.0105i -0.0048 + 0.0105i -0.0001 - 0.0002i -0.0001 + 0.0002i
0.0000 - 0.0000i 0.0000 + 0.0000i -0.0021 - 0.0306i -0.0021 + 0.0306i
0.0000 - 0.0000i 0.0000 + 0.0000i -0.0082 - 0.0041i -0.0082 + 0.0041i
1.0000 - 0.0000i 1.0000 + 0.0000i 0.0047 - 0.0009i 0.0047 + 0.0009i
0.0000 + 0.0003i 0.0000 - 0.0003i 1.0000 - 0.0000i 1.0000 + 0.0000i
0.0000 + 0.0003i 0.0000 - 0.0003i 0.1422 - 0.2597i 0.1422 + 0.2597i
-0.0761 - 0.1539i -0.0761 + 0.1539i -0.0012 - 0.0029i -0.0012 + 0.0029i
0.0000 - 0.0000i 0.0000 + 0.0000i -0.0289 - 0.1105i -0.0289 + 0.1105i
0.0000 - 0.0000i 0.0000 + 0.0000i -0.0276 - 0.0078i -0.0276 + 0.0078i
```

Columns 5 through 8

```
0.0000 + 0.0000i 0.0000 - 0.0000i 0.0000 0.0000
0.0000 + 0.0000i 0.0000 - 0.0000i 0.0000 -0.0001
0.0000 - 0.0000i 0.0000 + 0.0000i 0.0000 0.0000
0.0000 + 0.0000i 0.0000 - 0.0000i 0.0000 0.0000
0.0000 - 0.0000i 0.0000 + 0.0000i 0.0000 0.0000
0.0000 + 0.0000i 0.0000 - 0.0000i 0.0000 0.0000
0.0000 + 0.0000i 0.0000 - 0.0000i -0.0004 0.0048
0.0000 - 0.0002i 0.0000 + 0.0002i 0.0011 0.0003
-0.0005 + 0.0003i -0.0005 - 0.0003i 0.0005 0.0001
0.0000 + 0.0001i 0.0000 - 0.0001i -0.0039 0.0461
-0.0001 + 0.0001i -0.0001 - 0.0001i 0.0566 0.0184
-0.0001 + 0.0006i -0.0001 - 0.0006i 0.0501 0.0212
0.0000 - 0.0001i 0.0000 + 0.0001i 0.0045 -0.0531
0.0055 + 0.0026i 0.0055 - 0.0026i -0.0337 -0.0119
-0.0016 - 0.0306i -0.0016 + 0.0306i -0.0302 -0.0138
0.0028 + 0.0007i 0.0028 - 0.0007i -0.0932 1.0000
-0.1002 + 0.1723i -0.1002 - 0.1723i 1.0000 0.3199
1.0000 - 0.0000i 1.0000 + 0.0000i 0.8703 0.3612
0.0001 - 0.0019i 0.0001 + 0.0019i 0.0593 -0.6932
0.0218 + 0.0058i 0.0218 - 0.0058i -0.1071 -0.0372
-0.0226 - 0.0933i -0.0226 + 0.0933i -0.0807 -0.0364
```

Columns 9 through 12

```
0.0000 0.0053 + 0.0002i 0.0053 - 0.0002i -0.0305 + 0.0102i
0.0000 -0.0101 - 0.0035i -0.0101 + 0.0035i 0.0887 - 0.0030i
0.0000 -0.0032 + 0.0030i -0.0032 - 0.0030i -0.0139 - 0.0124i
0.0000 -0.0004 - 0.0030i -0.0004 + 0.0030i 0.0086 + 0.0257i
0.0000 -0.0010 + 0.0060i -0.0010 - 0.0060i -0.0026 - 0.0746i
0.0000 0.0020 + 0.0015i 0.0020 - 0.0015i -0.0104 + 0.0117i
0.0000 -0.0178 - 0.0534i -0.0178 + 0.0534i 0.0532 + 0.0503i
-0.0007 -0.0252 + 0.0112i -0.0252 - 0.0112i -0.0465 - 0.1357i
0.0006 -0.0134 + 0.0065i -0.0134 - 0.0065i -0.0418 - 0.0483i
-0.0003 -0.0267 - 0.0402i -0.0267 + 0.0402i 0.0292 + 0.0079i
-0.0352 -0.0274 - 0.0027i -0.0274 + 0.0027i -0.0368 - 0.0991i
0.0575 -0.0290 - 0.0051i -0.0290 + 0.0051i -0.0475 - 0.0713i
0.0004 0.0263 + 0.0385i 0.0263 - 0.0385i -0.0280 - 0.0076i
0.0208 0.0264 + 0.0012i 0.0264 - 0.0012i 0.0383 + 0.0923i
-0.0344 0.0277 + 0.0038i 0.0277 - 0.0038i 0.0454 + 0.0657i
-0.0084 0.0437 + 0.1732i 0.0437 - 0.1732i -0.1205 - 0.0284i
-0.6219 0.1441 + 0.1058i 0.1441 - 0.1058i 0.0068 + 0.6760i
1.0000 0.1685 + 0.0825i 0.1685 - 0.0825i 0.3259 + 0.4834i
0.0053 1.0000 - 0.0000i 1.0000 + 0.0000i -0.6252 + 0.6291i
0.0662 0.0815 - 0.1596i 0.0815 + 0.1596i 1.0000 - 0.0000i
-0.0922 0.0848 - 0.1350i 0.0848 + 0.1350i 0.6583 - 0.1414i
```

Columns 13 through 16

```
-0.0305 - 0.0102i -0.0636 -0.1048 0.0750 - 0.1208i
0.0887 + 0.0030i -0.0605 -0.1010 -0.2792 + 0.2640i
-0.0139 + 0.0124i -0.0631 -0.1046 0.0246 - 0.0003i
0.0086 - 0.0257i 1.0000 1.0000 -0.2120 - 0.1027i
-0.0026 + 0.0746i 0.9517 0.9643 0.4832 + 0.4143i
-0.0104 - 0.0117i 0.9927 0.9981 -0.0047 - 0.0404i
0.0532 - 0.0503i 0.0004 0.0011 0.0069 + 0.0207i
-0.0465 + 0.1357i 0.0074 0.0052 -0.1215 - 0.2002i
-0.0418 + 0.0483i -0.0006 -0.0008 0.0132 + 0.0386i
0.0292 - 0.0079i 0.0004 0.0008 0.0004 + 0.0045i
-0.0368 + 0.0991i -0.0001 -0.0002 -0.0052 - 0.0579i
```

# Table C.4.10 (cont'd)

```
-0.0475 + 0.0713i 0.0000 0.0000 0.0119 + 0.0163i
-0.0280 + 0.0076i -0.0006 -0.0009 -0.0003 - 0.0043i
0.0383 - 0.0923i 0.0001 0.0002 0.0059 + 0.0546i
0.0454 - 0.0657i 0.0000 0.0000 -0.0107 - 0.0155i
-0.1205 + 0.0284i 0.0177 0.0165 -0.0137 - 0.0155i
0.0068 - 0.6760i 0.0007 0.0010 -0.0281 + 0.3413i
0.3259 - 0.4834i 0.0001 0.0000 -0.1271 - 0.0643i
-0.6252 - 0.6291i 0.2650 0.2620 -0.2281 - 0.0270i
1.0000 + 0.0000i -0.0232 -0.0193 1.0000 + 0.0000i
0.6583 + 0.1414i 0.0002 0.0000 -0.2537 + 0.1376i
```

Columns 17 through 20

```
0.0750 + 0.1208i 0.0223 - 0.2503i 0.0223 + 0.2503i 0.0067 - 0.0156i
-0.2792 - 0.2640i -0.0328 + 0.0095i -0.0328 - 0.0095i -0.1436 + 0.0745i
0.0246 + 0.0003i -0.0770 + 0.6552i -0.0770 - 0.6552i 0.1123 - 0.0469i
-0.2120 + 0.1027i -0.3807 + 0.0107i -0.3807 - 0.0107i -0.0171 - 0.0050i
0.4832 - 0.4143i 0.0200 + 0.0478i 0.0200 - 0.0478i 0.0958 + 0.1409i
-0.0047 + 0.0404i 1.0000 - 0.0000i 1.0000 + 0.0000i -0.0631 - 0.1115i
0.0069 - 0.0207i 0.0343 + 0.0120i 0.0343 - 0.0120i -0.0081 + 0.0237i
-0.1215 + 0.2002i 0.0794 + 0.0004i 0.0794 - 0.0004i 0.0641 + 0.0675i
0.0132 - 0.0386i -0.1410 - 0.0219i -0.1410 + 0.0219i -0.0256 - 0.1112i
0.0004 - 0.0045i 0.0054 + 0.0056i 0.0054 - 0.0056i -0.0010 + 0.0072i
-0.0052 + 0.0579i 0.0212 - 0.0001i 0.0212 + 0.0001i 0.0469 + 0.0303i
0.0119 - 0.0163i -0.0694 - 0.0183i -0.0694 + 0.0183i -0.0225 - 0.1054i
-0.0003 + 0.0043i -0.0051 - 0.0055i -0.0051 + 0.0055i 0.0010 - 0.0069i
0.0059 - 0.0546i -0.0201 + 0.0005i -0.0201 - 0.0005i -0.0452 - 0.0274i
-0.0107 + 0.0155i 0.0646 + 0.0184i 0.0646 - 0.0184i 0.0213 + 0.0987i
-0.0137 + 0.0155i -0.0326 - 0.0080i -0.0326 + 0.0080i -0.0031 - 0.0274i
-0.0281 - 0.3413i -0.1228 - 0.0232i -0.1228 + 0.0232i -0.2180 - 0.2539i
-0.1271 + 0.0643i 0.4832 - 0.0771i 0.4832 + 0.0771i 0.2477 + 0.6373i
-0.2281 + 0.0270i -0.3096 + 0.1880i -0.3096 - 0.1880i -0.2180 - 0.1101i
1.0000 - 0.0000i -0.0302 + 0.3327i -0.0302 - 0.3327i -0.4264 + 0.4516i
-0.2537 - 0.1376i 0.3597 - 0.8707i 0.3597 + 0.8707i 1.0000 + 0.0000i
```

Column 21

```
0.0067 + 0.0156i
-0.1436 - 0.0745i
0.1123 + 0.0469i
-0.0171 + 0.0050i
0.0958 - 0.1409i
-0.0631 + 0.1115i
-0.0081 - 0.0237i
0.0641 - 0.0675i
-0.0256 + 0.1112i
-0.0010 - 0.0072i
0.0469 - 0.0303i
-0.0225 + 0.1054i
0.0010 + 0.0069i
-0.0452 + 0.0274i
0.0213 - 0.0987i
-0.0031 + 0.0274i
-0.2182 + 0.2539i
0.2477 - 0.6373i
-0.2180 + 0.1101i
-0.4264 - 0.4516i
1.0000 - 0.0000i
```

eigad =

1.0e+02 *

```
-0.3418 + 4.3639i
-0.3418 - 4.3639i
-0.5307 + 3.8043i
-0.5307 - 3.8043i
0.8175 + 0.4294i
0.8175 - 0.4294i
-0.0495 + 0.6412i
-0.0495 - 0.6412i
0.4738
0.3852
0.3417
0.2942
0.0002
0.0438
```

## Table C.4.10 (cont'd)

```
0.0696
0.1143
0.0598
0.1229
```

vad =

Columns 1 through 4

```
0.0045 + 0.0383i  0.0045 - 0.0383i  0.0080 + 0.0431i  0.0080 - 0.0431i
0.0023 + 0.0029i  0.0023 - 0.0029i -0.0054 - 0.0042i -0.0054 + 0.0042i
0.0001 + 0.0004i  0.0001 - 0.0004i  0.0003 + 0.0005i  0.0003 - 0.0005i
1.0000 + 0.0000i  1.0000 - 0.0000i  1.0000 + 0.0000i  1.0000 + 0.0000i
0.0814 + 0.0008i  0.0814 - 0.0008i -0.1300 + 0.0295i -0.1300 - 0.0295i
0.0115 - 0.0018i  0.0115 + 0.0018i  0.0147 - 0.0042i  0.0147 + 0.0042i
-0.0055 - 0.0725i -0.0055 + 0.0725i -0.0113 - 0.0821i -0.0113 + 0.0821i
0.0018 - 0.0066i  0.0018 + 0.0066i  0.0070 + 0.0102i  0.0070 - 0.0102i
-0.0001 - 0.0008i -0.0001 + 0.0008i -0.0007 - 0.0010i -0.0007 + 0.0010i
-0.0019 + 0.0248i -0.0019 - 0.0248i -0.0030 + 0.0217i -0.0030 - 0.0217i
-0.0001 + 0.0011i -0.0001 - 0.0011i -0.0001 - 0.0016i -0.0001 + 0.0016i
0.0009 + 0.0123i  0.0009 - 0.0123i  0.0020 + 0.0140i  0.0020 - 0.0140i
-0.0001 + 0.0058i -0.0001 - 0.0058i  0.0004 + 0.0065i  0.0004 - 0.0065i
-0.0001 + 0.0005i -0.0001 - 0.0005i -0.0005 - 0.0007i -0.0005 + 0.0007i
-0.0003 + 0.0001i -0.0003 - 0.0001i -0.0004 + 0.0002i -0.0004 - 0.0002i
0.0000 - 0.0033i  0.0000 + 0.0033i  0.0001 - 0.0028i  0.0001 + 0.0028i
0.0000 - 0.0002i  0.0000 + 0.0002i  0.0001 + 0.0003i  0.0001 - 0.0003i
-0.0004 - 0.0029i -0.0004 + 0.0029i -0.0007 - 0.0033i -0.0007 + 0.0033i
```

Columns 5 through 8

```
-0.1817 + 0.1206i -0.1817 - 0.1206i  0.2245 - 0.0725i  0.2245 + 0.0725i
0.0650 + 0.0214i  0.0650 - 0.0214i -0.2190 - 0.0899i -0.2190 + 0.0899i
0.0052 - 0.0367i  0.0052 + 0.0367i  0.0663 + 0.2109i  0.0663 - 0.2109i
1.0000 - 0.0000i  1.0000 + 0.0000i  0.0163 - 0.9434i  0.0163 + 0.9434i
-0.2165 - 0.3200i -0.2165 + 0.3200i -0.7161 + 0.6867i -0.7161 - 0.6867i
-0.1308 + 0.1511i -0.1308 - 0.1511i  1.0000 - 0.0000i  1.0000 + 0.0000i
0.3028 - 0.1677i  0.3028 + 0.1677i -0.4135 + 0.0159i -0.4135 - 0.0159i
-0.1572 - 0.0268i -0.1572 + 0.0268i  0.3863 + 0.2442i  0.3863 - 0.2442i
-0.0026 + 0.0639i -0.0026 - 0.0639i -0.0516 - 0.4451i -0.0516 + 0.4451i
0.0047 + 0.0024i  0.0047 - 0.0024i  0.0034 + 0.0003i  0.0034 - 0.0003i
-0.0001 - 0.0011i -0.0001 + 0.0011i -0.0013 - 0.0015i -0.0013 + 0.0015i
-0.0414 + 0.0158i -0.0414 - 0.0158i -0.0121 + 0.1561i -0.0121 - 0.1561i
-0.0284 + 0.0240i -0.0284 - 0.0240i  0.0269 - 0.0085i  0.0269 + 0.0085i
0.0168 - 0.0020i  0.0168 + 0.0020i -0.0275 - 0.0067i -0.0275 + 0.0067i
0.0030 - 0.0132i  0.0030 + 0.0132i -0.0151 + 0.0434i -0.0151 - 0.0434i
-0.0029 - 0.0026i -0.0029 + 0.0026i  0.0026 - 0.0023i  0.0026 + 0.0023i
-0.0015 + 0.0009i -0.0015 - 0.0009i -0.0009 + 0.0046i -0.0009 - 0.0046i
0.0129 - 0.0073i  0.0129 + 0.0073i -0.0113 - 0.0259i -0.0113 + 0.0259i
```

Columns 9 through 12

```
0.0267 0.4460 0.1591 -0.8247
0.1433 0.2380 0.0711 -0.8855
0.1173 0.1971 0.0050 -0.9813
-0.0356 -0.5623 -0.1374 0.6047
-0.2536 -0.3793 -0.1160 0.7878
-0.2553 -0.3035 -0.0099 0.9683
0.0210 -0.4949 -0.1031 0.7121
-0.1363 -0.2605 -0.1411 0.9242
-0.1381 -0.1460 0.0030 1.0000
0.0004 -0.0011 0.0007 0.0011
0.0001 -0.0007 -0.0004 0.0008
-0.0206 0.0074 -0.0108 0.0729
0.5036 0.2350 1.0000 -0.0926
1.0000 -0.3880 -0.5867 0.0620
0.2451 1.0000 -0.2792 0.0968
-0.7483 0.1895 -0.1498 0.0090
-0.2002 -0.2525 0.2345 -0.0669
-0.1506 -0.4624 -0.1497 -0.0634
```

Columns 13 through 16

```
1.0000 0.0840 1.0000 0.1269
0.9883 -0.0383 -0.4421 -0.0836
0.9998 -0.0437 -0.4693 -0.0040
0.9990 0.0685 0.5911 0.0572
0.9929 -0.0124 -0.2527 -0.0070
```

# Table C.4.10 (cont'd)

```
0.9994 -0.0243 -0.2496 -0.0026
0.9954 0.0262 0.0985 -0.0099
0.9970 -0.0614 -0.2520 0.1158
0.9993 -0.0192 0.0582 -0.0706
-0.0002 0.0002 0.0001 0.0006
0.0000 0.0002 0.0000 0.0002
0.0001 0.0188 -0.0041 -0.0049
0.0000 0.2555 0.0697 0.6519
-0.0001 0.3216 0.0232 0.3530
0.0002 0.5320 -0.0012 -0.1347
-0.0001 0.3777 0.0666 1.0000
0.0003 1.0000 0.0285 -0.9601
0.0002 0.6023 0.0274 0.6374

Columns 17 through 18

1.0000 0.0332
-0.0070 -0.1815
-0.8430 0.2334
0.6500 0.0073
-0.0004 -0.0673
-0.5035 0.0443
0.2709 -0.0125
-0.3271 0.0274
-0.0846 -0.1254
0.0001 -0.0001
0.0000 -0.0003
-0.0055 0.0132
0.1117 -0.0732
0.0831 -0.4905
0.0441 0.3337
0.1358 -0.7182
0.1375 -0.3446
0.0908 1.0000


detjj =

 -3.2336e+30


detd =

 9.6001e+20


detda =

 -3.3683e+09


detad =

 7.7356e+26


condjj =

 2.5317e+06


condd =

 61.6129


condda =

 1.2151e+06


condad =

 2.9276e+06


vtt =
```

## Table C.4.10 (cont'd)

```
1.0000 0.0156 -0.2700
-0.5389 1.0000 -0.4010
0.0836 0.0051 1.0000


eigtt =

1.0e+03 *

-0.1158
-1.5233
-0.0302
```

## Table C.4.11 Output for algebraic/dynamic 170 MVar(without exciter in)

eigjj =

```
-26.3797 +52.4173i
-26.3797 -52.4173i
 47.7826
 40.2813
 38.8519
-12.6304 +24.9974i
-12.6304 -24.9974i
 -9.6232 +18.7806i
 -9.6232 -18.7806i
 24.6874
 22.2368
-16.5881
 20.1955
-15.8172
 -4.1193 +15.0161i
 -4.1193 -15.0161i
 -5.2809 +13.6434i
 -5.2809 -13.6434i
 10.4417 + 0.5833i
 10.4417 - 0.5833i
  9.0174
  6.9834
 -0.4966 + 1.5689i
 -0.4966 - 1.5689i
  1.4438
 -0.1346 + 1.1794i
 -0.1346 - 1.1794i
 -0.0585 + 0.7173i
 -0.0585 - 0.7173i
 -0.0544 + 0.6062i
 -0.0544 - 0.6062i
  0.5180 + 0.1080i
  0.5180 - 0.1080i
  0.0338
  0.1944
```

eigd =

```
-12.4605 +25.2025i
-12.4605 -25.2025i
 47.7826
 40.2851
 38.8534
 -9.4218 +18.7836i
 -9.4218 -18.7836i
 -5.3122 +13.7008i
 -5.3122 -13.7008i
 24.6893
 22.2731
 20.2200
  1.2223
  1.7561
  7.1667
 10.5407 + 0.6607i
 10.5407 - 0.6607i
  8.9260
```

eigda =

```
-26.5444 +52.2305i
-26.5444 -52.2305i
 -3.8928 +14.9079i
 -3.8928 -14.9079i
-16.4681
-15.1809
 -0.3277 + 1.6990i
 -0.3277 - 1.6990i
 -0.0478 + 1.1154i
 -0.0478 - 1.1154i
 -0.0683 + 0.6982i
 -0.0683 - 0.6982i
 -0.0630 + 0.6124i
 -0.0630 - 0.6124i
 -0.1048
 -0.0636
  0.2004
```

vda =

Columns 1 through 4

```
 0.0000 - 0.0000i  0.0000 + 0.0000i  0.0000 + 0.0000i  0.0000 - 0.0000i
 0.0000 + 0.0000i  0.0000 - 0.0000i  0.0000 - 0.0000i  0.0000 + 0.0000i
 0.0000 + 0.0000i  0.0000 - 0.0000i  0.0000 - 0.0000i  0.0000 - 0.0000i
 0.0000 + 0.0000i  0.0000 - 0.0000i  0.0000 - 0.0000i  0.0000 + 0.0000i
 0.0000 - 0.0000i  0.0000 + 0.0000i  0.0000 + 0.0000i  0.0000 - 0.0000i
 0.0000 - 0.0000i  0.0000 + 0.0000i  0.0000 - 0.0000i  0.0000 + 0.0000i
-0.0002 + 0.0003i -0.0002 - 0.0003i  0.0000 + 0.0000i  0.0000 - 0.0000i
 0.0000 + 0.0000i  0.0000 - 0.0000i -0.0011 + 0.0007i -0.0011 - 0.0007i
 0.0000 + 0.0000i  0.0000 - 0.0000i  0.0000 + 0.0000i  0.0000 - 0.0000i
 0.0001 + 0.0000i  0.0001 - 0.0000i  0.0000 + 0.0002i  0.0000 - 0.0002i
 0.0000 + 0.0000i  0.0000 - 0.0000i  0.0000 + 0.0007i -0.0001 - 0.0007i
-0.0048 - 0.0105i -0.0048 + 0.0105i  0.0000 - 0.0002i  0.0000 + 0.0002i
 0.0000 - 0.0000i  0.0000 + 0.0000i -0.0021 - 0.0305i -0.0021 + 0.0305i
```

## Table C.4.11 (cont'd)

```
1.0000 + 0.0000i 1.0000 - 0.0000i 0.0042 - 0.0001i 0.0042 + 0.0001i
0.0000 + 0.0003i 0.0000 - 0.0003i 1.0000 + 0.0000i 1.0000 - 0.0000i
-0.0761 - 0.1539i -0.0761 + 0.1539i -0.0006 - 0.0027i -0.0006 + 0.0027i
0.0000 - 0.0000i 0.0000 + 0.0000i -0.0288 - 0.1105i -0.0288 + 0.1105i
```

Columns 5 through 8

```
0.0000 0.0000 0.0053 - 0.0005i 0.0053 + 0.0005i
0.0000 -0.0001 -0.0098 - 0.0036i -0.0098 + 0.0036i
0.0000 0.0000 -0.0036 + 0.0044i -0.0036 - 0.0044i
0.0000 0.0000 -0.0008 - 0.0030i -0.0008 + 0.0030i
0.0000 0.0000 -0.0010 + 0.0060i -0.0010 - 0.0060i
0.0000 0.0000 0.0029 + 0.0016i 0.0029 - 0.0016i
-0.0002 0.0048 -0.0194 - 0.0542i -0.0194 + 0.0542i
0.0011 0.0003 -0.0236 + 0.0095i -0.0236 - 0.0095i
0.0000 -0.0001 -0.0050 + 0.0087i -0.0050 - 0.0087i
-0.0022 0.0460 -0.0259 - 0.0409i -0.0259 + 0.0409i
0.0566 0.0177 -0.0241 - 0.0038i -0.0241 + 0.0038i
0.0026 -0.0530 0.0256 + 0.0392i 0.0256 - 0.0392i
-0.0336 -0.0114 0.0233 + 0.0025i 0.0233 - 0.0025i
-0.0538 1.0000 0.0405 + 0.1699i 0.0405 - 0.1699i
1.0000 0.3070 0.1203 + 0.0994i 0.1203 - 0.0994i
0.0342 -0.6921 1.0000 + 0.0000i 1.0000 - 0.0000i
-0.1069 -0.0356 0.0772 - 0.1388i 0.0772 + 0.1388i
```

Columns 9 through 12

```
-0.0307 + 0.0075i -0.0307 - 0.0075i -0.1340 + 0.0562i -0.1340 - 0.0562i
0.1203 + 0.0040i 0.1203 - 0.0040i -0.1202 + 0.3121i -0.1202 - 0.3121i
-0.0429 - 0.0103i -0.0429 + 0.0103i 0.4469 - 0.4506i 0.4469 + 0.4506i
0.0079 + 0.0272i 0.0079 - 0.0272i 0.0983 + 0.1823i 0.0983 - 0.1823i
-0.0011 - 0.1078i -0.0011 + 0.1078i 0.4594 + 0.1272i 0.4594 - 0.1272i
-0.0075 + 0.0388i -0.0075 - 0.0388i -0.7012 - 0.5714i -0.7012 + 0.5714i
0.0305 + 0.0363i 0.0305 - 0.0363i 0.0180 + 0.0139i 0.0180 - 0.0139i
-0.0376 - 0.1464i -0.0376 + 0.1464i -0.0956 - 0.1393i -0.0956 + 0.1393i
-0.0210 + 0.0069i -0.0210 - 0.0069i -0.0271 + 0.0199i -0.0271 - 0.0199i
0.0160 + 0.0076i 0.0160 - 0.0076i 0.0055 - 0.0004i 0.0055 + 0.0004i
-0.0300 - 0.0969i -0.0300 + 0.0969i -0.0085 - 0.0666i -0.0085 + 0.0666i
-0.0154 - 0.0074i -0.0154 + 0.0074i -0.0053 + 0.0002i -0.0053 - 0.0002i
0.0316 + 0.0907i 0.0316 - 0.0907i 0.0093 + 0.0628i 0.0093 - 0.0628i
-0.0658 - 0.0244i -0.0658 + 0.0244i -0.0199 + 0.0127i -0.0199 - 0.0127i
-0.0194 + 0.6341i -0.0194 - 0.6341i -0.0311 + 0.3969i -0.0311 - 0.3969i
-0.4222 + 0.3308i -0.4222 - 0.3308i -0.0470 + 0.2400i -0.0470 - 0.2400i
1.0000 + 0.0000i 1.0000 - 0.0000i 1.0000 + 0.0000i 1.0000 - 0.0000i
```

Columns 13 through 16

```
0.0757 - 0.1654i 0.0757 + 0.1654i -0.1048 -0.0636
-0.2599 + 0.3043i -0.2599 - 0.3043i -0.1011 -0.0605
-0.0132 + 0.0829i -0.0132 - 0.0829i -0.1046 -0.0631
-0.2799 - 0.0948i -0.2799 + 0.0948i 1.0000 1.0000
0.5350 + 0.3693i 0.5350 - 0.3693i 0.9643 0.9517
0.1361 + 0.0076i 0.1361 - 0.0076i 0.9981 0.9926
0.0175 + 0.0286i 0.0175 - 0.0286i 0.0011 0.0004
-0.1202 - 0.1793i -0.1202 + 0.1793i 0.0052 0.0074
-0.0217 + 0.0082i -0.0217 - 0.0082i -0.0008 -0.0005
0.0020 + 0.0060i 0.0020 - 0.0060i 0.0008 0.0004
-0.0056 - 0.0590i -0.0056 + 0.0590i -0.0002 -0.0001
-0.0018 - 0.0059i -0.0018 + 0.0059i -0.0009 -0.0006
0.0063 + 0.0556i 0.0063 - 0.0556i 0.0002 0.0001
-0.0233 - 0.0171i -0.0233 + 0.0171i 0.0165 0.0177
-0.0281 + 0.3481i -0.0281 - 0.3481i 0.0010 0.0007
-0.3167 + 0.0340i -0.3167 - 0.0340i 0.2620 0.2650
1.0000 + 0.0000i 1.0000 - 0.0000i -0.0193 -0.0233
```

Column 17

```
-0.0166
-0.0651
0.0428
-0.0828
-0.3247
0.2137
0.1094
0.2565
-0.5464
-0.0022
-0.0183
```

0.001
0.01
0.02
0.12
0.31
1.0

eigac

1.0

Table C.4.11 (cont'd)

```
0.0019
0.0170
0.0298
0.1217
0.3195
1.0000


eigad =

1.0e+02 *

-0.5787 + 4.1551i
-0.5787 - 4.1551i
-0.2333 + 4.0727i
-0.2333 - 4.0727i
 1.1720
 0.5331
 0.4652
 0.3840
 0.3406
-0.0397 + 0.0947i
-0.0397 - 0.0947i
-0.0272
 0.1799
 0.0002
 0.0717
 0.1080
 0.0578
 0.1147


vad =

Columns 1 through 4

0.0071 + 0.0395i  0.0071 - 0.0395i  0.0041 + 0.0412i  0.0041 - 0.0412i
-0.0030 + 0.0019i -0.0030 - 0.0019i  0.0015 - 0.0023i  0.0015 + 0.0023i
0.0000 + 0.0000i  0.0000 - 0.0000i  0.0000 + 0.0000i  0.0000 - 0.0000i
1.0000 + 0.0000i  1.0000 - 0.0000i  1.0000 + 0.0000i  1.0000 - 0.0000i
-0.0117 + 0.0740i -0.0117 - 0.0740i -0.0185 - 0.0544i -0.0185 + 0.0544i
0.0003 - 0.0001i  0.0003 + 0.0001i  0.0003 - 0.0000i  0.0003 + 0.0000i
-0.0103 - 0.0752i -0.0103 + 0.0752i -0.0043 + 0.0779i -0.0043 + 0.0779i
0.0084 - 0.0005i  0.0084 + 0.0005i -0.0019 + 0.0016i -0.0019 - 0.0016i
0.0000 + 0.0002i  0.0000 - 0.0002i  0.0000 - 0.0001i  0.0000 + 0.0001i
-0.0033 + 0.0236i -0.0033 - 0.0236i -0.0013 + 0.0232i -0.0013 - 0.0232i
-0.0009 - 0.0003i -0.0009 + 0.0003i  0.0007 - 0.0002i  0.0007 + 0.0002i
0.0017 + 0.0125i  0.0017 - 0.0125i  0.0007 + 0.0129i  0.0007 - 0.0129i
0.0003 + 0.0060i  0.0003 - 0.0060i -0.0002 + 0.0062i -0.0002 - 0.0062i
-0.0006 + 0.0000i -0.0006 - 0.0000i  0.0002 - 0.0001i  0.0002 + 0.0001i
-0.0004 + 0.0001i -0.0004 - 0.0001i -0.0004 + 0.0001i -0.0004 - 0.0001i
0.0002 - 0.0031i  0.0002 + 0.0031i -0.0001 - 0.0031i -0.0001 + 0.0031i
0.0002 + 0.0000i  0.0002 - 0.0000i -0.0001 + 0.0000i -0.0001 - 0.0000i
-0.0006 - 0.0030i -0.0006 + 0.0030i -0.0004 - 0.0031i -0.0004 + 0.0031i

Columns 5 through 8

-0.1691 -0.4676 -0.5694 0.5856
0.0391 -0.1514 -0.1552 0.3322
0.0006 0.0135 0.0684 0.2440
1.0000 1.0000 1.0000 -0.7344
-0.3048 0.3848 0.3641 -0.5210
-0.0043 -0.0353 -0.1438 -0.3762
0.2728 0.6283 0.7716 -0.6520
-0.1205 0.1184 0.1542 -0.3630
0.0072 -0.0367 -0.1035 -0.1917
0.0067 0.0030 0.0030 -0.0015
-0.0011 0.0006 0.0009 -0.0008
-0.0433 -0.0993 -0.1438 0.0279
-0.0295 -0.1436 0.2545 0.2850
0.0129 -0.0619 0.8122 -0.4344
0.0051 0.0604 0.3564 1.0000
-0.0007 0.0711 -0.5686 0.2005
-0.0018 -0.0023 -0.2017 -0.2458
0.0132 0.0395 -0.1012 -0.4846

Columns 9 through 12
```

## Table C.4.11 (cont'd)

```
0.0051 -0.1377 + 0.0079i -0.1377 - 0.0079i -0.1132
-0.0612 0.0691 - 0.0277i 0.0691 + 0.0277i -0.0588
-0.0944 -0.1689 - 0.2889i -0.1689 + 0.2889i -0.1947
0.0192 -0.1654 + 0.0876i -0.1654 - 0.0876i -0.1294
0.0440 0.0715 - 0.0725i 0.0715 + 0.0725i -0.0646
0.1188 -0.3834 - 0.2565i -0.3834 + 0.2565i -0.2127
0.0583 -0.0255 - 0.0037i -0.0255 + 0.0037i -0.0873
-0.0012 -0.2003 - 0.1946i -0.2003 + 0.1946i -0.1526
0.1050 -0.5400 + 0.5091i -0.5400 - 0.5091i -0.3548
0.0010 0.0000 - 0.0001i 0.0000 + 0.0001i 0.0001
-0.0002 0.0000 + 0.0000i 0.0000 - 0.0000i 0.0000
-0.0249 1.0000 + 0.0000i 1.0000 - 0.0000i 1.0000
1.0000 0.0061 + 0.0329i 0.0061 - 0.0329i 0.0789
-0.5759 0.0145 + 0.0387i 0.0145 - 0.0387i 0.0888
-0.2920 0.4109 + 0.1760i 0.4109 - 0.1760i 0.6362
-0.1643 -0.0021 + 0.0316i -0.0021 - 0.0316i 0.0781
0.2385 0.1206 + 0.1938i 0.1206 - 0.1938i 0.4522
-0.1387 0.0497 + 0.2218i 0.0497 - 0.2218i 0.3293
```

Columns 13 through 16

```
0.2274 0.9991 1.0000 0.1573
0.1805 0.9876 -0.5230 0.0608
1.0000 1.0000 -0.3165 0.3496
-0.0120 0.9981 0.5796 0.0643
-0.0303 0.9921 -0.2894 0.0523
-0.2176 0.9994 -0.1645 0.0860
-0.0073 0.9945 0.0719 0.0327
-0.1766 0.9968 -0.2198 0.0384
-0.7867 0.9990 0.0632 -0.1530
0.0000 -0.0002 0.0001 0.0003
-0.0001 0.0000 0.0000 0.0003
-0.4410 -0.0082 -0.0904 -0.4647
0.0833 -0.0013 0.1077 0.2990
-0.1380 -0.0016 0.0821 0.6510
-0.0202 -0.0068 0.0169 -0.3734
-0.2326 -0.0015 0.1437 1.0000
0.1317 -0.0062 0.1683 0.5480
0.4848 -0.0047 0.0621 -0.6801
```

Columns 17 through 18

```
1.0000 -0.0649
0.0677 0.1430
-0.8430 0.0536
0.6633 -0.0307
0.0530 0.0438
-0.5141 0.0095
0.3084 0.0222
-0.3284 -0.0886
-0.1242 0.0305
0.0002 -0.0004
0.0001 0.0000
-0.0787 -0.1402
0.1873 -0.4009
0.1875 0.0488
0.1438 -0.1015
0.2626 -0.2914
0.4132 1.0000
0.2254 -0.9740
```

detjj =

1.8175e+26

detd =

9.6001e+20

detda =

1.8932e+05

detad =

# Table C.4.11 (cont'd)

```
-4.9559e+24

condjj =
2.5408e+06

condd =
61.6129

condda =
1.2208e+06

condad =
2.9173e+06

vtt =
1.0000 0.0155 -0.2002
-0.4906 1.0000 -0.4246
-0.0017 -0.0002 1.0000

ett =
1.0e+03 *

-0.1140
-1.5191
0.0002
```

## Table C.4.12 Output for algebraic/dynamic 150 MVar(without exciter in)

eigjj =

```
-26.3461 +52.4058i
-26.3461 -52.4058i
 51.3629
 46.8155
 42.7175
-14.6136 +27.9829i
-14.6136 -27.9829i
-12.2939 +22.5771i
-12.2939 -22.5771i
 27.4704
 25.4227
 -7.5743 +16.7980i
 -7.5743 -16.7980i
 23.4856
-16.5863
-15.9151
 -3.9477 +14.9444i
 -3.9477 -14.9444i
 13.4571 + 0.8996i
 13.4571 - 0.8996i
 11.7788
  9.8842
  5.6831
  3.5289
 -0.3585 + 1.3749i
 -0.3585 - 1.3749i
 -0.2236 + 1.1036i
 -0.2236 - 1.1036i
 -0.0709
 -0.0843 + 0.7979i
 -0.0843 - 0.7979i
 -0.0497 + 0.6402i
 -0.0497 - 0.6402i
 -0.0349 + 0.5984i
 -0.0349 - 0.5984i
```

eigd =

```
-14.4530 +28.1474i
-14.4530 -28.1474i
-12.1199 +22.5681i
-12.1199 -22.5681i
 51.3628
 46.8168
 42.7216
 -7.4686 +16.7592i
 -7.4686 -16.7592i
 27.4743
 25.4621
  3.7091
 23.5039
  5.7289
 10.0391
 11.7581
 13.5198 + 0.9173i
 13.5198 - 0.9173i
```

eigda =

```
-26.4666 +52.2684i
-26.4666 -52.2684i
 -3.8998 +14.9699i
 -3.8998 -14.9699i
-16.5234
-15.6538
 -0.3235 + 1.3987i
 -0.3235 - 1.3987i
 -0.2121 + 1.0817i
 -0.2121 - 1.0817i
 -0.0688
 -0.0932 + 0.7924i
 -0.0932 - 0.7924i
 -0.0632 + 0.6368i
 -0.0632 - 0.6368i
 -0.0340 + 0.6039i
 -0.0340 - 0.6039i
```

vda =

Columns 1 through 4

```
 0.0000 - 0.0000i  0.0000 + 0.0000i  0.0000 + 0.0000i  0.0000 - 0.0000i
 0.0000 + 0.0000i  0.0000 - 0.0000i  0.0000 - 0.0000i  0.0000 + 0.0000i
 0.0000 + 0.0000i  0.0000 - 0.0000i  0.0000 - 0.0000i  0.0000 - 0.0000i
 0.0000 + 0.0000i  0.0000 - 0.0000i  0.0000 - 0.0000i  0.0000 + 0.0000i
 0.0000 - 0.0000i  0.0000 + 0.0000i  0.0000 + 0.0000i  0.0000 - 0.0000i
 0.0000 - 0.0000i  0.0000 + 0.0000i  0.0000 - 0.0000i  0.0000 + 0.0000i
-0.0002 + 0.0003i -0.0002 - 0.0003i  0.0000 + 0.0000i  0.0000 - 0.0000i
 0.0000 + 0.0000i  0.0000 - 0.0000i -0.0012 + 0.0006i -0.0012 - 0.0006i
 0.0000 + 0.0000i  0.0000 - 0.0000i  0.0000 + 0.0000i  0.0000 - 0.0000i
 0.0001 + 0.0000i  0.0001 - 0.0000i  0.0000 + 0.0000i  0.0000 - 0.0000i
 0.0000 + 0.0000i  0.0000 - 0.0000i -0.0001 + 0.0005i -0.0001 - 0.0005i
-0.0048 - 0.0105i -0.0048 + 0.0105i  0.0000 - 0.0000i  0.0000 + 0.0000i
 0.0000 - 0.0000i  0.0000 + 0.0000i -0.0021 - 0.0304i -0.0021 + 0.0304i
```

# Table C.4.12 (cont'd)

```
1.0000 + 0.0000i 1.0000 - 0.0000i 0.0011 + 0.0000i 0.0011 - 0.0000i
0.0000 + 0.0001i 0.0000 - 0.0001i 1.0000 - 0.0000i 1.0000 + 0.0000i
-0.0759 - 0.1538i -0.0759 + 0.1538i -0.0001 - 0.0007i -0.0001 + 0.0007i
0.0000 - 0.0000i 0.0000 + 0.0000i -0.0286 - 0.1101i -0.0286 + 0.1101i
```

Columns 5 through 8

```
0.0000 0.0001 0.0098 - 0.0057i 0.0098 + 0.0057i
0.0001 0.0000 -0.0057 - 0.0085i -0.0057 + 0.0085i
0.0000 0.0000 -0.0025 + 0.0014i -0.0025 - 0.0014i
0.0000 0.0000 -0.0054 - 0.0058i -0.0054 + 0.0058i
0.0000 0.0000 -0.0049 + 0.0052i -0.0049 - 0.0052i
0.0000 0.0000 0.0014 + 0.0015i 0.0014 - 0.0015i
-0.0001 0.0046 -0.0239 - 0.0688i -0.0239 + 0.0688i
0.0012 0.0001 -0.0141 - 0.0006i -0.0141 + 0.0006i
0.0000 0.0000 -0.0027 + 0.0020i -0.0027 - 0.0020i
-0.0008 0.0440 -0.0184 - 0.0395i -0.0184 + 0.0395i
0.0565 0.0062 -0.0088 - 0.0039i -0.0088 + 0.0039i
0.0010 -0.0508 0.0181 + 0.0381i 0.0181 - 0.0381i
-0.0335 -0.0039 0.0086 + 0.0033i 0.0086 - 0.0033i
-0.0207 1.0000 0.0344 + 0.1399i 0.0344 - 0.1399i
1.0000 0.1086 0.0376 + 0.0446i 0.0376 - 0.0446i
0.0131 -0.6673 1.0000 - 0.0000i 1.0000 + 0.0000i
-0.1065 -0.0122 0.0431 - 0.0570i 0.0431 + 0.0570i
```

Columns 9 through 12

```
-0.0211 + 0.0096i -0.0211 - 0.0096i -0.0028 -0.0014 - 0.0557i
0.3153 - 0.0592i 0.3153 + 0.0592i -0.0161 -0.0190 - 0.0115i
-0.0225 + 0.0056i -0.0225 - 0.0056i 0.0325 -0.0932 + 0.7924i
0.0123 + 0.0171i 0.0123 - 0.0171i 0.0410 -0.0692 + 0.0099i
-0.1077 - 0.2704i -0.1077 + 0.2704i 0.2339 -0.0116 + 0.0253i
0.0089 + 0.0191i 0.0089 - 0.0191i -0.4726 1.0000 + 0.0000i
0.0080 + 0.0352i 0.0080 - 0.0352i -0.0674 -0.0001 - 0.0004i
0.0044 - 0.1819i 0.0044 + 0.1819i -0.1980 0.0318 - 0.0007i
-0.0079 + 0.0016i -0.0079 - 0.0016i 1.0000 0.0010 + 0.0252i
0.0047 + 0.0119i 0.0047 - 0.0119i 0.0000 0.0003 + 0.0012i
-0.0169 - 0.1040i -0.0169 + 0.1040i -0.0018 0.0115 + 0.0034i
-0.0045 - 0.0115i -0.0045 + 0.0115i 0.0001 -0.0003 - 0.0012i
0.0194 + 0.0984i 0.0194 - 0.0984i 0.0017 -0.0110 - 0.0029i
-0.0184 - 0.0390i -0.0184 + 0.0390i -0.0016 -0.0026 - 0.0040i
-0.1174 + 0.6150i -0.1174 - 0.6150i 0.0095 -0.0614 - 0.0361i
-0.3674 + 0.0157i -0.3674 - 0.0157i -0.0261 -0.0484 - 0.0021i
1.0000 - 0.0000i 1.0000 + 0.0000i -0.2649 -0.0643 + 0.1435i
```

Columns 13 through 16

```
-0.0014 + 0.0557i -0.0632 + 0.6368i -0.0632 - 0.6368i 0.0247 + 0.0252i
-0.0190 + 0.0115i -0.0696 + 0.0344i -0.0696 - 0.0344i -0.2307 + 0.1592i
-0.0932 - 0.7924i 0.0137 + 0.1141i 0.0137 - 0.1141i 0.0055 + 0.0181i
-0.0692 - 0.0099i 1.0000 + 0.0000i 1.0000 - 0.0000i 0.0393 - 0.0431i
-0.0116 - 0.0253i 0.0643 + 0.1029i 0.0643 - 0.1029i 0.2842 + 0.3661i
1.0000 - 0.0000i 0.1753 - 0.0389i 0.1753 + 0.0389i 0.0293 - 0.0107i
-0.0001 + 0.0004i -0.0454 - 0.0205i -0.0454 + 0.0205i 0.0011 + 0.0127i
0.0318 + 0.0007i 0.0555 - 0.0561i 0.0555 + 0.0561i -0.0855 - 0.2350i
0.0010 - 0.0252i -0.0030 + 0.0095i -0.0030 - 0.0095i -0.0092 + 0.0021i
0.0003 - 0.0012i -0.0076 - 0.0126i -0.0076 + 0.0126i 0.0000 + 0.0010i
0.0115 - 0.0034i 0.0168 - 0.0139i 0.0168 + 0.0139i -0.0078 - 0.0572i
-0.0003 + 0.0012i 0.0071 + 0.0123i 0.0071 - 0.0123i 0.0000 - 0.0010i
-0.0110 + 0.0029i -0.0156 + 0.0135i -0.0156 - 0.0135i 0.0084 + 0.0538i
-0.0026 + 0.0040i 0.0549 + 0.0298i 0.0549 - 0.0298i -0.0026 - 0.0038i
-0.0614 + 0.0361i -0.1135 - 0.0614i -0.1135 + 0.0614i -0.0162 + 0.3433i
-0.0484 + 0.0021i 0.6760 - 0.2197i 0.6760 + 0.2197i -0.0514 - 0.0115i
-0.0643 - 0.1435i 0.1964 + 0.2958i 0.1964 - 0.2958i 1.0000 - 0.0000i
```

Column 17

```
0.0247 - 0.0252i
-0.2307 - 0.1592i
0.0055 - 0.0181i
0.0393 + 0.0431i
0.2842 - 0.3661i
0.0293 + 0.0107i
0.0011 - 0.0127i
-0.0855 + 0.2350i
-0.0092 - 0.0021i
0.0000 - 0.0010i
-0.0078 + 0.0572i
```

# Table C.4.12 (cont'd)

```
0.0000 + 0.0010i
0.0084 - 0.0538i
-0.0026 + 0.0038i
-0.0162 - 0.3433i
-0.0514 + 0.0115i
1.0000 + 0.0000i
```

eigad =

1.0e+02 *

```
-0.5717 + 6.6050i
-0.5717 - 6.6050i
-0.4252 + 4.2282i
-0.4252 - 4.2282i
 1.3999
 0.6388
 0.5068
 0.4490
-0.0727 + 0.1284i
-0.0727 - 0.1284i
 0.3764
 0.0147
 0.2142
 0.0423
 0.1057
 0.1361
 0.0972
 0.1411
```

vad =

Columns 1 through 4

```
0.0229 + 0.0184i 0.0229 - 0.0184i 0.0237 + 0.0385i 0.0237 - 0.0385i
0.1072 + 0.0210i 0.1072 - 0.0210i 0.0014 - 0.0003i 0.0014 + 0.0003i
0.0000 + 0.0000i 0.0000 - 0.0000i 0.0000 + 0.0000i 0.0000 - 0.0000i
0.8852 - 0.1741i 0.8852 + 0.1741i 1.0000 + 0.0000i 1.0000 + 0.0000i
1.0000 - 0.0000i 1.0000 + 0.0000i 0.0107 - 0.0055i 0.0107 + 0.0055i
0.0001 - 0.0001i 0.0001 + 0.0001i 0.0003 - 0.0001i 0.0003 + 0.0001i
-0.0130 - 0.0457i -0.0130 + 0.0457i -0.0079 - 0.0817i -0.0079 + 0.0817i
-0.0039 - 0.0555i -0.0039 + 0.0555i 0.0020 - 0.0013i 0.0020 + 0.0013i
0.0008 - 0.0001i 0.0008 + 0.0001i 0.0000 + 0.0000i 0.0000 - 0.0000i
0.0036 + 0.0335i 0.0036 - 0.0335i -0.0024 + 0.0238i -0.0024 - 0.0238i
-0.0007 + 0.0082i -0.0007 - 0.0082i 0.0000 + 0.0001i 0.0000 - 0.0001i
0.0020 + 0.0070i 0.0020 - 0.0070i 0.0012 + 0.0125i 0.0012 - 0.0125i
0.0003 + 0.0035i 0.0003 - 0.0035i 0.0001 + 0.0059i 0.0001 - 0.0059i
0.0003 + 0.0038i 0.0003 - 0.0038i -0.0001 + 0.0001i -0.0001 - 0.0001i
-0.0002 + 0.0001i -0.0002 - 0.0001i -0.0004 + 0.0001i -0.0004 - 0.0001i
-0.0008 - 0.0046i -0.0008 + 0.0046i 0.0000 - 0.0031i 0.0000 + 0.0031i
0.0000 - 0.0018i 0.0000 + 0.0018i 0.0000 - 0.0000i 0.0000 + 0.0000i
-0.0006 - 0.0017i -0.0006 +.0.0017i -0.0005 - 0.0030i -0.0005 + 0.0030i
```

Columns 5 through 8

```
-0.1203 -0.3594 -0.2669 0.4988
0.0036 -0.0703 0.0203 0.1766
0.0005 0.0107 0.1237 0.2187
1.0000 1.0000 0.5347 -0.7785
-0.3274 0.3434 0.1300 -0.5131
-0.0037 -0.0295 -0.2408 -0.3498
0.2483 0.5604 0.4327 -0.6367
-0.1097 0.0954 0.0536 -0.3101
0.0063 -0.0293 -0.1529 -0.1900
0.0079 0.0036 0.0020 -0.0020
-0.0006 0.0003 0.0003 -0.0004
-0.0367 -0.0850 -0.1081 0.0337
-0.0242 -0.0946 0.4244 0.0180
0.0107 -0.0226 1.0000 -0.5059
0.0040 0.0527 0.6754 1.0000
-0.0004 0.0348 -0.6918 0.3307
-0.0018 -0.0052 -0.3365 -0.2443
0.0110 0.0279 -0.2298 -0.3698
```

Columns 9 through 12

## Table C.4.12 (cont'd)

```
-0.1095 + 0.0146i -0.1095 - 0.0146i 0.0837 0.1190
0.0594 + 0.0061i 0.0594 - 0.0061i -0.0385 0.0679
-0.0834 - 0.2511i -0.0834 + 0.2511i -0.0423 0.0985
-0.1622 + 0.1034i -0.1622 - 0.1034i -0.0481 0.1328
0.0988 - 0.0256i 0.0988 + 0.0256i -0.0363 0.0898
-0.3278 - 0.3285i -0.3278 + 0.3285i 0.0494 0.1087
-0.0078 + 0.0268i -0.0078 - 0.0268i -0.0169 0.1033
-0.1466 - 0.2044i -0.1466 + 0.2044i -0.0533 0.0888
-0.6487 + 0.6086i -0.6487 - 0.6086i 0.0612 0.1898
0.0000 - 0.0001i 0.0000 + 0.0001i 0.0008 0.0001
0.0000 + 0.0000i 0.0000 - 0.0000i -0.0001 0.0000
1.0000 - 0.0000i 1.0000 + 0.0000i -0.0221 1.0000
0.0060 + 0.0138i 0.0060 - 0.0138i 1.0000 0.1271
0.0132 + 0.0228i 0.0132 - 0.0228i -0.5807 0.1387
0.3465 + 0.1138i 0.3465 - 0.1138i -0.1321 0.7413
0.0014 + 0.0144i 0.0014 - 0.0144i -0.1446 0.1326
0.0937 + 0.1120i 0.0937 - 0.1120i 0.1934 0.6406
0.0063 + 0.1562i 0.0063 - 0.1562i -0.1934 0.5611
```

Columns 13 through 16

```
0.2272 0.9374 1.0000 0.1261
0.1514 1.0000 -0.4078 -0.3692
1.0000 0.9405 -0.2802 -0.2107
-0.0216 0.8469 0.5439 0.0407
-0.0508 0.8768 -0.1946 -0.1984
-0.1948 0.8099 -0.1330 -0.0582
-0.0224 0.7822 0.1012 -0.0702
-0.1591 0.7752 -0.1506 -0.0434
-0.7483 0.6601 0.0275 0.0590
0.0000 -0.0001 0.0003 -0.0001
0.0000 0.0000 0.0000 -0.0002
-0.4308 -0.4482 -0.1129 0.2820
0.0669 -0.1554 0.1136 -0.1066
-0.0983 -0.1753 0.1024 -0.5877
-0.0567 -0.5488 0.0011 0.2598
-0.1926 -0.2014 0.1751 -0.7983
0.1602 -0.6647 0.1677 -0.7431
0.3786 -0.5734 0.0447 1.0000
```

Columns 17 through 18

```
1.0000 -0.2090
-0.0630 0.2264
-0.4876 -0.1397
0.5959 -0.0901
-0.0143 0.0554
-0.2566 -0.0353
0.2172 0.0106
-0.1708 -0.1073
-0.0464 0.1091
0.0003 -0.0005
0.0000 0.0000
-0.1414 0.0354
0.1581 -0.4904
0.1561 -0.0571
0.0465 0.0567
0.2394 -0.5149
0.2777 1.0000
0.1374 -0.9298
```

detjj =

-6.0095e+29

detd =

1.7207e+23

detda =

-3.4925e+06

detad =

# Table C.4.12 (cont'd)

```
  3.4649e+28

condjj =
  1.4727e+05

condd =
  17.6983

condda =
  1.2449e+05

condad =
  9.0097e+04

vtt =
  1.0000  0.0025 -0.0674
 -0.1803  1.0000 -0.1320
 -0.0006  0.0000  1.0000

ett =
  1.0e+03 *

 -0.0935  0  0
  0 -2.4353  0
  0  0 -0.0001
```

# LIST OF REFERENCES

# LIST OF REFERENCES

1.  R.A. Schlueter, 'and colleagues', "Voltage Stability and Security Assessment," EPRI Final Report EL-5967 on Project RP 1999-8, 1988.

2.  R.A. Schlueter, et al., "reactive Supply On-Line Criteria," Section 7, Proceedings of Workshop on Bulk Power Voltage Phenomena: Voltage Stability and Security, Potosi, MO, September 1988.

3.  R.A. Schlueter, et al., "Unification of Static and Dynamic Tests for Voltage Collapse: A Tutorial," Submitted to IEEE Transactions on Power Systems.

4.  R.A. Schlueter, et al., "Methods for Determining Proximity to Voltage Collapse," presented at Power Engineering Society Winter Meeting, February 4-9, 1990, Atlanta, Georgia.

5.  W.R. Lachs, "Voltage Collapse in EHV Power Systems," paper presented at the IEEE PES Winter Meeting, New York, NY, January 29 to February 3, 1978.

6.  W.R. Lachs, "System Reactive Power Limitations," paper presented at the IEEE PES Winter Meeting, New York, NY, February 4-9, 1979.

7.  V.A. Venikov, V.A. Stroev, V.I. Idelchick, and V.I. Tarasov, "Estimation of Electrical Power System Steady-State Stability in Load Flow Calculations," IEEE Trans. on Power Apparatus and Systems, Vol. PAS-94, No. 3, May/June 1975.

8.  J. Carpentier, R. Girard, E. Scano, "Voltage Collapse Proximity Indicators Computed from an Optimal Power Flow," Proceedings of 8th Power System Computation Conference, Helsinki, 1984.

9.  A.G. Costi, "Voltage Stability and Security Assessment for Power Systems," Dissertation for the Ph.D., submitted to Michigan State University in January 1987.

11. Y. Tamura, H. Mori, and S. Iwamoto, "Relationship between Voltage Instability and Multiple Load Flow Solutions in Electric Power Systems," IEEE Trans. on PAS, Vol. PAS-102, No. 5, May 1983.

12. Y. Tamura, Y. Nakanishi, and S. Iwamoto, "On the Multiple Solution Structure, Singular Point and Existence Conditions of the Multiple Load-Flow Solutions," IEEE PES Winter Meeting, New York, NY, February 3-8, 1980.

13. Y. Tamura, K. Iba, and S. Iwamoto, "A Method for Finding Multiple Load-Flow Solutions for General Power Systems," IEEE PES Winter Meeting, New York, NY February 3-8, 1980.

14. S. Abe, Y. Fukunaga, A. Isono, and B. Kondo, "Power Systems Voltage Stability," IEEE Trans. on Power Apparatus and Systems, Vol. PAS-101, No. 10, pp.3830-3840, October 1982.

15. J. Medanic, M. Illic, and J. Christensen, "Discrete Models of Slow Voltage Dynamics for Under Load Tap-Changing Transformer Coordination," presented at the 1986 IEEE Summer Power Meeting, Mexico City.

16. M. Illic and J. Medanic, "Strategies for Real Time Voltage Var Monitoring, Communications, and Control," submitted to IEE 1986.

17. M. Illic and J. Medanic, "Modeling and Control of Slow Voltage Dynamics in Electric Power Systems," presented at the 1986 IFAC Symposium on Large Scale Systems and Applications, Switzerland.

18. C.C. Liu, "Characterization of a Voltage Collapse Mechanism Due to the Effects of On-Line Tap Changers," Proceedings of IEEE International Symposium on Circuits and Systems, San Jose, CA, May, 1986.

19. P.W. Sauer and M.A. Pai, "Steady-State Stability and Load Flow," Proceedings of the 27th Conference on Decision and Control, Austin, Texas, December 1988.

20. C.L. DeMarco, "A Large Deviations Model for Voltage Collapse in Electric Power Systems," Proceedings of IEEE International Symposium on Circuits and Systems, San Jose, CA, May 1986.

21. J. Zaborszky, "Some Basic Issues in Voltage Stability and Viability," Proceedings: Bulk Power System Voltage Phenomena-Voltage Stability and Security, EPRI EL-6183, Project 2473-21, January 1989.

22. C.C. Liu and F.F. Wu, "Steady State Voltage Stability Regions of Power Systems," Proceedings of the Conference on Decision and Control, pp. 488-493, December 1984.

23. P.M. Anderson and A.A. Fouad, "Power System Control and Stability," The Iowa State University Press, 1977.

24. James M. Ortega, "Matrix Theory," Plenum Press, New York, 1987.

25. Arthur R. Bergen, "Power System Analysis," Prentice-Hall, Inc., New Jersey, 1970.

26. Samuel D. Conte and Carl de Boor, "Elementary Numerical Analysis, An Algorithmic Approach," McGraw-Hill, Inc., 1980.

27. H.G. Kwatny, A.K. Pasrija, and L.K. Bahar, "Static Bifurcations in Electrical Power Networks: Loss of Steady State Stability and Voltage Collapse," IEEE Trans. on Circuits and Systems, Vol. CAS-33, No. 10, Oct. 1986, pp.981-991.

28. P. Booremans, A. Calvaer, J.P. de Reuck, J. Gooserens, E. Van Geert, J. Van Hecke, and A. Van Ranst, "Voltage Stability: Fundamental Concepts and comparison of Practical Criteria," International Conference on Large High Voltage Electric Systems, Cigre 38-11, Aug. 1984.

29. H. Glavitch and P. Kessel, "Estimating the Voltage Stability of a Power System,"

1985 PICA conference paper, San Francisco, May 1985.

30.  George McPherson, "An Introduction to Electrical Machines and Transformer," John Wiley & Sons, Inc., 1981.